The Potential of Renewable Energy Sources and Integrated Energy in the ENTSO-E

A Techno-Economic Potential Analysis within an Energy Balance Assessment

Von der Fakultät für Maschinenbau, Elektro- und Energiesysteme
der Brandenburgischen Technischen Universität Cottbus–Senftenberg
zur Erlangung des akademischen Grades eines
Doktor der Ingenieurwissenschaften (Dr.-Ing.)

genehmigte Dissertation

vorgelegt von

M.Sc.

Mark Sebastian Kuprat

geboren am 11. Mai 1983 in Berlin

Vorsitzender:	Prof. Dr.-Ing. Georg Möhlenkamp
Gutachter:	Prof. Dr.-Ing. Harald Schwarz
Gutachter:	Prof. Dr.-Ing. Harald Fien
Tag der mündlichen Prüfung:	10. Oktober 2022

DOI: https://doi.org/10.26127/BTUOpen-6139

Vorwort

Die vorliegende Dissertation entstand während meiner Tätigkeit als Promovend und wissenschaftlicher Mitarbeiter am Fachgebiet Energieverteilung und Hochspannungstechnik der Brandenburgischen Technischen Universität Cottbus-Senftenberg. Die Arbeit steht im Zeichen der Klima- und Energiekrise, der Pandemie und politischer Zerwürfnisse, welche sich insbesondere in der Energieversorgungssicherheit und dem gesellschaftlichen Zusammenhalt manifestieren.

Herrn Prof. Dr.-Ing. Harald Schwarz danke ich herzlich für die langjährige Betreuung und Förderung, für seine Anregungen und Diskussionsbeiträge sowie für die Übernahme des ersten Gutachtens.

Herrn Prof. Dr.-Ing. Harald Fien danke ich für das der Arbeit entgegengebrachte tiefgreifende Interesse, die stetige Begleitung und die fachübergreifenden Diskussionen sowie für die Übernahme des zweiten Gutachtens.

Mein Dank gilt auch dem Verband Europäischer Übertragungsnetzbetreiber (ENTSO-E), dem Statistischen Amt der Europäischen Union (Eurostat) und der Gemeinsamen Forschungsstelle (JRC), welche die Arbeit begleitet und diskutiert sowie wertvolle Daten zur Verfügung gestellt haben.

Des Weiteren gilt mein Dank allen Freunden, Kollegen und Angehörigen des Fachgebietes Energieverteilung und Hochspannungstechnik, die sich durch tatkräftige Unterstützung und konstruktive Diskussionsbeiträge an dieser Arbeit beteiligten. Mein ganz besonderer Dank gilt dabei Herrn Dr.-Ing. Klaus Pfeiffer, der die Arbeit mit aufrichtiger Hingabe und in intensiver Zusammenarbeit von Beginn an begleitet hat.

Cottbus, im November 2022

Mark Sebastian Kuprat

“All energy is only borrowed and one day you have to give it back.”

- J. Cameron

Abstract

This analysis aims at the investigation of the techno-economic RES potentials and to minimize GHG emissions in the ENTSO-E. The ENTSO-E represents one of the world's largest economic regions with a GDP of 19,835 billion US dollar (23 %) and a primary energy consumption of 29,705 TWh (18 %). ENTSO-E is coined with high degrees of fossil energy dependencies (49.9 %) from third-party countries and contributes 3,517 Mt CO_{2eq} (9 %) to global GHG emissions. The Primary Sources onshore wind, offshore wind, utility-scale PV, and CSP techno-economic potentials are assessed via GIS-based georeferenced spatial analysis. Solar rooftop potentials are calculated based on a per capita approach. The Secondary Sources bioenergy, hydropower, geothermal, and hydrokinetic energy potentials are approximated based on meta-analysis. Primary and Secondary Sources potentials are input into the IES linear optimization model to simulate an energy system with high shares of RES and PTX. It is found that RES-based primary energy production potentials account for 13,492 TWh and energy dependency could be reduced by 6,482 TWh to 20.5 %. Compared to the base year 1990, the direct GHG emission reduction amounts to 3,246 Mt CO_{2eq} (70.7 %). This reduction does not correspond with the EU reduction target of 80–95 %. Hence, RES-based fuel imports, such as synthetic fuels and hydrogen, from third-party countries become necessary, to substitute fossil fuels and reduce domestic emissions. Additional GHG reduction potentials are suspected in the indirect emission sectors agriculture and waste management. In reference to the Sankey methodology, the analysis entails comprehensive energy flow balances for the ENTSO-E 2016 and 2050 energy systems. The ENTSO-E member countries exhibit heterogeneous properties regarding RES potentials, GHG emissions, and energy dependencies, and, hence, must be assessed individually. Integrated energy systems with high shares of RES and PTX represent a promising means to decrease direct energy use and non-energy use emissions as well as energy dependencies significantly.

List of Content

Compendium: Relevant content, charts, and figures can be found in the Compendium of this work, as referred to in the main body.

Annex CD: Digital data, calculations, tables, and files of this work are referred to as Annex CD and are not included in this publication.

List of Figures

List of Tables

Glossary

Anthropogenic Emissions		Emissions of greenhouse gases, precursors of GHG, and aerosols caused by human activities.
Carbon Dioxide Equivalent	CO_{2eq}	Metric measure used to compare the emissions from various greenhouse gases on the basis of their global-warming potential (GWP) by converting amounts of other gases to the equivalent amount of carbon dioxide with the same global warming potential.
Direct Emissions		Energy and non-energy use related emissions of combustion and non-combustion processes.
Downstream Processes		All energy conversion and transformation processes that are located in the final energy consumption sector.
Emission Inventory		Emission inventory account for the amount of pollutants emitted to the atmosphere and contain the total emissions for specific GHG that are originating from all source categories in a certain geographical area and within a specified time span, usually a specific year.
Energy Commodities / Energy Products		Solid fuels, oils, gases, renewables, wastes, heat, and electricity.
Energy Conversion and Transformation		All processes that refer to the conversion of primary energy sources into secondary energy sources, such as power plant combustion, refining processes, and PTX.
Energy Use		Combustion of energy products for the purpose of electricity, heat, and mechanical energy provision.
Final Energy Consumption	FEC	All energy commodities that enter the final energy consumption sectors after exports, conversion and transformation, losses, exchanges, and bunkering.
Global Warming Potential	GWP	The heat absorbed by GHG, expressed as a multiple of the heat that would be absorbed by the same mass of carbon dioxide.
Greenhouse Effect		Natural process by which radiation from the atmosphere warms earth’s surface to a temperature above a degree that makes it habitable. This natural effect is increased by anthropogenic GHG emissions.

Greenhouse Gases	GHG	Gases that absorb and emit radiant energy within the thermal infrared range causing the greenhouse effect.
Gross Inland Consumption		Primary energy consumption subtracted by exports and bunkering.
Indirect Emissions		Agriculture and waste management emissions, including wastewater emissions.
Intercellular		All energy conversion, flows, and exchanges between cells.
Intracellular		All energy conversion, flows, and demands within a single cell.
Land Use, Land-Use Change, and Forestry	LULUCF	Greenhouse gas inventory sector that covers emissions and removals of GHG resulting from direct human-induced land use, land-use change, and forestry activities.
Net Imports		All primary energy consumption imports minus exports.
Non-Energy Use		Non-combustion of energy products consumed as raw materials in the chemical, petrochemical, and other industries not to produce energy.
Primary Energy		Energy commodities that have not been subjected to any human engineered conversion process, such as natural gas, mineral oils, solar radiation, wind, solid and nuclear fuels.
Primary Energy Consumption	PEC	All energy commodities that enter the energy system via domestic production, imports, and stock changes.
Primary Energy Production		All primary energy commodities produced, mined, or extracted domestically.
Primary Sources		Onshore wind power plants, offshore wind power plants, utility-scale photovoltaic power plants, CSP, PV and solar thermal rooftops.
RES-based Energy Conversion		Electricity and heat production of renewable energy sources.
Secondary Energy		Products of primary energy conversion and transformation processes, such as electricity, district heat, refined fuels, and hydrogen.
Secondary Sources		Bioenergy, hydropower, geothermal, wave, ocean, and tidal power plants.

List of Symbols and Indices

H^+		Ionized hydrogen
H_2		Molecular hydrogen
H_2O		Water
N_2O		Nitrous oxide
O_2		Molecular oxygen
O^{2-}		Ionized oxygen
O_3		Ozone
SF_6		Sulfur hexafluoride
$\dot{V}$	$m^3 \cdot s^{-1}$	Volume flow
V_m	$m^3 \cdot mol^{-1}$	Volumetric molar mass
Ar		Argon
CH_4		Methane
CO_2		Carbon dioxide
CFC		Chlorofluorocarbons
CO		Carbon monoxide
COP	pu	Coefficient of Performance
E	J	Energy
He		Helium
KOH		Potassium hydroxide
M	$kg \cdot mol^{-1}$	Molar mass
N		Nitrogen
$NaOH$		Sodium hydroxide
Ne		Neon
OH^-		Hydroxide ion
P	W	Active power
Q	var	Reactive power
T	K	Temperature
U	V	Voltage
V	m^3	Volume
W	$kWh \cdot m^{-3}$	Wobbe index
d	pu	Relative density
n	mol	Amount of substance
p	bar	Pressure

pu		per unit
t	s	Time
w	$m \cdot s^{-1}$	Flow rate
ΔH_R	$J \cdot mol^{-1}$	Enthalpy of reaction
η	pu	Efficiency
ρ	$kg \cdot m^{-3}$	Density
τ	s	Temporal integration variable

List of Abbreviations

1G	First Generation
2G	Second Generation
3G	Third Generation
ACER	Agency for the Cooperation of Energy Regulators
AEL	Alcaline Electrolysis
AUE	Area Use Efficiency
BEV	Battery Electric Vehicles
BKB	Brown Coal Briquettes
CAPEX	Capital Expenditure
CCGT	Combined Cycle Gas Turbine
CDDA	Common Database on Designated Areas
CESA	Continental Europe Synchronous Area
CGDD	The French General Commission on Sustainable Development
CHP	Combined Heat and Power
CINEA	European Climate, Infrastructure and Environment Executive Agency
CLC	CORINE Land Cover
CLMS	Copernicus Land Monitoring Service
$CO_{2\,eq}$	Carbon Dioxide Equivalent
COP	Conference of the Parties
CORINE	Coordination of Information on the Environment
CSP	Concentrated Solar Power
CSV	Comma-separated Values
DNI	Direct Normal Irradiance
EC	European Commission
EDGAR	Emissions Database for Global Atmospheric Research
EEA	European Environment Agency
EEC	European Economic Community
EEZ	Exclusive Economic Zone
EF	Emission Factor
eff.	efficiency
EGS	Enhanced Geothermal System
EIA	Environmental Impact Assessment
EJ	Exajoule

El.	Electricity
EMODnet	European Marine Observation and Data Network
ENTSO-E	European Network of Transmission System Operators for Electricity
ESRI	Environmental Systems Research Institute
ETS	Emission Trading Scheme
ETSO	European Transmission System Operators
EU	European Union
EU-27	27 European Union Member States
Eurostat	European Statistical Office
EWEA	European Wind Energy Association
FCE	Fuel Cell Engine
FCEV	Fuel Cell Electric Vehicles
FEC	Final Energy Consumption
FLH	Full Load Hours
GAMS	General Algebraic Modeling System
GCEV	Grid Connected Electric Vehicles
GDP	Gross Domestic Product
GDR	German Democratic Republic
GHG	Greenhouse Gas
GIS	Geographic Information Systems
GMST	Global Mean Surface Temperature
Gt	Gigaton
GTP	Gas-to-Power
GWP	Global Warming Potential
HCNGV	Hydrogen Compressed Natural Gas Vehicles
HCV	Hydrogen Combustion Vehicles
HTP	Heat-to-Power
ICE	Internal Combustion Engine
IEA	International Energy Agency
IES	Integrated Energy System
IPCC	Intergovernmental Panel on Climate Change
IPCC-RA	IPCC Reference Approach
IPCC-SA	IPCC Sectoral Approach
IRENA	International Renewable Energy Agency
IRES	International Recommendations for Energy Statistics

ISO	International Organization for Standardization
IUCN	International Union for Conservation of Nature
ktoe	Thousands of Tons of Oil Equivalent
LCOE	Levelized Cost of Electricity
LHP	Large Hydropower Plants
LPG	Liquified Petroleum Gas
LULUCF	Land Use, Land Use Change, and Forestry
MERRA	Modern-Era Retrospective Analysis for Research and Applications
METAVER	Metadaten Verbund
Mt	Megaton
NDA	Nationally Designated Areas
NDC	Nationally Determined Contributions
NREL	National Renewable Energy Laboratory
NUTS	Nomenclature of Territorial Units for Statistics
O&M	Operations and Maintenance
ODU	Oxidized During Use
OPEX	Operational Expenditure
OPSD	Open Power System Data
OTEC	Ocean Thermal Energy Conversion
p.p.	Percentage Points
p.u.	Per Unit
PB	Peat Briquettes
PCI	Projects of Common Interest
PEC	Primary Energy Consumption
PEM	Polymer Electrolyte Membrane
PJ	Petajoule
PP	Power Plant
ppmv	Parts per Million Volume Fraction
PSH	Pumped-Storage Hydroelectricity
PT	Parabolic Through
PTC	Power-to-Chemicals
PTG	Power-to-Gas
PTH	Power-to-Heat
PTL	Power-to-Liquids
PTM	Power-to-Mobility

PTP	Power-to-Power
PTX	Power-to-X
PV	Photovoltaic
R/P	Reserves to Production
RES	Renewable Energy Sources
RG	Regional Groups
RG	Regional Group
SAC	Special Area of Conservation
SAM	System Advisor Model
SARAH	Surface Solar Radiation Data Set Heliosat
SBP	Specific Boiling Point / Industrial Spirits
Scand.	Scandinavia
SF	Storage Fraction
SHARES	Short Assessment of Renewable Energy Sources
SHP	Small Hydropower Plants
SI	International System of Units
SM	Solar multiple
SNG	Synthetic Natural Gas
SOEC	Solid Oxide Electrolysis Cell
SPA	Special Area of Protection
TCA	Trade and Cooperation Agreement
TSO	Transmission System Operators
TTW	Tank-to-Wheel
TWh	Terawatt-hour
TYNDP	Ten-Year Network Development Plan
UNCLOS	United Nations Convention on the Law of the Sea
UNFCCC	United Nations Framework Convention on Climate Change
UNSD	United Nations Statistics Division
USSE	Utility-scale solar energy
USSR	Union of Soviet Socialist Republics
VTG	Vehicle-to-Grid
W	Watt
WDPA	World Database on Protected Areas
WTW	Well-to-Wheel
XTP	X-to-Power

1. Introduction

1.1 Background and Motivation

Secure, affordable, and sustainable supply of energy serves as the foundation for any developed society and prosperity. Since the industrial revolution of the 19th century, mankind has become dependent on fossil fuels that substituted biomass as the dominant energy source. The energy intensity of fossil energy commodities, such as coal, mineral oil, natural gas, and uranium, accelerated human growth and development at an unprecedented velocity. [Priet2013] The world population has grown from about 1.3 billion in 1850 to 7.8 billion inhabitants in 2020 [UNC2020]. During the so-called petroleum age, the total energy consumption increased from about 10 exajoules (EJ) to far more than 450 EJ and the atmospheric concentration of carbon dioxide (CO_2) increased from 285 parts per million volume (ppmv) fraction to 411 ppmv [NOAA2020] [Priet2013]. In the meanwhile, anthropogenic greenhouse gas (GHG) emissions have reached 42 gigatons (Gt) carbon dioxide equivalent (CO_{2eq}) emissions per year. Those GHG emissions are projected to account for 52–58 Gt CO_{2eq} in 2030 [IPCC2019].

According to the Intergovernmental Panel on Climate Change (IPCC), the global mean surface temperature (GMST) exhibits an increase of 1.0 °C compared to pre-industrial levels. GMST is likely to exceed 1.5 °C between 2030 and 2052 if it continues to increase at the current rate. This increase of GMST comes along with significant near and long-term risks for the ecosystem and its inhabitants. Those tipping points entail the reduction of terrestrial carbon sinks due to the thawing of permafrost (boreal tipping point), the forest decline in the Amazon region (Amazon tipping point), and the global sea level rise. These impacts are regarded as irreversible. [IPCC2019] [UBA2020]

To minimize the probability of occurrence of the risks that come along with global warming, the world community aims at the reduction of anthropogenic GHG emissions. The first legal and globally accepted GHG reduction framework was given by the United Nations Framework Convention on Climate Change (UNFCCC) in Kyoto 1997. The Kyoto Protocol is the international treaty which extends the UNFCCC of Rio de Janeiro 1992. The Kyoto Protocol entered into force in 2005 and aims at the objective to inhibit global warming by reducing GHG concentrations in the atmosphere to a level that prevents dangerous anthropogenic interference with the climate system. [UN1998]

The most prominent successor of the Kyoto Protocol is the 21st Conference of the Parties 2015 (COP 21). Commonly it is referred to the 1.5 °C goal of the Paris Agreement, which determines the GMST increase to not exceed 2.0 °C and preferably limit it to not more than 1.5 °C compared to the pre-industrial era. [UN2015] Therefore, the remaining total carbon budget for the 1.5 °C objective amounts to approximately 580–770 Gt CO_{2eq} for a 50 % probability of limiting global warming to 1.5 °C (even chance) and 420–570 Gt CO_{2eq} for a 66 % probability (two-thirds chance) [IPCC2019].

In 2019, the European Commission (EC) has proclaimed the goal to become the first climate neutral continent within the framework of the European Green Deal [EC2019b]. Climate neutrality is defined as the offset of anthropogenic GHG emissions with carbon sinks. However, this term and its definition remains controversial. [IASS2015] The global consensus of mitigating climate change and limiting global warming to 1.5–2.0 °C is commonly referred to reducing the CO_{2eq} emissions by 80–95 % compared to the predefined base year 1990. [CEU2009a] [CEU2009b]. In consideration of the European Green Deal policy initiative, this work is concerned with the investigation of the technical feasibility and implementation of the GHG reduction objective in Europe.

Not only due to increasing CO_{2eq} concentrations but also in the face of scarce resources, the transformation of the energy systems becomes inevitable. In reference to 2019, hard coal and lignite reserves show a reserves-to-production (R/P) ratio[1] of 132 years. Whereas natural gas is estimated to 51 years and mineral oil to 50 years. [BP2020] Based on the currently identified resources, uranium is reported to last for 120 years [OECD2018]. Alternative large-scale energy sources, such as nuclear fusion, are not yet available and the future technical availability of those technologies is insecure [Crast2017] [Wess2017]. In the face of depleting resources and the lack of suitable alternatives, fossil resources must be subsidized at large scale. Hence, global warming and depleting fossil resources make it inevitable to substitute fossil fuels in the short and medium term. Minimizing the risks of global warming caused by anthropogenic GHG emissions at an early stage prevents mankind being compelled to find alternative energy sources in a post global warming world at a later stage of the 21st century.

Natural evidence, international treaties, and national legal frameworks are the prevailing drivers for reducing GHG emissions. Those reductions can be technically implemented by reducing energy consumption, increasing the efficiency of energy conversion, and substituting fossil fuels with renewable energy sources (RES). [IRENA2018a] The ongoing transformation of the energy sector poses the critical path, whereby the energy transition is mainly driven by RES-based electricity production. In this regard it seems obvious, that not only the increase of RES but also the conversion of electricity into other energy commodities and consumption sectors is of utmost importance to effectively decarbonize the energy system. This implies the development of integrated energy systems by the means of power-to-x (PTX) technologies. Those PTX technologies refer to their most prominent representatives power-to-heat (PTH), power-to-gas (PTG), and power-to-mobility (PTM) that enable the large-scale utilization of growing RES-based electricity production in the final energy consumption sectors. Hence, integrated energy systems (IES) based on PTX technologies with high shares of RES represent a promising means to decrease anthropogenic GHG emissions holistically and at large scale. [Aman2018] [Hirs2018]

[1] The R/P ratio is calculated by dividing the reserves remaining at the end of a year by the production in that year [BP2020]. The R/P ratio is subject to some uncertainties, such as extraction costs [OECD2018].

1.2 Objectives and Structure

As this work is concerned with the investigation of the feasibility of the GHG emission reduction targets in Europe 2050, the 80–95 % reduction goal is the subject of investigation. Since the European Union (EU) is a political construct which is exposed to external factors, such as accession and withdrawal negotiations, this work focuses on the European Network of Transmission System Operators for Electricity (ENTSO-E) area as the reference model region for the coherent European energy system.

Since the late 1990s, numerous countries promote the deployment of RES via various subsidy schemes, such as feed-in tariffs and market premiums. Consequently, especially large-scale onshore wind, offshore wind, and photovoltaic (PV) power plants have been erected. These power plants increased the RES share in the European electricity sector to more than 34 % in 2016. [EEA2018a] [EUROS2019a] However, the electricity sector covers only 21 % of the total energy demand. Thus, the total RES share of final energy consumption amounts to less than 17 %. [EUROS2019a] The significant energy demands are rather located in the heat and transport sectors. Those sectors are not yet sufficiently addressed by the energy transition and rely predominantly on fossil fuels. To achieve the GHG reduction goals, the RES-based electricity production must be increased tremendously and transferred into the energy consumption sectors within the framework of integrated energy[2] and by the means of PTX. [EC2018a] [IRENA2018a]

Since the deployment of various RES technologies is exposed to distinctive technical, economic, environmental, and social restrictions, which come along with strong limitations and competition of land use, the availability of RES is of special interest. In consideration that most RES-based energy conversion is unilateral concentrated in the electricity sector, the core research questions of this work are stated as the following:

(a) How are the current (2016) and future (2050) energy balances of the ENTSO-E countries composed? What amounts of primary energy, energy transformation, and final energy are input per ENTSO-E country?
(b) Which quantities of RES-based energy conversion are technically feasible? Where and to what extend can RES-based energy converters be deployed?
(c) By what means can the RES-based energy be converted into the other demand sectors? What is the potential role of PTX for integrated energy systems?
(d) To what extend is the ENTSO-E able to become independent from third-party energy imports? Which countries exhibit primary energy production surpluses or deficits as indicated by net positive and negative energy imports?
(e) How and to what extend is the GHG emission reduction goal of 80–95 % compared to the base year 1990 achievable?

[2] Integrated Energy Systems (IES) are generally referred to as resource efficient energy systems with high shares of RES and PTX technologies. Those systems are typically coined with high grades of digitalization and automation in order to synchronize supply and demand. [Hirs2018] [Palen2019] [Wu2019]

In the following, those questions are assessed for the ENTSO-E as a whole and for each ENTSO-E country individually. To investigate the core research questions this work is composed of five major sections, which comprise the following investigations:

(a) Status quo analysis of current energy balances and GHG emission inventories.
(b) Investigation of PTX potentials and implications for integrated energy systems.
(c) GIS and review-based techno-economic analysis of RES potentials.
(d) Energy system optimization and modelling with high shares of RES and PTX.
(e) Status 2050 analysis of future energy balances and GHG emission inventories.

To provide an overview of the current energy flows, demands, and conversions, a detailed analysis of the European energy systems is conducted and illustrated in energy flow charts (Sankey diagrams) for the energy balance reference year 2016. Moreover, the past and current GHG emissions are assessed and illustrated in form of CO_{2eq} emission inventories to evaluate previous impacts on GHG emissions and to derive future needs for action. To best consider the techno-economic RES potentials, a detailed site assessment by means of geographic information systems (GIS) for the most promising RES technologies onshore wind power, offshore wind power, utility-scale photovoltaic (PV), and concentrated solar power (CSP) plants is carried out, based on techno-economic, environmental, and social impact factors. Other technologies, such as solar rooftops, bioenergy, hydro power, and geothermal power plants, are considered via technical and literature review as well as meta-analysis.

To account for potential energy flows, conversions, and losses in a European energy system with high shares of RES, a linear optimization model has been developed in the General Algebraic Modeling System (GAMS). The model input is based on the techno-economic RES potential analysis and scenario assumptions of future energy demands, in conjunction with the corresponding production and demand profiles. The optimization variable of the objective function is based on the minimization of GHG emissions. As a distinctive feature, the optimization model considers PTX technologies. The PTX technologies are represented by its most prominent derivatives PTH, PTG, and PTM. Those PTX technologies represent the key technologies to account for energy conversion from the electricity sector and to enable RES consumption across all demand sectors. As a result, the energy balances of future energy systems with high shares of RES are assessed and illustrated as energy flow charts by the means of Sankey diagrams. Moreover, the corresponding GHG emissions are analyzed according to the resulting GHG emission inventories and their implication regarding the GHG reduction goals.

The final evaluation aims at the demonstration of a European energy system with high shares of RES and PTX. The proposed and hereinafter discussed methods are meant to investigate how and to what extent a climate neutral economy in the vision of the European Green Deal can be created in the ENTSO-E 2050. However, techno-economic, environmental, and social restrictions are considered an addressed thoroughly.

2. Status quo

2.1 ENTSO-E Model Region

To harmonize and liberalize the EU energy markets, the First Energy Package was adopted in 1996 to account for non-discriminatory market access, transparency and regulation, consumer protection, interconnection support, and security of supply. The first package was followed by the Second, Third, and Fourth Energy Package, with the objectives to ensure a functioning internal energy market along with adequate levels of interconnection and generation capacities. [Ciu2020] [EP2019]

However, the liberalization of Europe's energy markets had made only limited progress and the objectives had not been achieved at the desired scale, leading to uncompetitive energy prices and persistent entry barriers for market participants. To accomplish the objectives of the First and Second Energy Package, much closer cooperation of the transmission grid operators (TSO) was required. Therefore, the Third Energy Package was adopted in 2009, which in turn created the European Network of Transmission System Operators for Electricity (ENTSO-E) and the Agency for the Cooperation of Energy Regulators (ACER), as the successor organizations of the former European Transmission System Operators (ETSO). [ENTSO2014] [EP2019]

The ENTSO-E is clustered into five synchronous areas[3] that comprise the regional groups (RG) Continental Europe, Nordic, Baltic, Great Britain, and Ireland - Northern Ireland as well as the two isolated systems Cyprus and Iceland (non-RG). The main objective of the ENTSO-E is to ensure the security of supply and system reliability, integration of RES into the power system, and completion of the internal energy markets together with ACER. The ENTSO-E and ACER objectives are the drafting of network codes, technical cooperation between TSO, publication of summer and winter outlook reports for electricity generation, and coordination of research and development plans. Those objectives are central to meet the EU energy policy objectives of affordability, sustainability, and security of supply. Moreover, ENTSO-E is responsible for the development of the pan-European network plans, implemented by the Ten-Year Network Development Plan (TYNDP). [Ciu2020] [ENTSO2014]

The regional group Continental Europe, also referred to as Continental Europe Synchronous Area (CESA), represents the largest synchronous electrical grid in the world. In 2019, the ENTSO-E represents 42 electricity transmission system operators from 35 countries across Europe. 26 of those permanent members are EU members and 9 are non-EU members, whereas Malta is the only EU country not being member of the ENTSO-E and Turkey has the status of an observer member. [ENTSO2019a] In 2021, UK left the European Union within the framework of the EU-UK Trade and Cooperation

[3] Synchronous areas are groups of countries which are connected via their respective power systems. Individual synchronous areas are interconnected through direct current interconnectors. [ENTSO2014]

Agreement (TCA), which also embraces the withdrawal from ENTSO-E and ACER [EPRS2021]. Based on the Joint Operational Programme Romania-Ukraine-Republic of Moldova 2007-2013 Common borders (JOP RO-UA-MD 2007-2013), the synchronization of the Ukrainian (UA) and Moldovan (MD) power systems has been under long-term supervision and was initiated on technical level in 2017. In March 2022 an emergency synchronization with CESA was successfully completed and the stability of the Ukrainian-Moldovan power systems is supported by the Continental European TSO. [EC2015a] [ENTSO2022] As the proposed model region is meant to best represent a robust and independent European energy system within the European Energy Union [EC2015b] [EC2020a], this analysis focuses on the status quo of ENTSO-E 2019. Therefore, a complete list of ENTSO-E 2019 members and corresponding ISO country codes can be found in **Annex I**. The ENTSO-E model region is depicted in **Fig. 1**.

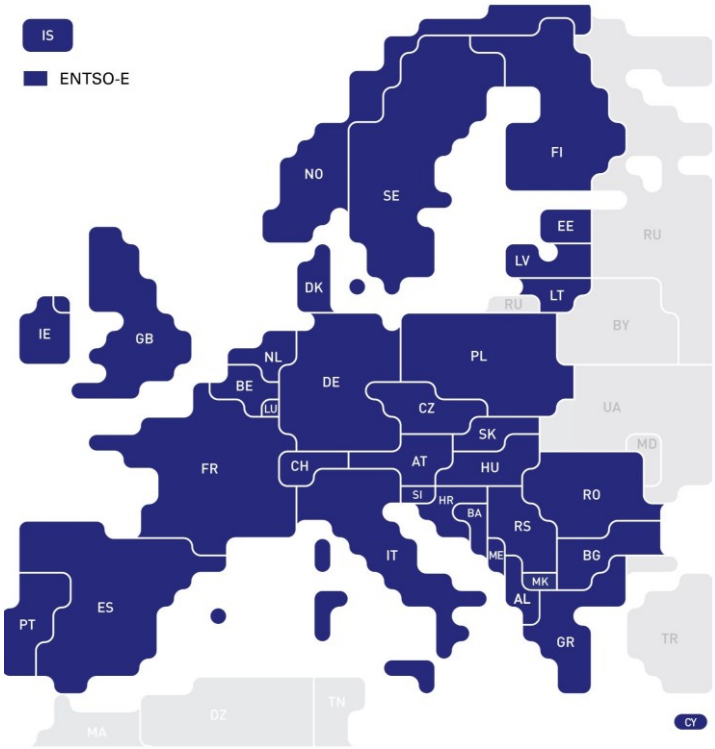

Fig. 1 Member countries ENTSO-E 2019
Source: In reference to [ENTSO2018a]

As depicted in **Annex I** and illustrated in **Fig. 1**, ENTSO-E 2019 comprises a total area[4] of 4,951,648 km^2, which accounts for 4 % of world total land area [WBG2019a] and more than 543 million inhabitants, who represent 7 % of total world population [WBG2019b]. The gross domestic product (GDP) is calculated as 19,835 billion US dollar, which accounts for 23 % of total world GDP [WBG2019c]. Total primary energy consumption amounts to 2,554,172 kiloton of oil equivalent (ktoe) or, equally, 29,705 terawatt-hours (TWh) per year, which represents 18 % of world primary energy consumption

[4] Land area refers to the total area of a country, excluding area under inland water bodies, national claims to continental shelf, and exclusive economic zones [WBG2019a].

[EUROS2018a] [IEA2019]. The total emissions accumulate to 3,505 Mt CO_{2eq} per year out of 38,017 Mt CO_{2eq} total world GHG emissions per year.[5] Hence, ENTSO-E accounts for 9% of world total GHG emissions [Crip2020a]. Together with the United States and China, ENTSO-E belongs to the largest economic and energy regions.

For the comprehensive understanding of the RES potentials and energy balances analysis, which comprises primary energy consumption (PEC), final energy consumption (FEC), imports, exports, and conversion and transformation, it becomes necessary to distinguish small-, mid-, and large-scale countries based on area size, population, and total GDP. As depicted in **Annex I**, the ENTSO-E countries exhibit heterogeneous characteristics. To provide a comprehensive classification regarding the absolute parameters, area size, population, and GDP per country are comparatively illustrated in **Annex II**. Therefore, countries such as France, Germany, UK, Spain, and Poland represent typical large-scale countries regarding all three parameters. Hungary, Ireland, Croatia, and Slovakia are typical mid-scale country representatives. Whereas small-scale countries are represented by Montenegro, North Macedonia, Estonia, and Cyprus. However, most countries exhibit diverse characteristics. Some small- and mid-scale area size countries such as Denmark, the Netherlands, and Belgium can be found in the top ranks of population and GDP. On the other hand, large-scale area countries such as Sweden, Norway, and Finland exhibit rather low population and moderate GDP. [WBG2019a] [WBG2019b] [WBG2019c] Therefore, the ENTSO-E model area comprises a heterogeneous composition of countries with diverse characteristics regarding size and economic activity. Hence, multifarious results for RES potentials, energy demands, efficiency gains, and correlated GHG emissions are anticipated on the country level.

According to those statistics and the technical nature of the ENTSO-E, the model region represents not only the 27 EU member states (EU-27), but also important European economies, such as UK, Norway, and Switzerland, which play a fundamental role for a holistic and sustainable European energy system. Therefore, the ENTSO-E is a representative and integral economic region, especially regarding its significant contribution of GDP and energy consumption. Third-party countries, such as Turkey[6], the Russian Federation, Ukraine, and Moldova, are not considered by this investigation. In 2019, those countries possess significant political and technical restrictions as well as insecurities towards the integration into the European energy system. However, the non-EU ENTSO-E countries represent an essential part of the European energy system analysis. To foster a uniform, holistic, and coherent analysis, the energy policies of the ENTSO-E member states are regarded as fully compliant with EU legislation and the European Energy Union towards 2050.

[5] The here presented GHG emissions are calculated based on direct and indirect emissions of the countries, excluding land use, land use change, and forestry (LULUCF).

[6] Turkey is not synchronously connected with continental Europe and regarded as observer member which does not yet possess the necessary robustness [ENTSO2015] [ENTSO2020].

2.2 Objectives of the European Energy Transition

The EU aims at the secure, sustainable, competitive, and affordable energy supply within the framework of the Energy Strategy and the Energy Union. The Energy Union is based on five dimensions, which comprise security and solidarity, internal energy market, energy efficiency, and climate action as well as research and innovation. [EC2015b] [EC2020a] In 2009, the Council of the European Union introduced a GHG abatement strategy for Europe and other developed economies that implies a CO_{2eq} emission reduction of 80–95 % until 2050 and compared to the base year 1990 [CEU2009a] [CEU2009b]. Therefore, GHG reduction targets until 2020 and 2030 for the EU emission trading scheme (ETS) and the non-emission trading scheme (non-ETS) sectors[7] have been defined [EC2013] [EPEC2018]. Until 2030 the EU ETS sector emissions shall be reduced by 43 % and the non-ETS sector emissions by 30 % compared to 2005. Those aims induce a GHG reduction of at least 40 %. However, the 2030 mid-term goals have recently undergone significant changes. [EPEC2018] In September 2020, the EC communicated an increase of the 2030 GHG reduction goals to at least 55 %. The new objective entails an ambitious increase and exceeds the previous one by 15 percentage points (p.p.) on the way to a climate neutral Europe in 2050. [EC2020a]

As a result of the Katowice Climate Change Conference (COP 24), uniform measuring and reporting standards on the emissions-cutting efforts of industrialized countries have been adopted [EP2018]. Within the framework of the Effort Sharing Decision, the GHG emission reduction targets are assessed and allocated individually for each member country. According to EU policy: "All sectors of the economy should contribute to achieving these greenhouse gas emission reductions, and all member states should participate in this effort, balancing considerations of fairness and solidarity." [EPEC2018] Due to the Effort Sharing Decision, not all EU countries contribute the same share of GHG reduction to the predefined targets. The efforts are rather distributed based on relative GDP per capita. [EPEC2018] [EUCO2014] The Paris Agreement 2015 requires each party to prepare, communicate, and maintain nationally determined contributions (NDC) that it intends to achieve. Those NDC represent the framework for national GHG emission reductions. [Delb2019] [UN2015]

According to the Clean Planet for All strategic long-term vision of the European Commission (2018), the EU commits to a climate neutral economy and defines pathways and key action areas to ecologically transform the economies [EC2018b]. Moreover, the Clean Energy for All Europeans Package of 2019 defines the legislative parameters to implement the Paris Agreement 2015 (COP 21) commitments [EC2019a]. In December 2019, the EC proclaimed the European Green Deal which comprises a catalogue of measures to become the first climate neutral continent by 2050 [EC2019b].

[7] The ETS is regarded as the key tool for cutting GHG emissions in the industry and aviation sector. However, the non-ETS sectors, i.e. the transport, agriculture, waste, and households, are not included. [Gruen2017]

2.3 Greenhouse Gas Emissions

Greenhouse Gases are natural components of Earth's atmosphere, which is composed of several layers of gases surrounding the planet and forming its planetary atmosphere. Among other functions, the atmosphere of Earth is absorbing ultraviolet solar radiation and warming the surface through heat retention, the so-called greenhouse effect. Nitrogen (*N*), oxygen (O_2), and argon (*Ar*) are the prevailing gases of the atmosphere. Beside those dominant gases, there are numerous trace gases, such as carbon dioxide (CO_2), carbon monoxide (*CO*), helium (*He*), hydrogen (H_2), methane (CH_4), neon (*Ne*), nitrous oxide (N_2O), and ozone (O_3). Among those trace gases, GHG are most prominently comprised by the radiatively active gases CO_2, CH_4, and N_2O. Those GHG represent the main drivers for the greenhouse effect. The greenhouse effect is described as a natural process by which radiation from the atmosphere warms earth's surface to a temperature above a degree that makes it habitable. This natural effect can be increased by anthropogenic GHG emissions. [Shur2019] [Tan2014] [UBA2020]

Anthropogenic activity, especially since the industrialization of the 19th century, comes along with additional emissions of radiatively active gases. Those anthropogenic emissions lead to higher concentrations of greenhouse gases and, in turn, amplify the greenhouse effect. Between 1750 and 2018, the concentration of CO_2 increased by 46 %, CH_4 by 150 %, and N_2O by 22 % compared to the pre-industrial era. To assess and compare the climate impact of various GHG, the global warming potential (GWP) of each GHG is referred to as carbon dioxide equivalent (CO_{2eq}). Over the course of the industrial era also completely new GHG gases, such as Chlorofluorocarbons (*CFC*) and Sulfur hexafluoride (SF_6), entered the atmosphere. [IPCC2019] [UBA2020] In order to distinguish among energy use and non-energy use GHG emissions, emissions are classified into direct and indirect emissions [EEA2021].

- Direct emissions: Energy and non-energy use related emissions
- Indirect emissions: Agriculture and waste management emissions

Energy use related direct emissions comprise all CO_{2eq} emissions that are related to direct combustion of fuels for the purpose of electricity, heat, and mechanical energy provision as well as fugitive emissions. Non-energy use direct emissions comprise all CO_{2eq} emissions that are related to industrial processes, such as GHG emitting processes in the chemical and raw materials industry. Indirect emissions are caused by non-energy use processes and refer to agriculture and waste management related emissions, which comprise waste and wastewater emissions. [Baum2018] [EEA2021]

ENTSO-E total GHG emissions accumulate to 4,591 Mt CO_{2eq} in the base year 1990 and 3,517 Mt CO_{2eq} in the GHG emissions reference year 2019. As depicted in **Fig. 2**, direct emissions consist of energy use processes and fugitive emissions that account for 77.8 %. Non-energy use processes account for 8.5 %. Indirect emissions consist of 10.4 % agriculture and 3.3 % waste management emissions. [Crip2020a] [EEA2021]

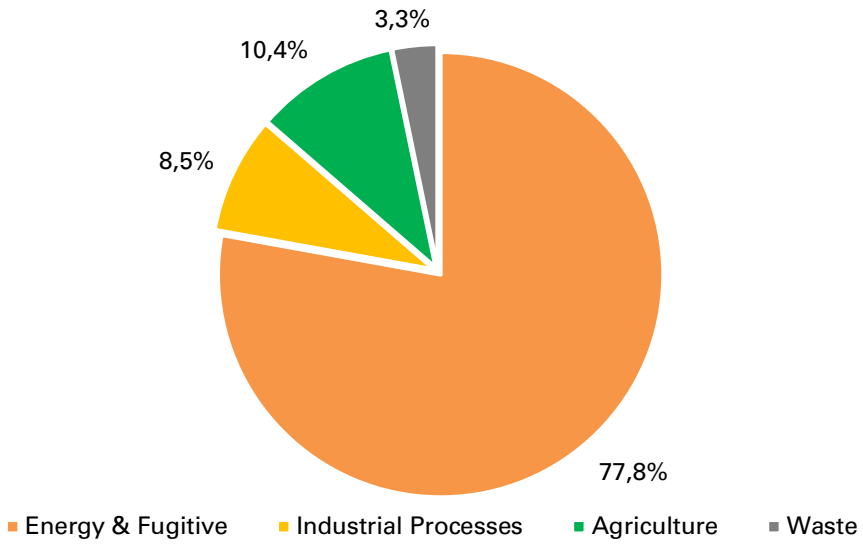

Fig. 2 Relation of process related GHG emissions EU 2019
Source: In reference to [EEA2021]

According to **Fig. 2**, direct and indirect GHG emissions are emitted by various processes in different energy sectors. The power industry contributes 28.9 %, the transport sector 26.8 %, the building sector 18.3 %, and the industry and commerce sector 16.8 % of total emissions, followed by others with 9.2 %, as indicated in **Fig. 3**. [Crip2020a]

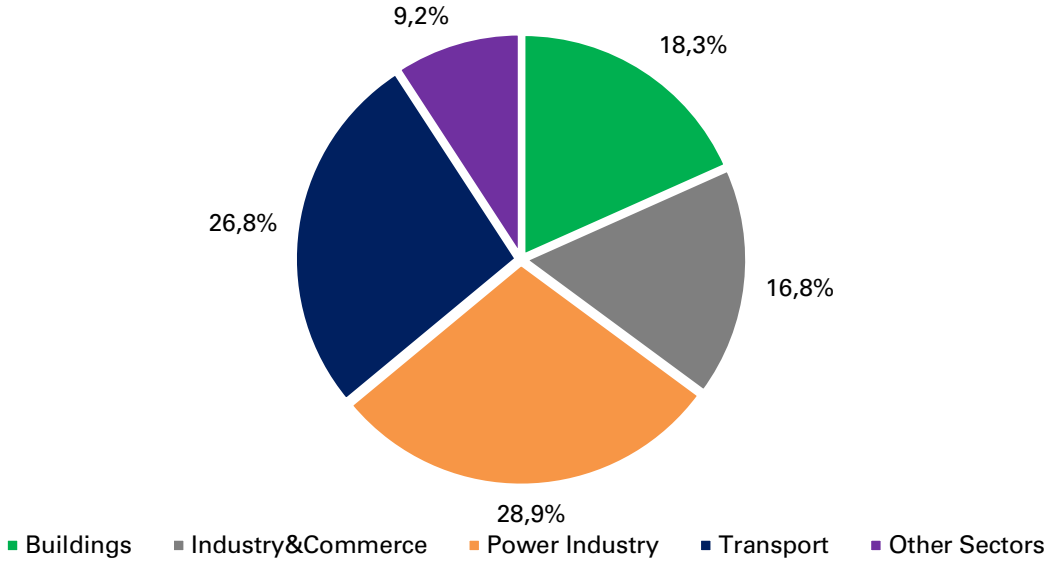

Fig. 3 Relation of sector related GHG emissions EU 2019
Source: In reference to [Crip2020a]

In reference to **Fig. 2** and **Fig. 3**, it is evident that combustion processes of fossil fuels in the sectors power industry, transport, buildings, and industry and commerce contribute the highest share of GHG emissions. Additional emissions can be found in agricultural, wastewater, and waste management processes. Moreover, fugitive emissions from leaks and other irregular releases contribute to indirect emissions. Emissions based on those processes are not directly related to fossil fuel combustion, as they are a result of biological and chemical processes. [Crip2020a] [EEA2021]

In reference to Crippa et al. (2020a) [Crip2020a] and the Fossil CO_2 Emissions of All World Countries Report [Crip2020b], the GHG emission repository analysis is based on the European Commission (EC) in-house Emissions Database for Global Atmospheric Research (EDGAR). The EDGAR database estimates country and sector-specific emissions of CO_2 as well as other GHG and air pollutants in reference to the latest available global statistics and state-of-the-art scientific knowledge of emission mechanisms for a wide range of anthropogenic activities.

The applied methodology is deemed to be fully transparent and in line with the most recent scientific literature. However, the EDGAR database includes uncertainties based on accuracy of the activity statistics, emission factors per type of fuel, separate reporting processes, and data gaps for specific sectors. The uncertainty bands are accurate within a bandwidth of ±0.5 % when based on robust statistical activity data for 1970–2015 and up to 2 % for the data of 2016–2019. The here presented GHG emissions are calculated in reference to direct and indirect emissions of the countries excluding land use, land use change, and forestry (LULUCF). Moreover, GHG emissions produced in third-party countries are not included. [Crip2020a] [Crip2020b] For the years 2010–2019 LULUCF is reported with a range of -300 Mt CO_{2eq} to -234 Mt CO_{2eq}. Hence, European LULUCF can be regarded as natural carbon sink, but with decreasing tendency. [EEA2021]

In reference to the EDGAR database, total GHG emissions in Mt CO_{2eq} per year are analyzed for each ENTSO-E country and the ENTSO-E entity. The data analysis refers to the relevant and available years 1990–2019. Due to regional coherency and better comparability of the disparate total emissions according to size and economic activity of countries, especially small- and mid-scale countries are aggregated to the regional groups Balkans, Baltics, Benelux, Scandinavia, and Others. Whereas large-scale countries such as Austria, Czechia, France, Germany, Italy, Poland, Portugal, Spain, and UK are treated as entities, here referred to as Nations. The defined geographic regional groups and corresponding countries are depicted in **Tab. 1**.

Tab. 1 Regional groups classification ENTSO-E

Region	Countries
Balkans	Albania, Bosnia and Herzegovina, Bulgaria, Croatia, Greece, Romania, Serbia and Montenegro, Slovenia
Baltics	Estonia, Latvia, Lithuania
Benelux	Belgium, Luxembourg, Netherlands
Scandinavia	Denmark, Finland, Iceland, Norway, Sweden
Others	Cyprus, Hungary, Ireland, Malta, Slovakia, Switzerland and Liechtenstein
Nations	Austria, Czechia, France, Germany, Italy, Poland, Portugal, Spain, United Kingdom

The regional classification fosters better understanding of regional variations of GHG emissions and differentiation among low- and large-scale emitting countries. Besides the prevailing primary energy commodities, GHG emissions are directly connected to population, economic activity, and weather conditions [IPCC2019] [UBA2020]. To comprehend the current state of mitigating climate change and to classify future GHG reduction goals, the past development and status quo of GHG emission repositories are investigated. Total emissions per region and country according to the EDGAR database are depicted in **Annex XXXIII** [Crip2020a]. **Fig. 4** illustrates total GHG emissions in Mt CO_{2eq} and GDP in billion USD from the base year 1990 to 2019 per region.

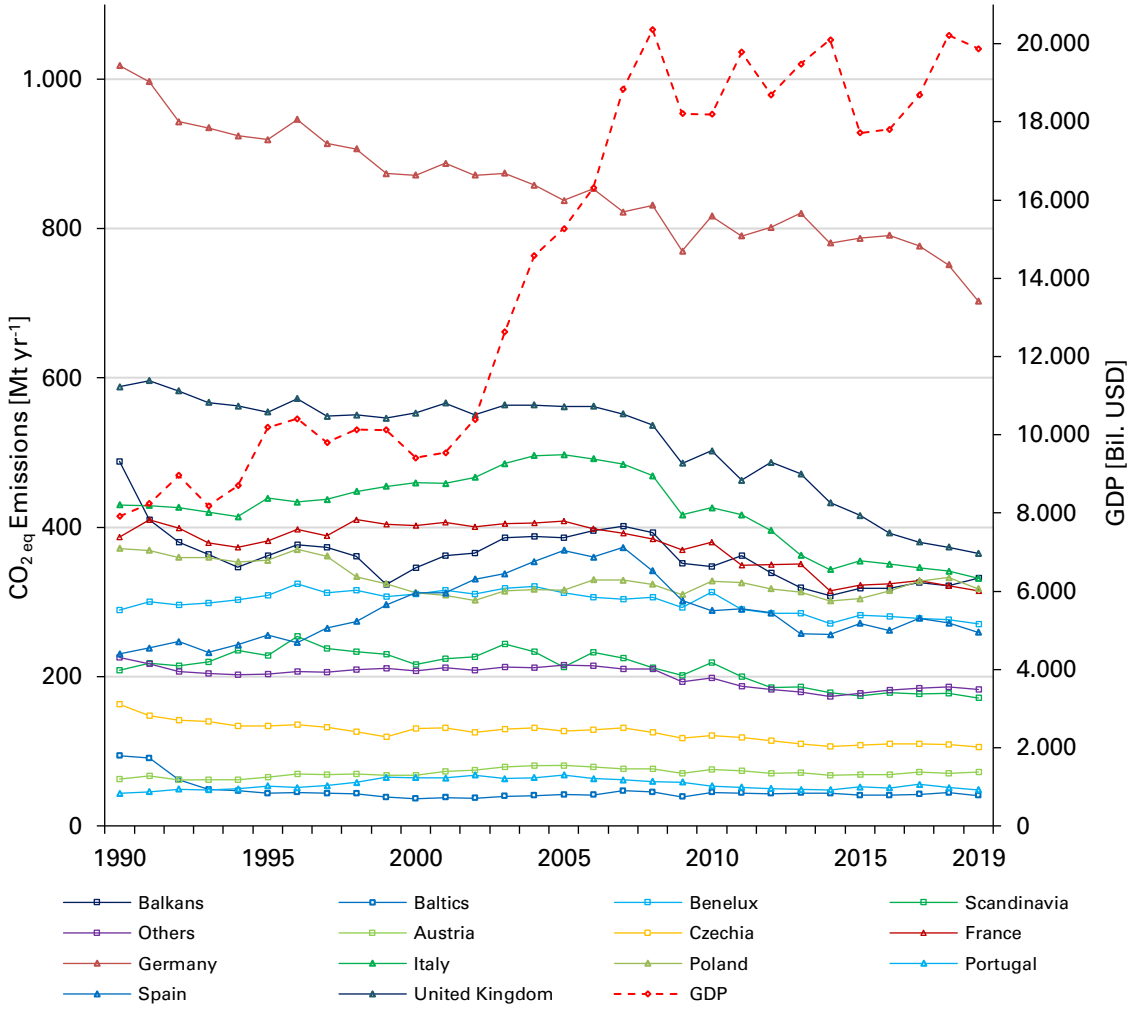

Fig. 4 GHG emissions per region and total GDP 1990–2019
Source: In reference to [Crip2020a] [WBG2019c]

According to **Fig. 4**, several countries and regions significantly decreased GHG emissions in the early 1990s. Among them, the Balkans, the Baltics, Czechia, (East) Germany, and Poland. Those regions belonged to the former Union of Soviet Socialist Republics (USSR) and faced a rapid deindustrialization after the Soviet Union collapsed in 1990 and so did the industrial emissions during the early 1990s. For Germany, this observation can be related to the former German Democratic Republic (GDR).

The subsequent period is coined with prosperity and economic growth that comes along with a trend to increasing GHG emissions. Especially, the period from 2000 to 2008 exhibits an immense GDP growth, whereas total GDP almost doubled. During this period most countries, such as the Balkans, the Baltics, Poland, Spain, Italy, and UK, show increasing GHG emissions. However, the large-scale countries France and Germany exhibit stagnating or even decreasing tendencies in face of economic growth. Here, particular effects, such as the early adoption of energy transition measures in Germany and the large nuclear power plant fleet of France, are deemed to significantly decrease relative GHG emissions. Moreover, the remaining countries possess comparatively larger GDP growth and, therefore, a relative GHG emissions increase.

The Global Financial Crisis of 2008 induced a remarkably sharp decline in the emissions of all regions due to inhibited economic activity across the globe. During the subsequent decade, GDP does not show significant increases but rather stagnates around 19 trillion USD. Simultaneously, GHG emissions are gradually reduced in most regions. Hence, most countries show a tendency to decreasing emissions mostly due to technological efficiency gains and increasing deployment of RES. Another reason is presumed in the continuous deindustrialization of post-industrial societies, which entails the externalization of CO_2 intensive production processes into third-party countries [Bell1999]. However, especially Poland exhibits increasing emissions during the last GPD growth period from 2015 to 2019. Hence, disproportionate economic growth paired with an above-average GHG emitting power plant fleet are suspected.

Analogous to the Global Financial Crisis, the COVID-19 pandemic caused a significant decrease of GHG emissions in 2020. Due to extraordinary impacts of the pandemic, the years 2020 and 2021 are not regarded by this analysis. However, the trend of decreasing emissions across the ENTSO-E continues and almost all countries show a decoupling of GHG emissions from GDP growth, at least to a certain extent and in the face of stagnating economic growth. In a wider sense, the last decade could be described as a steady state period[8]. From 1990 to 2019, increasing shares of RES and energy efficient technologies have reduced GHG emissions by 21 %, which accounts for an average GHG emission decrease of 0.89 % per year. Simultaneously, GDP increased by 151 %, which accounts for an average GDP increase of 3.54 % per year (compare **Fig. 4**).

For a regional comparison of total GHG emissions, CO_{2eq} emissions are aggregated into absolute emission classes. Those classes are displayed in heat maps per country and across the ENTSO-E. The heat maps indicate the absolute GHG emission classes in different colors, whereas pink represents high, purple and blueish colors average, and turquoise low emitting countries. Total GHG emissions in Mt CO_{2eq} per emission class and country are depicted in the heat map of **Fig. 5**.

[8] A steady-state economy is an economy made up of a constant stock of physical wealth and capital as well as a constant population size. In effect, it does not grow in the course of time. [Daly1974] [Kers2009]

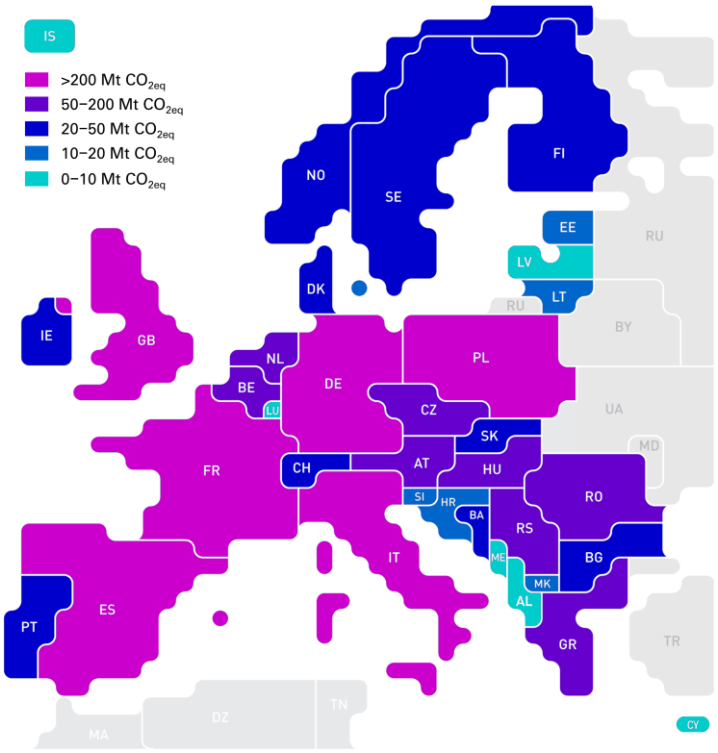

Fig. 5 GHG emissions heat map ENTSO-E 2019
Source: In reference to [Crip2020a]

As depicted in **Fig. 5**, the large-scale central European countries Germany (703 Mt CO_{2eq}), UK (365 Mt CO_{2eq}), Italy (332 Mt CO_{2eq}), Poland (318 Mt CO_{2eq}), France (315 Mt CO_{2eq}), and Spain (259 Mt CO_{2eq}) exhibit the largest amounts of GHG emissions, with each more than 200 Mt CO_{2eq}. Remarkably, Germany emits more than the second largest emitting countries UK and Italy together. France, as the second largest country by GDP and population size (compare **Annex I** and **Annex II**), occupies only the fifth rank, mostly due to the large share of nuclear power generation in the power sector. Poland, as the smallest of those economies, occupies the fourth rank presumably due to the large share of coal-based electricity production. In total, those six large-scale emitting countries account for two-thirds (2,392 Mt CO_{2eq}) of the ENTSO-E total emissions. Low emitting countries are prevailingly identified in the Balkans and the Baltics. The Benelux (except Luxembourg), Scandinavia, the south-eastern European countries, Switzerland, Portugal, and Ireland possess average GHG emissions.

The quantitative GHG emission development for the relevant years 1990–2019 is based on the analysis according to Crippa et al. (2020a) [Crip2020a]. As presented in **Chapter 2.2**, the future GHG reduction scenarios Business-as-Usual, 55 % Reduction (2030), 65 % Reduction (2030), 80 % Reduction (2050), and 95 % Reduction (2050) are anticipated based on the EU GHG reduction goals until 2050. To compare previous emission development trends and the implications of future GHG abatement measures in the ENTSO-E, total GHG emissions from 1990–2019 and the future scenarios for 2030 and 2050 in Mt CO_{2eq} per year are depicted in **Fig. 6**.

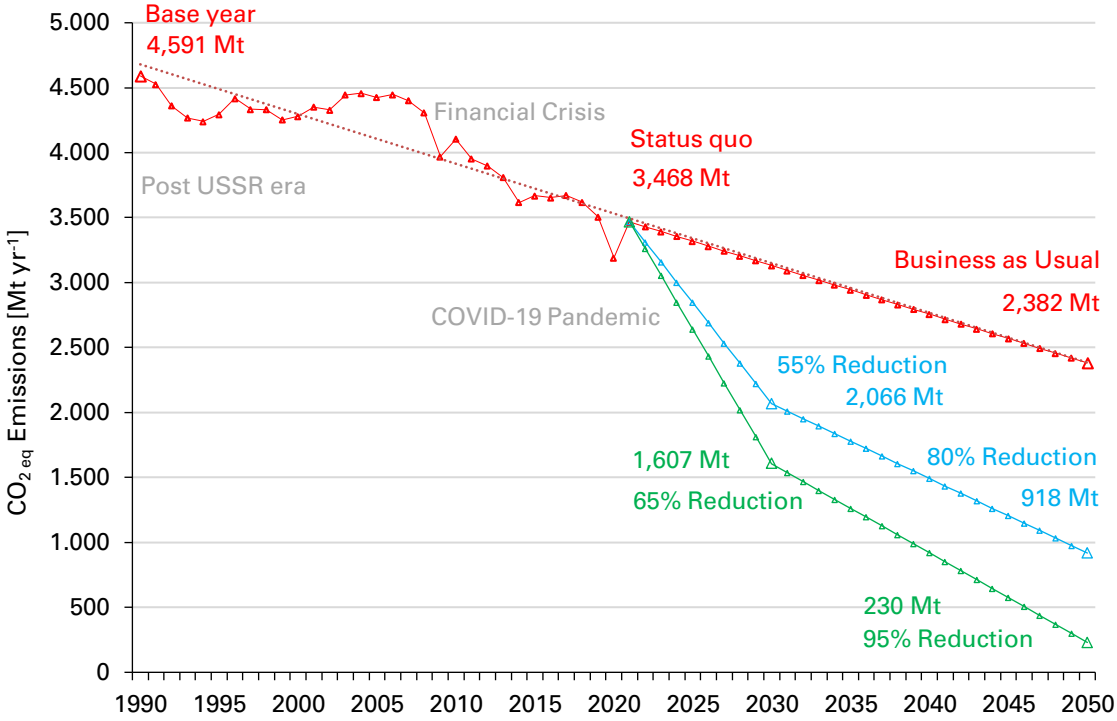

Fig. 6 GHG reduction 1990–2019 and scenarios 2020–2050 ENTSO-E
Source: In reference to [Crip2020a] [EC2018b] [EC2020a]

As depicted in **Fig. 6**, the 1990–2019 quantitative GHG emission development for the ENTSO-E is correlated with the impacts of the aforementioned historic events. Due to the latest economic crisis caused by the COVID-19 pandemic of 2020, the GHG emission curve entails a significant decline for 2020. According to Liu et al. (2020), the total decline of global CO_2 emissions is estimated as 9% due to inhibited economic activity and reduced transport emissions [Liu2020]. In reference to the European Statistical Office (Eurostat) (2021), European emissions 2020 decreased by 10% compared to the previous year. [Euros2021a] Therefore, the 2020 GHG emissions are calculated in reference to a decrease of 10% compared to 2019 and adjusted for 2021, with the average decrease of 1990–2019 based on the pre-pandemic values of 2019.

The mid-term GHG reduction goals of 2030 are based on the latest policy initiative of the EC regarding the increase of the previous goals of 40% to at least 55% for 2030 accounted for in the 55% reduction scenario [EC2020a]. To account for the more ambitious 2050 scenario of 95% reduction, the 2030 mid-term goal was increased to 65% in the 65% reduction scenario. The linear curve progression of the scenarios 2020–2050 is due to the yearly linear decrease of emissions according to the scenarios. Real world emission curves will not show a linear progression, but rather fluctuating progression due to dynamic real-world processes and changing parameters over time.

2.4 Energy Balances Analysis

Energy balances represent the statistical accounting of energy commodities and their flow in the economy. Energy balances give a comprehensive overview of the total amount of energy extracted from the environment, imported, exported, transformed, and consumed by end-users. They also inform about the relative contribution of each energy commodity, such as fuels and energy products. Energy balances allow for studying the overall domestic energy markets and monitoring impacts of energy policies. Moreover, they offer a complete and holistic view on the energy composition in a compact format, such as on energy consumption of the whole economy and of individual sectors. Hence, energy balances are regarded as key instrument to provide data in a suitable form to understand and analyze the implication of energy in the economy. Moreover, energy balances provide the major input for impact assessments in the field of energy policies and underpin the European Energy Strategy. [EUROS2018b]

The investigation of the European energy balances is based on the European Statistical Office (Eurostat) Energy Balance Sheets 2016 DATA (2018 Edition) publication [EUROS2018a] and the Energy Balances in the MS Excel File Format (2018 Edition), referred to as May 2018 Edition [EUROS2018b]. The energy balance sheets entail comprehensive energy balance matrices. Each matrix is arranged in columns and rows that are referenced by a specific code. The columns contain various categories of energy products, also referred to as energy commodities. Those categories embrace energy products, such as solid fuels, oils, gases, renewables, wastes, nuclear heat, derived heat, and electricity. Whereas each category consists of a wide range of energy commodities. The energy categories and the corresponding products and fuels are depicted in **Tab. 2**.

Tab. 2 Fuels and energy product categories of Eurostat energy balances
Source: In reference to [EUROS2018b]

Category	Energy Products and Fuels
Solid fuels	Anthracite, coking coal, other bituminous coal, sub-bituminous coal, lignite, patent fuels, coke oven coke, gas coke, coal tar, BKB, peat, peat products, oil shale and oil sands
Oils	Crude oil, natural gas liquids, refinery feedstocks, oxygenates, other hydrocarbons, refinery gas ethane, LPG, motor gasoline, aviation gasoline, gasoline type jet fuel, kerosene type jet fuel, other kerosene, naphtha, gas/diesel oil, fuel oil, white spirit and SBP, lubricants, bitumen, petroleum coke, paraffin coke, paraffin waxes, others
Gases	Natural gas, coke oven gas, blast furnace gas, gasworks gas, other recovered gas
Renewables	Hydro power, wind power, tide, wave and ocean, solar thermal, solar PV, solid biomass, charcoal, biogas, renewable municipal wastes, bio gasoline, biodiesel, bio jet kerosene, other liquid biofuels, geothermal
Wastes	Industrial wastes, municipal wastes
Heat	Nuclear heat, derived heat
Electricity	–

The Eurostat energy balances present all statistically significant energy commodities and their production, transformation, and consumption by different type and per economic sector industry, transport, households, trade and commerce, agriculture, and fishery as well as non-specified. Moreover, energy balances do not only cover the EU-27 countries, but also data for Norway, UK, and the non-EU Balkan countries. Switzerland is the only European country not covered by the Eurostat statistics. Hence, the Swiss energy balance must be anticipated in compliance with the Eurostat methodology.

Within each energy balance matrix, the energy products and fuels columns of **Tab. 2** are vertically arranged in rows (blocks). Those blocks indicate the energy flows from primary energy consumption (top block), over energy conversion and transformation as well as distribution losses (center block), to final energy and non-energy consumption (bottom block). This concept quantitatively accounts for all energy commodities entering, exiting, and being used within the national territory of a given country during a reference period of an entire year. The vertical blocks and the corresponding energy flows are depicted in **Tab. 3**. [EUROS2018a] [EUROS2018b]

Tab. 3 Energy flows and categories of Eurostat energy balances
Source: In reference to [EUROS2018b]

Category	Energy Flow
Energy supply (gross inland consumption)	Primary production, Recovered and recycled products, imports, stock changes, exports, bunkers, direct use
Energy transformation and distribution losses (conversion)	Conventional thermal power stations, nuclear power stations, coke ovens, blast furnaces, gas works, refineries & petrochemical industry, district heating plants, patent fuel plants, BKB & PB plants, coal liquefaction plants, for blended natural gas, liquid biofuels blended, charcoal production plants, gas-to-liquids plants, not specified transformation, distribution losses
Final energy and non-energy consumption (available final consumption)	**Industry sector** (iron & steel, chemical & petrochemical, non-ferrous metals, non-metallic minerals, transport equipment, machinery, mining & quarrying, food, beverages & tobacco, paper, pulp & printing, wood & wood products, construction, textile & leather, not elsewhere specified), **transport sector** (rail, road, domestic aviation, domestic navigation, pipeline transport, not specified transport), **other sectors** (commercial & public services, households, agriculture & forestry, fishing, not specified other), **final non-energy consumption**

The energy balance matrix with its categories, fuels, products, and flows are complying with the International Recommendations for Energy Statistics (IRES) and the respective coding [UN2018], as depicted in **Annex CD**. In early 2019, the dataset is available for each calendar year from 1990–2016. The original energy balances are expressed in the metric energy unit thousands of tons of oil equivalent (ktoe). The methodology is based on the physical energy content method. The general principle of this method is that primary energy is regarded as the first energy form in the production process, which is subsequently used for various energy purposes. [EUROS2018a] [EUROS2018b]

For directly combustible energy commodities, such as coal, crude oil, natural gas, biomass, and waste, primary energy is regarded as the inherent energy content. For commodities that are not directly combustible, the application of this principle leads to the attribution of heat as the primary energy form for nuclear, geothermal, and solar thermal power plants and to the attribution of electricity as the primary energy form for PV, wind, hydro as well as tide, wave, and ocean power plants. [EUROS2018a]

To properly assess the Eurostat energy balances data base, it is important to comply with the Eurostat methods regarding data computation. To calculate gross inland consumption, the energy outputs exports and bunkers are subtracted from total primary energy consumption. Hence, gross inland consumption comprises the cumulated primary production, other sources, net imports, recycled products, and stock exchanges, as indicated in **Eq. (2.1)**. [EUROS2018a] [EUROS2019f]

$$\begin{aligned} gross\_inland\_consumption \\ &= primary\_production + other\_sources + imports \\ &+ recycled\_products + stock\_changes - exports \\ &- bunkers \end{aligned} \tag{2.1}$$

Based on the calculation of gross inland consumption of **Eq. (2.1)**, available final consumption is calculated by subtraction of transformation input, consumption of the energy branch, and distribution losses from the sum of gross inland consumption, transformation output, and exchanges, as indicated in **Eq. (2.2)**. [EUROS2018a]

$$\begin{aligned} available\_final\_consumption \\ &= gross\_inland\_consumption \\ &- transformation\_input + transformation\_output \\ &+ exchanges\_transfers\_returns \\ &- energy\_branch\_consumption - distribution\_losses \end{aligned} \tag{2.2}$$

For some derived products, such as electricity, the value of gross inland consumption represents only the amount of net trade. For other derived products, such as petroleum products, the value of gross inland consumption represents the amount of net trade, stock changes, and consumption in the international marine bunkers. [EUROS2018a]

Statistical difference is a measure of the quality of data. In this data set it reflects the statistical balance between supply and consumption of energy. A zero value might be a result of the methodological approach. Zero values attribute for non-surveyed elements of energy, such as not elsewhere specified, stock changes, and distribution losses. The statistical difference is calculated according to **Eq. (2.3)**. [EUROS2018a]

$$\begin{aligned} statistical\_difference \\ &= available\_final\_consumption \\ &- final\_non\_energy\_consumption \\ &- final\_energy\_consumption \end{aligned} \tag{2.3}$$

In some cases, low values of statistical difference might indicate data of higher quality than a dataset with a statistical difference equal to zero. The value of gross inland consumption in the original data set can also be negative. Negative values for energy products available for final consumption indicate inaccuracies in statistical data collections or reporting. [EUROS2018a] **Equations (2.1)–(2.3)** and the data peculiarities are accounted for in the data analysis and evaluation, as depicted in the digital attachment **Annex CD**. For computational ease, negative values are set zero.

The Eurostat statistical data collection is based on joint annual questionnaires. Therefore, the data collection system has shown some weaknesses based on non-availability, confidentiality, negligibility, and real zero data. Those cases are shown as zero values in the questionnaire and as blank cells in the data tables. [EUROS2018a] The methodological failure of the data gathering cannot be accounted for in this evaluation and must be regarded as a statistically induced data deviation.

Based on the data availability of 2018, ENTSO-E energy balances are analyzed and displayed for the reference year 2016. In case of newly published energy balances, those balances are not regarded by this research due to the exceptional high time requirement regarding the drawing of the corresponding energy flow diagrams (Sankey diagrams). For better comprehensibility and uniformity with this analysis and to account for future energy systems based on high shares of RES-based electricity conversion, the original energy unit tons of oil equivalent (ktoe) is converted into terawatt-hours (TWh), according to the conversion factor $f_{ktoe\_TWh}=0.01163$ [EUROS2019b].

To date, Switzerland is the only ENTSO-E country not regarded by the Eurostat data set. To account for the Swiss energy balances in correspondence to the Eurostat (2018 Edition) methodology, an approximating method is chosen. Austria is the direct neighbor of Switzerland and possesses similar features regarding the alpine geographic location, inhabitants, and economic status. With only little deviation of 760 ktoe, primary energy consumption of Austria 1990 (25,033 ktoe) equals the primary energy consumption of Switzerland 2016 (24,273 ktoe) [EUROS2019a].

To account for this particular deviation, the Austria 1990 data is adjusted by the factor $f_{swiss}=0.97$ to represent the Swiss energy balances. The major difference between both countries is the utilization of nuclear energy. Switzerland belongs to the forerunners of nuclear energy utilization, whereas Austria does not use nuclear energy sources. The electricity generation based on nuclear energy is accounted for according to swissnuclear (2016) [SN2016]. The Swiss RES-based electricity generation is calculated based on data of the International Energy Agency (2018) [IEA2018].

Data extraction, aggregation, and sorting of the MS Excel file format energy balances for each of the 35 ENTSO-E countries is conducted via tailor-made input, output, and conversion forms, which allow for a precise data analysis according to **Annex CD**. The total ENTSO-E entity sheet is gathered via accumulation of the country data sheets.

In reference to **Tab. 3**, the data are aggregated and codified for the categories primary energy, energy commodities, energy conversion, sector consumption, and energy flows. A major weakness of the Eurostat data set is to correctly address for RES shares in the electricity and heat sector. Both sectors are supplied by combined heat and power (CHP) plants that can also be fueled with RES, such as biomass and biogas. The deviation of direct RES-based electricity production represented by wind and PV power plants and the indirect RES-based electricity production represented by biomass and biogas CHP plants is adjusted for the total RES share of each country based on the Eurostat (2017) Short Assessment of Renewable Energy Sources (SHARES) data [EUROS2017]. The missing RES CHP output for electricity and heat is calculated based on the SHARES data and adjusted for the actual RES input. As a simplification, the original classification of the economic sectors industry, agriculture, fishery, and non-specified is aggregated and those sectors are combined to the sector industry.

To picture the results of the comprehensive and in-depth analysis of the Eurostat energy balances, the energy flows for each ENTSO-E country are depicted as energy flow diagrams in the Sankey methodology. Those Sankey diagrams serve as a graphic illustration of energy and commodity flows, whereby those flows can be combined, split, and traced through a series of stages. These stages comprise the conversion, transformation, transport, consumption, and losses of energy and commodities. The width of each stream represents the quantitative amount of commodities or energy within the flow. Sankey diagrams are typically used to visualize energy transfers between processes. Thus, they are suitable for visually representing complex energy balances. [EUROS2018a] The original energy commodities and transformation processes of the Eurostat energy balances are described in **Tab. 2** and **Tab. 3**. To better represent and distinguish particular energy flows, the energy products and fuels of **Tab. 2** are aggregated into the following categories.

- RES electricity
- Electricity import
- Other sources (non-energy products, wastes, and others)
- Mineral oils
- Natural gas
- Biofuels
- RES heat

The energy flow diagram of the ENTSO-E 2016 in **Fig. 7** serves as a template to elaborate the chosen methodology and to illustrate the representation method of Sankey diagrams. The full series of the 35 ENTSO-E countries and the ENTSO-E entity Sankey diagrams of 2016 are depicted as landscape format in **Fig. 1–36** of the **Compendium**.

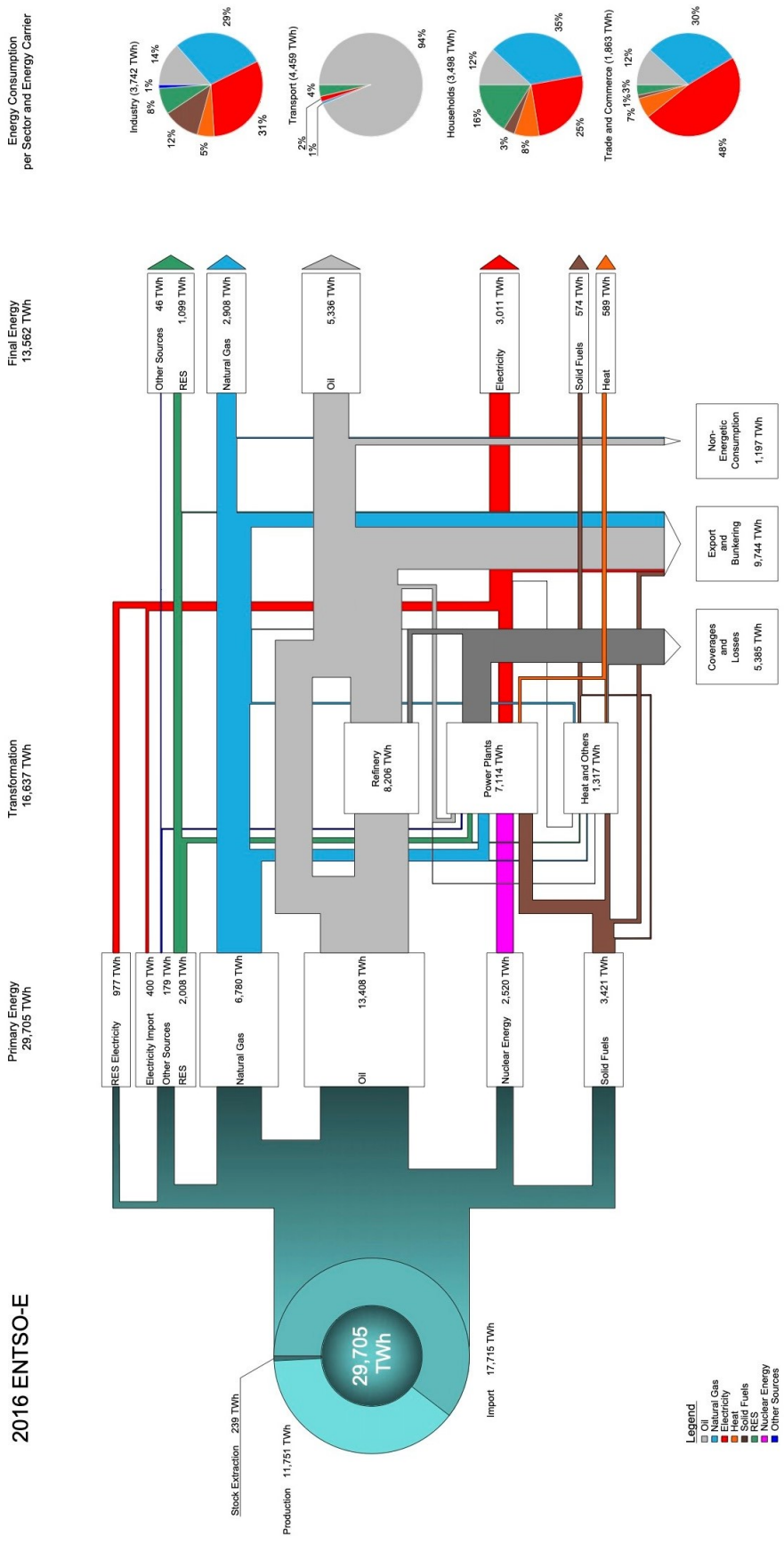

Fig. 7 Sankey energy flow diagram ENTSO-E 2016
Source: In reference to [EUROS2018b]

According to the methodology of Eurostat (2018a) and (2018b), Sankey diagrams are based on a series of nodes connected by energy flows. The energy flows represent input and output of energy commodities and the black nodes events or processes, such as imports, transformation, and final energy consumption (FEC). Energy commodities from production, imports, and stock extraction enter the energy balances on the left-hand site (primary energy) and exit on the right-hand site as exports, losses, non-energetic consumption, and final energy consumption. The center part of the diagram indicates those energy commodities that are used in their original form and those which go through conversion and transformation processes (transformation).

In accordance with the Sankey methodology, commodities are either directly supplied for final energy consumption or converted via transformation processes. Natural gas used for heating purpose in the household sector is an example of a commodity being used in its original form and, thus, directly carried over. Whereas natural gas that is transformed into electricity in thermal power plants represents an energy commodity that goes through a transformation process. The presented analysis of the ENTSO-E Sankey diagram and its respective energy flows is representative for all 35 ENTSO-E countries. However, primary energy consumption, transformation, final energy consumption, and the dominant energy commodities vary from country to country due to diverse historic, geographic, and environmental circumstances, as comprehensively depicted in the Sankey diagrams for each country in **Fig. 1–36** of the **Compendium**. The Sankey diagrams have been manually drawn as vector graphics in the Autodesk AutoCAD ARX version 23.0 software 2019.

In reference to **Fig. 7**, primary energy consumption represents the total available energy before energy conversion, transformation, export, and bunkering. It is anticipated that future energy systems are dominated by RES-based primary energy production, foremost electricity producers such as wind and PV power plants. Hence, the Sankey representation of wind- and solar-based RES converters refers to net primary energy. All energy related processes are represented by the SI system unit Watt (W), to account for future electricity dominated energy systems and to facilitate comprehension.

Primary energy consumption accounts for 29,705 TWh. Out of those, 11,751 TWh (39.6 %) refer to domestic primary energy production and 17,715 TWh (60.4 %) are imported within or across the ENTSO-E borders. Stock extraction accounts for a minor amount of 239 TWh (<1 %). 16,637 TWh (56.0 %) of those energy commodities are transformed in refineries, power plants, district heating plants, and others. 13,068 TWh (44.0 %) are carried over for direct use purpose. Energy branch consumption, coverages, and distribution losses account for 5,385 TWh (18.1 %). 9,744 TWh (32.8 %) are exported or bunkered and 1,197 TWh (4.0 %) are utilized for non-energy consumption, such as industrial processes. Final energy consumption accounts for 13,562 TWh (45.7 %).

Hence, the primary to final energy consumption conversion efficiency accounts for 81.9 %. However, this efficiency does not represent the overall efficiency, as various energy processes in the final energy consumption sector come along with additional energy losses due to downstream energy conversion and related energy losses. For instance, those downstream processes can be found in the utilization of final energy commodities for industrial processes, internal combustion engines of vehicles, and heating devices. The detailed utilization of final energy commodities per economic sector is displayed on the right-hand side of the Sankey diagrams. The quantitative and relative energy consumption of the sectors industry, transport, households, and trade and commerce are depicted by the final energy consumption charts in **Fig. 8**.

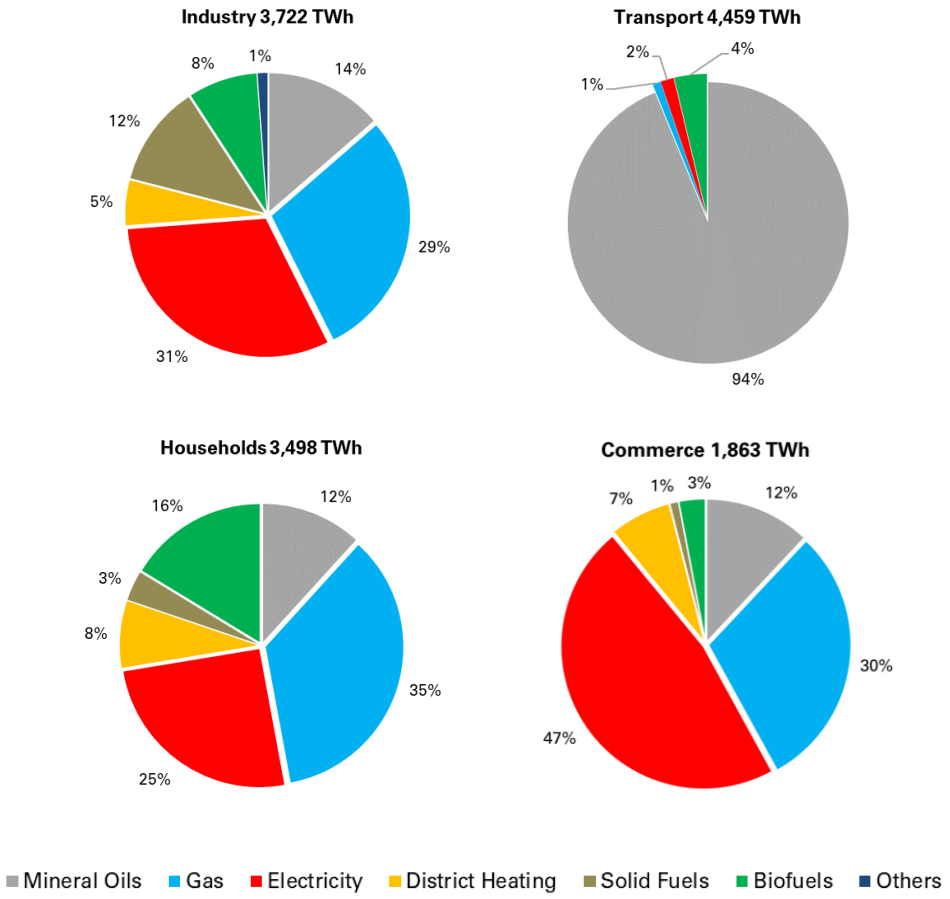

Fig. 8 Final energy consumption per sector ENTSO-E 2016
Source: In reference to [EUROS2018b]

As indicated in **Fig. 7** and **Fig. 8**, the economic sectors industry 3,722 TWh (27.4 %), transport 4,459 TWh (32.9 %), household 3,498 TWh (25.8 %), and trade and commerce 1,863 TWh (13.7 %) account for the total final energy consumption of 13,562 TWh. The sectors industry, households, and trade and commerce are dominated by a heterogeneous composition of the energy commodities mineral oils, gas, electricity, district heating, solid fuels, biofuels, and other sources. On the contrary, the transport sector relies predominantly on mineral oils (93.8 %).

In reference to **Eq. (2.1)**, the ENTSO-E gross inland consumption accounts for 19,961 TWh. Out of those primary energy commodities, 9,991 TWh (50.1 %) are produced and consumed domestically within the ENTSO-E and 9,970 TWh (49.9 %) account for net imports. Those net energy imports from third-party countries are denoted as energy dependency rate [EUROS2020].[9] Hence, the ENTSO-E 2016 total energy dependency rate accounts for 49.9 % of gross inland consumption. Among the prevailing conventional fuels, the net energy imports and corresponding dependency rates per commodity account for 5,488 TWh mineral oil (79.4 %), 2,939 TWh natural gas (64.6 %), and 1,143 TWh solid fuels (38.2 %). [EUROS2018b] To assign energy import dependencies of the EU-28 to particular energy commodity exporting countries, the origin and corresponding ratios of the predominant commodities are depicted in **Tab. 4**.

Tab. 4 Origin and ratios of EU-28 fossil fuel imports 2019
Source: In reference to [EUROS2022a]

Natural / Liquified Gas		Crude Oil		Hard Coal		Uranium	
	[%]		[%]		[%]		[%]
Russia	34.4	Russia	26.8	Russia	43.5	Russia	19.8
Norway	13.2	Iraq	8.9	U.S.	16.8	Kazakhstan	19.6
Qatar	12.6	Nigeria	7.8	Australia	13.1	Niger	15.3
Algeria	8.3	Saudi Arabia	7.7	Colombia	7.7	Australia	14.4
Nigeria	5.4	Kazakhstan	7.3	South Africa	2.7	Canada	11.6
U.S.	4.8	Norway	6.9	Canada	2.2	Namibia	9.6
U.K.	2.1	U.S.	5.2	Kazakhstan	2.1	Uzbekistan	4.8
Trinidad/Tobago	1.9	U.K.	4.9	Mozambique	1.5	South Africa	0.9
Others	17.3	Others	24.5	Others	10.5	Others	4.0

As depicted in **Tab. 4**, the prevailing fossil fuels in the EU-28 are imported from various countries. Remarkably, all major energy commodities are imported from the Russian Federation, foremost hard coal (43.5 %), natural gas (34.4 %), crude oil (26.8 %), and uranium (19.8 %). Therefore, a significant energy dependency for all energy commodities from Russia is identified. Comparatively large import shares from other countries (others) represent a diverse import portfolio, whereas small import shares from other countries denote particular strong dependencies on a limited number of countries. Hence, the large share of other suppliers for crude oil (24.5 %) and natural gas (17.3 %) implies a rather diverse origin of supply, whereas the low contribution of others for hard coal (10.5 %) and uranium (4.0 %) implicates particular strong dependencies on the major suppliers. In reference to the model region ENTSO-E, those dependencies are likely to be underestimated, as imports from Norway and UK must be internalized and, thus, energy dependencies from third-party countries are increased.

[9] The energy dependency rate denotes the proportion of energy that an economy must import. It is defined as net energy imports divided by gross inland consumption and expressed as a percentage. Negative dependency rates indicate net exporter and positive rates net importer. If the energy dependency rate is greater 100 %, corresponding energy commodities are stocked and bunkered. [EUROS2020] [EUROS2022b]

Quantitative and relative import dependencies of the aforementioned fossil fuel commodities and electricity per country are depicted in **Annex IV**. Total net energy import quantities and dependency rates per country are depicted in **Annex III**. As illustrated in **Fig. 9**, net energy imports are denoted by bluish columns on the upper side of the diagram. Whereas net energy exports (negative imports) are denoted by the greenish antipode columns. The percentage indication depicts the dependency ratio of net imports or exports from gross inland consumption.

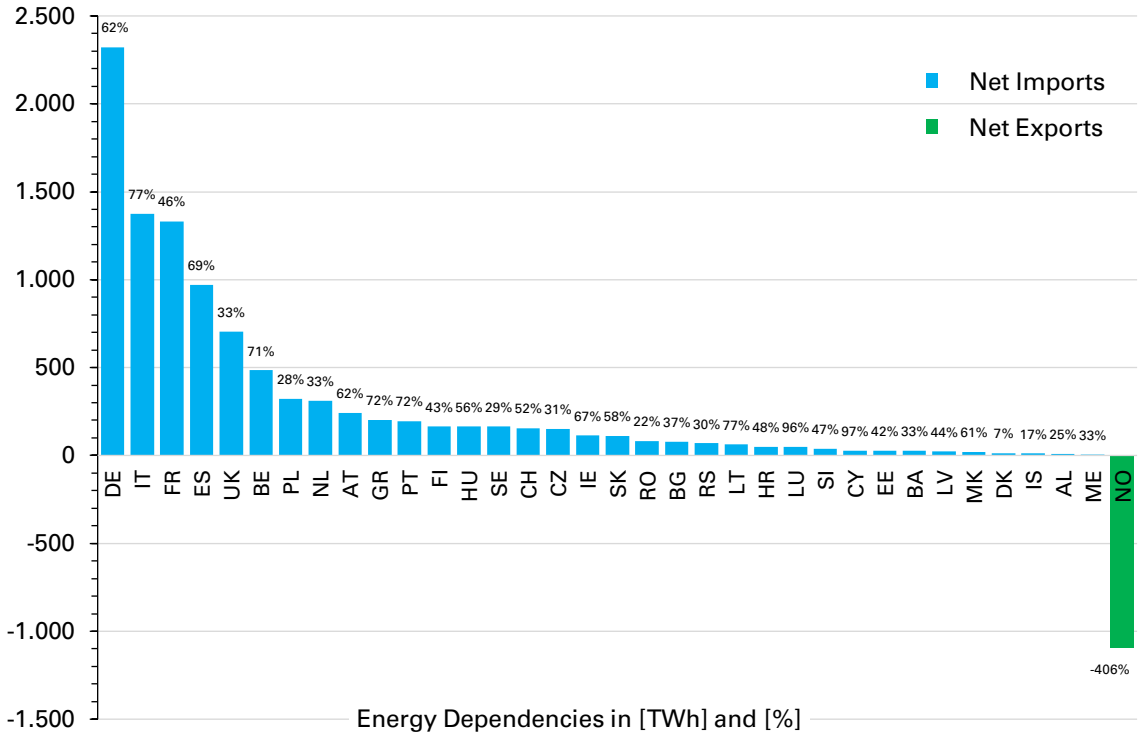

Fig. 9 Energy dependencies per country 2016
Source: In reference to [EUROS2018b]

As depicted in **Fig. 9**, the ENTSO-E exhibits a heterogenous composition of countries with high and low dependency rates. Net energy imports are quantitatively led by Germany (2,323 TWh), Italy (1,373 TWh), and France (1,332 TWh), which account for more than half (50.4 %) of net energy import quantities. Together with the subsequent countries Spain (969 TWh), UK (705 TWh), Belgium (484 TWh), Poland (321 TWh), and the Netherlands (310 TWh), those eight countries account for more than three-quarters (78.4 %) of net imports. The oil and gas rich country Norway represents the only country which exhibits negative net imports, equal to 1,095 TWh net exports. This export is slightly greater than the net import demand of Spain, but accounts for only 21.8 % of the net import demand of the three largest net import countries Germany, Italy, and France. Hence, the remaining 9,970 TWh must be imported from third-party countries.

Norway (-405.6 %) is the only ENTSO-E country with negative net import dependencies and, hence, represents a net export country. At the lower end, countries such as Denmark (7.2 %), Iceland (16.7 %), Romania (22.1 %), UK (22.8 %), Albania (25.0 %),

Poland (28.3 %), Sweden (28.7 %), Serbia (30.3 %), and the Netherlands (33.2 %) possess particular low dependency rates with less than 35 % of gross primary energy consumption. Remarkably, especially mid- and large-scale countries (compare **Annex I** and **Annex II**), such as Denmark, UK, and the Netherlands, are among those countries with low dependency rates, due to significant domestic fossil fuel reserves, foremost mineral oil and natural gas. Poland exhibits large shares of domestic solid fuels, such as lignite and hard coal, whereas Iceland covers most of its energy demand by domestic geothermal heat and electricity production. Norway, Denmark, and Sweden exhibit significant shares of domestic RES and fossil fuel production. Norway possess large amounts of hydropower electricity production and Denmark is excelling in wind power, whereas all three countries export mineral oil and natural gas due to superior domestic reservoirs. [EUROS2018b] Hence, large shares of domestic RES and fossil fuel production are decreasing energy dependency rates significantly. Those domestic production potentials are heterogeneously distributed across the ENTSO-E and may rely on RES or fossil fuel production potentials or a combination of both.

On the other hand, Luxembourg (95.9 %), Cyprus (96.6 %), Italy (77.0 %), Lithuania (76.8 %), Portugal (72.5 %), Greece (71.5 %), Belgium (71.4 %), Spain (69.5 %), Ireland (67.5 %), Germany (62.4 %), Austria (62.1 %), and North Macedonia (61.3 %), exhibit the highest dependency rates with each more than 60 %. Those large energy dependencies are due to large energy consumption shares and inferior domestic RES and fossil fuel production potentials, which make energy imports, foremost mineral oil and natural gas, necessary. Among the large-scale countries, France (46.2 %) exhibits a moderate energy dependency rate, due to large shares of nuclear power production. Since nuclear energy is based on uranium, which in 2019 is foremost imported from Russia (19.8 %), Kazakhstan (19.6 %), Australia (14.4 %), Canada (11.6 %), Namibia (9.6 %), Uzbekistan (4.8 %), South Africa (0.9 %), and, particularly in the case of France, from Niger (15.3 %), the comparatively low energy dependency rate of France is not comprehensible. France does not possess large fossil fuel, nor uranium deposits, but primary energy consumption is dominated by 1,210 TWh (37.1 %) nuclear energy (**Fig. 13** of the **Compendium**). [EUROS2018b] [EUROS2021b] Moreover, the uranium exporting countries, as introduced in **Tab. 4**, do not belong to the overseas territories of France [EP2018b]. Hence, a statistical error in the Eurostat energy balances is anticipated

Analogous to the energy dependency analysis methodology, the electricity dependencies of each country are under investigation. Unlike the energy dependencies of **Fig. 9**, in which only Norway is indicated as net export country, the ENTSO-E is composed of a heterogeneous mixture of net electricity export and import countries. Hence, the focus on electricity exchanges among countries accounts for the increasing significance of the energy commodity electricity within the framework of the energy transition. Moreover, electricity exchange among various European electricity systems contributes to security of supply and interoperability. Total net electricity import quantities and dependency rates per country are depicted in **Annex III** and **Fig. 10**.

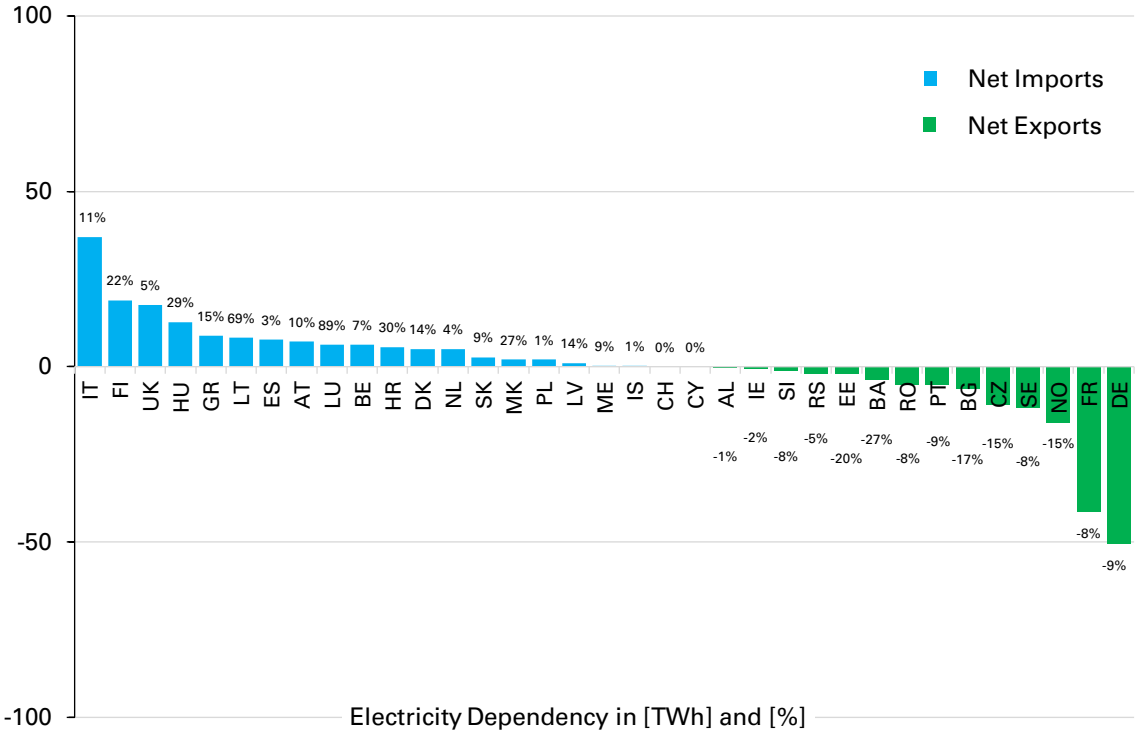

Fig. 10 Electricity dependencies per country 2016
Source: In reference to [EUROS2018b]

As depicted in **Fig. 10**, net electricity imports are led by Italy (37 TWh), Finland (19 TWh), UK (18 TWh), Hungary (13 TWh), Greece (9 TWh), Lithuania (8 TWh), Spain (8 TWh), and Austria (7 TWh), with each more than 5 TWh net electricity imports. Out of the net electricity import countries, Luxembourg (88.9%), Lithuania (69.2%), Croatia (30.5%), Hungary (28.5%), North Macedonia (26.5%), Finland (21.6%), Greece (14.6%), Denmark (14.2%), Latvia (13.9%), and Italy (11.4%) exhibit the highest electricity dependency ratio, with each more than 10% of gross inland electricity consumption. Among those countries, Italy, Finland, Hungary, Greece, and Lithuania possess comparatively large electricity demands and only moderate electricity production potentials. Hence, they represent electricity net import dependent countries in absolute and relative terms. Whereas countries such as UK and Spain exhibit large net electricity imports, but those account only for an inferior share of gross inland electricity consumption, indicated by the low electricity dependency rate.

On the contrary, Germany (51 TWh), France (42 TWh), Norway (16 TWh), Sweden (12 TWh), Czechia (11 TWh), Bulgaria (6 TWh), Portugal (5 TWh), and Romania (5 TWh) represent the leading net electricity export countries. Out of the net export countries, Bosnia (-26.8%), Estonia (-20.1%), Bulgaria (-16.6%), Czechia (-15.4%), Norway (-15.0%), Portugal (-9.4%), Germany (-8.5%), Romania (-8.4%), Sweden (-8.1%), and France (-8.1%) exhibit the highest net electricity export ratios (negative imports), with each more than -8%. Hence, the aforementioned countries are coined with superior electricity production potentials. Among the large-scale countries, especially Germany and France possess significant electricity export potentials, due to

robust and large power plant fleets. However, Germany as electricity export leader in the reference year 2016 is an exception, as France represents commonly the leading European electricity export country. The exception is due to comparatively large RES-based electricity feed-in in Germany and simultaneous power plant outages in France 2016, which is referred to as capacity shock. [EUROS2019f] [Rin2018]

During the Eurostat Energy balance sheets 2016 DATA (2018 Edition) [EUROS2018b] analysis, a failure in the assignment of the category *B_100112 direct_use* has been identified. The sub-category *B_100112 direct_use* belongs to the category *B_100900 gross_inland_consumption* and therefore must not subtracted from it. As a result of the correspondence with Eurostat in September 2018, *B_100112 direct_use* and *B_100110 primary_product_receipts* have been removed from the supply side in the updated energy balance sheets 2017 DATA - 2019 Edition [EUROS2019f] and the national country questionnaires for primary data acquisition have been updated. Hence, a failure of *err=0.12%* in the energy balances could be eliminated, which accounts for approximately 35 TWh (compare updated calculation method in **Eq. (2.1)** and the Eurostat 2018 correspondence in **Annex CD**). [Kup2018]

3. Integrated Energy

3.1 Power-to-X

The vast deployment of renewable energy sources (RES) is the prerequisite for a significant reduction of greenhouse gas emissions. Moreover, the shift to a renewable energy supply decreases the dependency on finite fossil fuels, such as coal, oil, gas, and uranium [10], that will be depleted in the mid and short term. Thus, RES are the only means to supply energy beyond depletable fossil fuels and to tackle the negative impacts that come along with global warming. Since the late 1990s, numerous countries promote the deployment of RES via various subsidy schemes. As a result, especially onshore wind, offshore wind, and photovoltaic (PV) power plants have been erected. Those powerplants increased the share of RES in the European electricity sector to approximately 34 % in 2016. [EEA2018a] [ENTSO2018b] [EUROS2019a]

However, the electricity sector contributes only 21 % to the final energy consumption and the total share of RES across all final energy consumption sectors accumulates to less than 17 % [Euros2019a]. The significant and vast energy demands are predominantly located in the heat and transport sector, which are barely permeated by RES. At present, those sectors rely strongly on fossil fuels and contribute a large proportion of GHG emissions. To achieve the carbon dioxide equivalent (CO_{2eq}) emission reduction goals of 80–95 % in 2050 compared to the base year 1990, the RES-based energy conversion must be increased tremendously and made available in all final energy consumption sectors on a large scale [EC2018a].

In integrated energy systems (IES) the electricity sector is interconnect with other energy consumption sectors via power-to-x (PTX) and x-to-power (XTP) technologies. The prevailing PTX applications comprise the power-to-heat (PTH), power-to-mobility (PTM), and power-to-gas (PTG) technologies. Moreover, electricity and gaseous energy commodity storages are integral components of integrated energy systems. Those storages are the key elements to decouple fluctuating RES-based production from energy consumption, which is characterized by rather inelastic demand profiles.

PTX technologies enable the conversion, transport, and storage of the increasing RES-based electricity production into the other demand sectors in form of electricity, heat, kinetic energy, and gaseous energy commodities. PTX represents the only means to effectively utilize the dominant RES-based electricity production and to convert it into useful energy for the prevailing energy consumption sectors. [DENA2018] [Kup2017b] [UBA2019] **Fig. 11** represents a schematic illustration of the integrated energy system under consideration of PTX technologies and the corresponding energy flows.

[10] For this analysis, uranium is regarded as fossil fuel as it belongs to the exhaustible resources.

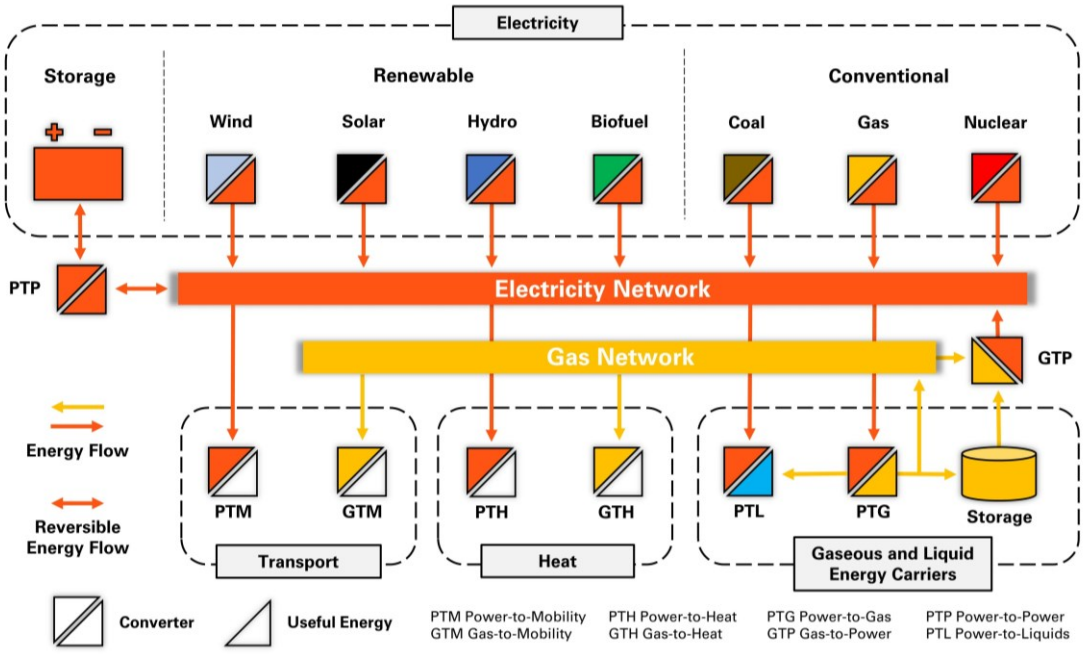

Fig. 11 Schematic illustration of PTX system integration
Source: In reference to [Kup2017b]

As depicted in **Fig. 11**, some PTX technologies can produce electricity in reversible XTP processes. For instance, unitized regenerative fuel cells can either produce hydrogen or convert hydrogen into electricity. Likewise, thermoelectric generators are able to convert heat into electricity via thermoelectric components. Moreover, grid connected stationary batteries can be charged and discharged. Those technologies are referred to as gas-to-power (GTP), heat-to-power (HTP), and power-to-power (PTP) technologies. In case of bidirectional charging of battery electric vehicles (BEV), the vehicle-to-grid (VTG) technology enables the discharging of the BEV battery and, therefore, turns the BEV into a storage system. [Kup2017b] [UBA2019]

The interconnection of energy sectors contributes to sustainable and efficient energy systems. Moreover, interoperability supports the network operation management[11]. The load shifting potential of PTX and the reverse operation of XTP technologies are salient features for the integrated energy system in order to balance the volatile RES-based electricity production and to compensate conventional power plant capacity. However, both energy conversions are coined with efficiency losses, limited field of application, and additional costs. As RES-based electricity production and financial resources are generally scarce, it is important to select the most efficient technology for the relevant applications. [FFE2017] [Kup2017a] [UBA2019]

[11] Network operation management comprises all measures to guarantee a secure and efficient operation of the electricity grids, such as ancillary services and network security measures. Those measures entail voltage and frequency control. [ENTSO2019c]

3.2 Power-to-Heat

PTH enables the conversion of electricity into useful heat and HTP vice versa. The predominant PTH technologies are represented by direct resistant heaters, such as heat elements and electric boilers, indirect resistant heaters, such as electrode boilers, and heat pumps. [Agora2014] [Bloes2018] **Fig. 12** illustrates the energy flows of the PTH and the HTP processes via the relevant technologies.

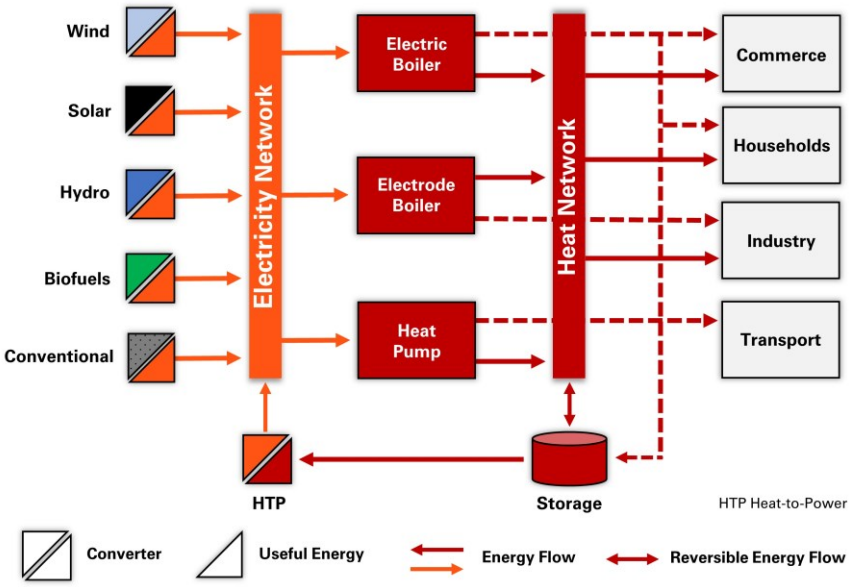

Fig. 12 Schematic illustration of PTH system integration

All PTH technologies are coined with high energy conversion efficiencies. The utilization of heat pumps can produce even more heat as electricity was input into the process due to the utilization of environmental heat according to the Carnot cycle. The efficiency of heat pumps is indicated by the coefficient of performance (COP). PTH technologies can be located centralized in a power plant and connected to a district heating system or decentralized, as part of a building or vehicle heating system in the economic sectors trade and commerce, households, industry, and transport. As part of heat supply, cooling in reference to air conditioning (AC) is regarded as reverse heat pump and, therefore, part of the PTH interface. All PTH technologies can be combined with small- and large-scale heat storage systems. [Bloes2018] [FFE2014] [Kup2017a]

Centralized PTH devices are increasingly integrated into combined heat and power (CHP) plants. Those power plants are generally more efficient than regular plants, but less flexible in the electrical operation due to heat supply obligations. The combination with a PTH device eases the ramping of CHP plants and, thus, guarantees the heat supply in case the CHP plant must ramp down due to disturbance, network bottlenecks, and redispatch measures of the transmission system operators (TSO). A prevailing advantage of PTH is the flexibility of the processes due to quick shutdown and restart times (ramping) as well as the thermal inertia of heat demand, which facilitates a high load shifting potential. In combination with properly sized heat storages, the load

shifting potential can be further increased. [Kup2017a] However, the transportation of heat in district heating systems and heat storage come along with additional energy losses due to heat convection, conduction, and radiation. Therefore, heat storages are rather regarded as short- and medium-term storages. [Bloes2018]

3.3 Power-to-Gas

The PTG technology enables the interconnection between the electricity and the gas sector. The PTG technology can be distinguished among two separated processes. The initial process comprises the production of hydrogen (H_2) via various electrolysis technologies that are based on the decomposition of water into H_2 and oxygen (O_2) by the means of electric power that forces a redox reaction between anode and cathode of the electrolyzer. The decomposition reaction is described in **Eq. (3.1)**. [Zapf2017]

$$H_2O \rightarrow H_2 + \frac{1}{2}O_2 \qquad \left[\Delta H_R^O = 286\,\frac{kJ}{mol}\right] \qquad (3.1)$$

The prevailing electrolysis technologies comprise the alkaline (AEL) electrolysis, the polymer-electrolyte membrane (PEM) electrolysis, and the solid oxide electrolysis cell (SOEC) electrolysis. Those technologies are basically distinguished among cell design, materials, chemical reaction, charge carriers, and process temperature. [Zapf2017]

AEL electrolyzer are based on aqueous electrolytes, such as potassium hydroxide (*KOH*) or sodium hydroxide (*NaOH*) and two perforated electrodes, which are separated by a diaphragm. AEL electrolyzer represent the most well established and mature electrolysis technology, that is coined with low costs and robust operation. On the contrary, the stable operation comes along with restricted operational flexibility in terms of ramping, slow reaction speeds, premature material degradation, and moderate operational efficiencies. PEM electrolyzer are based on bipolar plates and a proton conducting solid polymer electrolyte. Engraved channels (flow fields) in the plates allow water and gas transportation. PEM electrolyzer are able to operate at high pressures and quick response times, wherefore they are suitable for intermittent gas production and storage. Due to the use of numerous noble metals, the capital expenditures for PEM electrolyzer are comparatively high. SOEC electrolyzer are based on electrodes separated by oxygen ions conducting and gas-tight solid electrolytes, which are operating at elevated temperatures of 600–800 °C. Due to the input of water that is vaporized by an external heat source, the electrolysis process is highly efficient and requires less electricity than the AEL or PEM technologies, but is also less flexible in the operation. [Kurz2015] [Götz2016] [Kup2017a] [Kurz2015] [Zapf2017]

Conversion losses of state-of-the-art electrolysis plants account for 23–46 %. Hydrogen is the chemical element with the lowest atomic weight and, thus, tends to diffusion. Therefore, technical limitations on the storage and distribution of hydrogen are posed. Depending on the H_2 gas quality indicated by the Wobbe index that serves as an indicator of the interchangeability of fuel gases, H_2 can be directly injected into the

natural gas pipeline infrastructure to supplement the natural gas composition. This supplemental injection of H_2 is limited by the capabilities of the gas distribution system and the gas quality requirements, leading to reported limits as low as 1–5 % or potentially as high as 17–20 % by volume. Alternatively, a separated gas infrastructure can be utilized for exclusive H_2 transportation and storage, avoiding gas quality reduction through supplementation. Complementary to the production of hydrogen via electrolysis, a fuel cell can be utilized to produce electricity and water (H_2O) out of H_2 and O_2, as described in **Eq. (3.2)**. [Götz2016] [Kurz2015] [Oes2017]

$$H_2 + \frac{1}{2} O_2 \rightarrow H_2O \qquad \left[\Delta H_R^O = -286 \frac{kJ}{mol}\right] \qquad (3.2)$$

As subsequent and optional process, H_2 can be further processed wit carbon dioxide (CO_2) to methane (CH_4) via methanation in a so-called Sabatier reaction. The methanation enables the injection of CH_4 in form of synthetic natural gas (SNG) into the gas distribution system without hard restrictions. The methanation reactions are depicted in **Eq. (3.3)** and **Eq. (3.4)**. The corresponding water gas shift reaction is depicted in **Eq. (3.5)**. [Schmi2017]

$$CO + 3H_2 \Leftrightarrow CH_4 + H_2O \qquad \left[\Delta H_O^R = -206 \frac{kJ}{mol}\right] \qquad (3.3)$$

$$CO_2 + 4H_2 \Leftrightarrow CH_4 + 2H_2O \qquad \left[\Delta H_O^R = -165 \frac{kJ}{mol}\right] \qquad (3.4)$$

$$CO + H_2O \Leftrightarrow H_2 + CO_2 \qquad \left[\Delta H_O^R = -42 \frac{kJ}{mol}\right] \qquad (3.5)$$

According to **Eq. (3.3)** and **Eq. (3.4)**, carbon monoxide (CO) and CO_2 react to CH_4 and H_2O. The CO_2 hydrogenation of **Eq. (3.4)** is a result of combining the CO hydrogenation and the reverse water gas shift reaction of **Eq. (3.5)**. The Sabatier reaction is an exothermic reaction that requires an external heat source of 300–400 °C and must be pressurized with approximately 20 bar in the presence of a catalyst. Thus, it comes along with additional efficiency losses accounting for 35–51 % compared to the electricity input of the upstream electrolysis. In consideration of the reconversion of SNG into electricity, the total efficiency decreases to 30–38 % in power plants and to 43–54 % in combined heat and power (CHP) plants. Alternatively, a microbial methanation in bioreactors can be conducted, based on metabolic processes of microorganisms. [Schmi2017] [Kraut2016] [Zapf2017] Due to the maturity of the catalytic methanation, the biological methanation is beyond the scope of this analysis.

The chemical properties of SNG are easier to handle than the properties of H_2, so it can serve as a long term and seasonal energy storage and transported in the natural gas pipeline infrastructure. Among the presented PTG technologies, there are various additional technologies, such as power-to-liquids (PTL) and power-to-chemicals (PTC),

that are based on the Fischer-Tropsch process. [Schmi2016] As those technologies are based on water electrolysis, and chemical methanation is regarded as the reference case of this analysis, those technologies are not presented in detail. **Fig. 13** illustrates the energy flows of the PTG and GTP system via the corresponding technologies.

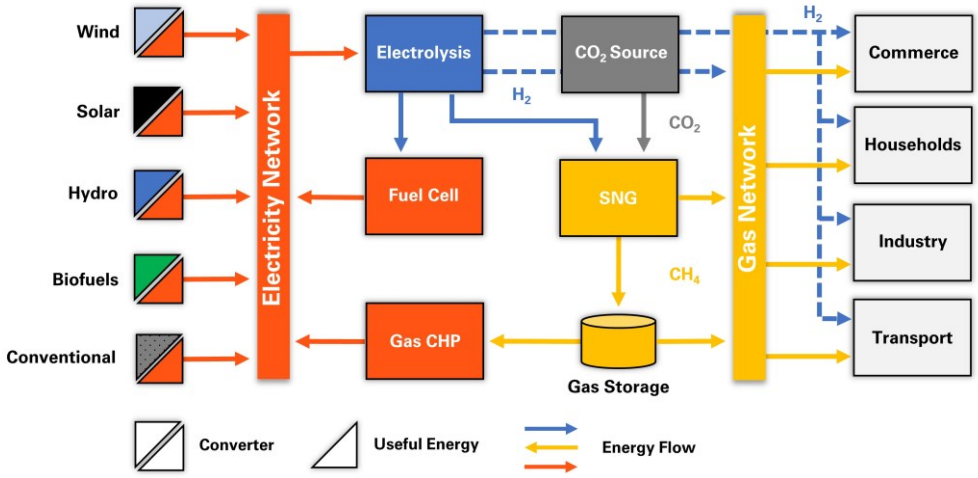

Fig. 13 Schematic illustration of PTG system integration

As indicated in **Fig. 13**, water electrolysis is the first stage of PTG processes. The electrolysis product H_2 can be used directly in the consumption sectors or stored and transported in the gas pipeline infrastructure, according to the prevailing limitations. According to the methanation processes, H_2 is reacted to CH_4 that can be injected into the gas pipeline infrastructure without restrictions and, thus, supplement the natural gas composition. Fuel cells and CHP plants are able to reconvert the synthetic gases into useful electricity, wherefore PTG represents a medium- and long-term means to store electricity, but comes along with significant energy losses. [Schmi2017] [Zapf2017]

3.4 Power-to-Mobility

PTM refers to the utilization of electricity in the transport sector. In a wider sense, also the usage of e-fuels and synthetic gases in internal combustion engine (ICE) and fuel cell engine (FCE) vehicles falls belongs to this category. According to this definition, those fuels are based on the PTG technology, foremost on the electricity-based H_2 production via electrolysis. Especially the fuel cell technology based on H_2 conversion into electricity for the purpose of traction energy, represents a promising PTM application. ICE, FCE, and battery electric vehicles (BEV) are characterized by different technical and economic parameters. The direct utilization of electricity in BEV and grid connected electric vehicles (GCEV), such as electric railways and streetcars, is highly efficient, whereas the electricity-based production of e-fuels and synthetic gases comes along with additional energy losses (compare **Chapter 3.3**). However, there are also advantages of gaseous and liquid energy commodities, such as transportability, long-term storability, and superior energy density. [Bozem2013] [Töp2017]

In comparison to BEV, which are equipped with a battery storage system, GCEV are directly connected to power lines. Thus, GCEV consume electricity directly and synchronous from the grid. Some GCEV, such as trolley trucks and buses, are equipped with a battery to bypass short distances, which are not supplied with power lines and to enable grid independent mobility. If enabled with the VTG technology, BEV can also be regarded as mobile storage systems and feed electricity into the grid. Therefore, BEV can actively provide ancillary services, such as frequency control and voltage stability. [Komar2018] [Oes2018] **Fig. 14** illustrates the energy flows of the PTM system.

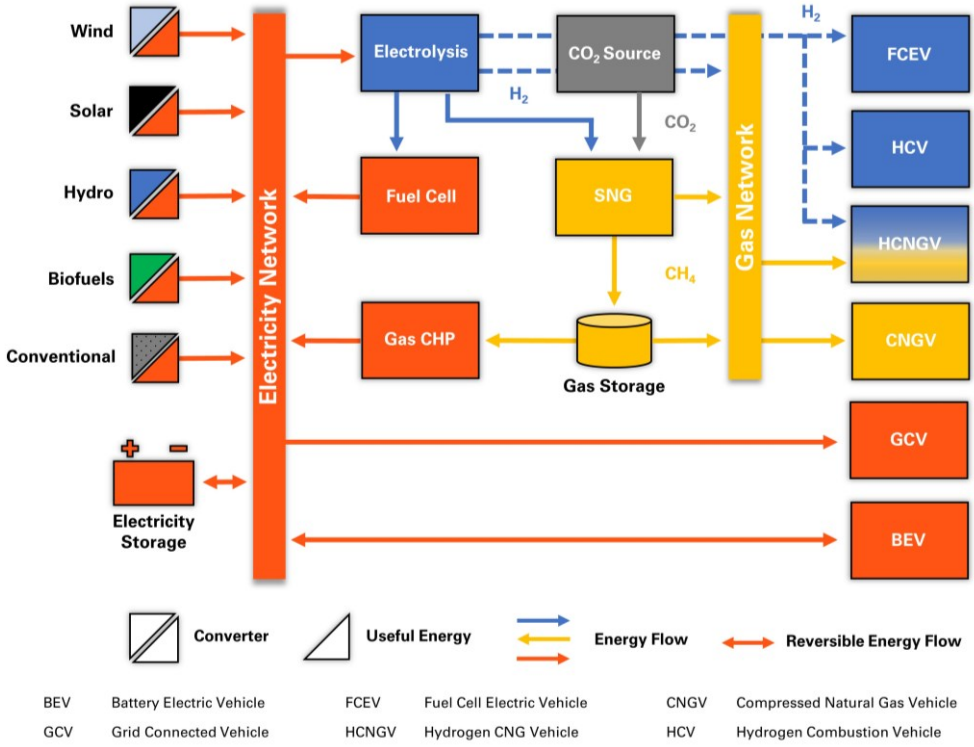

Fig. 14 Schematic illustration of PTM system integration

As per definition, **Fig. 14** entails the PTG process of **Chapter 3.3** to emphasize the potential utilization of e-fuels and synthetic gases in the transport sector. In this regard, H_2 can be utilized as gaseous fuel in fuel cell electric vehicles (FCEV), hydrogen combustion vehicles (HCV), and, complemented with SNG in hydrogen compressed natural gas vehicles (HCNGV). Alternatively, compressed natural gas vehicles (CNGV) can be fueled with SNG as a product of the PTG methanation process. The prevailing advantages of gaseous and liquid fuels in the transport sector are the long-term storage ability, the high energy density that enables high range, and the maintain of common user behavior. The overall well-to-wheel (WTW) efficiency strongly depends on the primary energy source and the energy conversion process used to provide the energy. WTW efficiencies are reported as low as 24 % for FCEV and as high as 75 % for BEV. The tank-to-wheel (TTW) efficiencies are reported as 40–60 % for FCEV and up to 95 % for BEV, depending on the operation mode. [Bozem2013] [Brun2015] [Lig2018] [Töp2017]

4. Renewable Energy Sources Potential Analysis

4.1 Objectives

The continued expansion of RES in the ENTSO-E, such as onshore wind power plants, offshore wind power plants, and utility-scale PV, will require the availability of areas for RES project development that are technically, economically, socially, and environmentally feasible. The deployment of RES is likely to disrupt local flora and fauna as well as local animal habitats. In this regard, RES expansion may alter or destroy breeding, feeding, migration, and flight paths of animals. Moreover, RES projects may lead to community conflicts regarding land value, shadowing issues, noise and light emissions as well as landscape and aesthetic impairments. Beyond monetary and policy incentives to support the deployment of RES, the extent to which suitable areas can be utilized within social and environmental constraints is likely become the prevailing restrictive factor. [BMVI2015] [Luetk2012] [Zaun2018] To best consider future potentials of RES-based energy conversion under consideration of these restrictive factors, the feasibility of RES project development is considered at a social, environmental, technical, and economic level. To assess the extent to which RES potentials can be exploited in the ENTSO-E member states, this analysis delineates two principal categories of RES: Primary Sources and Secondary Sources.

Primary Sources are RES that are expected to be the main drivers of RES growth as well as those that are most directly impacted by limitations to available land. The potential of Primary Sources is based on various geographic, climatic, regulatory, economic, and social factors. Given these factors, geographic information system (GIS) tools are used to comprehensively analyze regional land coverage within each of the ENTSO-E member states and to determine the resulting rated power P_r potential. Secondary Sources are those RES that are expected to have limited, minimal, or generally uncertain future impacts in comparison to Primary Sources and, therefore, are analyzed on the basis of meta-analysis literature review. The here regarded Primary and Secondary Sources and the corresponding assessment methods are comprehensively depicted in **Tab. 5**.

Tab. 5 Primary and Secondary Sources technology classification

Category	Technology	Assessment Method
Primary Sources	Onshore wind power plants, offshore wind power plants, utility-scale photovoltaic power plants, concentrated solar power (CSP)	GIS
	Rooftop solar (PV and solar thermal)	Approximation
Secondary Sources	Bioenergy (biomass, biogas, and biofuels), hydropower, geothermal, wave, ocean, and tidal power plants	Literature review

4.2 Primary Sources Land Coverage and Protected Area

Increasing RES-based energy supply is dependent on both, suitable RES technologies and availability of land area. Theoretical energy potentials often state the abundance of available RES based on technical and economic factors, while understating the impacts of environmental, social, and regulatory restrictions. As large-scale RES projects continue to propagate, easily attainable and convertible land areas become scarce and face increasing social and regulatory restrictions. Existing tools to account for social and environmental impacts, such as environmental impact assessment (EIA), are likely to underestimate community needs and concerns. Hence, conflicts may arise among developers, communities, and concerned parties. [Lars2008] [Luetk2012] [Zaun2018]

Major impacts on flora and fauna comprise the degradation of habitats, the disruption of breeding, feeding, and migration patterns as well as the creation of habitat competition. RES projects are also likely to impact societies and are reported to impair landscapes, diminish aesthetic appeal, conflict with cultural or heritage significance, and decrease general land value. [BMVI2015] [Zaun2018] Hence, it becomes necessary to carefully account for those areas that are prone to the aforementioned environmental and social impacts. Areas within the ENTSO-E that hold social, national, ecological, or environmental value are designated as either Natura 2000 or Nationally Designated Areas (NDA). NDA classifications are based on the Common Database on Designated Areas (CDDA) inventory. [EEA2013a] [IUCN2008]

As per European designation for special protections, Natura 2000 designations are specific to the EU member states and are nationally delineated to establish areas for species protection and biodiversity, according to the Habitats Directive (92/43/EEC) and Birds Directive (79/409/EEC). Under these directives member states designate areas as either Special Areas of Conservation (SAC) or Special Protection Areas (SPA). Natura 2000 consists of 27,852 conservation sites with a total area of 1,358,125 km^2. This area represents 17.9 % of the EU land territory and 9.7 % of its marine waters. Natura 2000 represents the largest coordinated network of protected areas in the world and serves as the principal tool for maintaining and restoring the conservation status of protected habitats and species. [EC2020b] [EEA2013a]

The CDDA inventory contains spatial data and information about protected areas and the national legislative instruments from 118,798 different sites that are located in 39 countries. The total coverage of CDDA amounts to 4,781,129 km^2. The dataset contains data on NDA and designated boundaries for the European Environment Agency (EEA) member and cooperating countries, whereas the dataset is divided into a national and an international section. The CDDA designation is nation-specific and has various subcategories, such as national parks, wilderness areas, and natural monuments. NDA are categorized in accordance with the International Union for Conservation of Nature (IUCN) categories, delineating the degree to which access, development, and

maintenance is necessary or permitted. Unlike Natura 2000, the CDDA represents the official source of protected area information from European countries to report to the World Database of Protected Areas (WDPA). [EEA2020] [IUCN2008]

Both, Natura 2000 and CDDA cover terrestrial and marine protected areas. **Fig. 15** illustrates the wide coverage of those designated and protected areas in the EU and the non-EU but ENTSO-E countries. Thereby, the locations of CDDA area are indicated by reddish surfaces and Natura2000 areas by greenish surfaces.

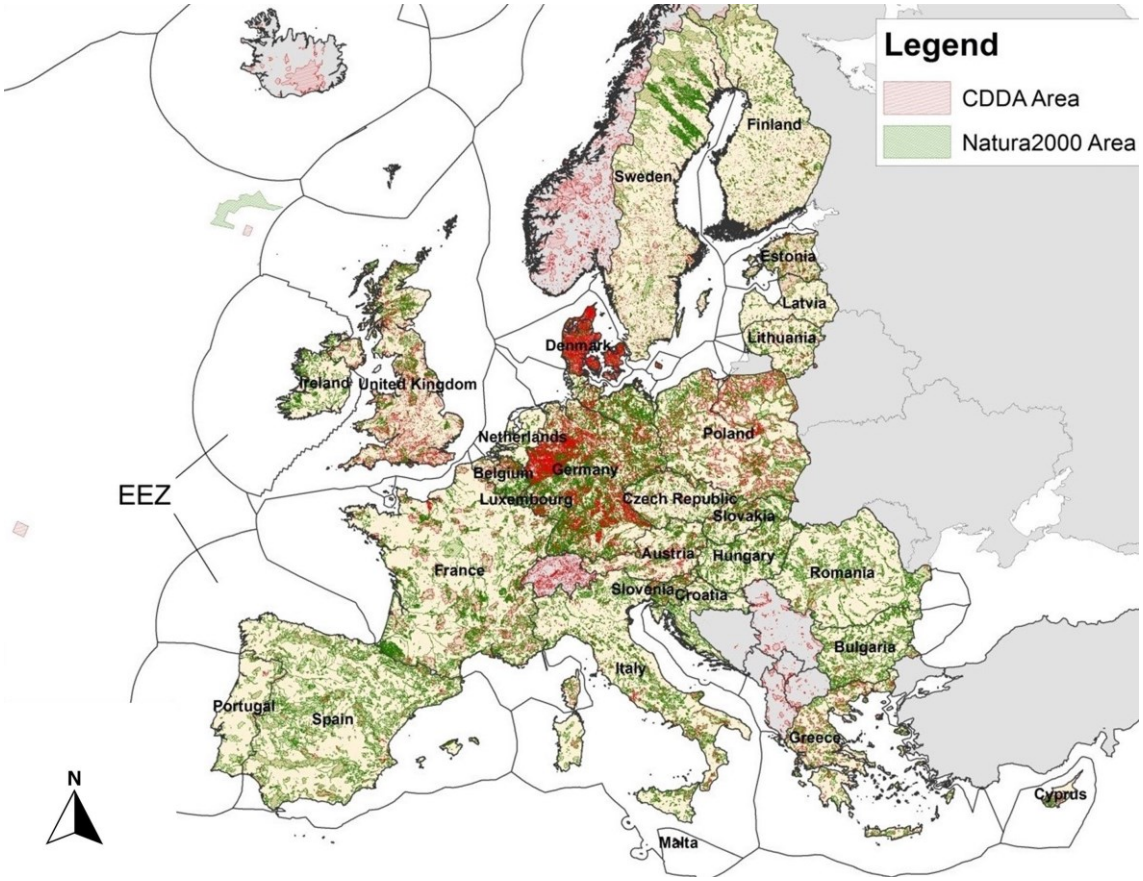

Fig. 15 CDDA and Natura 2000 protected areas EU and ENTSO-E
Source: In reference to [Kup2020a]

According to **Fig. 15**, EU-specific Natura 2000 and international CDDA designated areas can be found across the ENTSO-E, whereas Natura 2000 categories are only designated to EU countries. Non-EU countries are exclusively covered by CDDA categories. Natura 2000 and CDDA areas show especially high densities in Denmark and Germany.

4.3 Primary Sources Geo-Spatial Analysis

Space requirements and direct impacts of large-scale RES projects, foremost PV and wind power plant projects, lead to conflicts regarding land use and, thus, limit the extent of practical and social acceptance of RES project development [BWE2012] [Lars2008] [Zaun2018]. To best analyze the potential for RES-based energy conversion in each ENTSO-E country and under consideration of those hard restrictions, the GIS software ArcMap from the Environmental Systems Research Institute (ESRI) is utilized to

visualize, measure, configure, and investigate spatial and geographic data. This geo-spatial analysis is based on CORINE Land Cover (CLC) spatial land-coverage data of the Copernicus Land Monitoring Service (CLMS). CLC data delineates 44 sub-classifications of land-area among the following five main categories. [CLMS2012] [CLMS2018]

- Artificial surfaces
- Agricultural area
- Forests
- Semi-natural areas
- Wetlands and waterbodies

Moreover, numerous additional geo-referenced spatial datasets to precisely account for geographical, environmental, physical, and regulatory impact factors in the GIS analysis are utilized, as outlined in **Tab. 6**.

Tab. 6 Environmental and social impact factors
Source: In reference to [Kup2020a]

Spatial Datasets		
Wind speed	Elevation & depth	Maritime traffic
Global irradiance	Slope & orientation	Oil & gas pipelines
Direct normal irradiance	Highway	Population density
Optimum PV angle	Railway	Annual ice formation
CDDA areas	Natura 2000 areas	National NUTS & EEZ

As an integral part of the geo-spatial analysis, the resulting spatial data is exported as comma-separated values (CSV) data files into MATLAB script. The script considers each individual land area per country and region and performs the subsequent calculations.

- Compute onshore wind and utility-scale PV annual energy conversion
- Apply Natura 2000 and CDDA availability factors
- Calculate levelized cost of electricity (LCOE) and apply economic limitations
- Apply suitability factors
- Aggregate and export regional data

The ArcGIS and MATLAB script-based geo-spatial analysis of each land area is performed in the following four sequential stages.

- Gross Potential Stage (GIS-based)
- Available Potential Stage (script-based)
- Techno-Economic Potential Stage (script-based)
- Suitable Potential Stage (script-based)

Each stage considers the annual energy conversion from each applicable technology before applying various factors, technical specifications, and limitations, as outlined in **Fig. 16** and discussed in the following chapters.

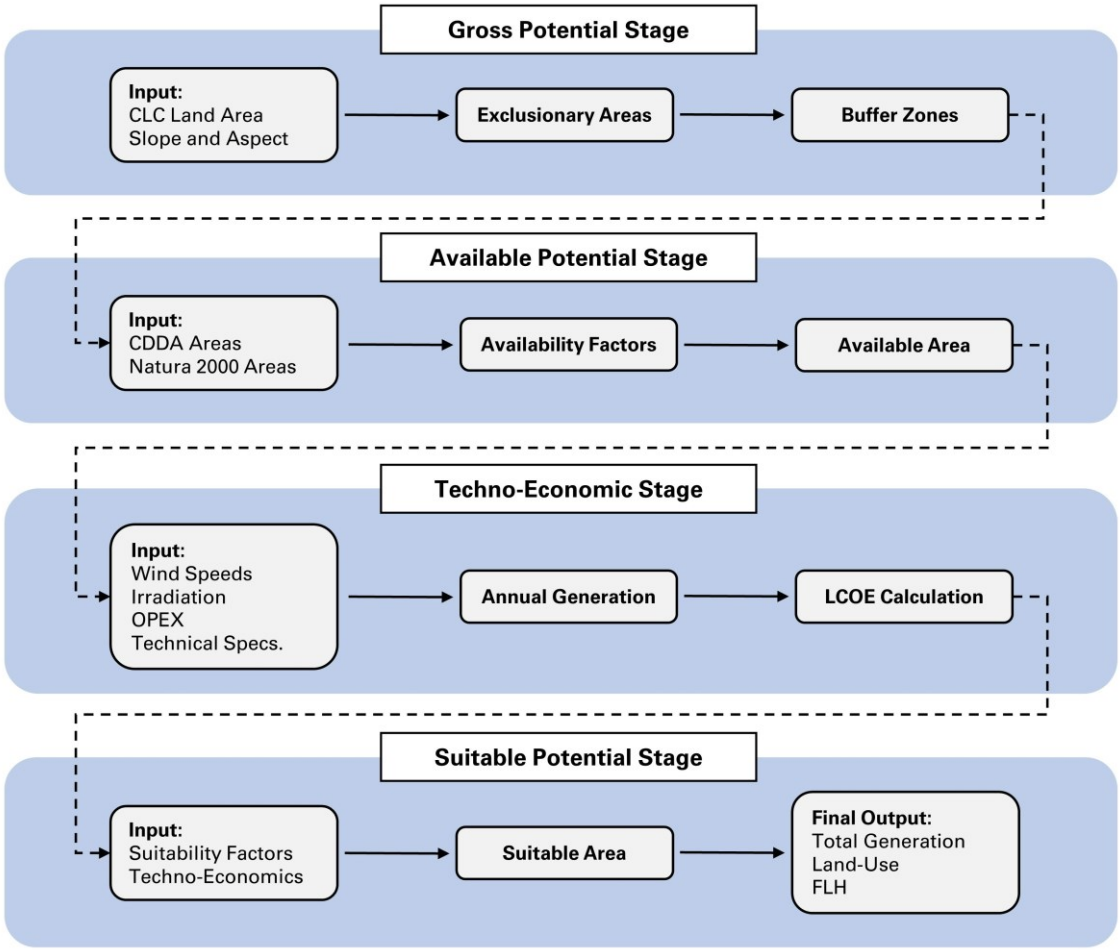

Fig. 16 Sequential stages of the geo-spatial potential analysis
Source: In reference to [Kup2020a]

4.3.1 Gross Potential Stage

In reference to the CLC inventory of CLMS (2012), specific exclusion zones are applied to each RES technology based on literature and technical review [CLMS2012]. According to this review, those land types are identified that are generally suitable for RES development. For instance, urban areas are excluded from onshore wind, utility-scale PV, and CSP project considerations. Irrigated areas, marshes, waterbodies, and beaches are excluded from onshore wind development. Likewise, forested areas, marshes, and waterbodies are excluded from utility-scale PV development. Based on technical guidelines, buffer zones are generated around exclusion areas, designating areas beyond sole exclusion areas that likewise cannot be used for RES development. Those exclusion areas and buffer zones may restrict wind power plant development from airports and adjacent area. Additional exclusion areas and geographic factors per RES technology are depicted in **Tab. 7**. [BMVI2015] [BWE2012] [EEA2009] [Sliz2013] [WE2017]

Tab. 7 Gross potential limiting factors per RES technology
Source: In reference to [Kup2020a]

Technology	Exclusion Areas	Geographic Exclusion Factor
Onshore wind	Urban, industrial, infrastructure, airport, sport and leisure, irrigated land, groves, plantations, beaches, dunes, sands, bare rock, marshes, water bodies	Slope, elevation
Offshore wind	Oil and gas pipelines, offshore wells and platforms, annual ice formation, maritime shipping routes	Depth
Utility-scale PV	Urban, infrastructure, ports, forests, grassland, beach, dune, sands, waterbodies	Slope, elevation, aspect
CSP	Urban, industrial, infrastructure, airport, sport and leisure, irrigated land, groves, plantations, beaches, dunes, sands, bare rock, marshes, water bodies	Slope, elevation, aspect, land geometry

In reference to the specific geographic features, geographic exclusion zones remove areas not feasible for RES development. In the case of onshore wind and utility-scale PV, these features comprise elevation and slope. Due to economic and performance considerations, utility-scale PV is furthermore limited to areas with a south-facing orientation. Analogous, CSP is limited by elevation, slope, and land geometry. The development of offshore wind power projects is restricted by ocean depth. Moreover, all infrastructure land areas, such as railways, streets, waterways, pipelines, and transmission lines, are entirely exempted from RES development.

The Gross Potential Stage utilizes the spatial data sets of **Tab. 6** and exclusion areas of **Tab. 7** to identify geo-referenced exclusion areas and to delineate buffer zones around those areas by the means of ESRI ArcMap software. Moreover, slope, aspect, and elevation data based on the CLC inventory are input into the analysis.

To account for various RES technologies additional data, such as average wind speeds and solar irradiance, are assigned to each individual location. In this regard, onshore wind power and utility-scale PV plant development is considered equally and in parallel stages. Thus, the resulting exclusion areas, buffer zones, and geologic restrictions are considered to account for overlapping and intersecting conflict areas, as illustrated at the example of the State of Brandenburg in **Fig. 17**.

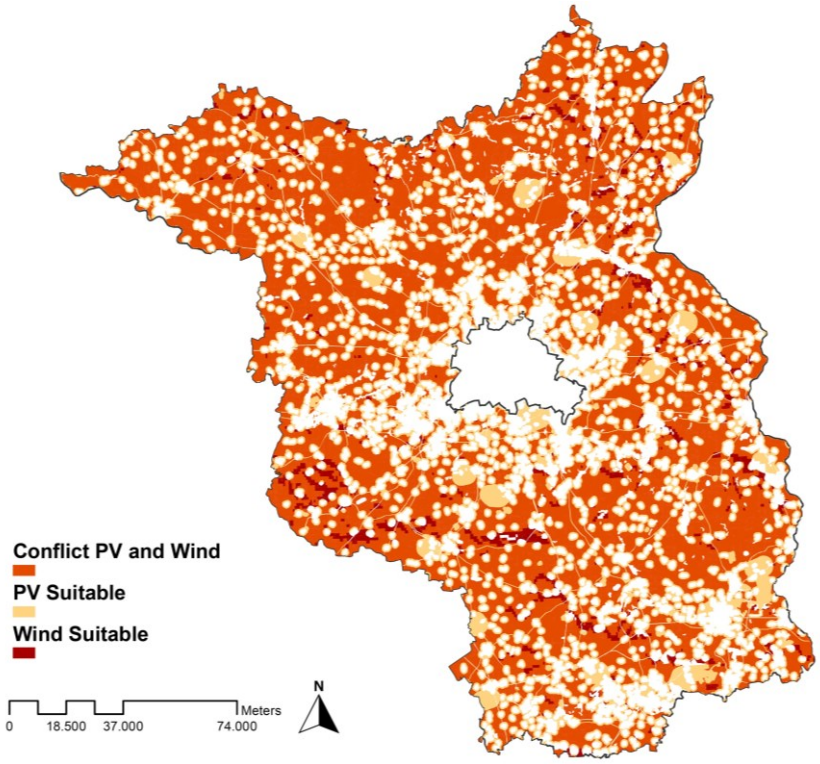

Fig. 17 Conflict PV and onshore wind areas in Brandenburg

As depicted in **Fig. 17**, land areas that are potentially suitable for onshore wind and utility-scale PV according to the previous stages of this analysis are considered as conflict areas. In the case that both onshore wind and utility-scale PV power plants are technically and economically feasible, the technology with potentially higher annual output is selected. As opposed to comparative LCOE, annual energy output is chosen as the decision criteria to better estimate maximum available energy while facing geological, technical, social, and regulatory limitations. As a result of the deterministic stages of this geo-spatial analysis, each land use percentage of a region represents how much of the total regional land area is used for either onshore wind or utility-scale PV.

4.3.2 Available Potential Stage

The Available Potential Stage restricts the total land and maritime areas that can be utilized for various RES technologies, based on ecological and regulatory factors. In reference to the designation of areas as Natura 2000, CDDA, or both, and based on the delineation by RES technology, quantitative availability factors are applied to represent varying levels of restrictions. Availability factors are derived from GIS-based RES analyses according to Sliz-Szkliniarz (2013), RES potential studies in reference to the German Federal Ministry of Transport and Digital Infrastructure (BMVi) (2015), and Zaunbrecher et al. (2018) [Sliz2013] [BMVI2015] [Zaun2018].

The development of RES in protected areas, such as nature reserves and wildlife sanctuaries, is not prohibited per se but subject to regulatory frameworks, municipal objections, and permitting processes specific to each country and region. Based on the

analysis of BMVi (2015), RES development in protected areas is qualitatively graded between hard restrictions and taboo. For instance, areas designated as national parks or strict nature reserves are considered taboo and are not further considered, whereas wilderness and protected areas as well as habitat and species management areas are less restricted. Hence, quantitative availability factors are defined between 1–10 %, as outlined in **Tab. 8**. [BMVI2015]

Tab. 8 Availability factors onshore wind, offshore wind, utility-scale PV
Source: In reference to [BMVI2015]

Type of Designation	Description	Onshore Wind	Offshore Wind	Utility-Scale PV
Natura 2000	Habitat and species protection	0.03	0.05	0.08
CDDA Ia	Strict nature reserve	-	-	-
CDDA Ib	Wilderness area	0.01	-	0.02
CDDA II	National park	-	-	-
CDDA III	Natural monument or feature	-	-	-
CDDA IV	Habitat and species management	0.01	-	0.02
CDDA V	Protect landscape or seascape	0.01	-	0.02
CDDA VI	Protected area with sustainable use of natural resources	0.05	-	0.10

According to **Tab. 8**, specific designated areas, such as national parks and national monuments, are strongly restricted regarding RES development. Whereas protected areas, although likewise restricted, may exhibit potential for RES development if adequately planned and precautionary measures are taken to address environmental concerns. The application of availability factors is conducted on a regional scale. In reference to a particular availability factor, the factor is applied to the entire composition of that specific land cover category. Thus, the total energy yield from the land cover category rather than a proportion for RES development is decreased. This method leads to a rather general estimation for each area and, to a certain extent, it reflects the limitations of GIS-based potential analysis.

4.3.3 Techno-Economic Potential Stage

To account for technical and economic limitations of RES projects, economic considerations based on the calculation of levelized cost of electricity (LCOE) as depicted in **Eq. (4.1)** are applied. Here, $R_{O\&M}$ describes the cost of operations and maintenance in EUR per kW represented by operational expenditures (OPEX), P_r the turbine rated power in kW, a the annuity in per unit (p.u.), I the initial capital cost per rated power in EUR per kW represented by capital expenditures (CAPEX), and E the annual energy yield in kWh [Sliz2013].

$$LCOE = \frac{R_{O\&M} \cdot P_r + a \cdot I \cdot P_r}{E} \tag{4.1}$$

According to **Eq. (4.2)**, the investment annuity a is defined as i the interest rate in percent and y the project lifetime in years [Sliz2013].

$$a = \frac{i(1+i)^y}{(1+i)^y - 1} \tag{4.2}$$

Based on **Eq. (4.1)** and **Eq. (4.2)**, the detailed calculation of LCOE and full load hours (FLH) as well as the underlying assumptions per RES technology are discussed in **Chapter 4.4** and summarized in **Tab. 9**.

Tab. 9 Competitive LCOE and FLH per technology
Source: [Bei2017] [Vart2015] [IRENA2012] [IRENA2017] [Kost2013] [Laem2017] [WE2017]

Technology	LCOE / FLH	Unit
Onshore Wind	100	EUR MWh^{-1}
Offshore Wind	75	EUR MWh^{-1}
Utility-scale PV	45	EUR MWh^{-1}
CSP	120	EUR MWh^{-1}
Rooftop PV	1,000	FLH

4.3.4 Suitable Potential Stage

To carefully account for potential RES development restrictions beyond those already considered, general suitability factors for onshore wind and utility-scale PV reference scenarios are defined based on designated land specification. Regarding onshore wind projects, Deng et al. (2015) anticipate a general suitability of 6 % for barren lands, pastures, and agriculture areas as well as 1 % for forested areas [Deng2015]. According to Sliz-Szkliniarz et al. (2013), the development of utility-scale PV is graded by land classification according to the subsequent categories [Sliz2013].

- Favorable
- Suitable-conflict
- Conflict-possible

In reference to Deng et al. (2015), suitability factors for utility-scale PV projects are defined as 3 % for barren land and pastures as well as 2 % for agriculture areas [Deng2015]. These factors are likewise anticipated and further adjusted based on the definition of Sliz-Szkliniarz et al. (2013) as the following qualitative grades [Sliz2013].

- 1.0 for favorable areas
- 0.8 for suitable-conflict areas
- 0.6 for conflict-possible areas

Analogous to the application of availability factors as introduced in **Chapter 4.3.2**, the application of suitability factors is conducted on a microscopic level and with a spatial resolution. The suitability factors for onshore wind and utility-scale PV power plants per CLC land category are depicted in **Tab. 10**.

Tab. 10 Suitability factors onshore wind and utility-scale PV
Source: In reference to [Deng2015] [Sliz2013]

CLC No.	CLC Land Category	Onshore Wind Factor	Utility-Scale PV Factor
121	Industrial and commercial units	-	0.250
123	Port areas	0.010	-
124	Airports	-	0.300
131	Mineral extraction sites	-	0.010
132	Dump sites	-	0.010
211	Non-irrigated arable land	0.120	0.016
212	Permanently irrigated land	-	0.016
213	Rice fields	-	0.012
221 222 223	Plantation: Vineyards, fruit, olives	-	0.012
231	Pastures	0.050	0.024
241 242 243	Cropland, cultivation, agriculture	0.020	0.016
244	Agro-forestry areas	0.020	0.024
321	Natural grasslands	0.100	0.024
311 312 313	Forest	0.020	-
322	Moors and heathland	0.100	-
323	Sclerophyllous vegetation	0.020	0.024
324	Transitional woodland-shrub	0.100	0.018
332	Bare rocks	-	0.030
333	Sparsely vegetated areas	0.020	0.030
334	Burnt areas	0.100	0.030

In reference to the set of suitability factors, each suitability factor is applied to the entire composition of the corresponding land category. Hence, the total energy yield from the land category, rather than a proportion for RES development, is reduced. Those suitability factors are applied consecutively to the previous three potential stages which consider geological, environmental, regulatory, technical, and economic factors. The application of generalized suitability factors does not allow for preferential treatment of specific areas over another. These factors rather represent a general approach towards estimating available land area and the resulting energy yield potential in reference to specific concerns, restrictions, and social limitations. Therefore, the approach results in a more general estimation for each land area.

4.3.5 Methodological Reference Case Brandenburg

This analysis considers the German Federal State of Brandenburg as a reference case to compare qualitative and quantitative assumptions to the status quo. Brandenburg exhibits a robust fleet of RES, but increasingly encounters municipal and regulatory objections as the expansion of RES continuous [Stef2018]. To account for plausibility of the method, spatial data of METAVER (2018) is utilized to gather the geo-referenced

locations of already existing or planned onshore wind turbines in Brandenburg and to compare them with the exclusion areas of the CLC spatial data analysis as described in **Chapter 4.3.1** [META2018]. The results of this comparative analysis at the example of a randomly chosen area in the south of Brandenburg are depicted in **Fig. 18**.

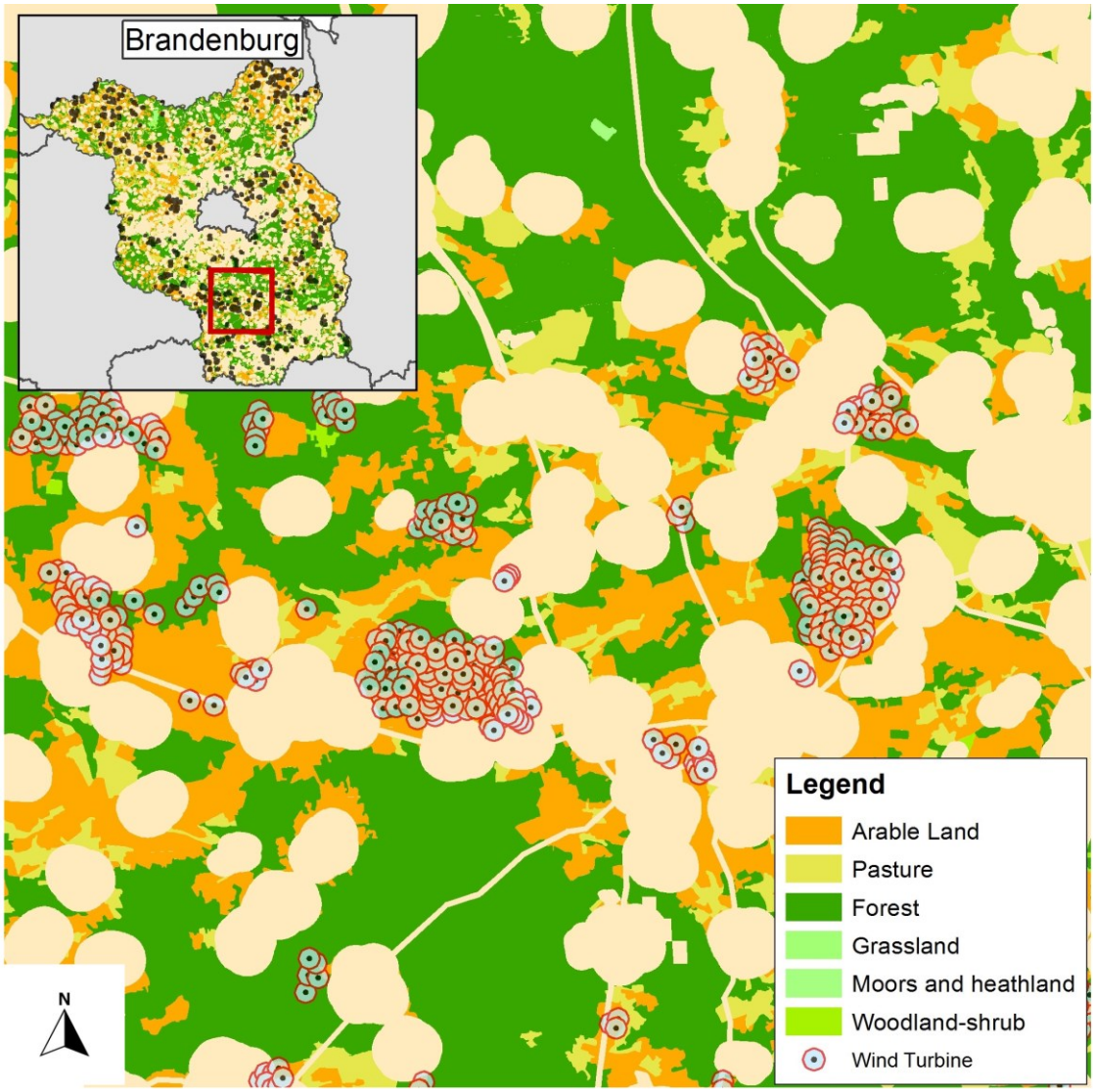

Fig. 18 Onshore wind analysis in Brandenburg
Source: In reference to [Kup2020a]

To best estimate the total surface space occupied by onshore wind turbines, a modest 400 m radial buffer-zone around each turbine is anticipated. As a result, 4,426 out of 4,596 of all existing turbines are shown to be located in areas considered as non-excluded by this analysis. This correlation represents a concordance rate of 96 %. In 2018, wind turbines with a total rated power of 6.85 GW, an average hub-height of 102 m, and an average rotor diameter of 82 m are in operation [META2018].

Compared to CLC land data, 80 % of this capacity is located in non-irrigated arable land, 11 % in coniferous forests, and 5 % in pastures. Furthermore, 11 % of non-restricted arable land and 12 % of woodland-shrubland was already utilized, followed by 9 % of natural grasslands and 4 % of coniferous forests. Under consideration of the restricted

area according to Natura 2000 and CDDA, 5 % of arable land and 4 % of heathland as well as 1 % of woodland, shrubland, and coniferous forests are utilized for non-excluded onshore wind power site development.

In total, 9 % of all available and non-excluded arable land had already been developed for onshore wind power in the reference area of Brandenburg 2018. The concordance rate of 96 % of the anticipated and the existing wind power sites implies a high accuracy of the presented method. Based on this result, the outcome of this site assessment is qualitatively reviewed and utilized to validate and to adjust the review-based assumptions regarding the definition of availability factors in **Chapter 4.3.2** and suitability factors in **Chapter 4.3.4**.

The 2012 Copernicus Land Monitoring Service (CLMS) guidelines consider utility-scale PV and wind power plant land covers [CLMS2012]. In consideration of RES development in commercial areas (CLC 121), 2012 land covers are reviewed. The review of the 2012 land covers in Brandenburg exhibits a significant share of areas classified as commercial due to utility-scale PV developments. However, no significant areas are indicated as commercial due to already existing wind power plants. To account for existing projects, this study considers commercial areas as viable for utility-scale PV and a general suitability factor is assigned based on the 2012 land cover review. In reference to 2018, it is anticipated that 20–30 % of CLC 121 land is covered by utility-scale PV power plants. As a result of the GIS analysis, a general utility-scale PV suitability of 25 % for commercial and industrial areas (CLC 121) is anticipated for the subsequent analysis.

Due to aviation security standards, the development of utility-scale PV as part of airports is commonly omitted [Luetk2012] [Sliz2013]. However, in consideration of the existence and growth of airport PV projects around the world and the development of PV panels that are non-reflective and, thus, not interfering with aviation security, PV development on airport sites is considered as part of this analysis [Kand2014]. Therefore, CLC class 124 specifically denotes airports and airfields. According to the CLC data of the 19 airports and airfields in Brandenburg, three had already been converted to utility-scale PV power plants and were reclassified as commercial (CLC 121). Nearly 20 % of the remaining airport and airfield area was still classified as CLC 124, but had already been converted, either completely or partially, into utility-scale PV. In reference to these inconsistencies, it is expected that approximately 30 % of existing airfield and airport area is available for utility-scale PV project development.

4.4 Primary Sources Potential Modeling

4.4.1 Onshore Wind Power Plants

Wind power plants are regarded as cost-competitive with gas- and coal-based electricity generation and come along with comparatively short construction times. In comparison to land-intensive PV power plants, only a small area of land is occupied by wind tower

foundations. Thus, alternative utilization, such as agricultural use, is possible. The rapid growth in the development of wind energy comes along with an increase in the size of wind turbines and decreasing competitive levelized costs of electricity (LCOE). Hence, wind power is coined with comparatively low LCOE. [Mil2020]

The prevailing environmental impacts of wind power development account for visual impairment and interference with bird flight paths, accompanied by land use conflicts with specific land uses sensitive to disturbance. During operation, disturbances from noise, shadow, and light emissions are likely. Moreover, ice throw may occur and interference with flight corridors and radio relay systems pose threats to aviation. Due to the dimensions of modern wind power systems, wind power plants may harm bird and bat populations. [Felb2014] [Mil2020]

Moreover, wind power plants are likely to alter landscape sceneries, which causes conflicts with residents, nature conservation, and recreational interests. Hence, the control of wind power plant expansion by spatial planning represents a fundamental instrument for mitigating negative impacts and to increase public acceptance. On a regional level, the determination of exclusion areas and safety distances for the development of wind power based on functional criteria represents the most essential planning tool. [Felb2014] [Mil2020] The following onshore wind power potential assessment methods are presented according to the geo-spatial analysis stages, as indicated in **Fig. 16** of **Chapter 4.2.**

Gross Potential Stage

Onshore wind project development is limited to open land types, such as grasslands, arable lands, and areas with only light vegetation. In consideration of the height of modern and future wind turbine towers, forested areas are deemed as potentially suitable areas for wind turbine erection. However, development in woodlands is limited due to environmental concerns as well as spatial access for construction and grid connections. [BFN2011] [Den2009] [Lars2018]

As indicated in **Tab. 7** of **Chapter 4.3.1**, onshore wind power plants are categorically excluded from municipality, urban, and recreational areas. Likewise, areas covered by highways, railways, transmission lines, and airport infrastructure are excluded. Moreover, areas with inadequate soil conditions regarding static and foundation aspects, such as marshes and bogs, are not considered. The construction of wind turbines near these excluded areas is likewise limited due to the afore mentioned environmental and safety considerations. Therefore, radial buffer zones are defined for each land cover type, as indicated in **Fig. 19**.

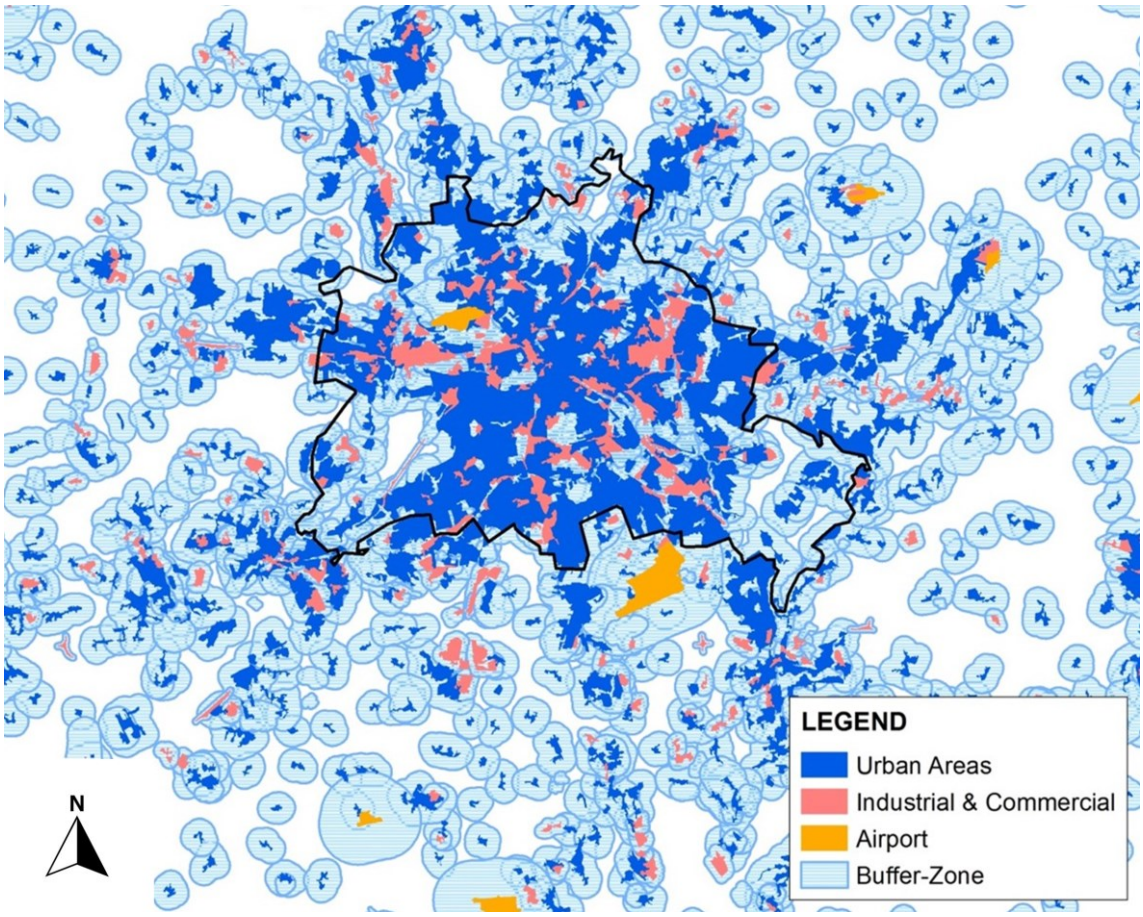

Fig. 19 Onshore wind buffer zones in the Berlin metropolitan region
Source: In reference to [Kup2020a]

Within those buffer zones as indicated by the light blue surface in **Fig. 19**, onshore wind project development is completely exempted. In reference to geological and topographic conditions, additional wind turbine construction restrictions are considered. Areas with elevations higher than 2,000 m are excluded due to decreased energy yield and limited accessibility. Land areas with prominent sloping of more than 3 % average slope per km^2 are excluded due to unfavorable roughness factors and wind characteristics as well as turbine construction limitations. [Kech2015] [Sliz2013] A comprehensive list of excluded land types and associated buffer zones as well as geological and topographic constraints is depicted in **Annex V**.

Available Potential Stage

Onshore wind power development in areas classified by the common database on designated areas (CDDA), such as national monuments, parks, and protected areas, is prohibited to prevent the degradation of land and interference with valued areas due to social, environmental, regulatory, and aesthetic concerns. In particular cases, nationally designated areas (NDA) are not entirely prohibited from wind power plant development, but are subject to more detailed review and restrictions as part of comprehensive environmental impact assessments (EIA). Moreover, areas additionally designated as habitat or species protection areas as per Natura 2000 databases are largely restricted,

in order to protect local ecologies and habitats as well as to prevent negative impacts on local species. As wind power plant development in those areas is generally omitted, development is not explicitly prohibited. Wind power plant development in those areas is rather subject to extensive review and permitting procedures. For areas designated as either Natura 2000 or CDDA availability factors for wind power are defined, in order to limit the amount of area that is considered for the spatial analysis. The complete set of availability factors for onshore wind power plant development in protected areas is depicted in **Tab. 8** of **Chapter 4.3.2**.

Techno-Economic Potential Stage

Regarding the Techno-Economic Stage of this analysis, only areas that exhibit sufficient annual wind availability are considered to ensure the economic viability of site developments. Based on the International Renewable Energy Agency (IRENA) (2017), wind locations that possess LCOE lower or equal to 100 EUR per MWh, which accounts for approximately 1,600 FLH, are considered [IRENA2017]. Total wind power plants development costs are calculated according to numerous capital costs based on turbine size, rated power, and site location as well as operations and maintenance costs. This analysis incorporates cost differences between different dimensions of wind turbines as well as their associated annual electricity production for each particular location. However, the proximity to existing transmission infrastructure is not directly considered. In those cases where various turbine dimensions are economically feasible, the turbine generating the most annual energy is selected.

Annual average electricity generation for each land area for onshore wind is based on average annual wind speeds, terrain roughness, turbine power rating, power curve, hub height, and rotor diameter [NREL2014]. Based on the National Renewable Energy Laboratory (NREL) System Advisor Model (SAM), the reference onshore wind turbines 1.8 MW Vestas V80, 2.5 MW Nordex N90, and 5 MW Areva Multibird are considered, as indicated in **Tab. 11** [NREL2016]. As the NREL selection of reference wind turbines is dated back to 2016, today the selection might be composed of more recent wind turbine versions. Due to steady innovation and constant change, newly arising technologies and corresponding parameters cannot be considered by this analysis. However, state of the art technologies have been selected.

Tab. 11 Reference wind turbine parameters
Source: In reference to [NREL2016]

Reference Turbines		Vestas	Nordex	Areva	Vestas
Model		V80 1.8	N90 2500 HS	Multibird	164
Operation Site		onshore	onshore	on- and offshore	offshore
Rated Power	[kW]	1,800	2,500	5,000	8,000
Hub Height	[m]	80	80	80	80
Rotor Diameter	[m]	80	90	116	164

In reference to Guedes et al. (2007), average annual wind speeds v_a at v_{10}=*10m* height are adjusted to the hub height h of each wind turbine reference model by applying generalized roughness factors Z based on land classification and corresponding roughness lengths in m, as indicated in **Eq. (4.3)** [Gued2007].

$$v_h = v_{10} \frac{ln\left(\frac{h}{Z}\right)}{ln\left(\frac{10}{Z}\right)} \tag{4.3}$$

The adjusted average annual wind speeds v_h are utilized to compute annual electricity generation based on the calculation of site-specific FLH. Therefore, the calculation of distribution curves is based on incremental wind speeds of v_i=*0.5 m per s* and accounts for average annual wind speeds v_a, rated wind speeds v_r, and wind speed class intervals dV, as indicated in **Eq. (4.4)**. [NREL2016]

$$f(v_r) = dV \left(\frac{\pi}{2}\right) \left(\frac{v_r}{{v_a}^2}\right) e^{-\frac{\pi}{4}\left(\frac{v_r}{v_a}\right)^2} \tag{4.4}$$

According to Sliz-Szkliniarz (2013), the FLH of each reference turbine are calculated by generating Rayleigh distribution curves based on the relationship between average annual wind speeds v_a and full load hours, as depicted in **Fig. 20** [Sliz2013].

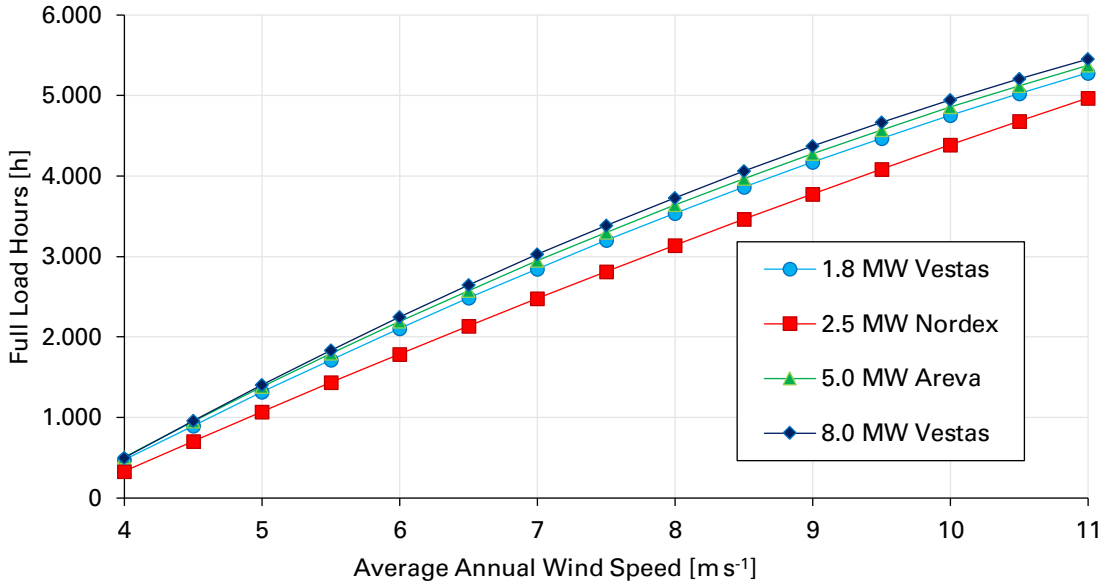

Fig. 20 Average wind speeds and FLH per reference turbine
Source: In reference to [Kup2020a]

The power curves of each onshore wind turbine are utilized to approximate annual energy yield E based on the average annual wind speed. To determine FLH based on particular annual average wind speeds v_a, the average annual energy yield E is compared to the turbine rated power P_r. In result, best-fit correlation equations are determined for each reference turbine, as indicated in **Eq. (4.5)** for Vestas V80 1.8 MW, **Eq. (4.6)** for Nordex N90 2.5 MW, and **Eq. (4.7)** for Areva Multibird 5.0 MW.

$$E_{1800,on} = -26.343v^2 + 1082.4v - 3435.2 \quad (4.5)$$

$$E_{2500,on} = -13.552v^2 + 866.07v - 2916.2 \quad (4.6)$$

$$E_{5000,on} = -29.332v^2 + 1135v - 3559.5 \quad (4.7)$$

The annual energy yield *E*, as calculated in **Eq. (4.5)–(4.7)**, is adjusted for turbine unavailability due to maintenance and repair as well as array efficiency. As proposed by the European Environment Agency (EEA) (2009), an availability factor of $f_a=0.83$ is anticipated for onshore wind turbines [EEA2009]. Assuming improved maintenance and monitoring practices in the scope of the year 2050, an onshore wind availability factor of $f_{a,on}=0.92$ is applied by this analysis.

Wind turbine spacing represents a crucial design parameter to ensure operational safety, wind recovery, and site access. Optimum turbine spacing is based on local wind patterns, prevailing wind directions, and land geography. As recommended by Lütkehus et al. (2012), this analysis considers wind turbine density as a function of turbine size, defining the necessary area per turbine by the specific turbine diameter *D* of 4D-by-4D to ensure adequate wind power plant topologies and to avoid negative performance impacts, such as shadowing issues. [Luetk2012] Due to economic considerations regarding grid connection and total project costs, a minimum plant size of two turbines is required to deploy a wind power plant in a suitable area. The turbine density calculation is adjusted by the factor $T_d=1.5$ to account for the location of turbines along the perimeter of a wind power plant. The total number and arrangement of wind turbines is dependent on natural geometries and prevailing wind directions of specific sites. Due to the holistic scope of this analysis, the presented spacing and siting method represents a rather generalized approach to approximate effective wind power.

The cost analysis of onshore wind projects is based on projected capital expenditures (CAPEX) and operational expenditures (OPEX). In reference to IRENA (2018), baseline onshore wind CAPEX and OPEX are anticipated as $CAPEX_{on}=1{,}520\ EUR\ per\ kW$ and $OPEX_{on}=47.5\ EUR\ per\ kW$ with a lifetime of $t_{yr}=25\ yr$ and investment interest rate of $i=4\ \%$ [IRENA2018b]. In reference to the parametric offshore wind power cost study of Freeman et al. (2016), whose results are anticipated as comparable to onshore wind turbine cost structures, CAPEX and OPEX of onshore wind turbines are adjusted for higher power ratings of large-scale turbines [Free2016]. As for offshore, similar improvements are expected for onshore, but to a lesser degree. Therefore, the 2030 values are utilized for onshore wind turbines. According to **Eq. (4.8)** and **Eq. (4.9)**, larger turbine sizes are adjusted linearly by 2 % cost reduction per kW.

$$CAPEX_{on,adj} = CAPEX - 0.02\ (P_r - 1{,}800) \tag{4.8}$$

$$OPEX_{on,adj} = OPEX - 0.02\ (P_r - 1{,}800) \tag{4.9}$$

To better reflect for economy of scales and continued cost reductions due to maturity of wind power technologies, CAPEX and OPEX are reported to significantly decrease. These cost reductions are projected to have greater effects on larger turbines and, thus, it is anticipated that the offshore cost reductions until 2030 suggested by Freeman et al. (2016) are representative for the onshore cost reductions until 2050. Therefore, CAPEX reduction of $CAPEX_{on,red}$=*1.8 %* and OPEX reduction of $OPEX_{on,red}$=*8 %* per MW are anticipated. [Free2016] The resulting $CAPEX_{on,2050}$ and $OPEX_{on,2050}$ are calculated according to **Eq. (4.10)** and **Eq. (4.11)**.

$$CAPEX_{on,2050} = CAPEX_{on,adj}\ (1 - CAPEX_{on,red} \cdot P) \tag{4.10}$$

$$OPEX_{on,2050} = OPEX_{on,adj}\ (1 - OPEX_{on,red} \cdot P) \tag{4.11}$$

The adjusted calculation of LCOE in reference to the adjusted average annual wind speeds v_a and based on **Eq. (4.1)–(4.11)** is indicated in **Fig. 21**.

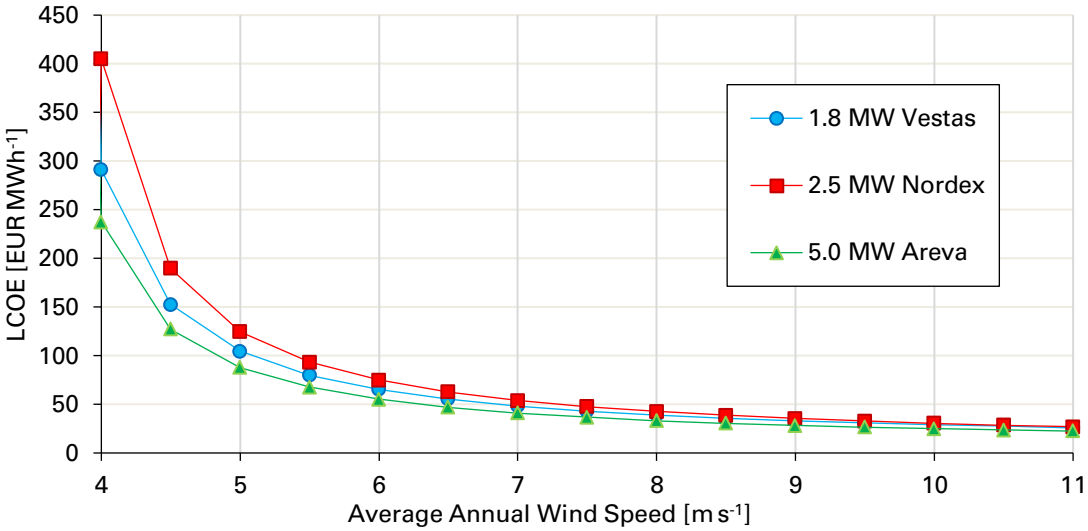

Fig. 21 Average wind speeds and LCOE per onshore turbine
Source: In reference to [Kup2020a]

Onshore wind projects are anticipated to be competitive at LCOE lower or equal to $LCOE_{on} \leqslant 100\ EUR\ per\ MWh$ or approximately 1,600 FLH and more [IRENA2018b].

Suitable Potential Stage

Finally, the general suitability of each land area is accounted for in reference to social and regulatory restrictions. The extent to which available and economically viable land

can be utilized for wind power development is generally less objective than the previously presented factors due to the numerous types of social concerns and the particular attitudes of local communities. As discussed in **Chapter 4.3.5**, the State of Brandenburg is investigated as the reference case to derive social and regulatory attitudes from existing onshore wind site developments and the related practical realization. Based on this reference case, suitability factors are defined and applied across all countries and regions of the ENTSO-E.

Suitability factors additionally impose onshore wind development restrictions by declaring land proportions that can be effectively utilized while maintaining social acceptance and regulatory requirements. In practice, these factors vary among each individual location. However, those site-specific factors are not regarded by this analysis due to the focus on a macroscopic perspective. The applied suitability factors are depicted in **Annex VIII**.

At present, there are only few seaports that have been utilized for onshore wind turbine erection, such as the ports of Hamburg and Rotterdam. In reference to the interference with logistic processes and cranes in operation, a marginal suitability factor is anticipated. Moreover, forested area is not generally prohibited for onshore wind turbine erection due to increased turbine heights that prevent unfavorable turbulences at hub heights and careful site assessments. [Luetk2012] [Free2016]

4.4.2 Offshore Wind Power Plants

To date, most ENTSO-E offshore wind power plants are located in relatively shallow seas on flat seabed in the southern Baltic Sea and the North Sea. However, siting of offshore wind power plants increasingly tends from nearshore shallow waters to offshore deep waters. Prevailing drivers for this development are the lack of space on land and conflict with residents claiming various disturbances from onshore and nearshore wind power plants. Moreover, the quality and yield of wind resources increases with greater distance from shore. Those advantages especially account for areas that are highly exposed to oceanic wind energies, such as the coastal areas of Portugal, Ireland, Scotland, and Norway. Offshore conflicts arise in reference to shipping routes and alternative uses of the seabed, such as fishing, pipelines, and cables. The prevailing environmental concerns regarding impacts on marine life in those areas relate to noise and sedimentation during the construction phase as well as habitat change and noise emissions during the operation phase. [Dahl2014]

As discussed in **Chapter 4.4.1**, the offshore wind potential analysis is based on the same methodology as onshore wind, but with notable differences [NREL2014]. As part of the Gross Potential Stage, first appropriate buffer zones along pipelines, cables, shipping lanes, and oil rigs are generated in ArcMap to create maritime exclusion zones. Consecutively, MATLAB code is used to interpret the resulting spatial data. In comparison to land-based RES technologies, no direct area competition with other

offshore technologies, such as tidal, wave, and ocean technologies or floating PV power plants, is considered as part of this analysis. Offshore wind power development is rather restricted by increasing costs related to the foundation type and distance to shore.

As a basic assumption and to correctly attribute for potential energy conversion, offshore wind turbines are only erected in the exclusive economic zones (EEZ) of each corresponding country. For this analysis, offshore wind power plants are classified and distinguished into the two subsequent mounting technologies.

- Foundation-based offshore wind turbines
- Floating offshore wind turbines

Unlike conventional offshore wind turbines, floating wind turbines enable offshore wind resources to be exploited in regions where ocean depths increase rapidly close to shore and it may facilitate access to deep water zones. Those far offshore sites generally come along with higher wind speeds and energy yield. However, floating wind turbines possess increased costs due to additional cabling and maintenance costs far offshore as well as costs of the floating foundation. Those additional costs must be offset by the superior energy yield that could be realized. [Mil2020]

The depth at which floating wind turbines become economically feasible is estimated from 30–50 m. Potentially attractive deep-water areas can be found close to the southwest tip of England, the Atlantic coast of Spain, and several areas in the Mediterranean. [Mil2020] Based on the European Wind Energy Association (EWEA) (2013), the deployment of foundation-based turbines is designated to depths less than 50 m due to technical and economic limitations. Whereas floating turbine construction is feasible at depths up to 100 m and more, but is likewise limited by several constraints, such as cable sagging and transmission costs. [EWEA2013] For this analysis it is assumed that floating-type turbines will not compete with foundation-type turbines at depths less than 50 m due to the increased costs and floating-type turbines are limited to depths of 100 m due to cable sagging and other technical transmission considerations.

Gross Potential Stage

The development of offshore wind power plants depends on local wind speeds, weather patterns, water depths, soil properties, and maritime ecologies. Considering maritime boundaries, each coastal country controls a specific EEZ as defined by the UN Convention on the Law of the Sea (UNCLOS). The EEZ of each country extends up to 200 nautical miles, which equals 370 km from the coast and delineates an area of national sovereignty and natural resource rights. [UN1994] For this analysis, the offshore electricity production potential of each EEZ is exclusively assigned to the corresponding country. As indicated in **Tab. 7** of **Chapter 4.3.1**, shipping lanes, pipelines, oil and gas wells, platforms, and areas of inhibitive annual ice formations are excluded and accounted for safety distances by specific buffer zones. A comprehensive list of excluded areas and the corresponding buffer zones is depicted in **Tab. 12.**

Tab. 12 Offshore exclusion areas and buffer zones
Source: In reference to [Kash2013] [Luetk2012]

Exclusion Area	Safety Distance
	[m]
Oil and gas pipelines	500
Oil and gas wells	500
Annual ice formations	1,000
Shipping routes	100
CDDA areas	0

In reference to **Tab. 12**, the resulting GIS-based exclusion areas are discussed at the example of the North Sea, as depicted in **Fig. 19**. With 7,600 vessels per year passing the shipping lanes of the North Sea, the North Sea belongs to one of the most frequented oceans in the world and accounts for a majority of seaborn trade. Moreover, plenty of resources are found in the North Sea, among them oil and natural gas as well as fishing resources. In recent years, the North Sea also became a hotspot for the development of offshore wind power sites. [CINEA2018]

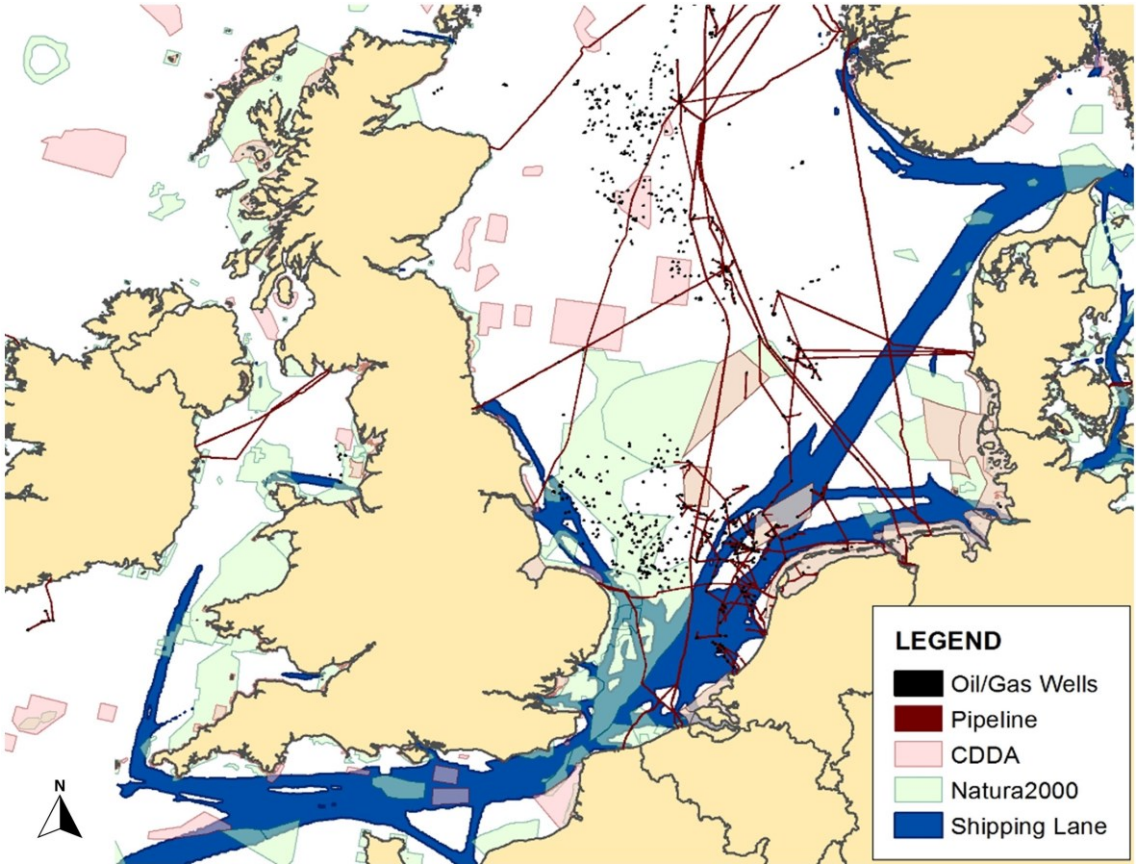

Fig. 22 Offshore exclusion areas in the North Sea

Fig. 19 demonstrates the manifold utilization of the North Sea for transportation, commerce, and natural protection among the adjacent countries. It is obvious, that there are plenty of conflicting interests between the different utilizations of the seabed and ocean surfaces. For instance, offshore wind power development is conflicting with

shipping lanes at the surface as well as pipeline and cable infrastructure on the ocean ground. Thus, the GIS analysis carefully considers those conflicting interests in accordance with the predefined exclusion areas and buffer zones of **Tab. 12**.

Available Potential Stage

Offshore wind projects are anticipated to be more likely socially and politically accepted due to their remote locations. However, offshore wind power plants are still subject to similar social constraints as onshore wind power plants in consideration of aesthetic, ecological, and conflict-of-interest concerns. In this regard, the European Marine Observation and Data Network (EMODnet) maps are compared. The EMODnet data indicates existing offshore wind power plants located in Natura 2000 areas, but offshore wind power plants are strictly omitted in areas due to CDDA classification. [EMO2018] Thus, nationally designated areas (NDA) as part of the CDDA are excluded from offshore wind power development for this analysis.

Additionally, areas designated as habitat or species protection areas in reference to the Natura 2000 databases are generally avoided in favor for the protection of local ecologies and to prevent threats to protected species, but not entirely prohibited. Hence, offshore wind power plant development in Natura 2000 areas is not explicitly excluded. The local authorities rather maintain the responsibility of defining and enforcing maritime protection standards. Therefore, offshore wind power sites are subject to extensive reviews and permitting procedures. For designated Natura 2000 offshore areas, a general availability factor of 5 % is defined to limit, but not completely exclude protected areas for offshore wind power development, as depicted in **Tab. 8** of **Chapter 4.3.2**.

Techno-Economic Potential Stage

Offshore wind power plant costs are predominantly based on turbine type, size, rated power, water depth, and distance to shore as well as operations and maintenance (O&M) costs. Analogous to the onshore wind analysis, costs of different wind turbine dimensions and the corresponding potential annual electricity generation are considered. The annual electricity generation of each maritime area is based on average annual wind speeds, wind flow quality, and wind turbine technology. To account for the annual offshore wind power electricity generation analysis, Areva Multibird 5 MW and Vestas 164 8 MW wind turbines with the corresponding parameters are considered, as indicated in **Tab. 11** of **Chapter 4.4.1**. [NREL2016]

In consideration of the height adjusted annual wind speeds, the correlated FLH of each turbine type are calculated in reference to the specific power and Rayleigh distribution curves, as introduced in **Fig. 20** of **Chapter 4.4.1**. The resulting FLH correlation equations are determined for each turbine based on the turbine power curves and wind distribution curves, as indicated in **Eq. (4.12)** for the Areva Multibird 5 MW and in **Eq. (4.13)** for the Vestas 164 8 MW [NREL2016].

$$E_{5000,off} = -29.332v^2 + 1135v - 3559.5 \quad (4.12)$$

$$E_{8000,off} = -33.572v^2 + 1211v - 3805.6 \quad (4.13)$$

To account for wind turbine unavailability due to maintenance and repair, the annual energy yield E_{off} in MWh as calculated in **Eq. (4.12)** and **Eq. (4.13)** is additionally adjusted. A general availability factor of f_a=*0.81* is recommended for offshore wind turbines. Due to improving maintenance and monitoring practices, the offshore availability factor is estimated as $f_{a,off}$=*0.90* [NREL2016].

In reference to Wind Europe (2017), offshore wind turbine density is based on rotor diameter D. As a basic planning principle, the turbine density per wind power plant is defined as 6D-by-9D [WE2017]. Analogous to onshore wind power development, CAPEX and OPEX are derived from IRENA (2018), with anticipated $CAPEX_{off}$=*4,462 EUR per kW* and $OPEX_{off}$=*114 EUR per kW*. The total lifetime is considered with t_{yr}=*30 yr* and an interest rate of *i=4 %* is assumed. [IRENA2018b] Base costs are adjusted according to turbine size and future cost reduction assumptions for offshore projects. Analogous to the onshore wind power calculation **Chapter 4.4.1**, future CAPEX reductions are anticipated as 1.8 % per MW and OPEX reductions as 8 % per MW [Free2016].

Based on Katsouris and Marina (2016), floating wind turbine designs come along with a 65 % increase in capital costs and 26 % in O&M costs compared to ground-mounted systems [Katso2016]. Thus, CAPEX and OPEX of floating wind turbines are adjusted by the factors $fCAPEX_{float}$=*1.65* and $fOPEX_{float}$=*1.25* to account for increased costs of material requirements as well as anchoring and mooring systems. Moreover, installation and transportation costs of floating wind turbines are regarded as superior compared to those of foundation-based wind turbines. The adjusted LCOE are depicted in **Fig. 23**.

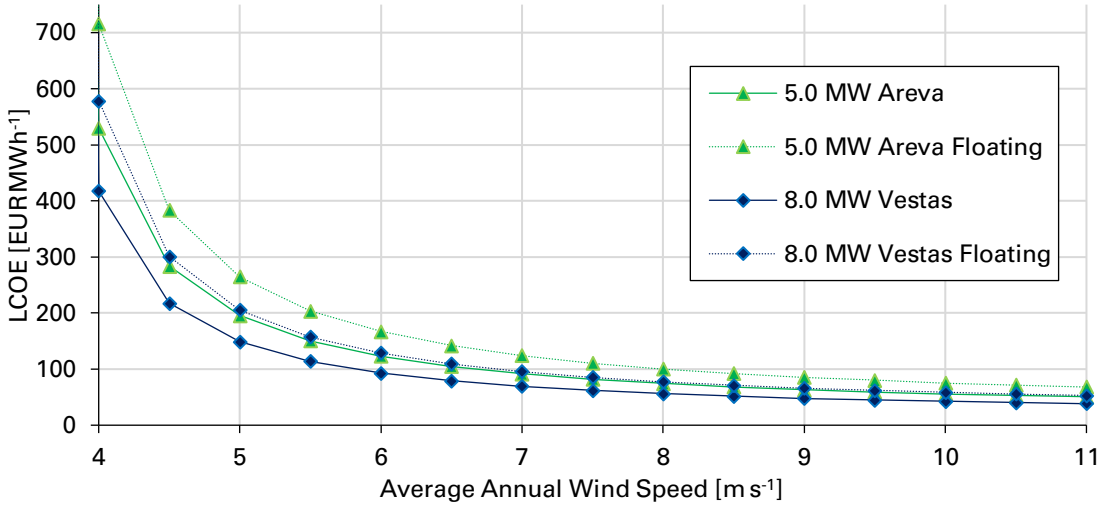

Fig. 23 Average wind speeds and LCOE per offshore turbine
Source: In reference to [Kup2020a]

Offshore wind power plants increase in costs as projects are developed with greater distance from shore. Based on the review of existing offshore wind power plants and in reference to the European Wind Energy Association (EWEA) (2013), LCOE of each marine area and minimum plant sizes are adjusted in accordance with distance from shore and increasing overall costs. The delineated offshore zones 1–4 and the corresponding adjustments are indicated in **Tab. 13**. [EMO2018] [EWEA2013]

Tab. 13 Offshore wind techno-economic adjustments
Source: In reference to [EMO2018] [EWEA2013]

Zone	Distance	LCOE Adjustment	Min. No. Units
	[km]	[EUR MWh^{-1}]	
Zone 1	0…10	0	3
Zone 2	10…30	3	5
Zone 3	30…50	10	10
Zone 4	>50	30	30

As indicated in **Tab. 13**, specific LCOE and offshore wind power plant sizes are assumed to increase with greater distance to shore, due to economic considerations regarding increasing overall and connection costs. The EEZ and the offshore zones 1–4 in the North and Baltic Sea for the adjacent countries Denmark, Germany, and the Netherlands are illustrated in **Fig. 24**.

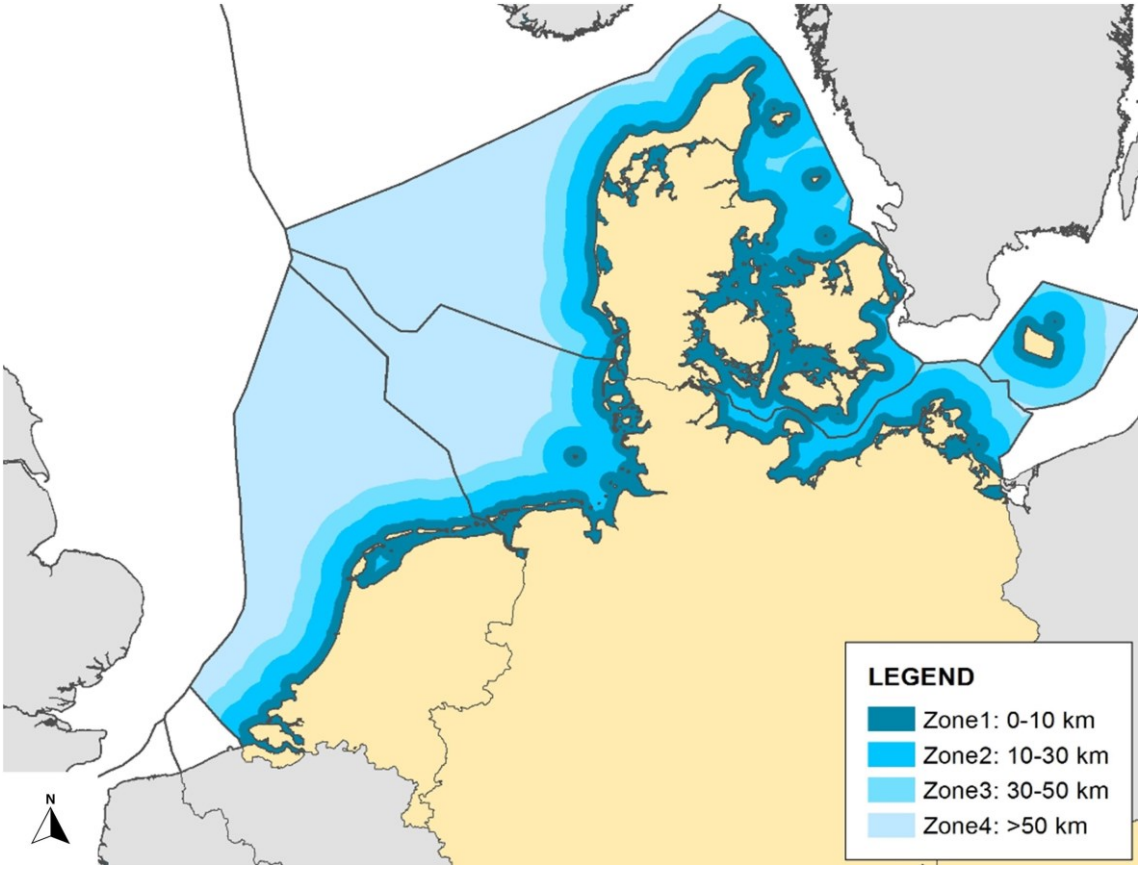

Fig. 24 Distance to shore zones 1–4 in the North and Baltic Sea

To account for wind recovery concerns, wind power plant turbine densities are decreased by 15 % in the case of large wind power plants with total area sizes of more than 10 km^2. As recommended by Beiter et al. (2017) and Wind Europe (2017), maritime areas that possess LCOE lower or equal to 75 EUR per MWh are considered as economically feasible for offshore wind power development. [Bei2017] [WE2017]

Suitable Potential Stage

In order to account for social, economic, and regulatory restrictions, the suitability of each maritime area is considered. Due to numerous types of social concerns, the extent to which available and economically viable maritime areas can be developed is generally less objective than various other factors constraining wind power development. For this analysis, general suitability factors are applied to account for those limitations, such as visual impairment and protection of recreational sites as well as naval training areas and fishing industry conflicts.

In reference to the review of specific suitability factors of the European Environment Agency (EEA) (2009), suitability factors are assigned in relation to distance to shore that is categorized by the distance zones 1–4. Moreover, each zone is adjusted to account for spatial exclusions, such as CDDA and Natura 2000 areas as well as maritime traffic routes. The suitability factors are correlated to the distance from shore according to the offshore zones 1–4, as depicted in **Tab. 14**. [EEA2009]

Tab. 14 Offhore wind suitability factors per shore distance zone
Source: In reference to [EEA2009]

Zone	Distance	Suitability
	[km]	
Zone 1	0…10	0.005
Zone 2	10…30	0.010
Zone 3	30…50	0.015
Zone 4	>50	0.030

4.4.3 Utility-Scale Photovoltaic Power Plants

Recent studies based on satellite data of operational utility-scale solar energy (USSE) plants, foremost represented by photovoltaic (PV) and concentrated solar power (CSP) plants, show that the area use efficiency (AUE) is up to six times lower than initial estimates. The development of USSE is subject to a diversity of constraints. Solar resource constraints entail the solar irradiance in a certain area, geographical constraints refer to slope and the existing use of areas, and regulatory constraints, such as the categorization as Natura 2000 and CDDA, address ecosystem and wildlife preservation concerns. [Ven2021]

Consequently, deserts and dry scrublands with high solar irradiance and generally low suitability for human activities are predestined for USSE developments. However, typical features of those areas, such as the lack of road, electricity, and water infrastructures as well as the remote character, complicate the large-scale construction, operation, and maintenance of USSE power plants. [Ven2021]

Recent analysis shows that USSE in densely populated areas is often developed on arable land that is potentially suitable for other productive uses, such as agriculture or forestry. Even though the simultaneous utilization of arable land for farming and solar energy conversion in the form of the recently emerging agricultural photovoltaic is promising, it is coined with increased costs and intensified land competition analogous to the utilization of arable land for bioenergy crops. Transforming arable land into USSE comes along with local impacts on biodiversity and aesthetic impairment. [Ven2021]

Hence, agricultural PV is addressed by the large-scale PV suitability factors of agricultural CLC areas, as depicted in **Tab. 10**. In the near future, the available rated power of solar PV is likely to overtake that of wind power plants. However, the generally lower capacity factor of PV power plants leads to an inferior total electricity generation. At present, large-scale PV power plants require considerable land area which, in turn, is effectively blocked for alternative utilization. [Mil2020]

Gross Potential Stage

The development of utility-scale PV power plants requires sufficient solar insolation for electricity generation as well as suitable terrain and surface gradation. Areas with excessive shadowing and canopy cover are inherently not suitable for PV power plants. As indicated in **Tab. 7** of **Chapter 4.3.1**, urban, port, and forested areas as well as railways, streets, waterways, lakes, marshes, and bogs are excluded from utility-scale PV development. Moreover, radial buffer zones are applied to those excluded areas to inhibit interference with shadowing effects and aesthetic concerns. Open, accessible, and flat areas, such as arable lands, grasslands, and sparsely vegetated areas, are favorable areas for utility-scale PV developments. In this regard, pastures, croplands, and cultivated areas are considered as potentially suitable.

Utility-scale PV power plants are likewise limited by topographic constraints. Due to limited accessibility and unfavorable terrain, areas with elevations greater than 2,000 m are excluded for PV development. As Europe is located in the Northern hemisphere, all north-facing areas with considerable gradients higher than 1 % average slope per km^2 are excluded due to lack of insolation and shadowing effects. Areas with excessive gradients, as defined with 3 % average slope per km^2 and regardless of geographic aspects, are likewise excluded due to inhibited accessibility and unfavorable conditions for PV power plants. [Ayd2013] [Sliz2013] Those excluded areas due to elevation and slope as well as the average values of the direct normal irradiance (DNI) in W per m^2 at the example of France are illustrated in **Fig. 25**.

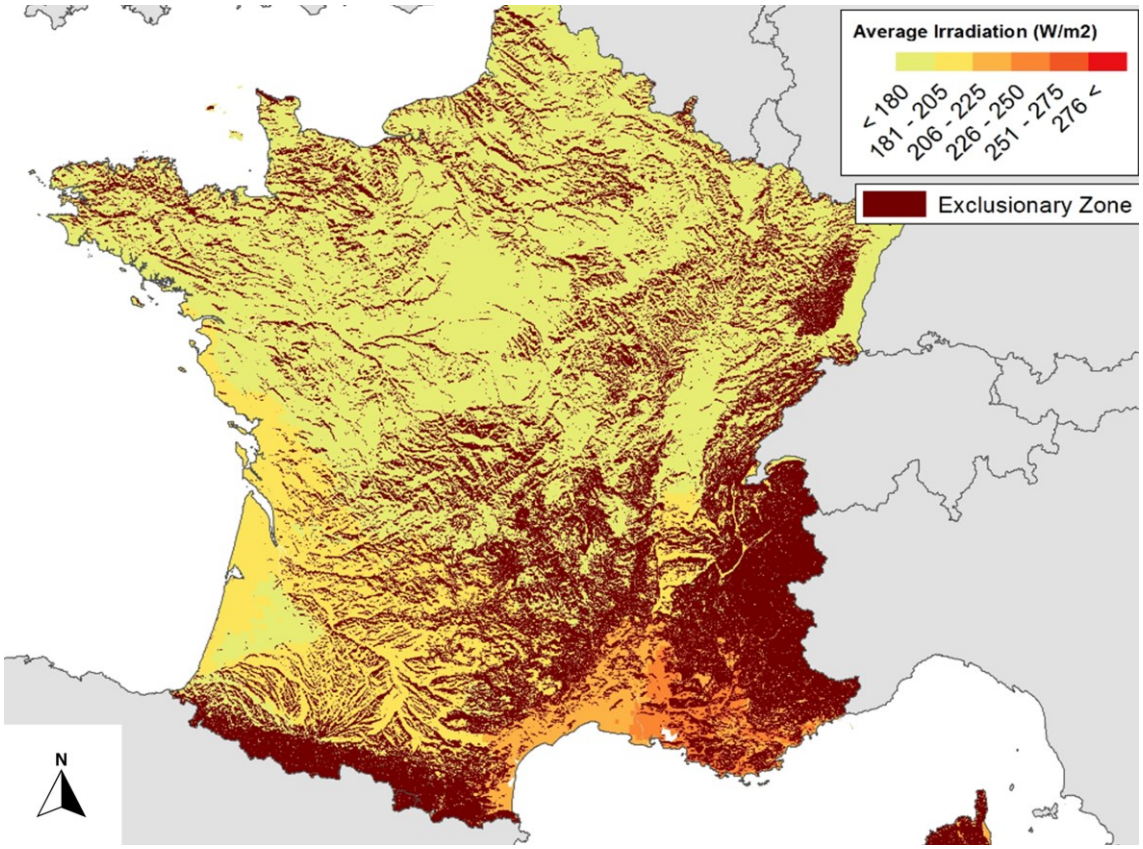

Fig. 25 Elevation and slope exclusion areas and DNI in France

As depicted in **Fig. 25**, utility-scale PV exclusion zones are indicated by dark red surfaces. Utility-scale PV exclusion areas are predominantly found in the high and low mountain ranges, due to elevation and slope. Those areas are identified in the French Alps, the Pyrenees, and the Cévennes. A comprehensive list of excluded land types, buffer zones, and geological constraints is depicted in **Annex VI**.

Available Potential Stage

Due to social, regulatory, ecological, and aesthetic concerns, utility-scale PV in nationally designated areas such as national monuments, parks, and national conservation sites is regarded as taboo in order to prevent the degradation of associated areas and the interference with local habitats. In specific cases, designated areas are not entirely prohibited, but subject to additional restrictions and profound environmental impact assessments (EIA). [Ayd2013] [Sliz2013]

Areas designated as habitat or species protection areas as per Natura 2000 database are largely avoided to protect local ecologies and to prevent negative impacts on local species, such as habitat destruction and migration disruption. For areas designated as either Natura 2000 or NDA/CDDA, specific availability factors are defined to restrict the specific area surface that is available for the spatial analysis. [BMVI2015] The applied availability factors are depicted in **Tab. 8** of **Chapter 4.3.2**.

Techno-Economic Potential Stage

Annual electricity generation from utility-scale PV projects is based on DNI, latitude, panel angle, and panel spacing. This analysis considers ground-mounted systems with a minimum rated power of 250 kW_p and favorably south-facing orientation as utility-scale PV power plants. Utility-scale PV is commonly based on standard 230 W_p panels with an average efficiency of η_p=*0.18* [BMVI2015]. Optimum panel angles are calculated based on the European Photovoltaic Geographical Information System (PVGIS). Total rated power is calculated in reference to the necessary minimum array spacing *S* [EC2017]. The relevant geometric properties of solar elevation and the corresponding array spacing are illustrated in **Fig. 26**.

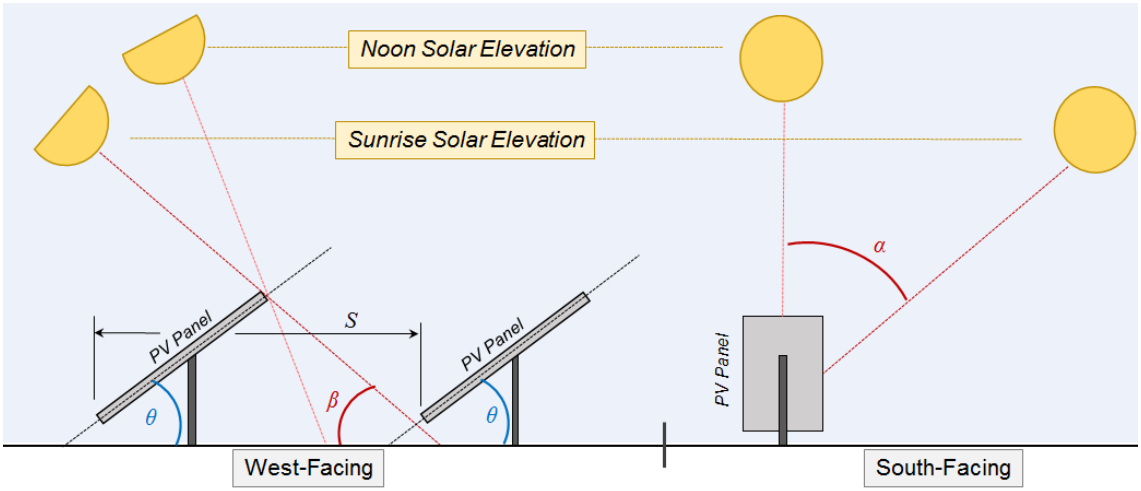

Fig. 26 PV panel array spacing and shading diagram
Source: In reference to [Sliz2013]

As indicated in **Eq. (4.14)**, the calculation of the minimum array spacing *S* per PV panel array is based on geometric properties of the constantly changing solar elevation. The calculation of the minimum array spacing aims at the minimization of shading issues and the corresponding array spacing, in order to increase effective rated power per area unit and utility-scale PV site [EC2018c] [Sliz2013].

$$S = \left(\frac{2\mathrm{L} \cdot \sin(\theta)}{\tan(\beta)}\right) \cdot \cos(\alpha) + L \cdot \cos(\theta) \tag{4.14}$$

As depicted in **Eq. (4.14)**, *L* delineates the solar panel length in m, Θ the panel tilt in (°), α the azimuth in (°), and β the solar elevation angle in (°) [Sliz2013]. To account for typical European solar elevations, irradiation and shading data from seven representative locations, which are well dispersed across latitudes and longitudes, are analyzed based on the boundary condition that constraints the effective operating time of PV power plants from 8 AM to 4 PM in February. The representative locations and the corresponding parameters in reference to **Fig. 26** are depicted in **Tab. 15**.

Tab. 15 Representative European solar locations and parameters
Source: In reference to [EC2017] [SM2019] [UO2007]

City	Location	Latitude	Longitude	Solar Elevation	Optimum Angle	Azimuth (180°)
		ϕ	λ	β	θ	α
Athens	GR	37.98° N	23.72° E	16.0°	32.0°	62.0°
Madrid	ES	40.42° N	3.69° W	14.5°	36.0°	61.0°
Rome	IT	41.89° N	12.49° E	14.0°	36.0°	62.0°
Paris	FR	48.86° N	2.35° E	10.0°	38.0°	60.0°
London	UK	51.51° N	0.13° W	9.0°	38.0°	59.0°
Berlin	DE	52.52° N	13.38° E	9.0°	38.0°	59.0°
Hamburg	DE	53.55° N	10.00° E	8.0°	38.0°	59.0°

In reference to **Tab. 15**, the irradiation and shading data from the dispersed European locations, based on the 8 AM to 4 PM operations schedule in February as the worst-case shading design and the spacing variable *S*, the relationship *K* between location, latitude, and realizable power is derived. As depicted in **Eq. (4.15)**, *K* represents the effective power per area in kW_p per ha and *x* the degree of latitude in (°). [EC2018c]

$$K = 3331.3 \cdot e^{-0.036x} \tag{4.15}$$

The resulting realizable rated power in kW_p per ha and the geographic reference to the corresponding latitude is depicted in **Fig. 27**.

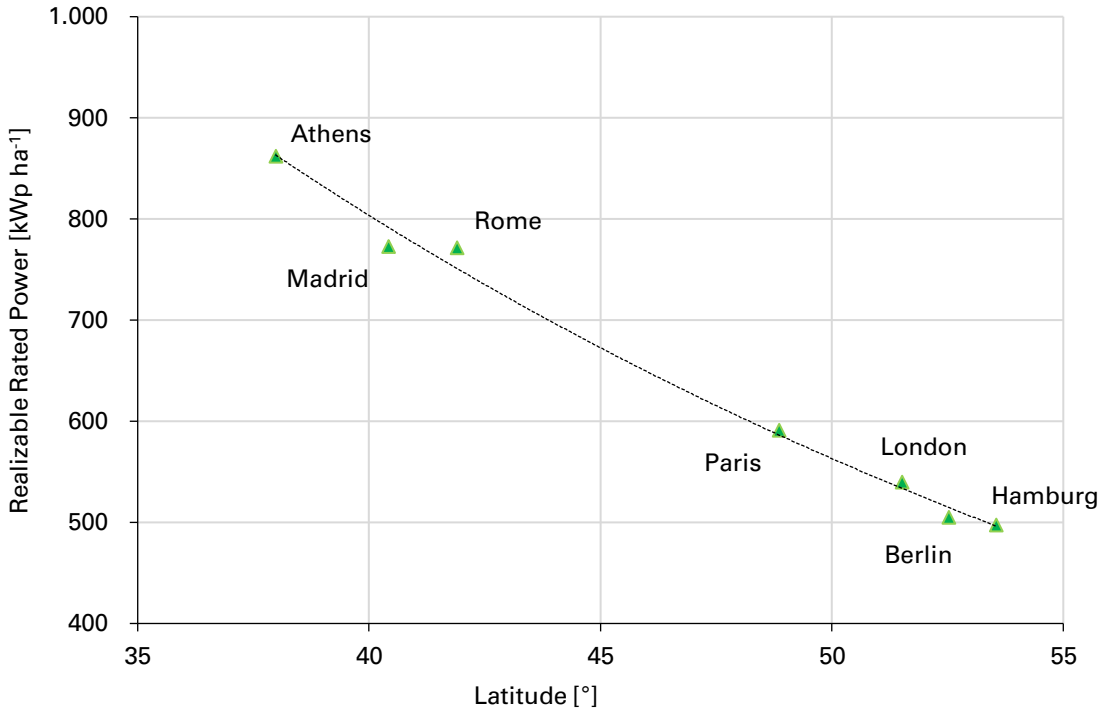

Fig. 27 Realizable PV rated power and latitude

The calculation of the effective PV panel area A_{PV} in **Eq. (4.16)** entails the effective power per area K and the site access factor η_a. To best account for additional space necessary for site access, construction, and maintenance, the average site access factor is anticipated as $\eta_a=0.65$. [EC2018c] [Sliz2013]

$$A_{PV} = K\left(\frac{1.632}{0.23}\right)\eta_a \tag{4.16}$$

The calculation of annual electricity generation E in **Eq. (4.17)** in kWh for each land area is based on the calculation of the average annual direct normal irradiance *DNI* in kWh per m², utilizable PV surface area A_{PV} in m², panel efficiency $\eta_{PV}=0.18$, and overall production factor $\eta_p=0.85$ to account for inadvertent shading, temperature coefficients of PV cells, total system losses, and general system availability [EC2018c] [Sliz2013].

$$E = \mathrm{DNI} \cdot A_{PV} \cdot \eta_{PV} \cdot \eta_p \tag{4.17}$$

As indicated in **Eq. (4.18)**, the full load hours (FLH) are calculated based on annual electricity generation E in kWh and the rated power P_r in kW_p [EC2018c] [Sliz2013].

$$FLH_{PV} = \frac{E}{P_r} \tag{4.18}$$

CAPEX and OPEX of utility-scale PV power plants are dependent on project size, location, and layout. The decreasing project costs of PV power plants due to economy of scales leads to increasing shares of O&M costs in total investments. In reference to Vartiainen et al. (2015), future CAPEX and OPEX are estimated as indicated in **Tab. 16**. The average project lifetime of utility-scale PV power plants is estimated as $t_{yr}=30\ yr$ and an interest rate of $i=5\ \%$ is anticipated. [Vart2015]

Tab. 16 Utility-scale PV CAPEX and OPEX
Source: In reference to [Vart2015]

Category	1 MW_p	50 MW_p
	EUR kW_p^{-1}	EUR kW_p^{-1}
CAPEX	380	300
OPEX	10	7.50

In consideration of future cost and project improvements, for this analysis $CAPEX_{USPV}=380\ EUR\ per\ kW_p$ and annual $OPEX_{USPV}=10\ EUR\ per\ kW_p$ are anticipated. The final LCOE for utility-scale PV power plants are calculated in reference to **Eq. (4.1)** of **Chapter 4.3.3**. The competitive LCOE by 2050 are estimated as 30 EUR per MWh in favorable areas [Vart2015]. Therefore, a general competitive $LCOE_{USPV} \leq 45\ EUR\ per\ MWh$ for utility-scale PV power plants is assumed.

Suitable Potential Stage

The suitability for utility-scale PV power plants of each land area is considered in order to account for regulatory and social limitations. Due to the numerous types of social concerns and the wide range of attitudes of local inhabitants, the extent to which available and economically viable land could be utilized is generally less objective than various other factors constraining utility-scale PV development.

Those areas that are suitable for utility-scale PV but not for onshore wind developments are regarded with a higher suitability factor to better represent areas, such as the peripheral areas alongside highways and railways, that are predestined locations for utility-scale PV development. The chosen suitability factors effectively define utility-scale PV development limitations by defining the extent to which a particular area is available, while maintaining social and regulatory acceptance. In practice, these factors may vary among each specific location. The applied suitability factors for utility-scale PV power plants per CORINE Land Cover (CLC) type are depicted in **Annex VIII**.

4.4.4 Concentrated Solar Power

Concentrated Solar Power (CSP) plants exploit the thermal energy of solar radiation to generate electricity. CSP is a rapidly growing renewable energy source with excellent predictability and dispatchability. There are various CSP technologies, such as parabolic trough, linear Fresnel, and solar towers as well as dish Stirling and solar chimney CSP plants. In 2016, more than 36 CSP plants of various sizes with a total rated power of 2.6 GW had been installed in the EU. This represents a share of more than 50 % of the 5.1 GW global CSP capacity. However, the development of CSP plants is facing strong financial pressures and only some areas with superior DNI are economically suitable. [Papa2018] Hence, CSP development is restricted to the limited number of countries with high levels of DNI, as represented by Greece, Portugal, and Spain.

As this analysis focuses on future large-scale CSP projects, only the parabolic through (PT) design is considered, due to its superior maturity and cost reduction potential. The reflective aperture size of CSP plants compared to the area necessary to provide the rated power, is defined as the solar multiple (SM). *SM=1* (SM1) describes a system with sufficient reflective area that is necessary to reach the rated system power, whereas *SM>1* describes a system with more than the necessary reflective area, which allows for excess production that can be thermally stored. SM are defined for 1 MW rated power with an electrical efficiency $\eta_{el}=0.15$ and a roundtrip efficiency for heat storage $\eta_{h}=0.12$ regarding the corresponding area size *A*. [IRENA2012] [Trieb2009]

- $A_{SM1} = 8{,}000 \frac{m^2}{MW_p}$
- $A_{SM2} = 16{,}000 \frac{m^2}{MW_p}$
- $A_{SM3} = 24{,}000 \frac{m^2}{MW_p}$

Analogous to the method for utility-scale PV plants of **Chapter 4.4.3**, the CSP potentials are analyzed and computed. However, notable topographic restrictions and divergent potentials are accounted for, as indicated in **Tab. 7** of **Chapter 4.3.1**. The resulting spatial data and corresponding DNI is interpreted within MS Excel worksheets. Due to the highly restrictive nature of CSP development and probability-based suitability factors for both onshore wind and utility-scale PV, CSP is not considered to be in area competition with other land-based RES technologies. To ensure economic feasibility and to provide effective means of energy storage, this analysis assumes a minimum project size of 50 MW_p rated power with storage (SM2), whereby projects can range up to 100 MW_p rated power with storage (SM3). Annual electricity generation is calculated via rated power in MW_p, average annual DNI in MWh per m^2, storage capacity SM2 and SM3 as well as plant electrical and storage-to-electrical round-trip efficiency in percent.

Gross Potential Stage

CSP plant siting requires significant amounts of space and suitable topography, such as flat and stable soil, as well as sufficient DNI. In this regard, areas that are excluded from CSP development are comparable to those excluded from utility-scale PV plants. A complete list of excluded land types and buffer zones is depicted in **Annex VII**. In consideration of land-use, the excluded land categories comprise areas such as forested areas, ports, and urban areas. In consideration of topography, land with no or minimal sloping with not more than 3 % slope per km^2 is necessary and must exhibit the defined minimum dimension to be of adequate size. Therefore, potential land areas are analyzed topographically regarding suitable land arrangement by comparing land area to its circumference. By this means it is ensured that selected areas are not irregularly shaped. Based on siting and average annual DNI, the resulting potential CSP sites at the example of the Spanish regions Andalusia and Murcia are depicted in **Fig. 28**.

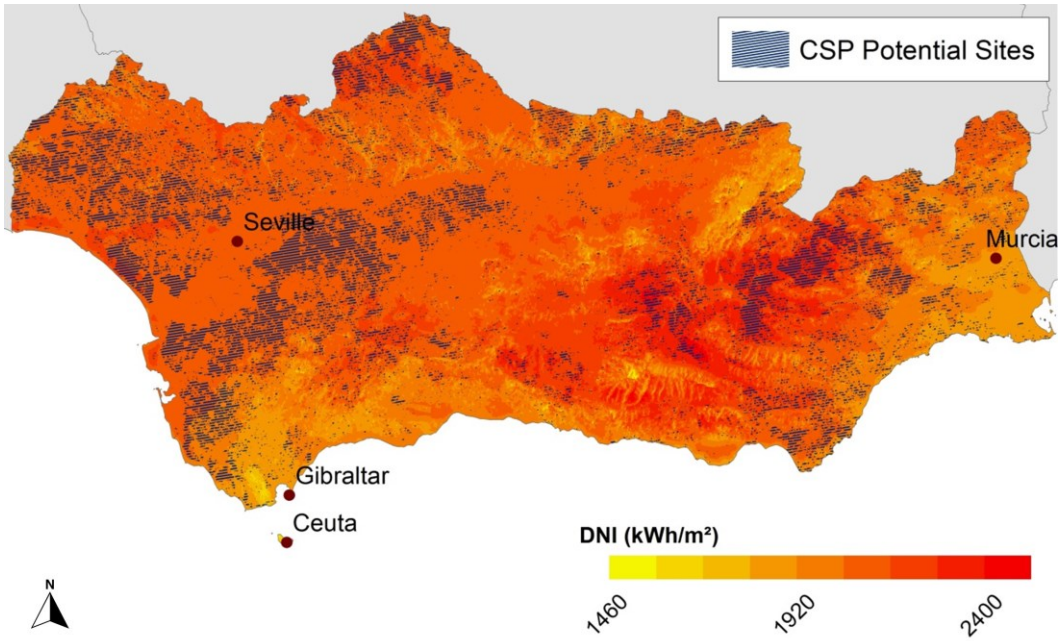

Fig. 28 Potential CSP sites in Andalusia and Murcia

Available Potential Stage

In comparison to other RES technologies, CSP plants are exceptional large and inherently intrusive. Therefore, only some areas with high DNI and no specific area utilization for alternative purposes are potentially suitable. Those areas are typically represented by sparsely vegetated areas and deserts. Thus, all land areas of ecological, biological, political, or national concern, especially those under the Natura 2000 and CDDA categorization, are not regarded as potentially viable and, therefore, excluded.

Techno-Economic Potential Stage

Based on IRENA (2012) and Kost et al. (2013), status quo costs for CSP power block investments are anticipated to decrease slightly and costs for operations and maintenance (O&M) as well as solar field and storage will reduce by 30–45 %. CAPEX is based on rated power in EUR per kW, project size in EUR per kW_{SM}, storage capacity in EUR per kWh, and overall electricity generation in EUR per kWh. [IRENA2012] [Kost2013] In reference to the advantageous energy storage potential of CSP, a competitive $LCOE_{CSP} \leqslant 120\ EUR\ per\ MWh$ is anticipated for the final calculation, as introduced in **Chapter 4.3.3**.

Based on the standard CSP plant SM1 it is anticipated that a solar field with an area A_{SM1} of 8,000 m^2 is sufficient to supply a 1 MW rated power CSP plant. CSP annual electricity generation E_{CSP} is based on DNI, specific solar-multiple, and electrical and storage efficiencies, as indicated in **Eq. (4.19)**.

$$E_{CSP} = A_{SM1} \cdot P \cdot DNI \cdot \eta_{el} + (SM - 1) \cdot A_{SM1} \cdot P \cdot DNI \cdot \eta_{sto} \tag{4.19}$$

In **Eq. (4.19)**, P represents the CSP plant's rated power in kW, DNI the average direct normal irradiation in kW per m^2, η_{el} the plant electrical efficiency, SM the solar multiple category, η_{sto} the storage-to-electrical efficiency, and A_{SM1} the solar field area for SM1 CSP plants. The CSP full load hours FLH_{CSP} are calculated based on annual electricity generation E_{CSP} in kWh and the rated power P_r in kW, as indicated in **Eq. (4.20)**.

$$FLH_{CSP} = \frac{E_{CSP}}{P_r} \tag{4.20}$$

CSP plants comprise various components with different capital and O&M costs as well as potential cost reductions until 2050. Those cost components and reduction potentials are depicted in **Tab. 17**.

Tab. 17 CSP plant component cost reduction potential
Source: In reference to [IRENA2012] [Kost2013] [Trieb2009]

Cost Component	Abbreviation	Costs	Unit	Cost Reduction 2050
Power block	C_{PB}	1,050	EUR kW^{-1}	5%
Project planning	C_{PR}	1,800	EUR kW^{-1}	15%
Storage unit	C_{ST}	100	EUR kWh^{-1}	45%
Solar field	C_{SF}	2,025	EUR kW^{-1}	40%
O&M	C_{OP}	0.04	EUR kWh^{-1}	30%

In order to calculate the LCOE for CSP plants in reference to **Eq. (4.1)** of **Chapter 4.3.3**, the initial capital costs I in EUR are calculated as indicated in **Eq. (4.21)**. Whereas C_{PB} represents the power block costs and C_{PR} the project planning costs in EUR per kW, P the rated power in kW, SM the solar multiple category, C_{ST} the storage unit costs in EUR per kWh, and C_{SF} the solar field costs in EUR per kW_p.

$$I = C_{PB} \cdot P + C_{PR} \cdot P \cdot SM + 6 \cdot C_{ST} \cdot (SM - 1) + C_{SF} \cdot P \cdot SM \tag{4.21}$$

As indicated in **Eq. (4.22)**, the O&M costs $R_{O\&M}$ are calculated based on specific costs, energy yield, and rated power. Whereas C_{OP} represents the total O&M costs in EUR per kWh, E_{CSP} the annual electricity generation in kWh, and P the rated power in kW.

$$R_{O\&M} = \frac{C_{OP} \cdot E_{CSP}}{P} \tag{4.22}$$

Suitable Potential Stage

Analogous to the utility-scale PV analysis of **Chapter 4.4.3**, the suitability for CSP plants of each land area is considered in order to thoroughly account for social and regulatory limitations. Due to numerous social concerns, local objections, and energy policies, the extent to which available and economically viable land can be utilized is generally less objective than the topographic factors constraining CSP developments. The applied suitability factors effectively define specific potentials of CSP plant developments by declaring the extent to which each land category is likely to be utilized for CSP plant developments while maintaining social and regulatory acceptance.

Therefore, arable land, grassland, and pastures as well as heathland, shrubland, and sparsely vegetated areas are considered as viable areas. In practice, suitability factors vary strongly among each individual location, based on the specific preferences and policies of local communities. The applied suitability factors are depicted in **Annex VIII**.

4.4.5 Photovoltaic and Solar Thermal Rooftops

Large shares of private and commercial buildings show a significant proportion of unoccupied roof space. Most of those buildings possesses a demand for heat and electricity. Hence, rooftops are suitable for PV and solar thermal panel installations. To effectively supply heat and electricity demands, annual solar-based energy conversion from rooftops considers both technologies. Analogous to the restrictions for utility-scale PV power plants, solar resource constraints for PV and solar thermal panels entail the annual DNI in a certain area and the land and area use efficiency (AUE). The limitation of AUE due to roof-access, chimneys, and windows reduces the effective potential of solar panel installations on rooftop spaces. Therefore, the potential solar rooftop production is dependent upon daylight hours, season, solar elevation patterns, roof tilt, available roof space, and shadowing effects. [Laem2017] [Ven2021]

In consideration of the actual available roof space that varies by region, building type, and roof type, an average rooftop availability is considered. Unlike the analysis of utility-scale PV in **Chapter 4.4.3** and CSP in **Chapter 4.4.4**, the solar rooftop analysis is not performed in the Primary Sources stages as introduced in **Chapter 4.3**, but rather based on an empiric analysis, which considers the specific population density in relation to average rooftop area per capita. Therefore, the potential effective rooftop area is derived from the International Energy Agency (IEA) (2016), that developed an empiric general relationship method between population density and effective rooftop area [IEA2016]. The corresponding population density p_d of each country is indicated by the population density map and the related population categories in **Fig. 29**.

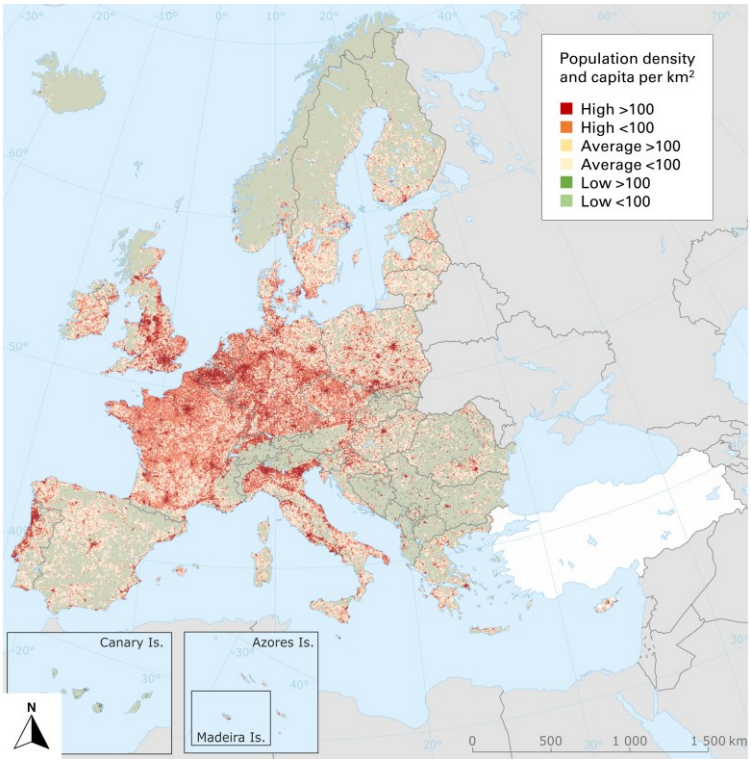

Fig. 29 Population density and capita per km²
Source: In reference to [EEA2018b]

As depicted in **Fig. 29** and in reference to Eurostat (2018c), the specific population density of each region is derived for the Level 3 classification of the Nomenclature of Territorial Units for Statistics (NUTS) [EUROS2018c]. The effective rooftop area is determined with the corresponding average annual irradiance derived from PVGIS [EC2017]. Based on average heat demand per household, 1.5 m² of the available rooftop area per capita is allocated to solar thermal production and anticipated to be sufficient to meet the general heat demand. The remaining space is designated for PV panel installation [BMVI2015] [Sliz2013]. The correlation between population density p_d in capita per m² and available rooftop area $A_{r,el}$ in m², excluding space for rooftop access and miscellaneous rooftop components, is described in **Eq. (4.23)** [IEA2016].

$$A_{r,el} = 172.3 \cdot p_d \cdot e^{-0.352} \tag{4.23}$$

Annual electricity generation from rooftop PV $E_{r,el}$ comprises the available rooftop area $A_{r,el}$ in m², annual *DNI* in kWh per m², and panel efficiency $\eta_{r,el}$*=0.14* [Laem2017]. In comparison to utility-scale PV, rooftop PV panel efficiency is generally inferior due to increased specific investment costs and various constraints for performance parameters related to rooftop installation, as indicated by $\eta_{r,el}$ in **Eq. (4.24)**.

$$E_{r,el} = A_{r,el} \cdot DNI \cdot \mu_{r,el} \cdot a \tag{4.24}$$

As depicted in **Eq. (4.24)**, average PV panel electricity generation $E_{r,el}$ is adjusted with the location adjustment factor a linearly between 40–80 % based on latitude *lat* in (°), to account for lesser availability due to shading and rooftop pitch angles as latitude increases. The calculation of a is depicted in **Eq. (4.25)**. [Laem2017]

$$a = -\frac{4}{3} lat + 86 \tag{4.25}$$

Analogous, solar thermal production $E_{r,th}$ is based on the available rooftop area $A_{r,th}$ in m², annual *DNI* in kWh per m², panel efficiency $\eta_{r,th}$*=0.65*, and the general availability factor f_a*=0.25* [Laem2017], as depicted in **Eq. (4.26).**

$$E_{r,th} = A_{r,th} \cdot DNI \cdot \mu_{r,th} \cdot f_a \tag{4.26}$$

Unlike the calculation of $E_{r,el}$, the calculation of $E_{r,th}$ as indicated in **Eq. (4.26)** is not adjusted to latitude in order to account for inferior shading issues and direct irradiance requirements of solar thermal panels. Rooftop PV and solar thermal are analyzed using micro-regional data according to the NUTS Level 3 classification for population, population density, geographic area, optimal tilt angle, and solar irradiation. The regional data set is exported in MS Excel and processed according to the methods discussed in **Chapter 4.3.3** and **Chapter 4.4.3**. Due to economic considerations, solar rooftop systems are anticipated to be restricted to areas with at least 1,000 FLH.

4.5 Secondary Sources Potential Analysis

4.5.1 Bioenergy

Bioenergy represents the oldest known and most widespread energy source across the world. There are numerous sources of bioenergy which vary on a regional level in availability and scale of utilization. Generally, biofuels can be classified into first generation (1G), second generation (2G), and third generation (3G) biofuels. 1G biofuels are sourced from starch, sugar, and oil of various plants, such as beet, corn, rapeseed, and soy plants. Those plants can be processed to produce biofuels, such as bioethanol and biodiesel. 2G biofuels, such as biomethane and cellulose ethanol, stem from different byproducts and crops that require additional processing to extract biofuels. Those byproducts comprise various forest residues, straw, bagasse, waste vegetable oil, and municipal solid waste. [Lack2017] [Rast2019]

3G biofuels are based on algae that is produced in ponds, tanks, or in the open sea. Algal fuel production is coined with high yields and minimal impact on freshwater resources. However, algal fuel production comes along with high energy input and demand for fertilizers. Moreover, algal fuels show a more rapid degradation than other biofuels. [Lack2017] [Li2013] Due to the immature and non-economic character, 3G biofuels are not further regarded by this analysis.

The availability of land and resource commitments for 1G and 2G bioenergy products is dependent upon land availability and legal restrictions as well as soil and climate suitability. The major restrictive factor is found in the global land use competition among food crops and energy crops. According to the model assumptions of the European Environmental Agency (EEA) (2013b) and Ruiz et al. (2015), the available resources of energy crops, such as sugar beet, forest residues, and oil crops, are converted into bioenergetic products via conversion processes, such as fermentation and transesterification. [EEA2013b] [Ruiz2015]

For this analysis, the energy yield of crops as energy source is considered in a holistic potential analysis. The major restrictions for energy crops are identified in the competition with food crops and the potential low energy density of biofuels. In reference to Ruiz et al. (2015), the calculation of potential bioenergy yields is based on the availability and restrictions of each country, taking into account land-use conflict, fuel demand, and fuel prices. In consideration of the three scenarios of the original study, the Low Bioenergy Scenario is referenced due to the aforementioned hard restrictions for 1G and 2G biofuels in Europe. The underlying assumptions for the Low Bioenergy Scenario comprise the subsequent criteria. [Ruiz2015]

- Strong sustainability criteria for biofuel production
- Low levels of stimulation measures for the production of biofuels
- Focus on efficient utilization of biomass, rather than mass application

Based on the Low Bioenergy Scenario, the annual biofuel potential is determined for each country, delineated by bioenergetic fuel type and the calorific value of each biofuel source. The biofuel potential is calculated in PJ per year, based on the specific conversion efficiencies as indicated in **Tab. 18**.

Tab. 18 Type of biofuel and conversion efficiency
Source: In reference to [Ruiz2015]

Type of Resource	Final Bioenergy Product	Type of Conversion	Conversion Efficiency
Sugar Beet	Ethanol	1G Fuel	0.70
Rapeseed	Bio-Diesel	1G Fuel	0.70
Oil Crops	Bio-Diesel	1G Fuel	0.70
Starchy Crop	Ethanol	1G Fuel	0.70
Grass Crop	Biomass	CHP	0.85
Willow	Biomass	CHP	0.85
Poplar	Biomass	CHP	0.85
Manure	Biogas	Gasification	0.80
Primary Residuals	Biogas	Gasification	0.80
Round Wood	Biomass	CHP	0.85
Primary Forestry	Biomass	CHP	0.85
Forestry Chips	Biomass	CHP	0.85
Forestry Sawdust	Biomass	CHP	0.85
Forestry Landcare	Biomass	CHP	0.85
Municipal Waste	Biomass	CHP	0.85
Sludge	Biogas	Gasification	0.80

4.5.2 Hydropower

Hydropower accounts for nearly 20 % of the global electricity supply and in several countries, such as Albania, Iceland, Latvia, Norway, Sweden, and Switzerland, hydropower represents the dominant source for electricity generation. Hydropower plants are generally classified into small hydropower plants (SHP) and large hydropower plants (LHP). LHP are categorized with a high rated power of 100 MW and more, that also involve the construction of dams and possess a significant storage capacity. However, those large-scale hydropower plants come along with severe impacts on the environment and local communities, such as described in the following. [Jia2017]

- Loss of habitat due to construction and land inundation
- Altered river flows and natural flooding cycles
- Diminishing water quality and aquatic ecology
- Displacement of people and communities
- Structural dam failure risks

Due to the negative impacts and the already high utilization of potential LHP sites, the general potential for further large-scale hydropower plant development in Europe is regarded as very restricted. However, there are significant potentials for small-scale hydropower plants. SHP are usually referred to as run-of-river or reservoir systems that

possess only little or no storage capacity and a rated power of less than 10 MW. Those run-of-river systems may also impact the environment, but to a much lesser and more controllable degree than LHP. Therefore, SHP are regarded as a potential and untapped renewable energy source in Europe. [Jia2017]

As the existing hydropower infrastructure in the ENTSO-E is at a well-developed stage, the already exploited potentials are referenced as the baseline for this analysis. Most of the remaining potential for the extension and development of hydropower can be found in run-of-river and reservoir SHP. The utilization of pumped-storage hydroelectricity (PSH) plants is excluded from this analysis as it is not regarded as a source of primary energy, but rather a means of energy storage.

For this analysis, the hydropower extension scenarios as projected by Capros et al. (2016) are considered as a liberal estimate of future hydropower potential in TWh per year [Cap2016]. The hydropower potentials of the non-EU countries are based on the analysis of the International Hydropower Association (IHA) (2017) [IHA2017].

4.5.3 Geothermal Energy

Unlike most renewable energy sources that are directly or indirectly derived from solar radiation, geothermal energy refers to the thermal energy generated and stored in the earth crust. The geothermal energy originates from the original formation of the planet and from radioactive decay processes. Geothermal energy is regarded as the most stable renewable energy source due to its constant utilization factor, which is independent from weather and seasonal influences. Moreover, geothermal energy can be utilized for electricity generation and heat production in district heating networks. [Mura2017]

Geothermal energy utilization is typical for countries with volcanic activity and high temperature basins, such as Iceland and Italy. More recently, less volcanic countries, such as France, Germany, and Switzerland, developed geothermal power plants within the enhanced geothermal system (EGS) concept. EGS is capable to generate electricity without the need for high grades of natural convective hydrothermal resources and naturally occurring heat, water, and rock permeability. Generally, geothermal power generation is classified into the two subsequent technologies. [Mura2017]

- Steam flash power generation from high-temperature of 150–370 °C
- Binary cycle power generation from low-temperature of 50–200 °C

In reference to non-residential large-scale EGS projects, the development of the geothermal energy sector in the ENTSO-E is projected as low-temperature binary heating systems, due to the economic potential and maturity of the technology. Future geothermal potentials as reported by Angelino et al. (2013) are anticipated by this analysis. On that basis, significant geothermal potential with LCOE less than 100 EUR per MWh are anticipated. [Angel2013] [Klaus2010]

According to Klaus et al. (2010), Germany shows a technical potential of 312 TWh per year for geothermal electricity production [Klaus2010]. However, the technical potential is not applicable due to economic considerations. The investigation rather implies, that

a current-guided conversion process is only economical, when the residual heat of low-temperature EGS is utilized for heating purposes. Therefore, the utilizable technical potential is further reduced to a gross production of 66 TWh per year and, in consideration of the self-consumption of each EGS plant, to a net production of 50 TWh per year. This represents a total reduction in the technical potential of 84 %. Analogous, Kirchner (2011) proposes a total gross potential of 300 TWh per year, which is likewise decreased to 66 TWh per year due to economic considerations and the present total heat demand in German district heating networks. Therefore, a reduction of 78 % is regarded as robust and applicable. [Kirch2011]

To carefully account for economic and technical limitations of the use of geothermal energy, the potentials proposed by Klaus et al. (2010) are considered by this analysis. Thus, the geothermal potentials of each ENTSO-E country investigated by Angelino et al. (2013) are scaled down by 84 %. Moreover, thermal energy production is anticipated as 2:1 ratio in comparison to electricity generation. For the non-EU countries of the ENTSO-E Bosnia and Herzegovina, Iceland, Norway, Serbia, and Switzerland, the geothermal energy potential is based on van Wees et al. (2013) [Wees2013]. North Macedonia possesses an economic potential of up to 600 GWh per year [Popo2004]. According to Nádor (2014) and Frasheri (2015), the deep geothermal potential for Albania and Montenegro is only marginal and not relevant [Nado2014] [Frash2015].

4.5.4 Hydrokinetic Energy

Another and more latent form of hydropower is called hydrokinetic power and refers predominantly to wave, current, and tidal power plants. Those power plants utilize the kinetic energy of the water flowing in oceans and rivers to generate electricity. Other forms, such as ocean thermal energy conversion (OTEC) and osmotic power plants are not regarded by this research due to their very conceptional nature. [Jia2017]

The continued development of marine-based electricity production illustrates the potential role of wave, current, and tidal technologies for future RES-based electricity generation [Ham2011]. Even though those novel technologies show technical potential, the sector largely remains in developmental and scaling stages. Reasons for the uncertainty of hydrokinetic potentials are found in the complexity of the mechanical engineering required to convert the oscillatory motion of the waves into a rotary motion that is needed for the generation of electricity. Moreover, the industrial interests in those technologies, which lack behind more mature technologies such as offshore wind power, is not yet commercialized. [Mil2020] Due to the unavailability of data regarding technical, economic, and spatial potentials, no geo-spatial analysis is performed.

As an assumption, it is postulated that the ENTSO-E countries that include hydrokinetic power technologies in their National Renewable Energy Action Plans (NREAP) will be able to double their 2020 NREAP goals by the year 2050. Those countries comprise France, Ireland, Portugal, Spain, the Netherlands, and UK. [JRC2018]

Beside those high potential countries, also Italy, Denmark, and Sweden exhibit considerable hydrokinetic energy development potential, albeit at lower levels. As an estimate, each of the three countries is anticipated to possess a total hydrokinetic electricity generation potential of 0.25 TWh per year. [JRC2018]

Unlike the optimistic potentials for hydrokinetic energy as proposed by some studies, such as Hammons (2011) who assumed more than 100 TWh per year for Western Europe [Ham2011], the assumptions made for this analysis are liberal and highly optimistic in consideration that hydrokinetic electricity generation accumulated to 0.47 TWh in 2007 and to 0.50 TWh in 2016 [EC2018a]. Therefore, the proposed potentials of IRENA (2014), which project the hydrokinetic electricity production potential to 4 TWh for the entire EU-28 by 2030, appear more applicable [IRENA2014].

4.6 Analysis and Evaluation

The renewable energy sources potential analysis of each of the 35 ENTSO-E countries is considered in two separate sections:

- Primary Sources
- Secondary Sources

Primary Sources, which comprise solar and wind-based technologies, are analyzed from a geo-spatial perspective to best consider technical, economic, environmental, and social aspects, as discussed in **Chapter 4.2–4.4**. The outcome of the geo-spatial analysis refers to the rated power potential of the respective RES technologies in GW.

Secondary Sources, such as bioenergy, geothermal energy, hydropower, and hydrokinetic energy, are considered via comparative meta-analysis, literature review, and technical analysis to investigate future RES potential for the ENTSO-E countries, as presented in **Chapter 4.5**. The resulting potentials are denoted as potential energy yield in TWh per country and year.

To best represent and discuss regional European differences, the United Nations Statistics Division (UNSD) geo scheme for Europe is chosen. Based on the UNSD scheme, ENTSO-E can be distinguished among the subsequent geographical areas. [UNSD2020]

- Eastern Europe
- Northern Europe
- Southern Europe
- Western Europe

This assignment of countries to specific European geographical regions serves the analytical convenience and does not imply any assumption regarding political or other affiliations of countries. It is rather meant to provide a brief overview of the regional RES potentials in the ENTSO-E. The regional classification is depicted in **Fig. 30**.

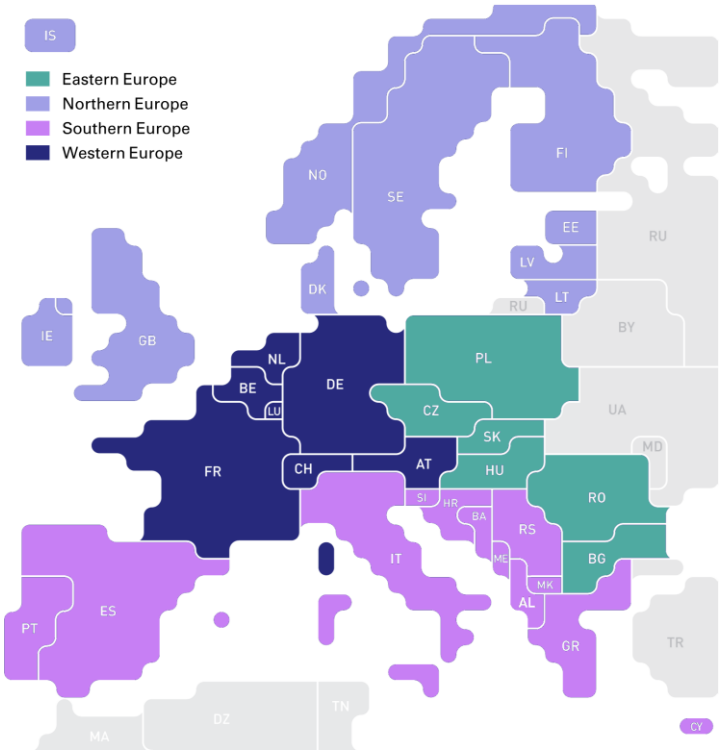

Fig. 30 Regional classification ENTSO-E
Source: In reference to [UNSD2020]

As indicated in **Fig. 30**, Europe and the corresponding ENTSO-E territory are classified into four geographic regions. Those regions are distinguished by latitudes and longitudes as well as particular geologic and climatic influences. Under this classification, Eastern Europe shows a rather homogeneous distribution of six mid-size countries, whereas the other regions are rather heterogeneously distributed. Northern Europe exhibits a share of large-scale countries, such as Norway and Sweden, as well as small-scale countries, such as the Baltic countries. Southern Europe is coined with the large-scale countries Italy and Spain as well as a large share of small-scale countries of the Balkans. Western Europe is dominated by the large-scale countries France and Germany, followed by Austria, Switzerland, and the Benelux countries.

4.6.1 Primary Sources Results

Based on the geo-spatial analysis and under consideration of numerous social, environmental, and technical limitations, it is found that 5,522 GW rated power of Primary Sources is techno-economical feasible across the ENTSO-E. Out of the 35 ENTSO-E member states, the largest countries with sufficient land area, particularly denoted by grassland, cropland, and arable lands, show the highest total net rated power potential. These high potential member states comprise France, Germany, UK, and Spain, followed by Poland, Italy, Sweden, and Iceland, with each more than 250 GW potential rated power of Primary Sources.

The medium potential countries are denoted by Finland, Romania, Denmark, the Netherlands, Norway, Ireland, Portugal, Greece, Latvia, Lithuania, Bulgaria, Hungary, Czechia, and Estonia, which show a potential of 50–200 GW. The low potential countries with a total potential less than 50 GW are represented by Austria, Belgium, Serbia,

Slovakia, Croatia, Bosnia, Switzerland, Albania, North Macedonia, Slovenia, Cyprus, Montenegro, and Luxembourg. The total rated power RES potentials per country and technology are depicted in **Fig. 31**.

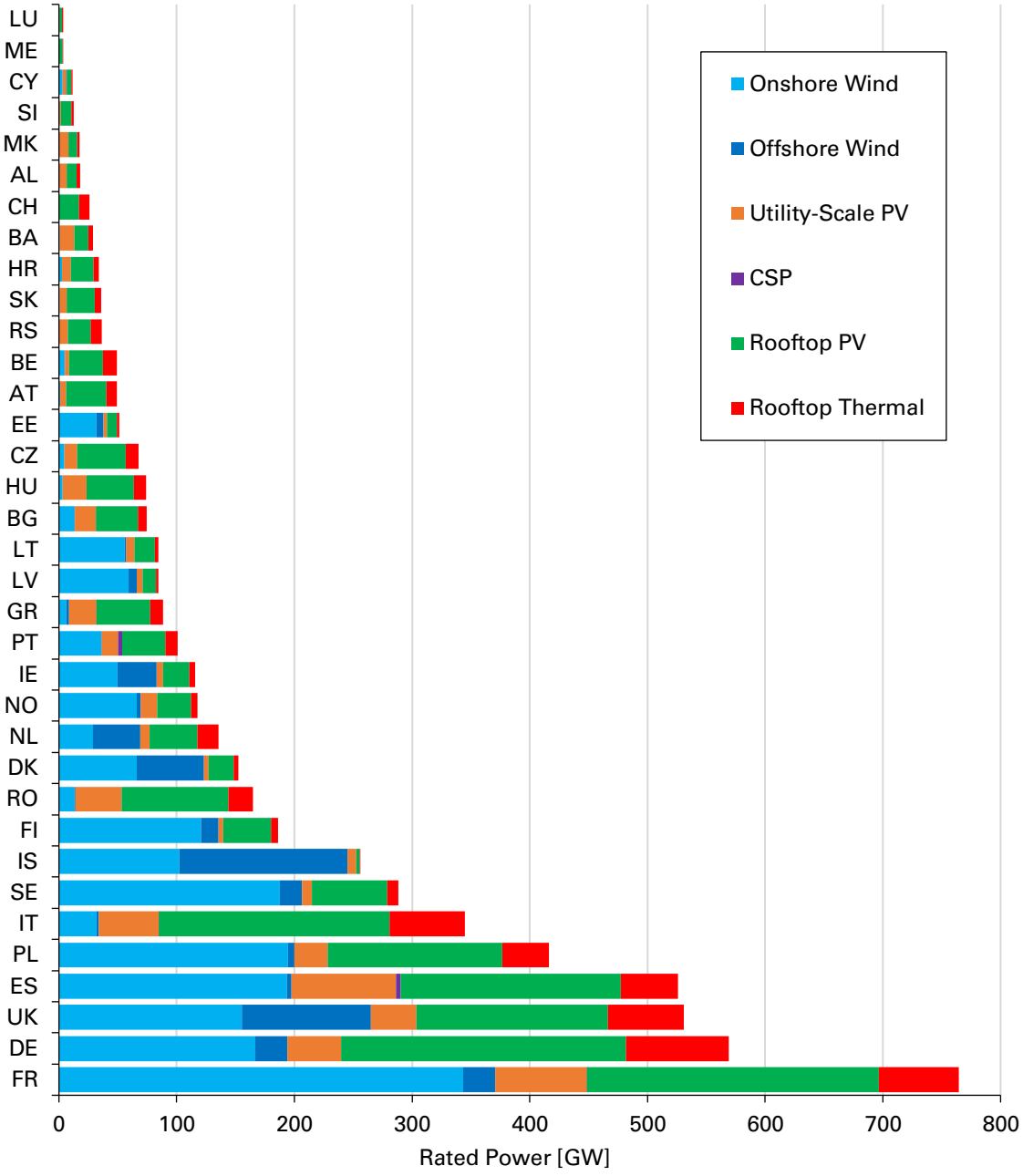

Fig. 31 Primary Sources rated power potential per country
Source: In reference to [Kup2020a] [Kup2020b]

As indicated in **Fig. 31**, the Primary Sources high potential countries are predominantly composed of the large-scale ENTSO-E countries. Thus, larger countries generally possess more available space for the deployment of land-intensive onshore RES technologies, such as onshore wind and utility-scale PV. However, other parameters, such as population density, average area slope, and availability of maritime and coastal areas as well as ocean depths, are affecting the potential of onshore and offshore RES.

Regardless the total size of the high potential countries, those countries possess a large proportion of plains which favor the onshore RES technologies potentials and

advantageous access to maritime and coastal areas for offshore RES technology deployment. Some countries, such as UK, Iceland, Denmark, the Netherlands, and Ireland, extraordinarily benefit from their comparative large coastal areas and corresponding EEZ, as expressed by the high shares of offshore wind potential. On the contrary, high ocean depths, such as observed in Norway and Portugal, may diminish the offshore wind potential. Likewise, a high proportion of mountainous areas is decreasing the potential for onshore wind and utility-scale PV deployments, as indicated by the alpine countries Austria and Switzerland.

Moreover, population density and corresponding density of settlements is hindering the potential of onshore RES technologies due to the proposed distance areas. This issue can be observed at the example of the two leading countries France and Germany. The onshore RES potential of Germany is significantly lower than the potential of France, due to the higher population density. However, the RES technologies rooftop PV and rooftop thermal benefit from a high population density and the corresponding availability of rooftop space. As discussed in **Chapter 4.4**, only some countries, such as Spain and Portugal, show high potentials for CSP plant developments due to the necessary availability of high direct normal irradiance and the corresponding CLC land categories. The total potential per Primary Source technology is depicted in **Fig. 32**.

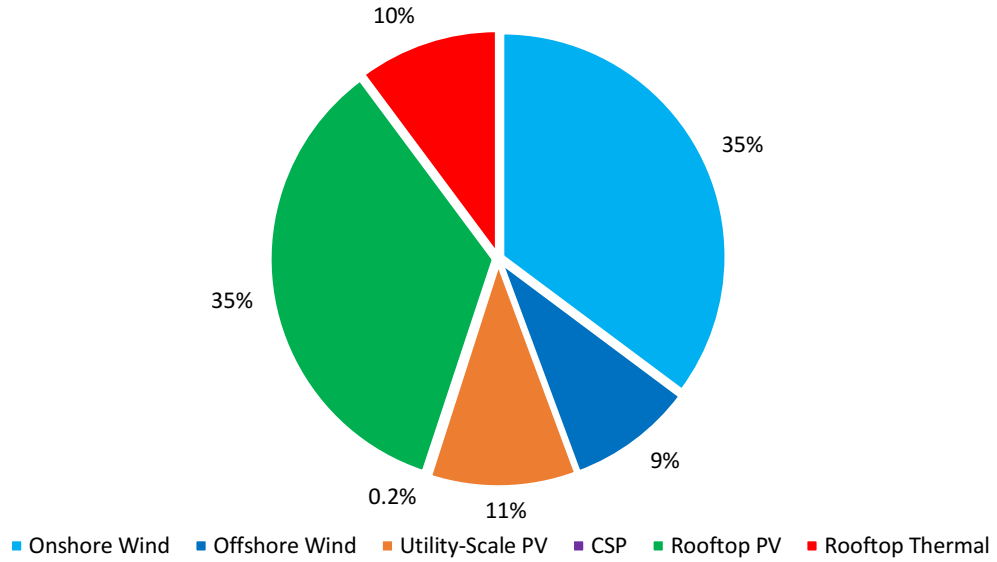

Fig. 32 Primary Sources potential per technology ENTSO-E

As indicated in **Fig. 32**, with each 35 % wind onshore and Rooftop PV possess the highest share of the 5,522 GW Primary Sources potential among the ENTSO-E, followed by utility-scale PV with 11 % and rooftop thermal with 10 %. Offshore wind contributes 9 % to the total share. CSP exhibits only a marginal share of 0.2 %. A comprehensive list of the Primary Sources potential per country and technology is depicted in **Annex IX**. The prevalence of protected areas, such as Natura 2000 and CDDA, poses a major restriction on the Primary Sources potentials. However, significant RES potential exists while minimizing the impact on protected areas. As countries define and approach future energy goals, the impact on local communities and environment must be considered in reference to social and environmental factors, as presented in this analysis.

For a regional comparison of the Primary Sources potentials, Primary Sources are aggregated to energy source classes and potential categories. Those classes and categories are displayed in heat maps per country and across the ENTSO-E. The heat maps indicate the absolute potential classes in colors, whereas pink indicates high potentials, purple and blueish colors average potentials, and turquoise low potentials.

Wind Power Potentials

For the consecutive technology-based analysis, the wind-based technologies onshore and offshore wind power are aggregated to the Primary Sources class wind power. Wind power exhibits a total potential of 2,449 GW across the ENTSO-E. The five absolute wind power potential classes in GW and the corresponding colors per country are illustrated in the heat map of **Fig. 33**.

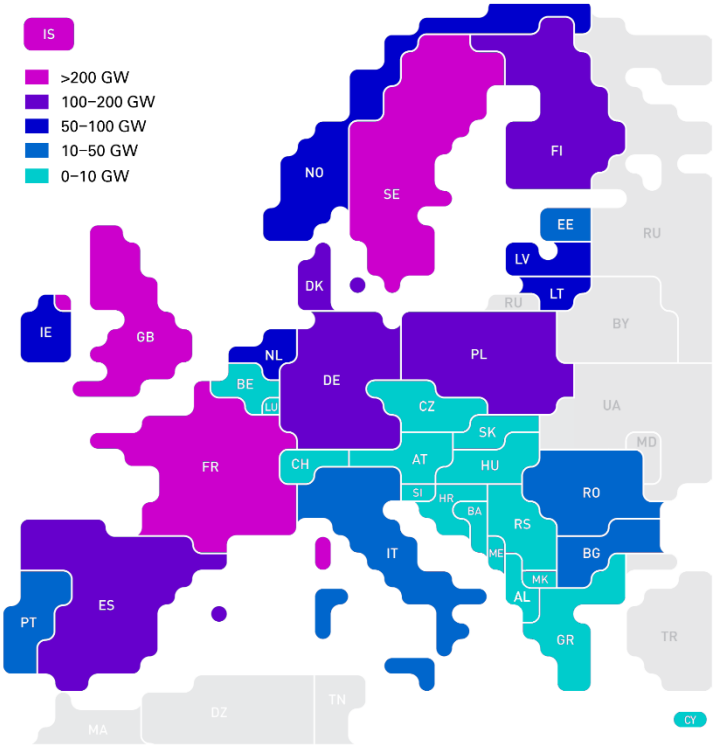

Fig. 33 Wind power potential heat map ENTSO-E

As indicated in **Fig. 33**, large surface countries with long coastal areas, such as France, UK and Sweden, possess the highest wind power potentials. Those potentials are largely based on the availability of land as well as the availability of nearshore and offshore areas for wind turbine erection. For wind power in general, it is important that the potential areas are not in close proximity to municipalities, wherefore population density and distribution is a crucial factor for the wind power potentials of each country. The population density impact can be observed at the example of Germany, which possess a significant area size, but also Europe's largest population.

Moreover, the prevailing water depths are crucial for the development of offshore wind power, which leads to the comparatively low potentials of countries with large coastal areas, such as Norway and Portugal. Those countries are generally suitable for offshore wind power development, but likewise limited by the prevailing water depths >100 m of

the corresponding EEZ (compare **Chapter 4.4.1** and **4.4.2**). Countries with comparatively low area size, limited access to shore, high average slopes, and high population densities show significant low potentials, as indicated by the Alpine countries Austria and Switzerland as well as the Balkan countries, for instance.

On the regional level, wind power dominates Northern and Western Europe due to the availability of suitable areas, particular large coastal areas, and favorable wind speeds. Eastern and Southern Europe exhibit only comparatively low shares of wind power, except Spain and Poland. Especially the area from Switzerland, across the Balkans, and down to Greece does not show high potentials mostly due to limited area size and high average slopes in the dominant mountainous areas of those countries.

Solar Electricity Potentials

The solar based electricity producing RES technologies utility-scale PV, CSP, and PV rooftops are aggregated to the category solar electricity. Solar electricity exhibits a total potential of 2,511 GW_p. The five absolute solar electricity potential classes in GW and the corresponding heat map colors per country are depicted in **Fig. 34**.

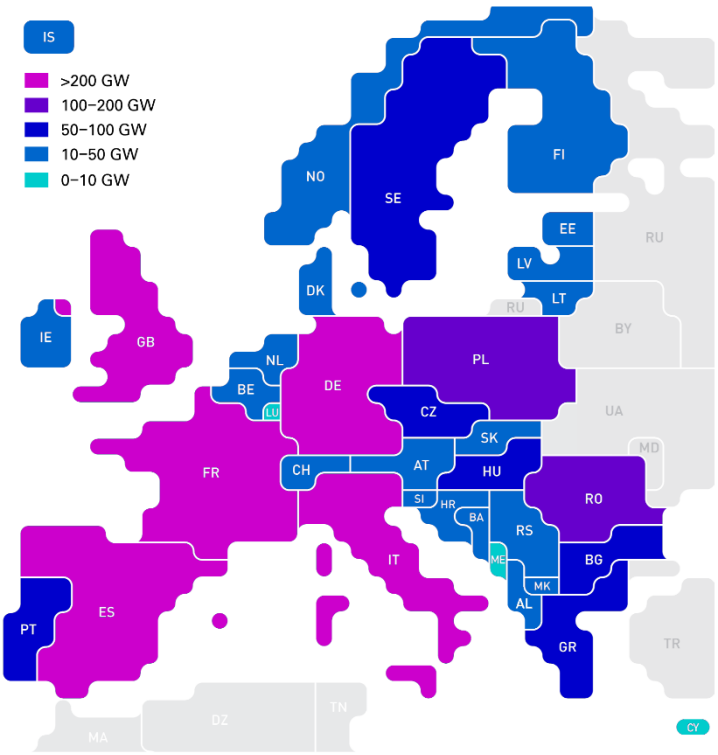

Fig. 34 Solar electricity potential heat map ENTSO-E

As indicated in **Fig. 34**, again, large-scale area countries France, Germany, Italy, Spain, and UK possess the highest solar electricity potentials. Utility-scale PV and CSP potentials largely depend on the availability of suitable land area as well as sufficient direct normal irradiance (compare **Chapter 4.4.3** and **4.4.4**).

Areas with high average slopes, as found in mountainous regions, negatively impact the potentials for those area intensive technologies. Moreover, population density and distribution affect the potential of utility-scale PV and CSP, but, unlike onshore wind power, much less due to the decreased radial buffer zones to municipalities.

On the contrary, high population densities and the corresponding shares of households and commercial buildings lead to a superior potential for PV rooftops due to the availability of roof area for PV panel installation. Thus, high potentials for PV rooftops can be found especially in France, Germany, Italy, Poland, Romania, Spain, and UK.

Whereas countries such as Finland, Norway, and Sweden possess significant area size, but solar electricity production potentials are limited due to large areas with high average slopes, insufficient direct normal irradiance, low population densities, and area competition with more favorable onshore wind power sites.

On the regional level, solar electricity exhibits particular high potentials in Western and Southern Europe, due to area availability for large-scale PV and CSP as well as high shares of solar rooftops. Especially the countries of the southern latitudes exhibit specifically high shares of direct normal irradiance and, therefore, potentially high solar yields per area that privileges the area utilization for large-scale PV and CSP over the deployment of onshore wind power.

Especially the Scandinavian countries of Northern Europe as well as the Alpine countries Austria and Switzerland are lacking suitable area for utility-scale PV due to high average slopes of the mountainous areas and the lack of south facing areas. Eastern Europe shows moderate solar electricity potential due to the moderate area size and availability of the countries, especially in Poland and Romania.

Solar Rooftop Potentials

Solar rooftops refer exclusively to solar thermal and PV panel installations. Those two technologies are in direct area competition with each other, as they share the same potential rooftop area. For this comparison, solar thermal and PV rooftop power potentials are aggregated to solar rooftops. The solar rooftop power rating comprises a total potential of 562 GW_p. The five absolute solar rooftops potential classes in GW and the corresponding heat map colors per country are depicted in **Fig. 35**.

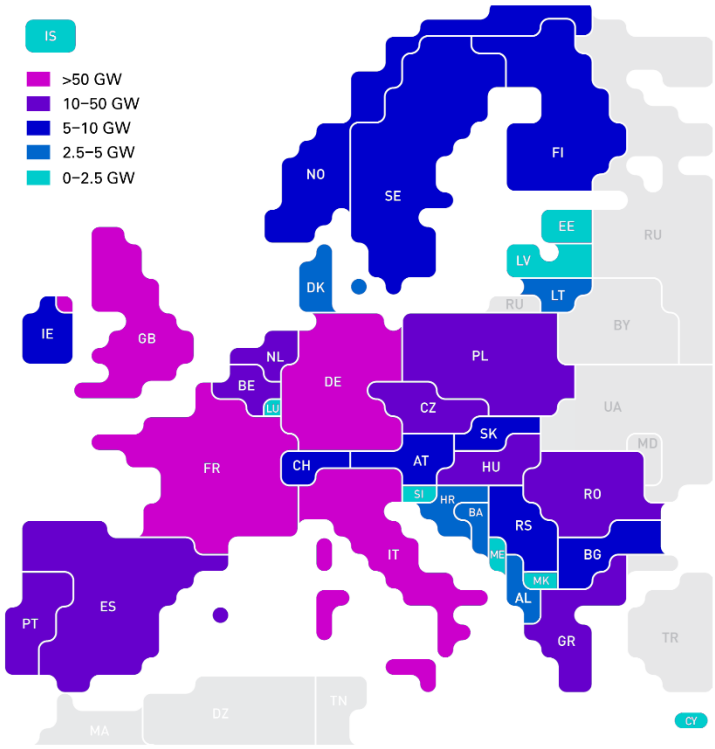

Fig. 35 Solar rooftops potential heat map ENTSO-E

As indicated in **Fig. 35**, high solar rooftops potentials are found in those countries with comparatively high population densities and the corresponding availability of rooftop area for solar thermal installations. Those countries comprise France, Germany, Italy, and UK, but also Belgium, Czechia, Greece, Hungary, the Netherlands, Poland, Portugal, Romania, and Spain. Unlike the PV rooftop potentials, solar rooftop potentials are capped by a per capita factor and, thus, do not exceed certain shares based on population (compare **Chapter 4.4.5**). Whereas the PV rooftop electricity potential is exclusively limited by the availability of rooftop area and do not directly correlate with population.

On the regional level, solar rooftop potentials are well dispersed across the ENTSO-E. The highest shares are found in Southern and Western Europe, followed by Eastern and Northern Europe. Especially high population density countries, such as Germany and UK, benefit from the availability of rooftop spaces. Countries with comparatively low population density, such as the Scandinavian and Baltic countries, exhibit only little solar rooftop energy potential.

4.6.2 Secondary Sources Results

Based on meta-analysis, literature review, and technical investigation, it is found that 4,263 TWh of Secondary Sources energy yield per year is techno-economical feasible across the ENTSO-E. Analogous to the Primary Sources analysis, especially large-scale countries with sufficient land area, particularly denoted by grassland, cropland, and arable lands, as well as favorable geologic and topographic conditions, exhibit the largest total net energy yield potential per year.

As depicted in **Annex X**, those high potential member states comprise France, Germany, Spain, Italy, and Poland, followed by Sweden, Romania, Norway, Iceland, and Hungary, which possess each more than 150 TWh potential energy yield per year. The medium potential countries are denoted by Austria, UK, Finland, Portugal, Czechia, Switzerland, Bulgaria, Greece, Denmark, the Netherlands, and Slovakia, which exhibit a potential energy yield of 50–150 TWh per year. The low potential countries with a potential less than 50 TWh are represented by Lithuania, Croatia, Latvia, Belgium, Serbia, Bosnia, Ireland, Slovenia, Albania, Estonia, North Macedonia, Montenegro, Luxembourg, and Cyprus. The energy potential per country and technology is illustrated in **Fig. 36**.

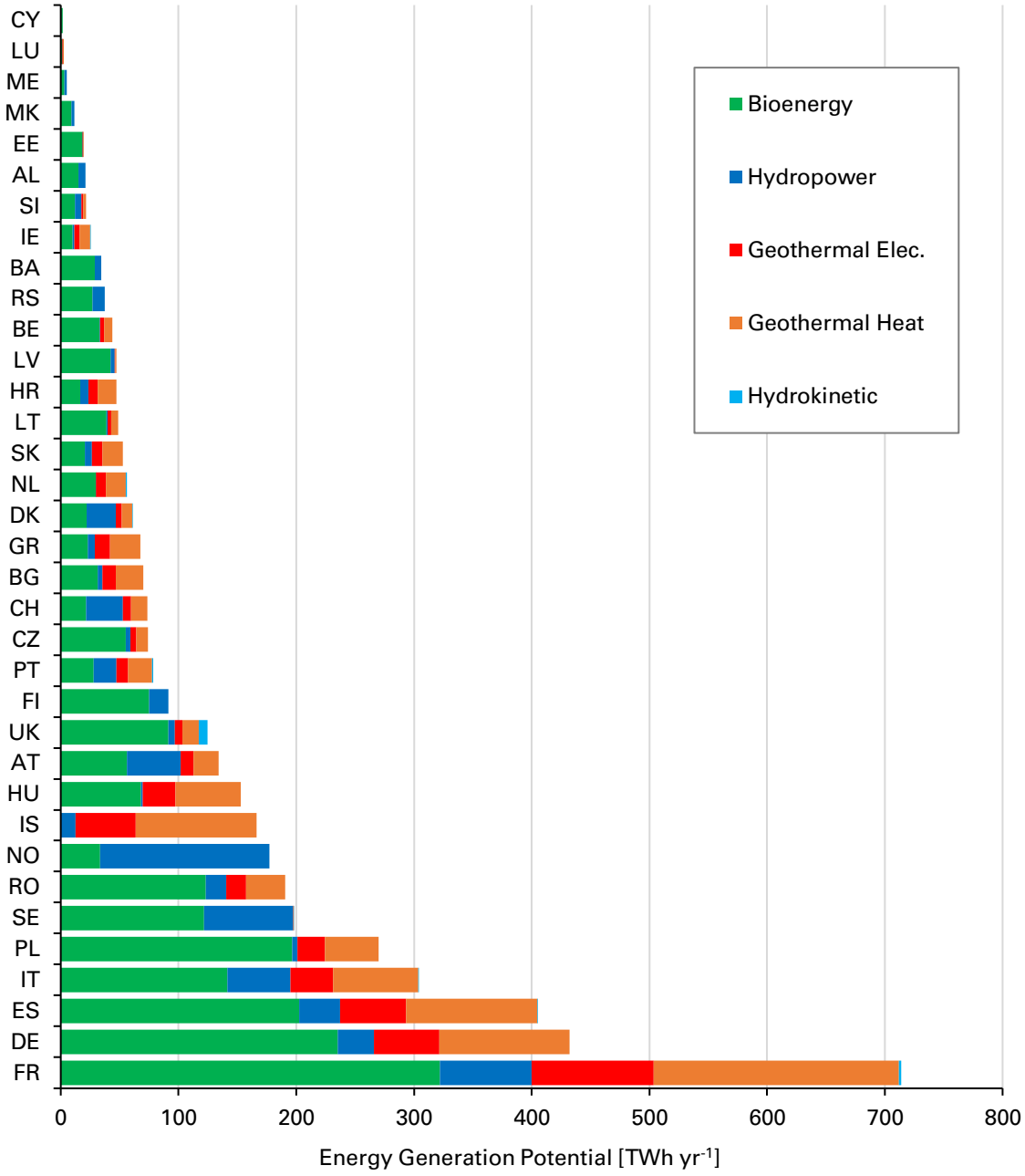

Fig. 36 Secondary Sources energy potential per country
Source: In reference to [Kup2020a] [Kup2020b]

As indicated in **Fig. 36**, the Secondary Sources high potential countries comprise the largest ENTSO-E countries by area size. Regarding the Secondary Sources analysis, larger countries generally possess more available land for farming and the corresponding residues as well as for cultivating energy crops, such as beet, corn, rapeseed, and soy plants. Due to the categorization of the Secondary Sources, the availability of hydropower and geothermal sources does impact the country ranking.

Especially those countries with prominent mountainous areas, such as Norway, France, Sweden, Italy, and Austria, exhibit significant high potentials due to the availability of small and large hydropower sources. Moreover, countries with comparably high potential of geothermal energy, such as France, Spain, Germany, Iceland, Italy, Hungary, Poland, and Romania possess significant high energy yield potentials regardless the availability of land for land-intensive RES technologies.

In comparison to the Primary Sources analysis, in which UK exhibits the third largest potentials, it is apparent that UK does not belong to the Secondary Sources high potential countries. Unlike the other high potential countries, such as France, Germany, and Spain, UK does not possess a significant biofuel and biomass potential due to high population density and unfavorable geology. Moreover, the hydropower and geothermal potentials are inferior and cannot be offset with the promising hydrokinetic potential.

As discussed in **Chapter 4.5.4**, hydrokinetic technologies can be found only in countries with access to maritime and coastal areas that possess the necessary conditions to develop those marine-based technologies, such as France and UK. The relative potentials per Secondary Source technology are depicted in **Fig. 37**.

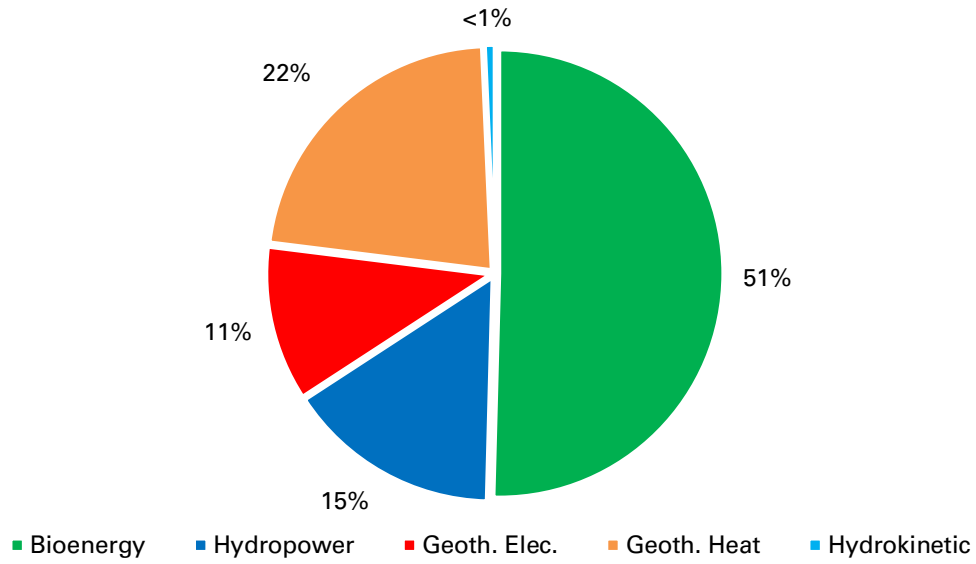

Fig. 37 Secondary Sources potential per technology ENTSO-E

As indicated in **Fig. 37**, bioenergy with 51 % contributes the highest share of the 4,263 TWh Secondary Sources energy yield potential per year, followed by 22 % geothermal heat. Geothermal electricity contributes 11 % and hydropower a share of 15 %. Hydrokinetic technologies exhibit only a marginal share of 0.3 %. A comprehensive list of the Secondary Sources potentials per country and technology is depicted in

Annex X. Analogous to the Primary Sources potentials analysis, Secondary Sources are aggregated to energy source classes and potential categories. Those classes and categories are displayed in heat maps per country and across the ENTSO-E.

Bioenergy Potentials

For the consecutive technology-based analysis, biofuels, biogas, and biomass production potentials are aggregated to the Secondary Sources class bioenergy. Bioenergy comprises a total potential of 2,157 TWh per year across the ENTSO-E. The five absolute bioenergy potential classes in TWh and the corresponding colors per country are depicted in the heat map of **Fig. 38**.

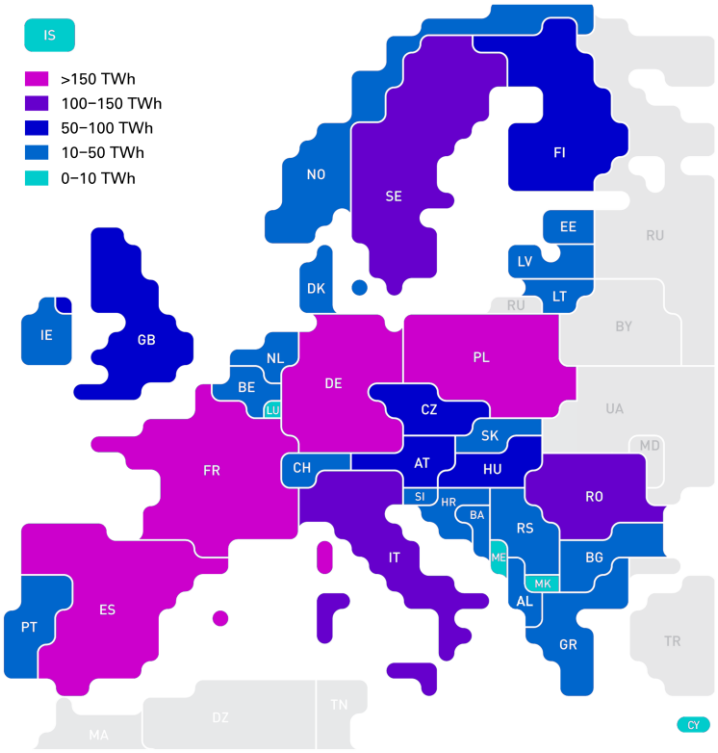

Fig. 38 Bioenergy potential heat map ENTSO-E

As indicated in **Fig. 38**, specifically high bioenergy potentials are identified in France, Germany, Spain, and Poland, followed by Italy, Sweden, and Romania. The regarded 1G bioenergy products are dependent upon land availability and legal restrictions as well as soil and climate suitability, whereas the major restrictive factor is found in the global land use competition among food crops and energy crops. Therefore, large area countries with large availability of abandoned agricultural areas and suitable soil qualities possess higher potentials than those countries with low agricultural area and poor soil qualities (compare **Chapter 4.5.1**).

On the regional level, comparatively high bioenergy potentials can be found across the ENTSO-E, as all countries possess a significant share of farming residues and land availability for bioenergy crops. Large-scale countries exhibit generally larger potentials due to the higher availability of agricultural land. Some countries, such as UK, show particular low bioenergy potentials due to high population densities and strong area competition among energy and food crops cultivation.

Hydropower and Hydrokinetic Energy Potentials

The hydrokinetic-based electricity production of the RES technologies hydropower and hydrokinetic energy are aggregated to the category hydro-kinetic power. Across the ENTSO-E, hydro-kinetic power comprises a total potential of 673 TWh per year. The five absolute hydro-kinetic power potential classes in TWh and the corresponding heat map colors per country are depicted in **Fig. 39**.

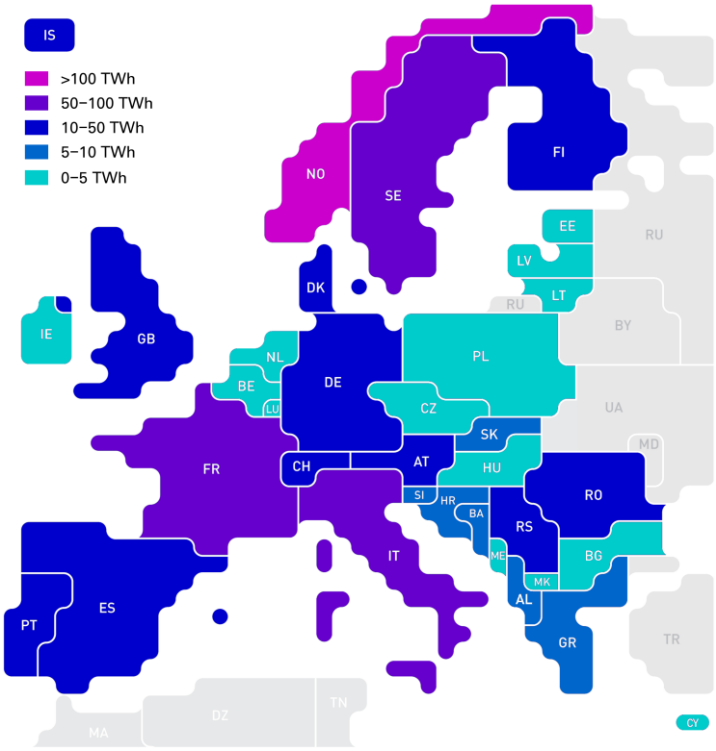

Fig. 39 Hydro-kinetic power potential heat map ENTSO-E

As indicated in **Fig. 39**, countries with large shares of suitable rivers and mountainous areas for small and large hydropower utilization as well as those with suitable and large shares of coastal area for hydrokinetic energy utilization possess the highest potentials for hydro-kinetic power (compare **Chapter 4.5.2** and **4.5.4**). Those countries which are especially suitable for hydropower utilization comprise Norway, France, Sweden, and Italy. Countries such as UK, the Netherlands, and Ireland exhibit only minor hydropower potential but rather large potential for hydrokinetic energy, due to large suitable coastal areas. Norway exhibits the highest potential within the ENTSO-E, due to superior conditions for small and large hydropower utilization. However, hydrokinetic power remains a comparatively inferior RES, whereby especially hydrokinetic energy is very much limited to specific technology applications and locations.

On the regional level, the hydrokinetic power potentials are very much concentrated in some regions of Western and Northern Europe, due to the favorable mountainous areas and corresponding kinetic potentials. The prevailing hydropower potentials are located in those countries, which are adjacent to the transalpine range and the Carpathians as well as in the Scandinavian countries. However, the major share of ENTSO-E countries shows only very little potentials for hydrokinetic power.

Geothermal Potentials

The geothermal heat and power energy output comprises a total potential of 1,433 TWh per year. The five absolute geothermal potential classes in TWh and the corresponding heat map colors per country are depicted in **Fig. 40**.

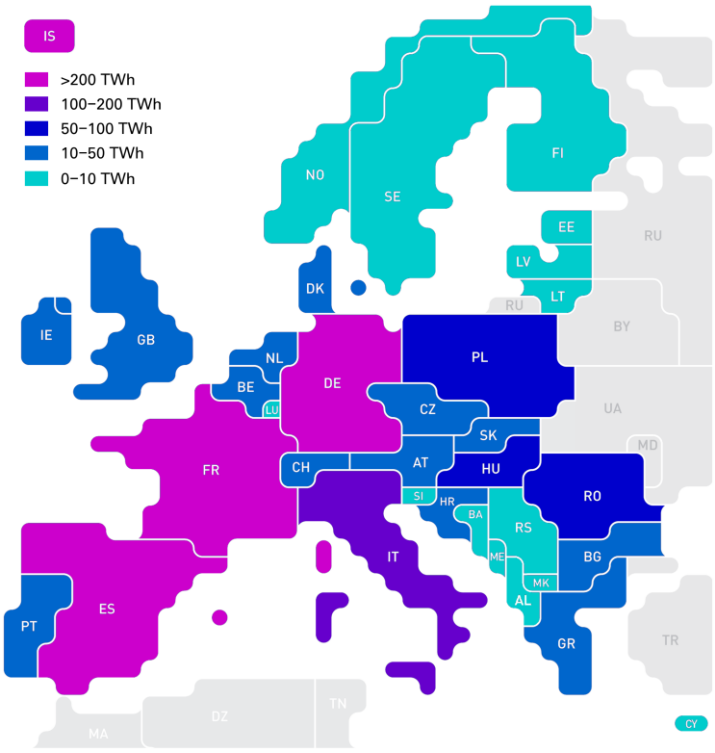

Fig. 40 Geothermal potential heat map ENTSO-E

As indicated in **Fig. 40**, particular high geothermal potentials can be found in France, followed by Spain, Germany, and Iceland. Moreover, Italy, Poland, Hungary, and Romania exhibit notable geothermal potentials. Geothermal energy sources are dependent on specific geologic conditions and, therefore, differ strongly among the ENTSO-E countries and regions (compare **Chapter 4.5.3**). High geothermal potentials are found in geologic active regions, which are identified in Western and Southern Europe as well as some regions in Eastern Europe. Except Iceland, Northern Europe exhibits only little potential for geothermal electricity generation and heat production.

5. Integrated Energy System Model

5.1 Objectives

Energy system models aim at the analysis of energy systems or sub-systems, such as the heat, gas, and power system. Generally, energy system models are concerned with various purposes, as stated in the subsequent instances. [Bhat2010]

- Improved energy supply system design and planning
- Enhanced understanding of present and future demand-supply interactions
- Energy and environment interactions

Energy system models utilize different techniques, such as mathematical and econometric methods as well as related methods of statistical and network analysis. Consequently, those models vary in terms of data and skill requirements, technology specification, and computing requirements. The scope of energy system models may differ in reference to purpose and focus. Engineering models focus on specific processes of components and sub-components. Whereas comprehensive models cover energy economy interactions at the national and international levels, often with the objective function of minimal system costs. Numerical calculations of those models are prone to complexity in reference to spatial resolution, number of interconnections, and system granularity. Thus, the grade of complexity of each model is strongly correlated with the need for computational power. [Bhat2010] [Hess2018]

To best consider high grades of spatial and temporal resolution in the face of limited computational power, various methods are available. First, the power transmission constraint can be neglected and the model region is treated as a so-called copper plate. However, transmission constraints and the limitation of transmission power are necessary to account for the intermittency of renewable energy sources. However, computational power reaches its limit when spatial resolution, data input, and the number of interconnections are increased. Second, the representative time slices approach provides an approximation of the temporal aspects of seasonal demand and RES-based energy conversion by reducing the need for computational power due to the calculation of representative time slices per season instead of complete time periods. Third, the grade of spatial and technical detail can be adjusted to decrease data input and the number of computational tasks. [Hess2018] [Knop2013] [Pfen2014] [Ponc2015] Hence, the here presented methods represent a tradeoff between model accuracy and computational ease as well as temporal and spatial resolution.

The integrated energy system (IES) model aims at the modelling and simulation of an energy system with high shares of RES and power-to-x (PTX) technologies. The generic model embraces the ENTSO-E area, but can be applied to any arbitrary model region. The IES model aims at the minimization of CO_{2eq} emissions across all energy demand sectors by the means of PTX and exploitation of the techno-economic RES potentials. Unlike cost-focused energy system models, the IES model research objective focuses on the investigation of how and to what extend the CO_{2eq} emission reduction targets as

introduced in **Chapter 2.2** can be technically realized. Moreover, the optimum distribution of PTX technologies is under investigation.

As basic input for the IES model, the ENTSO-E energy balances as introduced in **Chapter 2.4** are adjusted regarding future efficiency gains and consumption patterns. Those energy balances as well as several profiles for electricity, heat, transport, and residual demand are adjusted to represent future energy demands, based on best estimate technology and efficiency assumptions. As discussed in **Chapter 3**, PTX technologies, such as power-to-mobility (PTM), power-to-heat (PTH), and power-to-gas (PTG), are the most promising means to effectively convert the dominant RES-based electricity production into the remaining energy consumption sectors. To best estimate total RES potential in the ENTSO-E as a basis for future low-emission energy supply, the techno-economic potentials of the prevailing RES technologies have been carefully assessed in **Chapter 4**. The outcomes of the techno-economic potential analysis serve as input for the model. The IES model output comprises primary energy conversion, energy transformation, and CO_{2eq} emissions. The IES model output is then utilized to create Sankey diagrams of the future ENTSO-E energy system, analogous to the energy balances analysis method as introduced in **Chapter 2.4**.

5.2 Methods

The linear unit commitment and extension model enables the optimization of large and complex energy systems within a cell-based model logic. The cell logic refers to single energy system cells, here regarded as countries and the total entity, represented by the ENTSO-E. The logic distinguishes among intracellular[12] and intercellular[13] energy flows. The intracellular energy flow method regards each cell as copper plate with unlimited transmission capacities and, thus, reduces the need for computational power significantly. The intercellular power flow method among the cells ensures appropriate representation of the intermittency of RES-based power supply, such as wind power and PV. The distinction among inter- and intracellular energy flows enables a high degree of data and temporal resolution, and to best account for seasonal effects and intermittencies within the constraint of available computational power.

The objective function of the IES model aims at the efficient coverage of energy demands and minimization of the total CO_{2eq} emissions by the means of linear optimization in the General Algebraic Modeling System (GAMS) for mathematical optimization. The reduction of those emissions strongly depends on the energy production and demand profile inputs as well as the selected energy transformation technology. For each time step, the model logic decides which utilization path is the most efficient in order to balance energy supply and demand and to minimize CO_{2eq} emissions via the simplex method of the IBM CPLEX solver. Unlike other energy system models, the IES model focuses on the physical availability of scarce RES-based energy

[12] Intracellular refers to all energy conversion, flows, and demands within a single cell.
[13] Intercellular refers to all energy conversion, flows, and demands between the cells.

sources and the reduction of CO_{2eq} emissions. The RES-based energy conversion profiles for each ENTSO-E country are derived from the techno-economic potential analysis of **Chapter 4**, which is based on technical and economic efficiencies, geospatial data, cost factors, and land use. The hourly electricity generation of wind onshore, wind offshore, and PV as well as the heat production of solar thermal rooftops is calculated based on the corresponding hourly wind and solar capacity factors of each country. All computation in the IES model is denominated in megawatt (MW) per hour (h), as indicated by the GAMS code in the digital **Annex CD**.

Within each cell, the power-to-power (PTP) interface describes the direct electricity supply from the generation to the demand side. In case electricity demand cannot be covered by RES electricity generation, combined cycle gas turbines (CCGT) serve as backup source to balance the system. Remaining energy demands per time step are covered by energy imports from third-party countries if they cannot be covered by domestic production. Therefore, additional CO_{2eq} emissions equal to the specific emission factor (EF) of natural gas are imposed to the GHG repositories.

Based on the input data, the energy flows are computed by the IES model logic for each time step representing one hour out of 8,760 hours per year. The computation complies with the equations edited in GAMS that comprise electricity generation, PTX conversion, energy balances and demands as well as electricity exchanges between adjacent cells. Moreover, technical restrictions, such as generation and conversion efficiencies are introduced. The linear optimization model is designed as generic and scalable logic, which can be applied to arbitrary energy systems and model regions. However, the focus lies on the RES and integrated energy potentials of Europe, which is represented by the ENTSO-E. Therefore, the model is introduced on a technical level, but refers to the 35 cells which each represent one of the 35 ENTSO-E countries.

5.3 Optimization Logic

The IES model is based on a deterministic optimization logic which comprises several energy cells and clusters. The IES model logic is applied to the 35 EU and non-EU ENTSO-E countries. As depicted in **Annex I**, each ENTSO-E country represents a particular cell and is labeled with the corresponding ISO country code. Each of those ENTSO-E countries possess specific energy conversion, transformation, and consumption patterns as well as individual energy system peculiarities. Within the IES model structure each of those cells are interconnected with the adjacent cells and able to exchange electricity as imports or exports. Each cell is regarded to balance energy conversion and demand on the intracellular level first, while utilizing PTX technologies to convert electricity into the other energy demand sectors. In case that a core cell is not able to balance electricity demand, electricity is either exported to or imported from adjacent cells on the intercellular level or, lastly, supplied by CCGT power plants.

5.3.1 Intercellular Model

The intercellular electricity exchange logic of the IES model requires a specification of cross-border transmission line capacities as represented by the capacity of each interconnection, to define the maximum power flow between each cell and per time step. According to Anderski et al. (2015), the transmission network model comprises the sum of all transmission line capacities which are in operation or likely to be implemented within the framework of the ENTSO-E Ten-Year Network Development Plan (TYNDP) [Ander2015]. In reference to the e-Highway 2050 Modular Development Plan of the Pan-European Transmission System 2050, the grid extension assumptions of the Large-Scale RES and 100% RES scenarios of Bakken et al. (2015) are taken into account [Bak2015]. The total transfer capacities are a result of the combination of the transmission capacities of Anderski et al. (2015) and Bakken et al. (2015). The resulting total transmission capacities between each country are depicted in **Fig. 41**.

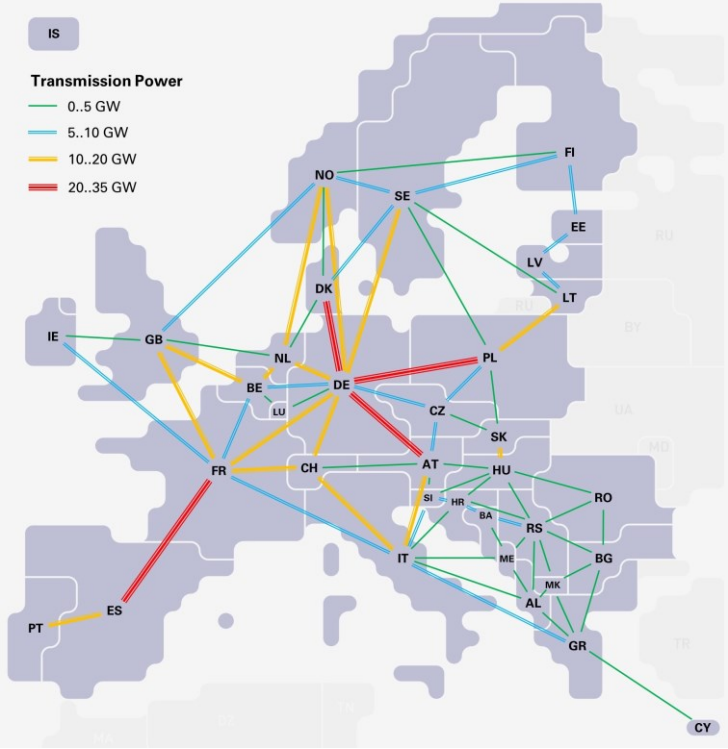

Fig. 41 Power transmission capacities ENTSO-E 2050
Source: In reference to [Kup2019] [Kup2020b]

As depicted in **Annex XI** and **Fig. 41** each cell can exchange electricity with adjacent cells restricted by the transmission capacities at the intercellular level. Major transmission capacities are identified in Western Europe, which represents a pivot point for intercellular electricity exchange due to its geographic location and the electricity demand and generation characteristic of the large-scale pivotal countries, such as France and Germany. As depicted by the red and yellow transmission lines, both countries are well connected to the adjacent countries Denmark, Norway, Sweden, Poland, Austria, Italy, Switzerland, Spain, and UK. Countries of the ENTSO-E peripheral areas, such as the Balkan and the Baltic countries, exhibit rather limited transmission capacities as indicated by the blue and green transmission lines. The at present existing

transmission lines are a result of historic electricity trade schemes. Whereas the TYNDP and e-Highway 2050 extension scenarios are based on assumptions regarding future energy demand and RES production clusters. Compared to the existing transmission line capacities as well as those lines being planned or under construction until 2030, the scenario projection suggest the reinforcement of transmission capacities among the pivotal countries, such as Belgium, France, Germany, the Netherlands, Norway, Poland, Spain, Sweden, and UK, by more than 10 GW.

5.3.2 Intracellular Model

At the intracellular level, each cell represents a domestic self-contained energy system that entails energy supply and demand as well as PTX conversion. Each cell is considered as a so-called copper plate and the transmission capacities are regarded as infinite. The model balances energy supply and demand on the intracellular level for each time step and cell. In case the balance does not equalize, the cells exchange electricity with each other and import fuels in the form of natural gas to cover the domestic energy demand on the intercellular level. Due to the short-term storage capacity of heat storages, long-term storage of heat is not considered by the IES model logic. In face of the potential overproduction of heat in particular time steps, a heat slack is introduced to the model logic. The heat slack serves as the means to deal with the heat surplus production of solar thermal rooftops or geothermal power plants, in case the heat supply exceeds demand, which may occur especially during summer periods. Unlike heat production, surplus electricity is either exported to adjacent countries or stored in batteries.

In each time step, the intracellular energy balances are offset by the hierarchical balancing logic. First, electricity and heat demand are supplied based on the RES-based electricity, heat, and biofuel production of each cell. Therefore, electricity, heat, and biofuels are supplied directly to the demand. Second, in case the supply cannot cover the corresponding demand, the demand is covered by the PTX interfaces. If available, electricity is imported from adjacent countries or produced by CCGT power plants. Third, in case the available energy supply sources are not sufficient, fuels are imported from the fossil fuel supply of third-party countries.

The primary to final energy consumption conversion in the intracellular model logic comes along with various energy conversion, transformation, and transmission losses as well as corresponding CO_{2eq} emissions. In reference to the subsequent introduction of the IES model logic, all relevant efficiencies η and emission factors EF are comprehensively listed in **Tab. 19**.

Tab. 19 Conversion efficiencies and emission factors
Source: In reference to [Kup2019] [Kup2020b]

Symbol	Description	Value	Unit
$\eta_{CCGT,el}$	eff. of CCGT electricity	0.65	
$\eta_{biomass,el}$	eff. of biomass electricity	0.25	
$\eta_{biomass,h}$	eff. of biomass heat	0.65	
$\eta_{biogas,el}$	eff. of biogas electricity	0.35	
$\eta_{biogas,h}$	eff. of biogas heat	0.50	
$\eta_{geo,el}$	eff. of geothermal electricity	0.20	
$\eta_{geo,h}$	eff. of geothermal heat	0.40	
η_{PTG-H2}	eff. of electrolysis	0.70	
η_{PTH}	eff. of PTH	1.30	
η_{PTC}	eff. of PTC	4.00	
η_{PTM}	eff. of PTM	0.95	
η_{BAT}	eff. of battery storage	0.95	
η_{STO}	eff. of gas storage	0.90	
$\eta_{el,trans}$	eff. of electricity transmission	0.90	
$\eta_{gas,trans}$	eff. of gas distribution	0.90	
EF_{SNG}	CO_{2eq} EF of natural gas	0.181	$t_{CO2}\ MWh_{th}^{-1}$
EF_{oil}	CO_{2eq} EF of oil	0.256	$t_{CO2}\ MWh_{th}^{-1}$
$EF_{mobility}$	CO_{2eq} EF of transport	0.219	$t_{CO2}\ MWh_{th}^{-1}$
$EF_{biomass}$	CO_{2eq} EF of biomass	0.341	$t_{CO2}\ MWh_{th}^{-1}$
EF_{biogas}	CO_{2eq} EF of biogas	0.178	$t_{CO2}\ MWh_{th}^{-1}$

The conversion losses depicted in **Tab. 19** refer to those losses that occur during the conversion of primary energy into secondary energy by various processes, such as power plant heat η_h and electricity η_{el} production as well as PTX η_{PTX} conversion. Moreover, storage and extraction losses of battery and gas storages are accounted for by η_{BAT} and η_{STO}. Additional electricity transmission and gas distribution losses after primary conversion are indicated by $\eta_{el,trans}$ and $\eta_{gas,trans}$.

GHG emissions of various combustion processes are indicated by the specific emission factors *EF* in tons of CO_{2eq} per thermal megawatt hour MWh_{th}. In reference to energy supply, demand, import, export, and PTX conversion, the IES model logic is introduced as energy conversion and transformation flow chart. According to the IES model flow chart in **Fig. 42**, the IES model logic is described in **Chapter 5.4–5.6**.

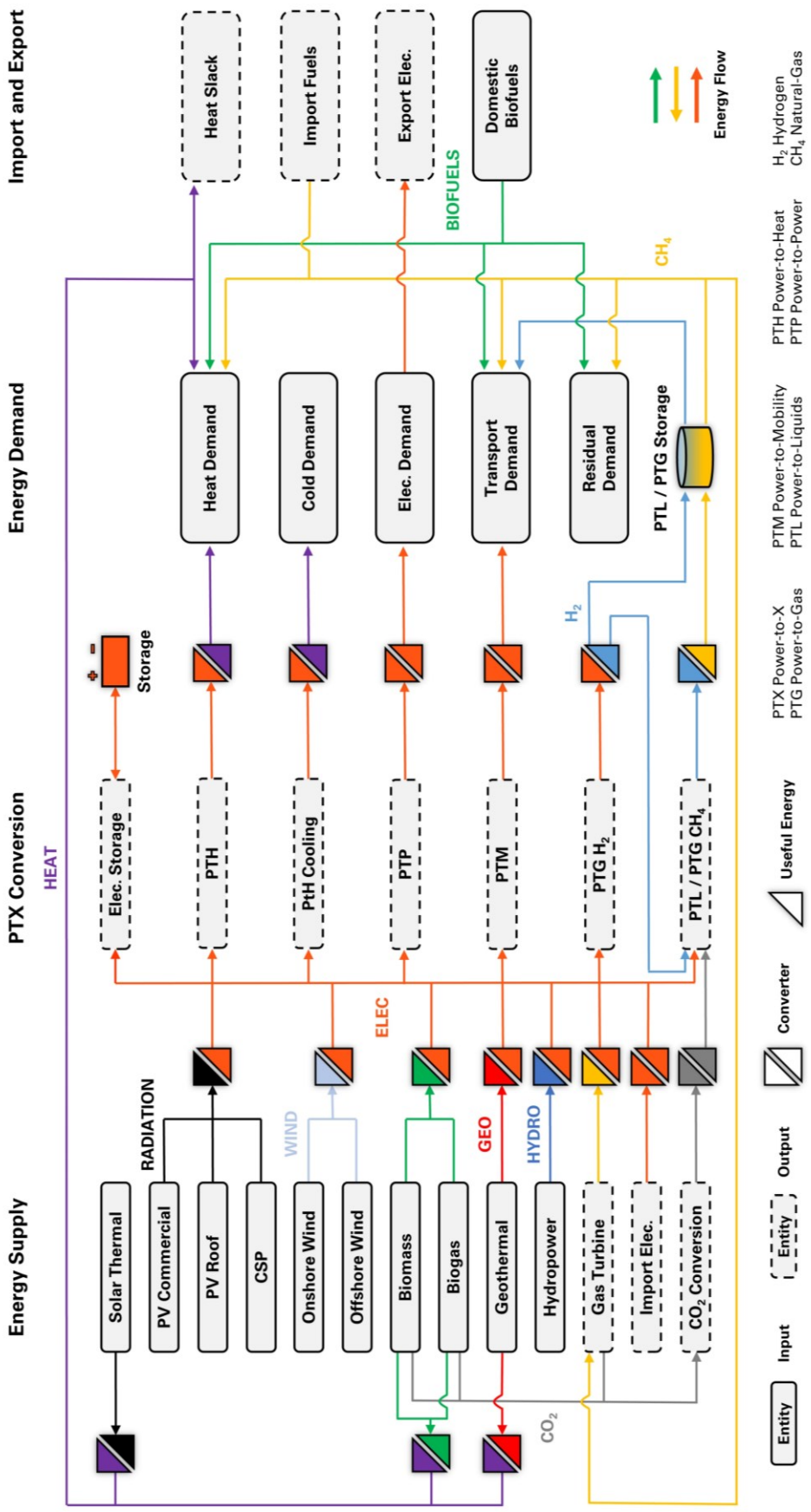

Fig. 42 Integrated energy system model flow chart
Source: In reference to [Kup2019] [Kup2020b]

5.4 Energy Supply

The total available energy supply of each cell and time step entails RES-based and CCGT power plants as well as the electricity transaction between the cells. RES technologies comprise wind, solar, biomass, biogas, hydro, and geothermal power plants. In reference to the Primary Sources, wind power is distinguished among onshore and offshore wind. Whereas solar power is composed of utility-scale PV, rooftop PV, and concentrated solar power (CSP), as indicated on the left-hand side of the IES model flow chart in **Fig. 42**. Depending on the corresponding technologies, electricity and heat is produced. As a peculiarity of biomass and biogas combined heat and power (CHP) as well as CCGT power plants, the CO_2 exhaust gases of the combustion processes are utilized as input for the PTG methanation process. To account for the techno-economic potentials of RES in each cell, the results of the techno-economic potential analysis of **Chapter 4** are utilized as input for the consecutive IES model calculation.

In order to compose the production profile for each Primary Source and cell, the total RES potential as introduced in **Chapter 4.4** and **Chapter 4.6.1** is multiplied with hourly capacity factors of the corresponding technology. The hourly onshore and offshore wind capacity factors and the historic solar averages are based on MERRA and MERRA-2 global meteorological reanalyzes as presented by Staffell and Pfenninger (2016) [Staf2016] as well as the Meteosat-based CM-SAF SARAH satellite dataset as introduced by Pfenninger and Staffell (2016) [Pfen2016]. Both are corrected for systematic bias by matching the simulations to the mean bias in modeling individual sites and examining the long-term patterns, variability, and correlation with power demand across Europe. The records of the wind capacity factors for the year 2015 are retrieved from the dataset 1980–2016 [ETH2016a] and the PV capacity factors from the dataset 1985–2016 [ETH2016b], as published on the open-source platform Renewables.ninja of the Swiss Federal Institute of Technology, that has been utilized for this analysis.

In comparison to the meteorologically dependent energy output of the Primary Sources, the Secondary Sources biomass, biogas, hydro, and geothermal power are only dispatchable within certain limitations. Therefore, those technologies are regarded as baseload power plants with constant power output per time step. For the model input, total Secondary Sources potentials as introduced in **Chapter 4.5** and **Chapter 4.6.2** are divided by 8,760 to account for the available energy of each hourly time step. From a resource efficiency perspective, increasing total output from a given input requires minimizing or effectively utilizing energy conversion losses [EEA2013b]. Therefore, cogeneration is anticipated as an optimal solution for efficient energy conversion. Thus, biomass, biogas and geothermal power plants are regarded as CHP plants.

Due to the focus on electricity as prevailing energy commodity of RES-based energy conversion, electricity demand is first supplied with the available RES-based electricity production. In each time step t, electricity demand is prioritized among other energy demands, such as heating, cooling, and transportation. In case the RES-based electricity production exceeds the demand, surplus electricity is converted into other energy

commodities via PTX technologies, such as PTH, PTG, and PTM. Moreover, surplus electricity production can be stored in battery storages or exported to adjacent cells. In the case of insufficient RES-based electricity production, electricity is supplied from the battery storages, imported from adjacent countries, or produced by the CCGT power plants. The electricity balancing logic of the IES model is described in **Eq. (5.1)**. The left-hand side of the equation represents the electricity supply and the right-hand side refers to the electricity demand of a specific cell *c*.

$$f_{eff,el} \cdot \left(E_{RES,el(t,c)} + STO_{dis(t,c)} + E_{CCGT,el(t,c)} + TRANS_{el(t,c)}\right) = D_{PTP(t,c)} + PTX_{(t,c)} + STO_{chrg(t,c)} \quad (5.1)$$

In **Eq. (5.1)** $E_{RES,el(t,c)}$ describes the RES-based electricity production per time step *t* and cell *c*, $STO_{dis(t,c)}$ the battery storage discharging electricity, $E_{CCGT,el(t,c)}$ the backup power plant electricity production, and $TRANS_{el(t,c)}$ the electricity transaction with adjacent cells. The supply side of the equation is multiplied with $f_{eff,el}=0.90$ to account for transmission and transaction losses, which are anticipated with 10%. $D_{PTP(t,c)}$ describes the electricity that flows through the PTP interface to the electricity demand side, $PTX_{(t,c)}$ the electricity that is input into the PTX interfaces, and $STO_{chrg(t,c)}$ the electricity that is stored in the battery storage. **Eq. (5.2)** describes the general equilibrium between the direct electricity supply and electricity demand side.

$$PTP_{(t,c)} = D_{el(t,c)} \quad (5.2)$$

In **Eq. (5.2)**, $PTP_{(t,c)}$ refers to the electricity input of the PTP interface and $D_{el(t,c)}$ the total electricity demand of the demand sectors industry, households, transport as well as trade and commerce. The RES-based electricity generation per time step *t* and cell *c* is represented by the aforementioned generation profiles per RES technology. Those generation profiles are based on the installed rated power and the capacity factors per cell and time step. The generation profiles of each RES technology are accumulated to the total RES-based electricity production $E_{RES,el(t,c)}$ and thermal production $E_{RES,th(t,c)}$ and input into the IES model logic.

5.4.1 Primary Sources

Wind Onshore and Offshore Generation Profiles

Based on the techno-economic potential analysis results of **Chapter 4.6.1**, hourly wind capacity factors for onshore wind $CAP_{wind,on}$ and offshore wind $CAP_{wind,off}$ are assigned to each cell. The onshore and offshore capacity factors for wind electricity generation are derived from Renewables.ninja for each hourly time step and ENTSO-E country if applicable as some countries do not possess offshore wind power sites [ETH2016a].

As depicted in **Annex IX**, the total installed onshore and offshore wind rated power $P_{wind(c)}$ is multiplied with the corresponding capacity factor $CAP_{wind}=0…1$ per time step, referencing the model input year 2015. **Eq. (5.3)** describes the wind electricity generation $E_{wind,el(t,c)}$ for onshore or offshore wind per time step *t* and cell *c*.

$$E_{wind,el(t,c)} = CAP_{wind(t,c)} \cdot P_{wind,el(c)} \quad (5.3)$$

Hence, total wind power generation curves for each of the 35 cells and the ENTSO-E entity are generated. The available hourly wind supply for 8,760 time steps per year are input into the consecutive simulation. A representative wind power generation profile at the example of the ENTSO-E is depicted in **Annex XII**.

Photovoltaic and Solar Thermal Generation Profiles

Solar production profiles are composed of solar electricity generation, such as utility-scale PV, rooftop PV, and CSP. Solar thermal energy conversion is represented by the heat production of solar thermal rooftops. Analogous to the wind power generation profiles, the electricity production of utility-scale PV and rooftop PV as well as the heat production of solar thermal rooftops is computed by multiplying the total installed capacity of each cell with the corresponding capacity factor $CAP_{sol}=0…1$ per time step, referencing the model input year 2015. The solar capacity factors for each hourly time step and ENTSO-E country are derived from Renewables.ninja [ETH2016b].

Eq. (5.4) describes the PV electricity generation $E_{PV,el(t,c)}$ per time step t and cell c. The total PV rated power $P_{PV,el(c)}$ for rooftop and utility-scale PV as depicted in **Annex IX,** is multiplied with the corresponding capacity factor $CAP_{sol}=0…1$ per time step, referencing the model input year 2015.

$$E_{PV,el(t,c)} = CAP_{sol(t,c)} \cdot P_{PV,el(c)} \quad (5.4)$$

The resulting total PV electricity generation profile at the example of ENTSO-E is depicted in **Annex XIII**. The total PV production is contained in **Annex CD**.

Eq. (5.5) describes the solar thermal production $E_{sol,th(t,c)}$ per time step and cell. Analogous to the PV electricity generation, the solar thermal production is computed. The total installed solar rooftop rated power per cell $P_{sol,th(t,c)}$ as depicted in **Annex IX,** is multiplied with the corresponding capacity factor $CAP_{sol}=0…1$ per time step, referencing the model input year 2015.

$$E_{sol,th(t,c)} = CAP_{sol(t,c)} \cdot P_{sol,th(c)} \quad (5.5)$$

The resulting solar thermal heat production profile at the example of the ENTSO-E is illustrated in **Annex XIV**. Total solar thermal heat production is depicted in **Annex CD**.

As introduced in **Chapter 4.4.4**, the electricity output of CSP plants is not a direct energy conversion, such as for PV and solar thermal production, but rather based on steam production for a thermal electricity generation process. To account for this peculiarity, a divergent approach to calculate the total electricity output $E_{CSP,el(t,c)}$ of CSP plants is chosen. To approximate the electricity generation per time step of the six countries that enable CSP production due to geographical and temperature

requirements, a ratio-based method is applied. Therefore, similar large area requirements for utility-scale PV and CSP as well as similar irradiance conditions are anticipated. Based on the computed average yearly electricity generation of utility-scale PV power and CSP plants as introduced in **Chapter 4**, the CSP ratio is multiplied with the model results of the utility-scale PV production per time step for Cyprus, Spain, France, Greece, Italy, and Portugal, as depicted in **Tab. 20**.

Tab. 20 CSP and utility-scale PV production ratios

Country	CSP Production	Utility-Scale PV Production	CSP Ratio
	[TWh]	[TWh]	
CY	3.30	6.63	0.498
ES	31.00	265.99	0.117
FR	0.50	145.36	0.003
GR	0.20	45.35	0.004
IT	0.30	125.38	0.002
PT	16.90	45.76	0.369

Consecutively, the CSP electricity production $E_{CSP,el(t,c)}$ per time step and cell is obtained by multiplying the CSP ratio with the corresponding utility-scale PV production $E_{USPV,el(t,c)}$, as indicated in **Eq. (5.6)**.

$$E_{CSP,el(t,c)} = Ratio_{CSP(c)} \cdot E_{USPV,el(t,c)} \tag{5.6}$$

The resulting CSP production $E_{CSP,el(t,c)}$ per time step and cell is accumulated with the utility-scale and rooftop PV electricity production.

5.4.2 Secondary Sources

As introduced in **Chapter 4**, the secondary sources bioenergy, hydrokinetic power, and geothermal energy are regarded as baseload supply technologies. Therefore, the energy supply per time step is regarded as constant and equalized across the 8,760 time steps per year. Thus, the total Secondary Sources energy output results $E_{sec(total,c)}$ of **Chapter 4.6.2** are divided by 8,760 to account for the energy supply $E_{sec(t,c)}$ per time step and cell, as described in **Eq. (5.7)**.

$$E_{sec(t,c)} = \frac{E_{sec(total,c)}}{8{,}760} \tag{5.7}$$

The result for each technology is input into the IES model supply side, based on the regarded energy commodities electricity $E_{sec,el(t,c)}$ and heat $E_{sec,th(t,c)}$. The resulting bioenergy, hydrokinetic power, and geothermal electricity generation profiles at the example of the ENTSO-E are depicted in **Annex XV**. The resulting bioenergy and geothermal heat production profiles at the example of the ENTSO-E are depicted in **Annex XVI**. The total Secondary Sources production is depicted in **Annex CD**.

5.4.3 Combined Cycle Gas Turbines

In order to ensure security of supply as well as to account for electricity network stability and secure provision of ancillary services in the IES model, CCGT power plants serve as a backup power supply. Since a fuel-switch to natural gas is anticipated, CCGT power plants represent the only power plants based on conventional fuels. As a general assumption regarding security of supply and sufficient provision of ancillary services, the minimum capacity of CCGT power plants $CAP_{CCGT,min(c)}$ per cell is limited to 25 % of the corresponding capacities in 2016, in reference to the Open Power System Data (OPSD) (2019) [OPSD2019]. According to the rapid ramping gradients of state-of-the-art CCGT power plants, it is anticipated that the CCGT power plants can be ramped up and down continuously and without delay. As depicted in **Eq. (5.1)**, CCGT power plants ramp up only in case RES electricity generation $E_{RES,el(t,c)}$, battery storage discharge $STO_{dis(t,c)}$, and electricity import $TRANS_{(t,c)}$ is not able to cover the electricity demand of a cell in the corresponding time step. Moreover, CCGT backup power plants are utilized to introduce the unit extension function into the model logic. Therefore, the CCGT backup power plant capacities per cell are extended, in case the 25 % minimum capacity for each cell is not sufficient to balance **Eq. (5.1)** at all time steps. The unit extension functions are introduced by **Eq. (5.8)–(5.10)**.

$$E_{CCGT,el(t,c)} > CAP_{CCGT,on(t,c)} \cdot R_{CCGT,\min(c)} \tag{5.8}$$

$$E_{CCGT,el(t,c)} < CAP_{CCGT,on(t,c)} \cdot t_{(h)} \tag{5.9}$$

$$CAP_{CCGT,on(t,c)} < CAP_{CCGT,r(c)} \cdot R_{CCGT,af} \tag{5.10}$$

In **Eq. (5.8)** $E_{CCGT,el(t,c)}$ represents the electricity production of CCGT power plants at each time step t in a cell c, which exceeds the particular power plant capacity $CAP_{CCGT,on(t,c)}$ that is actually producing electricity multiplied with the minimum capacity per cell $R_{CCGT,min(c)}$. **Eq. (5.9)** describes the relation between the backup power plants electricity generation $E_{CCGT,el(t,c)}$ and the particular available power plant capacity $CAP_{CCGT,on(t,c)}$, whereby generation is less than the available capacity per hourly time step. **Eq. (5.10)** requires the available power plant capacity $CAP_{CCGT,on(t,c)}$ to succeed the rated power plant capacity $CAP_{CCGT,r(t,c)}$ multiplied with the power plant availability factor $R_{CCGT,af}$. CCGT power plant availability is anticipated with $R_{CCGT,af}=0.85$ and a minimum load of $R_{CCGT,min(c)}=0.30$.

5.4.4 Import Fuels

Import fuels serve as backup supply for the heat, transport, and residual demands as well as to fuel the CCGT backup power plants. Fuels are imported in case the domestic production of heat, biofuels, and PTX cannot cover the corresponding demand per time step. The import sources for fossil fuels $I_{fuel(t,c)}$ are regarded as infinite and serve as backup to maintain the equilibrium of non-electricity supply and demand at all times. The equilibrium between supply and demand is described by **Eq. (5.11)**.

$$E_{PTH(t,c)} + E_{PTM(t,c)} + E_{PTG(t,c)} + E_{RES,th(t,c)} + E_{bio(t,c)} + I_{fuel(t,c)} = D_{heat(t,c)} + D_{trans(t,c)} + D_{res(t,c)} + D_{CCGT,th(t,c)} \quad (5.11)$$

The supply side of **Eq. (5.11)** comprises the corresponding PTX conversion $E_{PTX(t,c)}$, the thermal generation of solar thermal, biomass and biofuel as well as geothermal power plants $E_{RES,th(t,c)}$, and the domestic biofuel supply $E_{bio(t,c)}$ per time step and cell. The demand side is composed of heat demand $D_{heat(t,c)}$, transport demand $D_{trans(t,c)}$, residual demand $D_{res(t,c)}$, and gas power plant demand $D_{CCGT,th(t,c)}$. In case the equilibrium is not balanced at any time step, fossil fuels $I_{fuel(t,c)}$ are imported.

5.4.5 Greenhouse Gas Emissions

In reference to the energy flow chart in **Fig. 42** and **Eq. (5.11)**, direct energy use GHG emissions of the IES model are exclusively caused by the combustion of fossil fuels $I_{fuel(t,c)}$ that are imported for the heat, transport, and residual demand sectors as well as the CCGT power plants. In reference to the Intergovernmental Panel on Climate Change (2014), the average carbon dioxide equivalent emissions of natural gas for stationary combustion refer to the emission factor $EF_{CH4}=0.181\ t_{CO2eq}\ per\ MWh_{th}$ [IPCC2014]. These emission factors may vary in accordance with the natural gas composition as well as gas supply and combustion processes quality. Thus, the emission factors reflect an average assumption for the GHG emissions of natural gas combustion, based on the calculation of CO_{2eq}. [UBA2016] The total GHG emissions $GHG_{fuel(t,c)}$ of each time step and cell are calculated based on the fossil fuel import $I_{fuel(t,c)}$, as described in **Eq. (5.12)**.

$$GHG_{fuel(t,c)} = I_{fuel(t,c)} \cdot EF_{CH_4} \quad (5.12)$$

Direct non-energy use emissions comprise emissions that occur in industrial processes, such as in the chemical and raw materials industry, that are not related to energy use direct combustion. Estimating CO_{2eq} emissions resulting from the non-energy use of fossil fuels, such as natural gas and mineral oils, is not straightforward as parts of the carbon embodied in these fossil fuels is first stored in chemicals with lifetimes ranging from days to decades. These chemicals lead to emissions during the use phase or in the waste treatment phase. In reference to asphalt and land filled plastics, these chemicals do not lead to emissions within a time span relevant for emission accounting. Apart from the emissions originating from the carbon embodied in synthetic organic chemicals, non-energy use may lead to industrial process emissions during the production of certain chemicals. In some processes, the hydrocarbon input is used both as fuel and as feedstock. Depending on the definition of non-energy use applied in the energy statistics, part of the carbon embodied in the non-energy use might also lead to CO_{2eq} emissions from fuel combustion. Therefore, the Intergovernmental Panel on Climate Change (IPCC) recommends the two subsequent principal methods of calculating national GHG emissions. [Egg2006] [Neel2005]

- Reference Approach (IPCC-RA)
- Sectoral Approach (IPCC-SA)

Due to the availability of non-energy use natural gas and mineral oil amounts as well as the straight-forward nature of the macroscopic method to assess complex non-energy use emissions from a myriad of industrial processes, the reference approach IPCC-RA is chosen. IPCC-RA enables the subtraction of the amount of fossil carbon stored from the total CO_{2eq} emissions calculated on basis of the total primary energy supply of a country. Hence, non-energy use emissions are calculated on the basis of total primary energy supply of each country by multiplying the non-energy use of a certain fuel with the specific emission factor and the storage fraction for this fuel. In reference to the IPCC Guidelines for National Greenhouse Gas Inventories (2006), the methods for calculating CO_{2eq} emissions from non-energy product are composed of a carbon content factor and a factor that represents the storage fraction (SF) of fossil fuel carbon that is oxidized during use (ODU). This concept is applied to oxidation during first use of lubricants and paraffin waxes and not to subsequent uses, such as energy recovery. For this analysis, the non-energy use CO_{2eq} emissions of natural gas and mineral oils are calculated in reference to **Eq. (5.13)**. [Egg2006] [Neel2005]

$$GHG_{non\_energy} = \mathrm{NEU}_{CH_4;Oil} \cdot EF_{CH_4;Oil} \cdot SF_{CH_4;Oil} \tag{5.13}$$

In **Eq. (5.13)** $NEU_{CH4;Oil}$ indicates the amount of the non-energy use commodity natural gas or mineral oil in MWh_{th}. $EF_{CH4;Oil}$ represents the emission factor, whereas the specific emission factor of mineral oil is anticipated with $EF_{oil}=0.256\ t_{CO2eq}\ per\ MWh_{th}$ [IPCC2014] [UBA2016]. In reference to Neelis et al. (2005), the storage fraction of natural gas is anticipated with $EF_{CH4}=0.33$ and the one for mineral oils with $EF_{oil}=0.5$ [Neel2005].

However, the IPCC-RA method comes along with some degree of methodologic failure in reference to the energy statistics that do not take into account the variety of downstream non-energy carbon flows through the economy, such as trade in synthetic organic chemicals. These flows might differ substantially between countries. For this reason, emissions resulting from the non-energy use of fossil fuels contribute considerably to the overall uncertainty in many national GHG emission inventories, especially in those countries with a large share of non-energy use relative to total primary energy consumption. [Neel2005] Hence, a sensitivity analysis is conducted in reference to the computational results according to **Eq. (5.13)** and the non-energy emissions 2019, as reported by the European Environment Agency (2021) [EEA2021]. It is found that the computational result of 374 Mt CO_{2eq} deviates 7 Mt CO_{2eq} from the reported 381 Mt CO_{2eq} emissions from industrial processes in the EU-28 of 2016. Hence, the IPCC-RA method is regarded as a robust and representative method to report non-energy emissions on the ENTSO-E country level (compare **Annex CD**).

5.5 Energy Conversion and Transformation

Energy conversion and storage represents the link between energy supply and demand. As depicted in **Fig. 42**, energy conversion and storage interfaces are located in the center of the IES model flow chart. In reference to **Chapter 3**, PTX interfaces are introduced to interconnect the electricity supply side with the demand side. Among

them, the PTP and PTM interfaces enable the transmission of electricity directly to the electricity demand. The PTH, PTC, PTG_{H2}, and PTG_{SNG} interfaces convert electricity into other energy commodities, such as gas and heat, in order to cover the energy demand in the corresponding consumption sectors.

5.5.1 Power-to-Heat

In reference to **Chapter 3.2**, PTH refers to the provision of heat and cold via the means of heat pumps, electric boilers, and air conditioners. Average heat pumps operate at an average coefficient of performance (COP) of $COP_{HP}=3.10$ [IEA2014]. The efficiency of electric boilers is anticipated as $\eta_{EB}=0.97$ [Yilm2017]. Due to the necessity of external heat sources for heat pumps and high temperature level needs for process energy, which are restricting the field of application for heat pumps, the ratio of electric boilers and heat pumps is anticipated as $R_{EB:HP}=0.85:0.15$. Based on **Eq. (5.14)**, the average conversion efficiency of PTH is computed as $\eta_{PTH}=1.30$.

$$\eta_{PTH} = 0.85 \cdot \eta_{EB} + 0.15 \cdot COP_{HP} \tag{5.14}$$

According to the COP of air conditioners (AC), which show an average efficiency range of $COP_{AC}=1.90…4.30$ for residential AC, the COP of AC in the PTC interface is regarded as $\eta_{PTH,AC}=4.00$ [Yilm2017].

5.5.2 Power-to-Gas

In reference to **Chapter 3.3**, PTG refers to the production of hydrogen and synthetic natural gas (SNG) via the means of electrolysis (PTG_{H2}) and methanation (PTG_{SNG}). The prevailing educts of the PTG process are water and carbon dioxide, which are converted by the means of electricity into the products hydrogen (H_2) and SNG. According to the IES model logic, PTG_{H2} is powered exclusively by surplus RES electricity. PTG_{SNG} is sourced with hydrogen from PTG_{H2} as well as captured carbon dioxide from biomass, biogas, and CCGT power plant exhaust gases. The water-based electrolysis PTG_{H2} represents the first process in the PTG conversion. Average electrical efficiencies of alkaline (AEL) and polymer-electrolyte membrane (PEM) electrolyzers range between 70–74 % [Lehn2014] [Purr2016]. Due to technical advance a conversion efficiency of $\eta_{PTG,H2}=0.75$ is anticipated. As indicated in **Fig. 42**, the produced H_2 can either be utilized in fuel cell electric vehicles (FCEV) in the transport sector or further react with CO_2 in the subsequent methanation process.

Constrained by the availability of CO_2 from power plant combustion processes, the methanation process PTG_{SNG} is supplied with H_2. In reference to the high economic utilization value, the remaining H_2 is exclusively available for the transport sector. Based on the meta-analysis of particular substance flows in common electrolyzer setups, an average H_2 production of 281.25 m^3 per 1 MW rated power is anticipated. Moreover, 1 m^3 CO_2 and 4 m^3 H_2 are necessary to produce 0.02 MWh_{SNG} at elevated pressures. In reference to the here regarded PTG_{SNG} process, a catalytic methanation in an environment of $T=300°C$ and $p=20\ bar$ is anticipated. In accordance with the ideal gas

law, the gravimetric emission factors for SNG, biomass, and biogas are converted into volumetric units V_{CO2}, as depicted in **Eq. (5.15)**.

$$V_{CO2} = \frac{\mathrm{n} \cdot \mathrm{R} \cdot \mathrm{T}}{p} \tag{5.15}$$

Eq. (5.15) comprises the temperature T in kelvin and pressure p in pascal as well as the ideal gas constant R and the amount of substance n. Based on the catalytic reaction conditions, the conversion factor is computed as $1\ kg\ CO_2 = 0.053\ m^3\ CO_2$. In reference to the ideal gas law of **Eq. (5.15)**, the volumetric emission factors of natural gas $EF_{SNG,v}$, biogas $EF_{biogas,v}$, and biomass $EF_{biomass,v}$ are calculated and input into **Eq. (5.16)**, in order to compute the total available CO_2 volume as input for the methanation process.

$$V_{CO2(t,c)} = EF_{SNG,v} \cdot \frac{E_{CCGT,el(t,c)}}{\eta_{\mathrm{CCGT,el}}} + EF_{biogas,v} \cdot \frac{E_{biogas(t,c)}}{\eta_{biogas,\mathrm{el}}} + EF_{biomass,v} \cdot \frac{E_{biomass,el(t,c)}}{\eta_{\mathrm{biomass,el}}} \tag{5.16}$$

In consideration of the meta-analysis results, a stoichiometric gas mixture is anticipated. The consecutive calculation of the H_2 input $H_{2,SNG(t,c)}$ and SNG output $E_{SNG(t,c)}$ is depicted in **Eq. (5.17)–(5.18)**.

$$H_{2_{SNG(t,c)}} = 4 \cdot CO_{2_{v(t,c)}} \tag{5.17}$$

$$E_{SNG(t,c)} = 0.02 \cdot CO_{2_{v(t,c)}} \tag{5.18}$$

Based on **Eq. (5.19)**, the remaining surplus hydrogen $E_{H2,trans(t,c)}$ is directly input into the gas storage and then supplied to the transport demand.

$$E_{H2,trans(t,c)} = PTGH_{2_{(t,c)}} \cdot \eta_{PTGH_2} - \frac{H_{2_{SNG(t,c)}}}{281.25} \tag{5.19}$$

In accordance with the energy flow chart in **Fig. 42**, the produced SNG $E_{SNG(t,c)}$ and the remaining hydrogen $E_{H2,trans(t,c)}$ are first supplied to the gas storage, before being supplied to the energy demands. Therefore, it enables the storage and supply of gaseous energy commodities across multiple time steps.

5.5.3 Power-to-Mobility

As introduced in **Chapter 3.4**, PTM refers to the utilization of electricity as well as liquid and gaseous fuels in the transport sector. As a simplification, those vehicles can be distinguished among light vehicles and heavy-duty vehicles. Based on this categorization, light vehicles comprise passenger cars, here regarded as battery electric vehicles (BEV), whereas heavy-duty vehicles represent trucks as well as shipping and aviation vessels. In reference to the IES model flow chart in **Fig. 42**, the transport demand is covered by electricity via the PTM interface as well as hydrogen, natural gas, and biofuels. To account for various energy intensities and range requirements, light vehicles in form of BEV are solely powered by electricity via the PTM interface. The BEV

charging process efficiency in the PTM interface is anticipated as η_{BEV}=0.95. As depicted in **Eq. (5.20)**, electricity supplied to the PTM interface $E_{BEV,el(t,c)}$ equals the electricity demand of BEV $D_{BEV,el(t,c)}$ per time step and cell divided by the BEV charging efficiency η_{BEV}, according to the BEV demand profile.

$$E_{BEV,el(t,c)} = \frac{D_{BEV,el(t,c)}}{\eta_{BEV}} \tag{5.20}$$

Heavy-duty vehicles are fueled with hydrogen, natural gas, and biofuels. The efficiency of combustion processes in the heavy-duty transport sector is regarded as η_{HD}=0.35. Those efficiencies are included in the absolute demand profiles of the transport sector.

5.5.4 Transmission, Distribution, and Storage

In reference to the IES model flow chart in **Fig. 42**, the battery storages serve as a storage interface for electricity, in order to store surplus electricity for the consecutive time steps. The gas storage represents a buffer-storage to supply hydrogen and SNG to the corresponding demand sectors. The gas storage is supplied with surplus hydrogen and SNG from the methanation process. The battery storage is based on the lithium-ion technology and, therefore, a charging and discharging efficiency of η_{BAT}=0.95 is anticipated. Due to compression and diffusion of the gaseous energy commodities, the gas storage efficiency is anticipated with η_{STO}=0.90. Battery storages are regarded as short-term storage to balance the electricity network, whereas gas storages are regarded as mid- and long-term storages to provide secure energy supply. To account for transmission and distribution losses, electricity transmission losses are regarded with $\eta_{el,trans}$=0.90 and gas distribution with $\eta_{gas,trans}$=0.90 (compare **Tab. 19**).

5.6 Energy Demand

As depicted by the IES model flow chart in **Fig. 42**, energy demand refers to the right-hand side of the energy flow chart. In reference to the IES model logic, energy demand accounts for the demand of energy in each time step and cell. Depending on the corresponding energy consumption sector, energy demand can be covered by various energy commodities, such as electricity, heat, natural gas, biofuels, hydrogen, and SNG. The demand sectors are distinguished by heat, cold, electricity, transport, and residual demand. Based on the analysis of the energy balances as introduced in **Chapter 2.4** as well as in reference to the standard load profiles for electricity, heat, and cold demand, the future energy demands for each ENTSO-E country are anticipated based on assumptions regarding energy efficiency gains and changing energy consumption patterns. To thoroughly account for future energy demand profiles, various scenarios and meta-studies are under consideration. In reference to the IES model logic, energy demand is regarded as a fixed input and represents the manipulated variable.

5.6.1 Heating and Cooling Demand

Heating and cooling demand is distinguished among hot water supply, space heating, and space cooling, and process heating and process cooling. The detailed analysis and

development of heating and cooling demand profiles for each ENTSO-E country is exhaustively elaborated in **Annex XVII**. To account for future efficiency gains and increasing energy demands due to technologic advance and changing energy consumption patterns, various assumptions are taken into account. Based on the trend scenario of Prognos et al. (2014), the absolute demand curves for heating and cooling of each country and final demand sector are adjusted [Prog2014].

In reference to Fleiter et al. (2017), the adjustments refer to the total heating and cooling demand of 2016 [Flei2017a]. Regarding the private households and trade and commerce, hot water supply as well as space heating and cooling are under consideration. Regarding the sectors industry and trade and commerce, process heating and process cooling demand curves are adjusted. The heating and cooling demand adjustment ratios in reference to the base year 2016 are indicated in **Tab. 21**.

Tab. 21 Future heat demand assumptions
Source: In reference to [Prog2014]

Type of Demand	Future Energy Demand
	Ratio
Hot Water	1
Space Cooling	2
Space Heating	0.5
Process Heating	0.9
Process Cooling	0.9

In reference to the IES model flow chart in **Fig. 42**, the domestic heating demand of each time step and cell is covered by various heat supply options. The IES model logic distinguishes among the following RES-based heat supply technologies.

- Solar thermal
- Biomass and Biogas CHP
- Geothermal
- PTH
- PTG_{SNG}
- Biofuels

The separated cooling demand is exclusively supplied by air-conditioners (AC) that are based on the adsorption chiller technology. AC are regarded as reversible heat pumps and introduced by the PTH_{cold} interface. Fossil fuel imports offset residual heat demand if the RES-based heat supply sources are not able to cover heat demand in each time step. The resulting total heating demand profile at the example of ENTSO-E is depicted in **Annex XX**. The total cooling demand profile is depicted in **Annex XXI**. The total heating and cooling demand for each ENTSO-E country is contained in **Annex CD.**

5.6.2 Electricity Demand

Each country possesses a specific electricity consumption pattern. For this analysis, the hourly country-specific electricity consumption is derived from historical data of ENTSO-E for the year 2015 [ENTSO2019b]. The electricity demand sector embraces various electricity demands in the final consumption sectors industry, private households, transport, and trade and commerce. Due to its manifold application options, electricity consumption is likely to comprise final energy demand applications and patterns that show cross-references to other energy application sectors. Those electricity demand patterns may refer to electric railway systems in the transport sector or electric heating in the heat sector. Therefore, the distinction among those sectors and attribution to particular applications is not straight forward.

As the purpose of this analysis is to investigate the energy demand coverage in each sector and to distinguish among various energy sources, it is intended to separate electricity demand for transportation and heating as well as cooling from the plain electricity demand profiles. To separate the electricity heating content, the country-specific electricity shares for space heating according to the European Statistical Office (Eurostat) (2019) [EUROS2019c] are subtracted from each electricity demand profile and accounted for in the heating profile. Analogous, the cooling demand is deducted, whereby a 100 % electrification rate is anticipated. Regarding the energy share of transportation in the ENTSO-E electricity demand profiles, it is anticipated that the share of electric transportation predominantly consists of electric trains. The average EU-28 electricity consumption for electric trains amounts to 2.3 % [EEA2016]. Thus, electricity demand of each country per time step is subtracted by 2.3 % of the total demand, to account for the transport demand that is covered by electricity supply. This approach might not capture the detailed intra-day electricity demand, due to peak and off-peak hours, nor it reflects country-specific characteristics of the train system. However, it allows a general estimation for the electricity share in the transportation sector. Regarding the IES model input, the electricity demand of BEV according to the calculation of **Annex XXIII** is added to the electricity demand profiles of each ENTSO-E country. To provide an overview of electricity consumption patterns, the one-year ENTSO-E load curve is depicted in **Annex XXII** and the separated BEV load profiles are depicted in **Annex XXIV** and **Annex XXV**.

5.6.3 Transport Demand

Transport demand embraces all kinds of transportation, such as commercial, public, aviation, and maritime transport. In reference to the hourly-based IES model, annual transport demand of ENTSO-E countries in 2050 is equally divided into 8,760 time steps. Based on different energy sources, the energy supply for transportation is classified into battery electric vehicles (BEV), fuel cell electric vehicles (FCEV), compressed natural gas (CNG) vehicles and biofuel and fossil fuel vehicles. As indicated in the IES model flow chart in **Fig. 42**, BEV are powered by electricity based on the BEV demand profile of each country. FCEV are fueled with hydrogen (H_2), which is produced via electrolysis in the

power-to-hydrogen (PTG_{H2}) process. CNG vehicles are fueled with imported natural gas or SNG from the PTG process. Biofuels stem from the domestic bioenergy production. Fossil fuels are imported in case the domestic fuel production does not cover the transport demand of each time step. For the IES model input, the electricity demand of BEV according to the calculation in **Annex XXIII** is subtracted from the transport demand in order not to double account for the BEV demand, which is already accounted for in the electricity demand profiles. The resulting transport demand at the example of ENTSO-E is depicted in **Annex XXVI**.

5.6.4 Residual Demand

Based on the energy balances evaluation in **Chapter 2.4**, residual demand refers to the demand that cannot be clearly categorized and attributed to a particular demand sector. In reference to the energy balance product categorization in **Tab. 3** of **Chapter 2.4**, those demands comprise energy demands for industrial and chemical processes, such as processes that can be found in the raw materials industry and other sectors, such as agriculture, forestry, and final non-energy consumption. Analogous to the transport demand method, residual demand is distributed equally across the 8,760 time steps and covered by domestic SNG and biofuel production. As depicted in **Fig. 42**, fossil fuel imports cover residual demand if SNG and biofuels cannot cover the demand of a particular time step. Natural gas serves as the exclusive fossil fuel source in the residual demand sector and contributes the corresponding CO_{2eq} emissions. The resulting residual demand at the example of the ENTSO-E is depicted in **Annex XXVI**.

5.7 Analysis and Evaluation

5.7.1 Primary Energy Consumption

In reference to **Chapter 2.4**, primary energy consumption refers to the total energy input of the IES model, as indicated on the left-hand side of the ENTSO-E 2050 Sankey energy diagram in **Fig. 58** and the energy flow charts in the **Compendium**. Primary energy represents the total available energy before energy conversion, transformation, export, bunkering, and final consumption. Since the ENTSO-E 2050 energy system is dominated by RES-based primary energy production, the Sankey representation of wind- and solar-based RES production refers to net primary energy production. Therefore, the primary energy input computation of the IES model refers to net primary energy conversion to not account for primary global irradiation and wind energy.

As depicted in **Annex XXVII**, total primary energy consumption of the ENTSO-E 2050 energy system accounts for 16,980 TWh. Those primary input is composed of a heterogenous mixture of primary energy conversion and commodities, such as onshore and offshore wind (5,780 TWh), utility-scale PV, rooftop PV, CSP (3,097 TWh), geothermal (621 TWh), and hydrokinetic (659 TWh) electricity production. RES-based heat production consists of geothermal heat (816 TWh) and solar thermal heat (362 TWh). Fuels are composed of biomass, biogas, and biofuels (2,157 TWh), mineral oils (1,547 TWh), natural gas (1,782 TWh), and other sources (159 TWh). Out of those

fuels, 1,165 TWh mineral oils and natural gas are input into the non-energy consumption sector for raw materials and chemical industry processes. In total, RES-based primary energy consumption contributes 13,492 TWh, which accounts for 79.5 % of total primary energy consumption. The relative share of primary energy consumption per technology and energy commodity is depicted in **Fig. 43**.

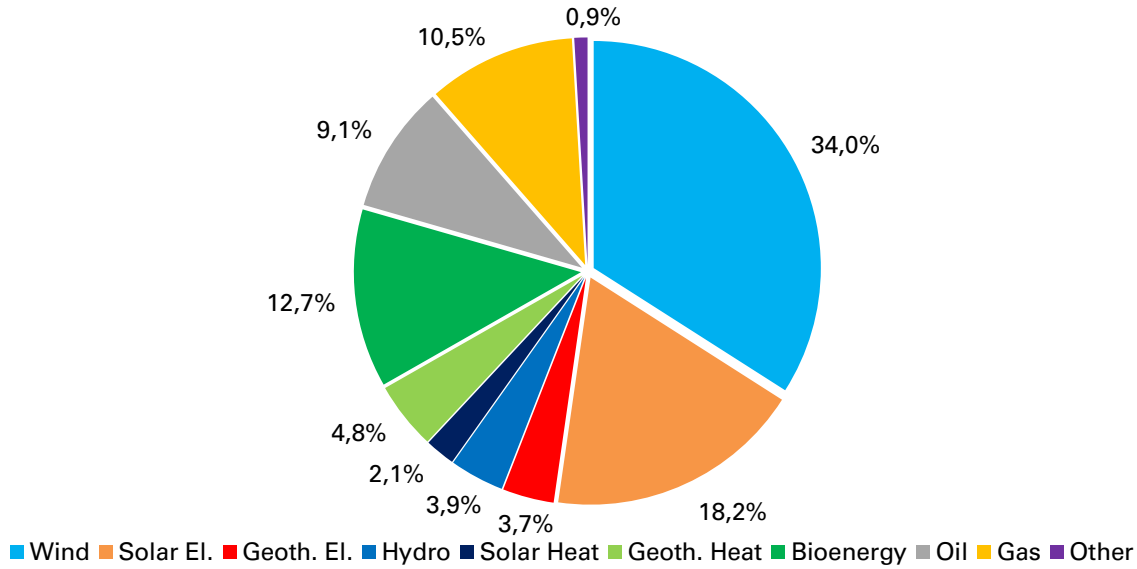

Fig. 43 Primary energy and non-energy consumption ratios ENTSO-E 2050

As indicated by **Fig. 43**, RES-based electricity production accounts for 59.8 % of total available primary energy. It is composed of onshore and offshore wind (34.0 %), utility-scale PV, rooftop PV, CSP (18.2 %), geothermal (3.7 %), and hydrokinetic (3.9 %) electricity production. RES-based heat production accounts for 6.9 % and consists of geothermal heat (4.8 %) and solar thermal heat (2.1 %) production. Fuels are composed of biomass, biogas, and biofuels (12.7 %), mineral oils (9.1 %), natural gas (10.5 %), and other sources (0.9 %) that contribute 33.2 % of total primary energy consumption.

Out of those fuels, 35.0 % of mineral oil and natural gas commodities are input into the non-energy use sector. Therefore, 35.0 % of primary energy fuels do not contribute to the energy related consumption and conversion processes, neither to energy associated GHG emissions. Hence, those industry process related resources are regarded by the non-energy use GHG emission calculation, as introduced in **Chapter 5.4.5**.

As depicted in **Annex XXVII**, the 35 ENTSO-E countries exhibit a heterogeneous mixture of primary energy consumption. In reference to **Chapter 4**, RES-based primary energy potentials are dependent on the geographic and topographic features and the specific parameters of each country, such as offshore access, country size, and population density. RES-based primary energy consumption refers to the domestic electricity and heat production of wind, solar, geothermal, and hydrokinetic RES converters and to the domestic biofuels production potential.

In reference to the IES model computation in **Chapter 5**, remaining primary energy consumption is covered by fossil fuel imports from third-party countries. **Fig. 44**

illustrates the quantities and distributions of energy technologies and commodities in reference to primary energy consumption per country.

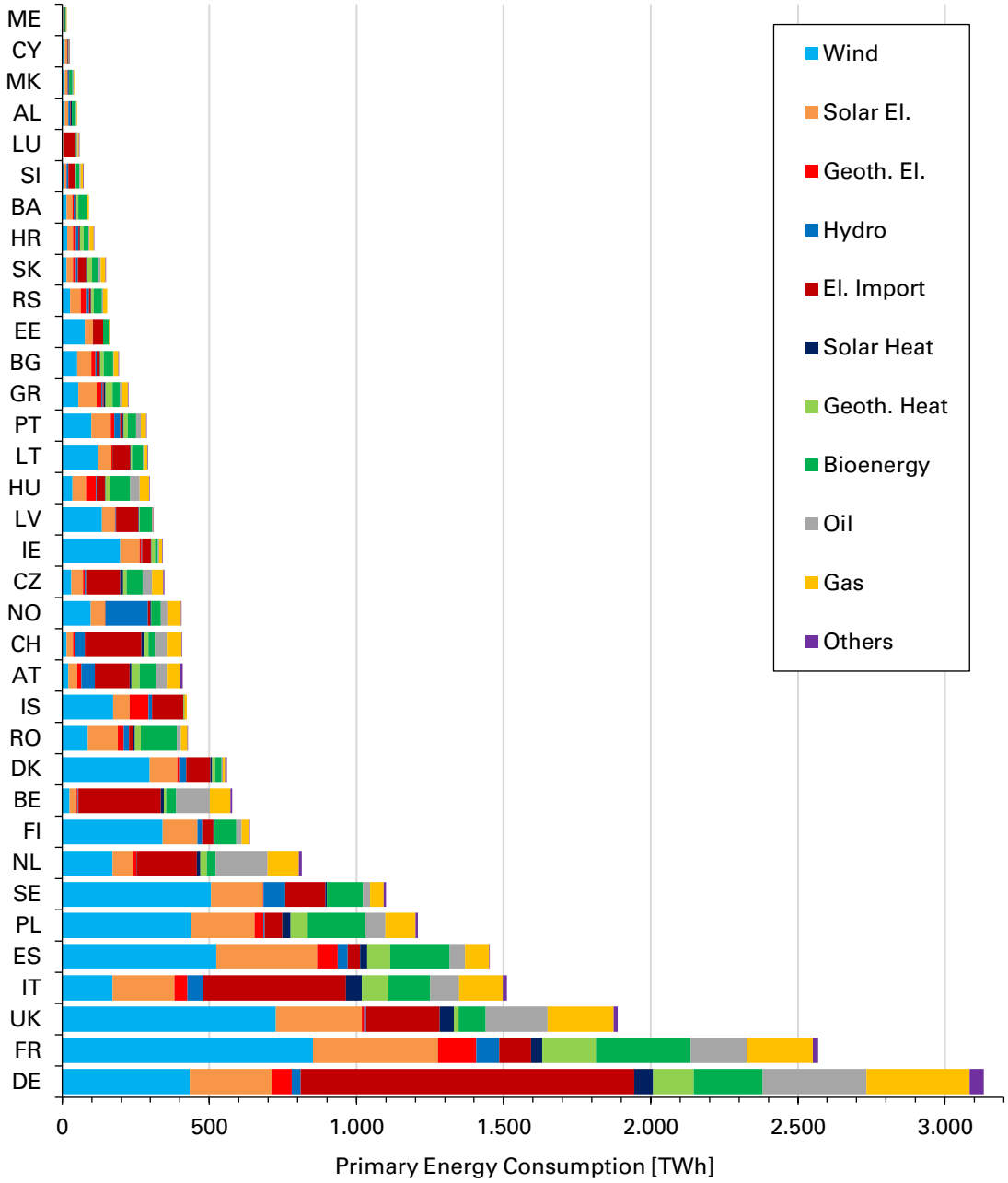

Fig. 44 Primary energy consumption per technology and country 2050

As indicated by **Fig. 44**, primary energy consumption is dominated by the large-scale countries Germany (3,132 TWh), France (2,569 TWh), UK (1,888 TWh), Italy (1,510 TWh), Spain (1,453 TWh), Poland (1,208 TWh), and Sweden (1,100 TWh), with each more than 1,000 TWh primary energy consumption. Thus, Germany (18.4 %), France (15.1 %), UK (11.1 %), Italy (8.9 %), Spain (8.6 %), Poland (7.1 %), and Sweden (6.5 %) exhibit the largest share of the 16,980 TWh total primary energy consumption. Remarkably, the 9,099 TWh of the four largest countries Germany, France, UK, and Italy contribute 54.1 % of primary energy consumption. Hence, only four out of thirty-five countries are consuming more than half of total primary energy. In consideration of

Spain, Poland, and Sweden, which account for another 3,761 TWh, the top seven countries exhibit more than three-quarters of primary energy consumption (76.4 %).

However, primary energy entails domestic energy production and imports, but does not account for potential electricity exports. Thus, primary consumption does not reflect the net energy demand of a country. For instance, Sweden and other countries with high net electricity exports, such as Denmark, Latvia, and Lithuania, do not belong to the leading final energy consumption countries (compare **Chapter 5.7.3** and **Annex XXX**). In order to correctly account for net energy demands it seems more appropriate to consider final energy consumption, which represents energy demand after energy imports, exports, losses, and transformation (compare **Chapter 5.7.5**).

Out of the large-scale countries (compare **Annex I** and **Annex II**), especially France (853 TWh), UK (726 TWh), Spain (524 TWh), Sweden (505 TWh), and Poland (437 TWh) exhibit an exceptional large onshore and offshore wind electricity production, due to high availability of onshore and offshore wind sites. Compared to that, Germany (434 TWh) possesses moderate wind potential, due to limited onshore and offshore access and high population densities. Other countries, such as Finland (341 TWh) and Denmark (297 TWh), exhibit considerable amounts of wind power electricity production due to favorable offshore wind site access. The aforementioned countries account for more than two-thirds (71.2 %) of total wind power production.

In reference to superior solar locations and share of available rooftop area and suitable areas for utility-scale PV and CSP, the solar electricity production is dominated by France (423 TWh) and Spain (342 TWh). The other large-scale countries UK (292 TWh), Germany (277 TWh), Poland (217 TWh), Italy (210 TWh), Sweden (178 TWh), and Finland (118 TWh) contribute an inferior share. In total, those countries account for 66.4 % of total solar electricity production. Hence, the solar power potential is more well dispersed across the ENTSO-E compared to the wind power potential, due to lesser restrictions and area dependencies.

In reference to the applied per capita methodology (compare **Chapter 4.4.5**), solar thermal rooftop heat production exhibits the strongest shares in Germany (63 TWh), Italy (53 TWh), UK (47 TWh), France (39 TWh), Poland (29 TWh), and Spain (24 TWh), which account for 70.4 % of total solar thermal production. Due to the capita-based methodology of rooftop-only installations, the potential is directly correlated with the population density of each country.

Depending on the particular topographic and geographic features, hydrokinetic and geothermal production potential is primarily country specific. Due to favorable mountainous locations, the largest hydrokinetic electricity production potential is identified in Norway (144 TWh), France (78 TWh), Sweden (76 TWh), Italy (54 TWh), and Austria (46 TWh), Spain (35 TWh), Switzerland (31 TWh), and Germany (31 TWh). Those countries account for three-quarters (74.9 %) of total hydrokinetic electricity production. The highest combined geothermal electricity and heat production is identified in France (313 TWh), Germany (208 TWh), Spain (147 TWh), Italy (136 TWh),

Poland (86 TWh), Iceland (68 TWh), Hungary (50 TWh), and Austria (43 TWh), which account for almost three-quarters (73.1 %) of total geothermal production.

Domestic bioenergy primary consumption is headed by France (322 TWh), Germany (235 TWh), Spain (203 TWh), Poland (197 TWh), Italy (141 TWh), Romania (123 TWh), Sweden (122 TWh), and UK (91 TWh), with each more than 90 TWh primary energy consumption. These countries account for 66.5 % of total bioenergy production, due to superior bioenergy potentials as investigated in **Chapter 4.5–4.6**.

Out of the 3,488 TWh conventional fuel imports of natural gas, mineral oils, and other sources, Germany (751 TWh), UK (450 TWh), France (432 TWh), the Netherlands (292 TWh), Italy (261 TWh), Belgium (192 TWh), Poland (177 TWh), and Spain (137 TWh) exhibit particular high shares. These countries account for more than three-quarters (77.2 %) of total fossil fuel imports. Therefore, those countries are prone to possess the highest shares of quantitative GHG emissions.

In reference to gross electricity imports, Germany (1,134 TWh) exhibits the largest share, followed by Italy (485 TWh), Belgium (282 TWh), UK (251 TWh), the Netherlands (205 TWh), and Switzerland (192 TWh), which account for more than two-thirds (68.2 %) of total electricity imports. The potential of electricity imports is restricted by the availability of RES-based electricity production of adjacent countries and the corresponding transmission capacities.

5.7.2 Energy Transformation, Exchanges, and Losses

Energy transformation, exchanges, and losses account for all energy conversion processes between primary and final energy consumption. Energy imports represent the energy and non-energy relevant mineral oils and natural gas derivates, in order to supply energy and non-energy demand that cannot be covered by domestic RES-based production. Those conventional sources might be supplied by domestic production of those countries which possess relevant gas and oil reservoirs, such as Norway, the Netherlands, UK, Romania, Italy, and Denmark [EUROS2022].

However, almost all of these countries signed declarations of renunciation to ban new explorations and to end conventional fuels extraction beyond 2050 [EUNEW2022] [IHS2021]. This development is also enforced by the EU fifth list of Projects of Common Interest (PCI) [EC2021].[14] Hence, for this analysis it is anticipated that future conventional fuel imports stem exclusively from third-party countries. Electricity imports and exports account for the intercellular energy exchange among the countries. However, the ENTSO-E entity does not exhibit any electricity exchange with third-party countries, as it is regarded as enclosed European electricity system entity.

Energy conversion and transformation embraces all processes that refer to the conversion of primary energy sources into secondary energy commodities and

[14] PCI are key infrastructure projects aimed at completing the European internal energy market in order to help the EU to achieve its energy and climate policy objectives [EC2021].

applications, such as power plant combustion, refining processes, and PTX. As depicted in the center part of the ENTSO-E Sankey diagram in **Fig. 58**, those conversion processes account for a total energy transformation of 10,793 TWh. The relative composition of energy conversion per technology is depicted in **Fig. 45**.

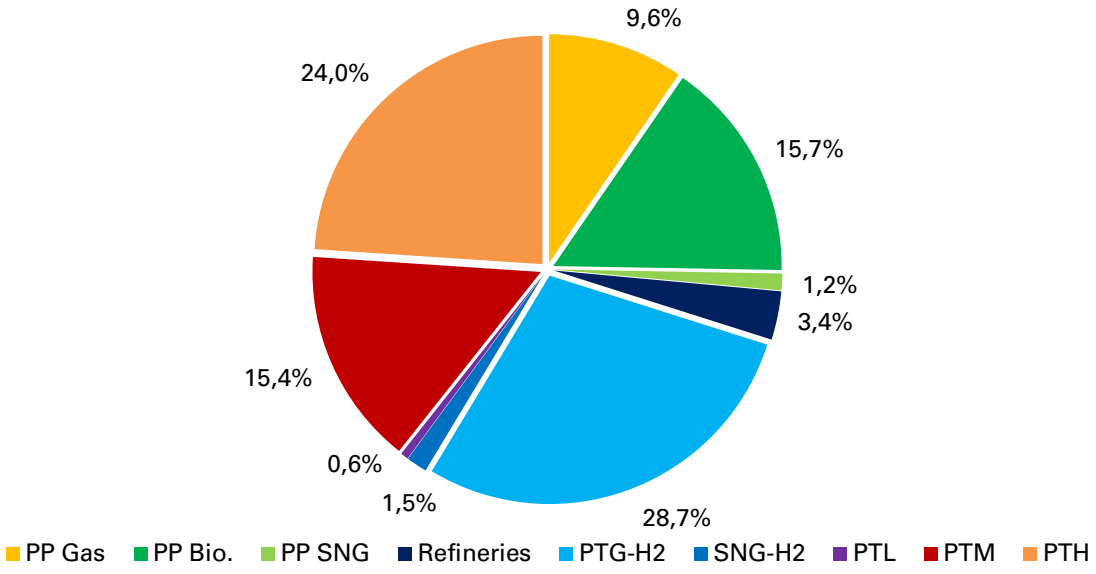

Fig. 45 Energy conversion and transformation ratios ENTSO-E 2050

The 10,793 TWh energy transformation and conversion account for 64.0 % of total primary energy consumption. Hence, almost two-thirds of primary energy consumption are further converted by various processes, whereas one-third is directly supplied to final energy consumption in the form of electricity and heat as well as liquid and gaseous fuels. As depicted in **Fig. 45**, PTG_{H2} (28.7 %) and PTH (24.0 %) contribute the largest share of energy conversion processes, followed by bioenergy combustion in power and heat plants (15.7 %) and PTM (15.4 %). Natural gas and SNG combustion in CCGT power plants (10.8 %), refinery processing (3.4 %) and SNG-H_2 (1.5 %) and PTL-H_2 (0.6 %) supply[15] exhibit minor contribution to energy conversion and transformation. Total PTX conversion accounts for 70.1 %, followed by 26.5 % power plant combustion, and 3.4 % refinery transformation. In reference to those processes and the corresponding exergy consumption (compare **Chapter 5.4**), 1,470 TWh (9.3 %) refer to process-related conversion losses and 1,644 TWh (10.4 %) to distribution losses. In total, energy conversion and distribution losses amount to 3,114 TWh (19.7 %)

Hence, the primary to final energy conversion and distribution efficiency accounts for 80.3 %. In comparison to 2016, energy conversion and distribution losses could be reduced by 2,271 TWh or 1.6 percentage points due to increased contribution of highly efficient transformation processes, such as PTP, PTM, and PTH, paired with a decrease of inefficient thermal combustion processes, such as power and heat plant combustion. However, those decrease is rather marginal as relatively large amounts of conversion processes, foremost PTX, are located in the energy conversion and transformation

[15] H_2-based SNG-H_2, PTL-H_2, and SNG production are input twofold into the conversion and transformation processes (compare **Fig. 42** in **Chapter 5.3.1**).

section rather than being attributed to final energy downstream processes. Analogous to the 2016 system, those downstream processes can be found in the utilization of final energy commodities for industrial processes, transport, and other applications.

In reference to **Annex XXXII**, the ENTSO-E countries exhibit a heterogeneous composition of energy conversion and transformation processes, which are depending on the availability of primary energy electricity, heat, and domestic biofuel production potentials as well as electricity import potentials from adjacent countries and total third-party fuel imports. The quantitative energy conversion and transformation inputs per country and technology are depicted in **Fig. 46**.

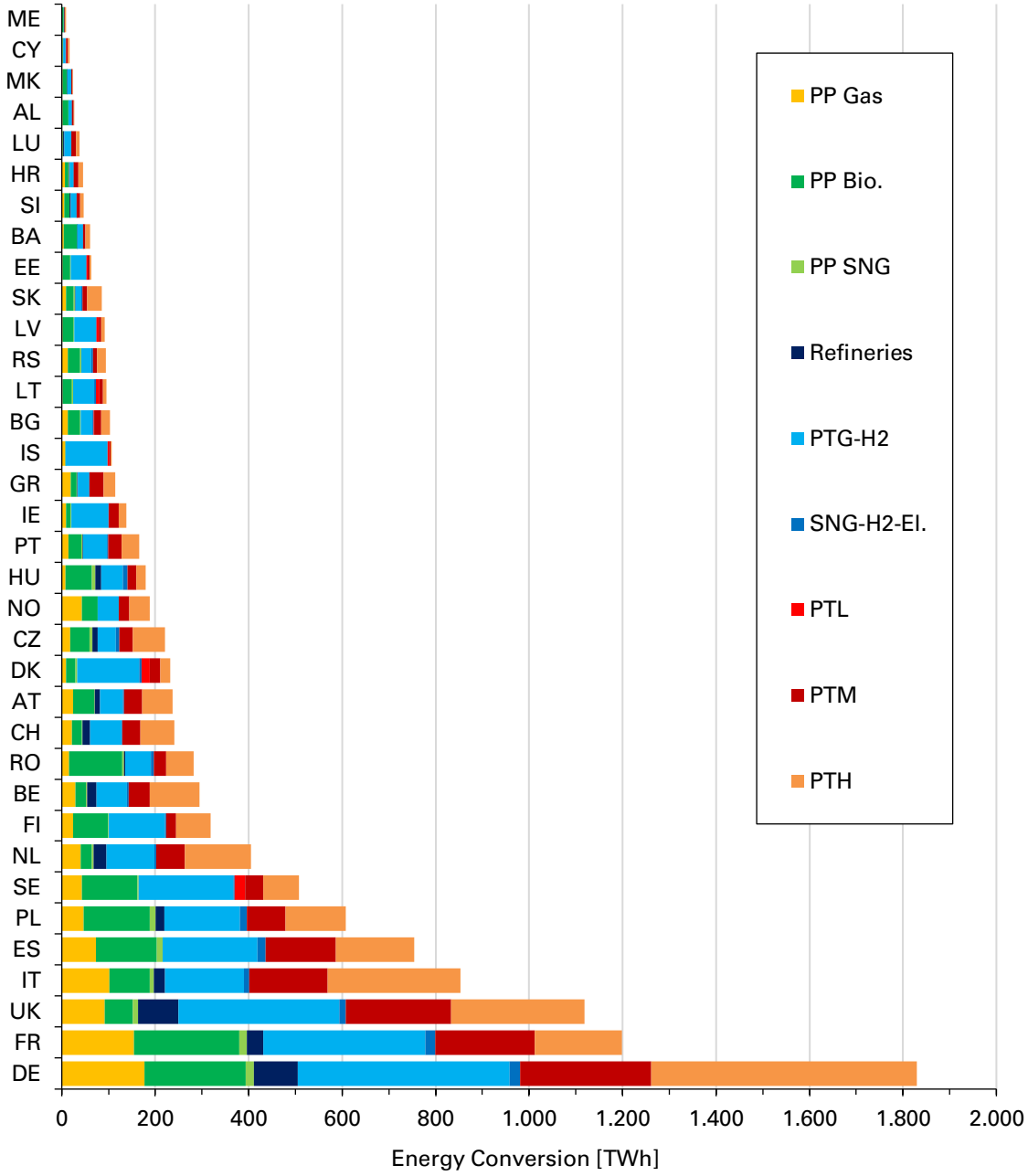

Fig. 46 Energy conversion and transformation per technology and country 2050

As indicated in **Fig. 46**, energy conversion and transformation input is headed by Germany (1,830 TWh), France (1,199 TWh), UK (1,118 TWh), Italy (854 TWh), Spain (754 TWh), Poland (608 TWh), and Sweden (507 TWh), with each more than 500 TWh.

This distribution resembles the country ranking of primary energy consumption (compare **Chapter 5.7.1**) that is dominated by large-scale countries and, hence, reflects the greater demands of those countries for primary energy consumption.

However, small-scale countries, such as Sweden, Finland, Belgium, Switzerland, Denmark, and Iceland, can be found in the upper ranks of the primary energy consumption and conversion ranking. Here, Sweden, Finland, Denmark, and Iceland belong to the high potential RES-based primary energy conversion countries and, therefore, exhibit a strong primary energy consumption share before electricity exports (compare **Fig. 44** and **Fig. 46**). Since exports are not deducted from primary energy consumption, it does not indicate the domestic energy demand. In this regard, gross inland consumption as per definition of **Eq. (2.1)** in **Chapter 2.4** is a more representative indicator for the evaluation of domestic primary energy demands.

Moreover, those countries possess a high contribution of energy conversion and transformation based on PTX, foremost based on PTG_{H2}. On the other hand, small-scale countries such as Belgium and Switzerland exhibit comparably high energy demands combined with inferior domestic RES-based production. Therefore, comparably large conventional fuel imports become necessary. Those energy demands are covered by fuel imports that are processed in refineries and power plants. Electricity imports that are converted in PTX processes, foremost by the utilization of PTH as well as PTG_{H2} and PTM, are necessary to offset the energy balance. This observation leads to the consideration of net energy imports and exports and the corresponding ratios, in the following denoted as energy dependency rates.

Analogous to the 2016 energy dependency analysis in **Fig. 9** of **Chapter 2.4**, energy dependency rates provide an overview of net energy imports and exports (negative imports) distributions of each country in reference to gross inland consumption, as depicted in **Eq. (2.1)**. These ratios denote those countries which exhibit net energy imports and those which possess net energy exports. However, the spread of total net domestic electricity exports (3,739 TWh) and energy imports (6,062 TWh) exhibits a total deviation of 2,323 TWh.

This deviation represents the ENTSO-E net import of conventional energy use fuels. Hence, the dependency rate accounts for 13.7 % of the energy use primary consumption imports. The remaining non-energy use import demand amounts to 1,165 TWh, which corresponds to a dependency rate of 6.9 %. Thus, the 3,488 TWh net import demand, which comprises 1,782 TWh natural gas, 1,547 TWh crude oil, and 159 TWh other sources, accounts for a total dependency rate of 20.5 %. Net import demands and energy dependency rates per country are depicted in **Fig. 47**.

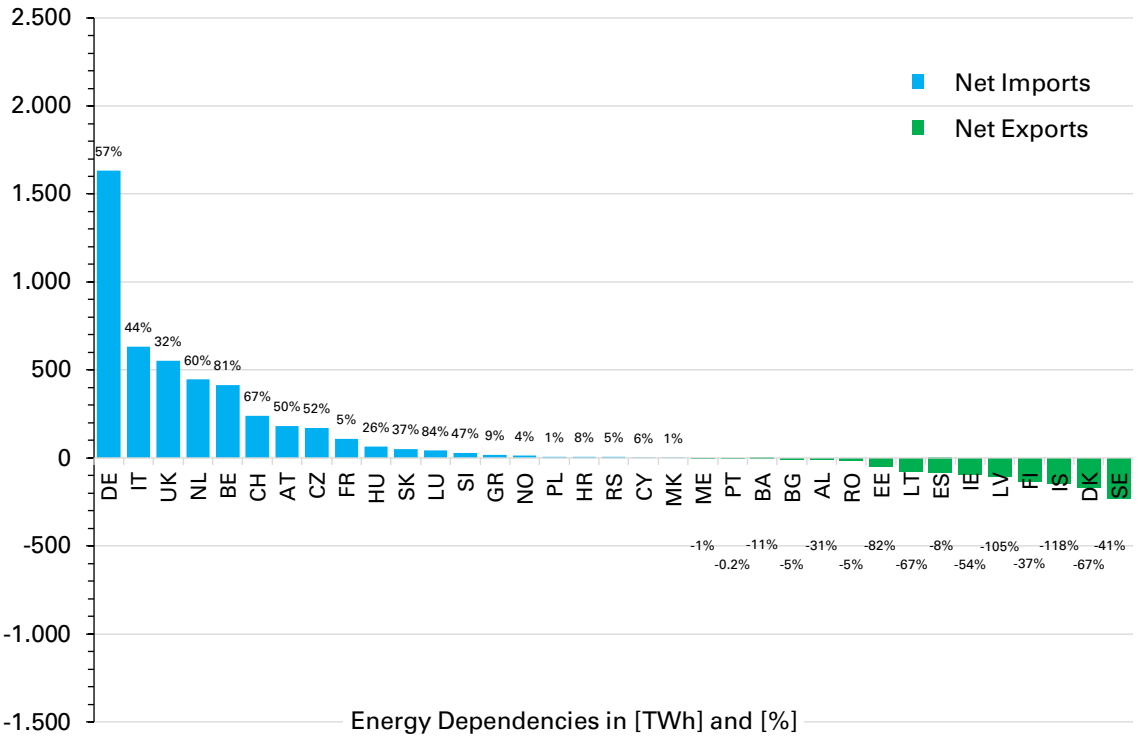

Fig. 47 Energy dependencies per country 2050

In reference to **Annex IV**, net primary energy imports are reduced by 6,482 TWh (65.0 %) compared to 2016. Therefore, the ENTSO-E 2050 energy dependency rate is effectively reduced by 29.4 percentage points. As depicted in **Fig. 47**, the energy dependency rates show a heterogeneous distribution. Quantitative net energy imports are headed by Germany (1,633 TWh), Italy (634 TWh), UK (551 TWh), the Netherlands (446 TWh), Belgium (415 TWh), Switzerland (240 TWh), Austria (180 TWh), Czechia (170 TWh), and France (108 TWh), with each more than 100 TWh.

In comparison to the ENTSO-E 2016 energy system as described in **Chapter 2.4**, significantly more countries represent net energy export countries. Among those 15 net export countries, Sweden (230 TWh), Denmark (169 TWh), Iceland (145 TWh), Finland (136 TWh), Latvia (105 TWh), Ireland (96 TWh), Spain (85 TWh), Lithuania (77 TWh), Estonia (50 TWh), and Romania (14 TWh) exhibit the largest net energy export potential, due to comparatively high RES potentials paired with moderate domestic energy demands. Accumulated, those countries exports are almost equal to the 2016 exports of Norway (compare **Chapter 2.4**).

In reference to **Chapter 4** and **Chapter 5.6**, those factors are significantly influenced by the individual topographic and geologic features, population and country size, as well as grade of industrialization and GDP (compare **Annex I** and **Annex II**). Among the net energy export countries, Iceland (-117.6 %), Latvia (-104.7 %), Estonia (-82.3 %), Denmark (-66.9 %), Lithuania (-66.8 %), Ireland (-53.8 %), Sweden (-41.3 %), and Finland (-36.6 %) exhibit the highest negative energy dependency rates. Thus, net export of those countries is superior to gross domestic consumption.

On the contrary, Luxembourg (83.9%), Belgium (81.4%), Switzerland (67.2%), the Netherlands (60.1%), Germany (56.7%), Czechia (52.0%), Austria (49.9%), Slovenia (46.9%), and Italy (44.0%) possess significantly high energy dependency rates. Hence, those countries are not able to offset domestic demand by RES-based production and electricity import potentials from adjacent countries. Therefore, those countries remain strongly dependent on energy imports from third-party countries.

In comparison to the 2016 dependency rates diagram in **Fig. 9** of **Chapter 2.4**, not all countries decreased net energy imports. Especially the mid- and large-scale countries with comparatively low energy dependencies in 2016, such as the Netherlands and UK increase energy dependency rates significantly due to lack of RES potentials, which could offset the large domestic fossil fuel exploitation in 2016. However, previously fossil fuel dependent countries, such as Denmark, Ireland, Poland, Romania, and Sweden, could substitute fuel consumption by RES production and significantly reduce energy dependencies. In reference to the specific features, Germany, Italy, UK, and Belgium remain in the top ranks of net energy import countries.

Among the large-scale countries, France, Spain, and Poland are able to significantly decrease absolute and relative import dependencies, whereas Spain profits from large net export potentials (85 TWh). Among the previously import dependent countries, especially Sweden, Finland, and Ireland possess superior net export potentials. Hence, the ENTSO-E 2050 energy dependencies largely depend on primary energy consumption, domestic RES-production, adjacent countries electricity export potential, and the particular demand for non-energy use fuel imports.

5.7.3 Primary and Secondary Electricity Production

Primary and Secondary (total) electricity production refers to primary energy commodities that are secondarily converted by power plants and the already converted primary energy electricity production of wind- and solar-based RES converters. Those converters are regarded by the Primary Sources potential analysis in **Chapter 4.3**. Primary Sources total electricity production per country is a result of the available rated power per technology and the anticipated capacity factor profiles, as introduced in **Chapter 5.4.1**. Secondary Sources total electricity production is derived from the Secondary Sources potential analysis as introduced in **Chapter 4.5**. CCGT gas power plant backup generation is derived from the IES model computation, as presented in **Chapter 5.4.3**. Therefore, CCGT power plants are ramped up in case the RES-based electricity generation is not sufficient to cover electricity demand of each time step.

Total secondary electricity production accounts for 11,280 TWh, which is utilized for conversion and transformation in the PTX stream or directly supplied through the PTP interface. As depicted in **Fig. 48**, total electricity production and the corresponding electricity mix show a heterogeneous distribution, which is composed of 94.0% RES-based and 6.0% conventional electricity production.

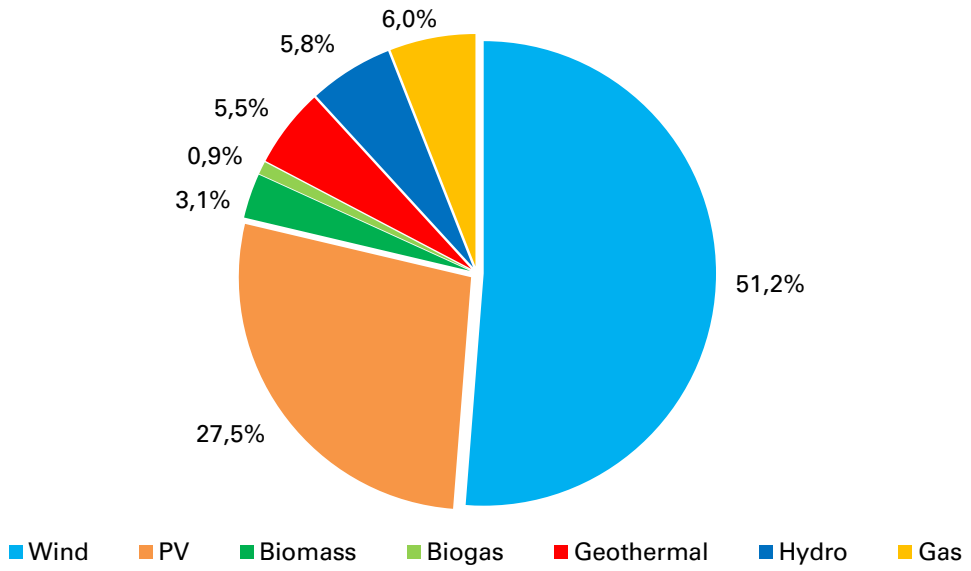

Fig. 48 Share of total electricity production per technology ENTSO-E 2050

As indicated in **Fig. 48**, total electricity production of the ENTSO-E 2050 energy system is composed of RES-based onshore and offshore wind (51.2 %), utility-scale PV, rooftop PV, and CSP (27.5 %), biomass and biogas (4.0 %), geothermal (5.5 %), hydrokinetic (5.8 %), and conventional CCGT (6.0 %) electricity production. Primary Sources onshore and offshore wind, utility-scale PV, rooftop PV, and CSP (78.7 %) contribute the highest share. Due to the intermittent non-dispatchable wind- and solar-based electricity production, those converters simultaneously exhibit the highest fluctuations and insecurities regarding security of supply. The dispatchable technologies biomass, biogas, geothermal, hydro, and CCGT power plants account for 21.3 % of total electricity production. Hence, 78.7 % of the electricity producers do not contribute to security of supply and system resilience, as they are non-dispatchable. The wind and PV power plant production can only be controlled within the framework of grid security measures, such as curtailment of excess power generation to account for secure network operation.

As depicted in **Annex XXVIII**, the composition of the Primary and Secondary Sources electricity production and the CCGT backup production exhibits a heterogeneous distribution across the ENTSO-E. In reference to the techno-economic potential analysis of **Chapter 4**, each ENTSO-E country possess a strongly individual composition of electricity production technologies. This distribution depends on the individual availability of RES-based electricity producers, predominantly determined by the specific geographic, topographic, and demographic features of each country. Moreover, the availability of surplus electricity production and sufficient transmission capacities in adjacent countries reduces the need for domestic CCGT backup electricity production. **Fig. 49** illustrates the quantities and distributions of secondary electricity production per country and technology.

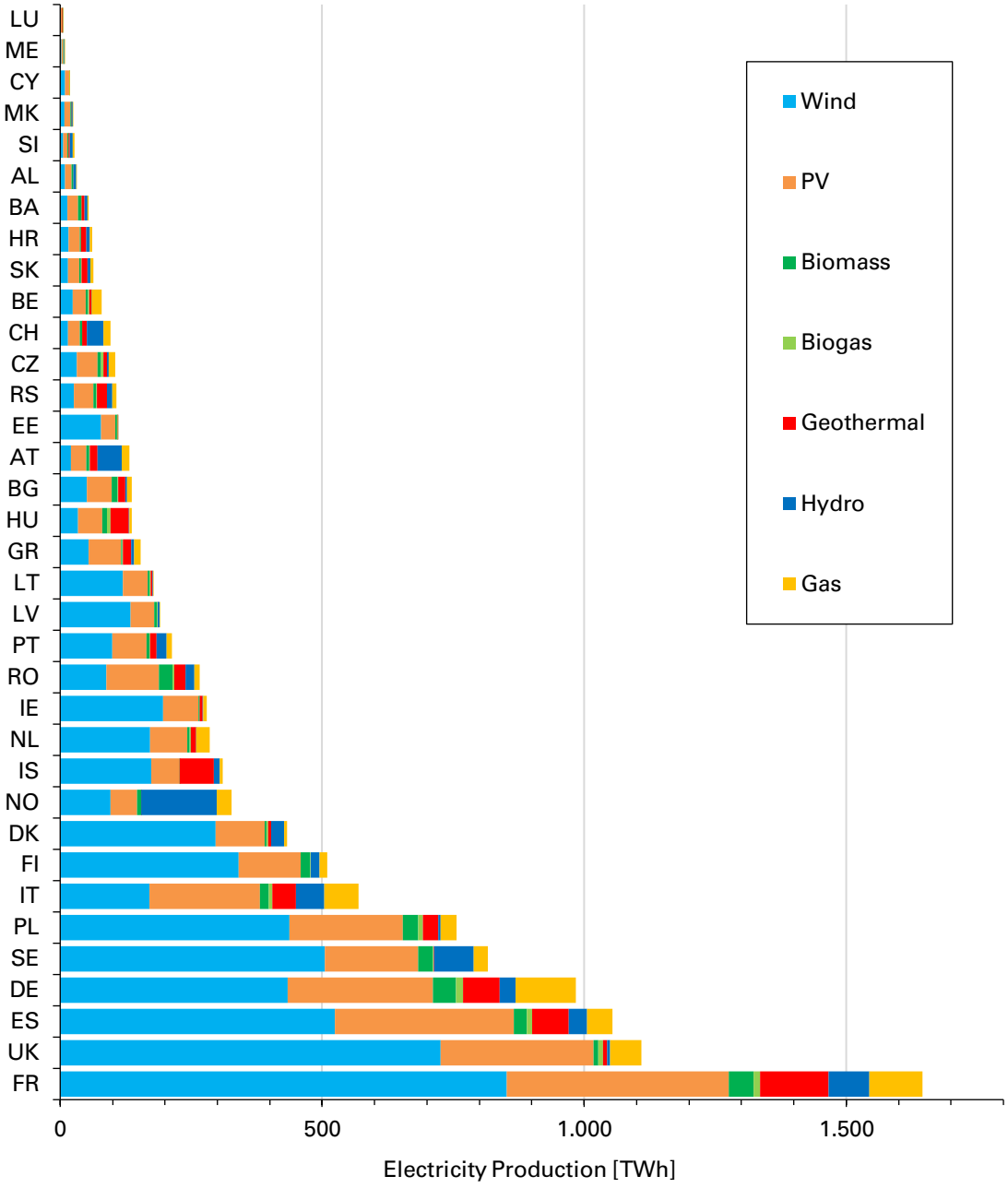

Fig. 49 Total electricity production per technology and country 2050

As depicted in **Fig 49**, France exhibits the largest total electricity production (1,645 TWh), followed by UK (1,109 TWh), Spain (1,053 TWh), Germany (984 TWh), and Sweden (817 TWh), with each more than 800 TWh. Those countries account for nearly half of total electricity production (49.7 %). Together with Poland (756 TWh), Italy (570 TWh), Finland (510 TWh), Denmark (433 TWh), Norway (327 TWh), and Iceland (310 TWh), those eleven countries account for 75 % of total electricity production. Among the ENTSO-E countries, Belgium (24.4 %), Luxembourg (23.0 %), Austria (14.8 %), Switzerland (14.8 %), Slovenia (12.2 %), Germany (11.7 %), Austria (11.6 %), Italy (11.6 %), and Czechia (11.4 %), with each more than 10 %, possesses a significantly high contribution of CCGT power plant electricity production. Countries such as Lithuania (0.4 %), Latvia (0.4 %), Estonia (1.1 %), Denmark (1.3 %), Iceland (1.6 %), and Ireland (2.2 %), exhibit only little contribution of CCGT backup power generation, due to high shares of RES-based electricity production and sufficient transmission

capacities to adjacent countries (compare **Annex XI**). As a result of the techno-economic potential analysis of **Chapter 4**, the electricity production composition depends strongly on the potential and availability of each technology, which differs significantly from country to country.

In reference to the electricity dependency analysis of **Chapter 2.4**, the electricity dependencies of each country are under consideration. As depicted in **Fig. 50**, the ENTSO-E is composed of net electricity export and import countries. Analogous to the electricity dependency illustration in **Fig. 10**, net electricity imports are denoted by bluish columns on the upper side of the diagram, whereas net electricity exports (negative imports) are denoted by the greenish antipode columns. The percentage indication depicts the ratio of net imports or exports from gross electricity inland consumption. Unlike the energy dependency analysis in **Chapter 2.4** and **Chapter 5.7.2**, electricity dependencies focus exclusively on net electricity imports and exports. Therefore, they account for the prevailing significance of the foremost primary energy commodity electricity in the energy system 2050.

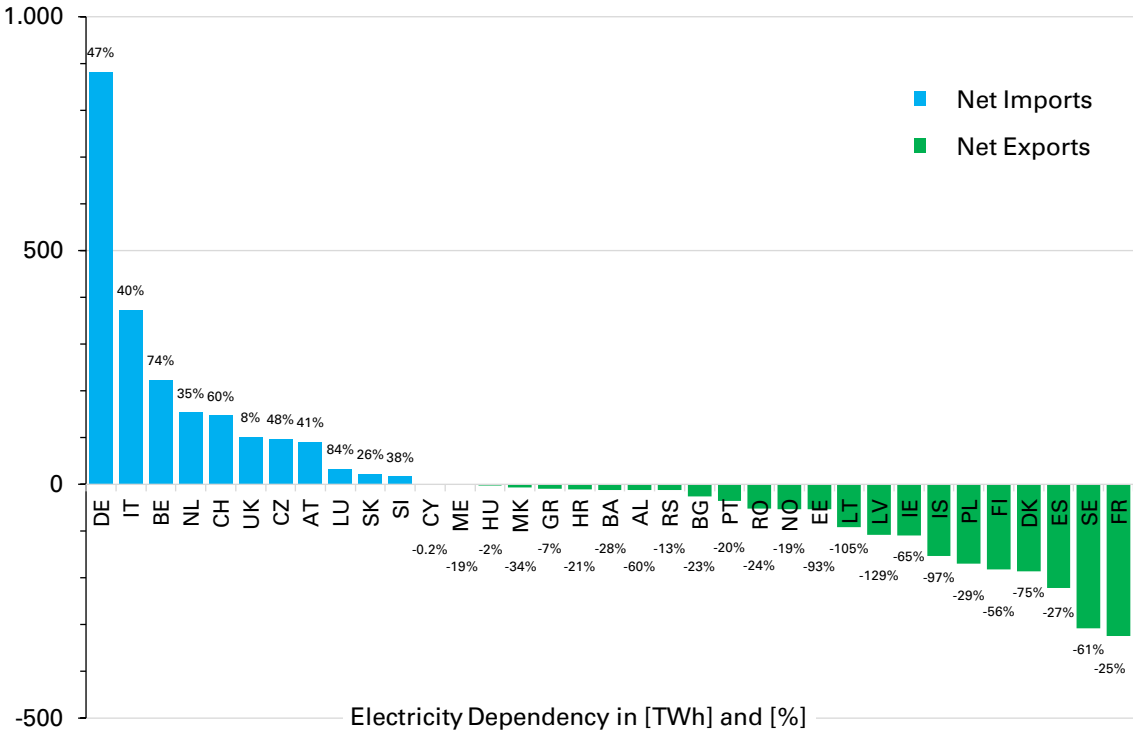

Fig. 50 Electricity dependency rates per country 2050

As depicted in **Annex XXXI** and **Fig. 50**, net electricity imports are led by Germany (882 TWh), Italy (373 TWh), Belgium (223 TWh), the Netherlands (154 TWh), Switzerland (148 TWh), UK (102 TWh), Czechia (97 TWh), and Austria (91 TWh), with each more than 90 TWh electricity imports. Out of the net electricity import countries, Luxembourg (84.0 %), Belgium (73.8 %), Switzerland (60.5 %), Czechia (48.1 %), Germany (47.3 %), Austria (40.8 %), Italy (39.6 %), and Slovenia (37.8 %) exhibit the highest electricity dependency ratio, with each more than 35 % of gross inland electricity consumption. Analogous to the energy dependency analysis, those countries possess comparatively large energy demands and only moderate RES-based production

potentials. Hence, they represent net import dependent countries in absolute and relative shares. Remarkably, the aforementioned countries exhibit particular low onshore and offshore wind potentials (compare **Chapter 4.6.1** and **Chapter 5.7.1**).

On the contrary, France (324 TWh), Sweden (308 TWh), Spain (222 TWh), Denmark (186 TWh), Finland (182 TWh), Poland (169 TWh), Iceland (153 TWh), Ireland (110 TWh), and Latvia (108 TWh) represent the leading total net electricity export countries, with each more than 100 TWh electricity surplus. Out of the net export countries, Latvia (-129.0 %), Lithuania (-104.6 %), Iceland (-97.3 %), Estonia (-92.9 %), Denmark (-75.2 %), Ireland (-64.6 %), Sweden (-60.7 %), Albania (-59.7 %), and Finland (-55.6 %) exhibit the highest net electricity export ratios (negative imports), with each more than 50 % of gross inland electricity consumption. In comparison to **Chapter 4.6.1** and **Chapter 5.7.1**, those countries exhibit significantly large shares of onshore and offshore wind power potentials. Whereas France, Spain, Poland, and Finland possess considerable large solar electricity potentials. Hence, those RES-based primary electricity production potentials become a major driver for future electricity exports.

As depicted in **Fig. 50**, the distribution of the 11 net electricity importers and 24 net electricity exporters exhibits a large spread, with more than twice export than import countries. In comparison to the electricity dependency of 2016 as depicted in **Fig. 10**, a diverse picture of net import and export countries is identified. Due to superior RES-based electricity production potentials, France remains the leading electricity export country. Whereas Italy stays among the largest electricity importers, due to inferior RES potentials. Germany switches its role from the leading net electricity export to the leading net import country, due to conventional power plant phase out and moderate RES potentials. Hence, the electricity dependency rate increases drastically. Likewise, Czechia, Denmark, Finland, Poland, and Spain exhibit remarkable shifts.

Since, no electricity is exchanged with non-ENTSO-E countries and the ENTSO-E is regarded as enclosed electricity system entity, total electricity dependency equals zero. Therefore, the electricity dependency rate corresponds to 0.0 %. However, a total of 3.739 TWh electricity is exchanged among the ENTSO-E countries. Hence, electricity imports and exports of the ENTSO-E 2050 Sankey diagrams in **Fig. 58** and in **Fig. 37** of the **Compendium** refer exclusively to the domestic exchange.

5.7.4 Primary and Secondary Heat Production

Analogous to primary and secondary electricity production, primary and secondary (total) heat production is derived from Primary and Secondary Sources. To not account for global total irradiation, primary energy of solar thermal rooftops equals secondary energy output, as introduced by the Primary Sources potential analysis of **Chapter 4.4.5**. Secondary Sources total heat production is derived from the Secondary Sources potential analysis as introduced in **Chapter 4.5–4.6**. Total heat production of solar thermal rooftops, biomass, biogas, and geothermal power stations is utilized to directly cover heat demand.

In case heat production of solar thermal rooftops and thermal power stations is not sufficient to cover the heat demand of each time step, additional heat is produced via the PTH interface. Total heat production amounts to a total of 5,348 TWh, which accounts for 31.5 % of primary energy consumption. Moreover, additional 1,072 TWh (16.7 %) of total primary heat production are slacked, due to the IES model logic as introduced in **Chapter 5.3.2**. Hence, there exists a superior heat production potential that cannot be utilize due to insufficient heat storages, especially during the summer period. The distribution of the 5,348 TWh total heat production (heat slack is not considered) per technology is depicted in **Fig. 51**.

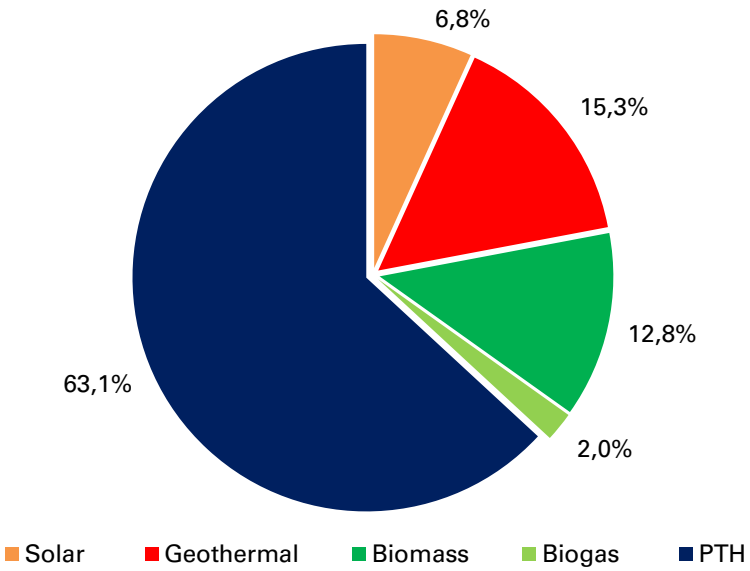

Fig. 51 Share of total heat production per technology ENTSO-E 2050

As indicated in **Fig. 51**, total heat production shows a heterogeneous picture, which is composed of 63.1 % PTH (3,376 TWh), 15.3 % geothermal (816 TWh), 14.8 % biomass and biogas (794 TWh), and 6.8 % solar thermal heat production (362 TWh). GHG emissions of the heat sector are exclusively caused by the secondary electricity mix of the PTH electricity input and the corresponding GHG emissions, which accounts for 6.0 % contributed by natural gas fueled CCGT power plants. Moreover, 1,072 TWh of solar thermal and geothermal primary heat production is slacked by the IES model logic, as it does not account for long-term heat storage. The heat slack accounts for 16.7 % of total heat production and represents a considerable amount of unused energy.

As depicted in **Annex XXIX**, the composition of primary and secondary heat production exhibits a heterogeneous distribution across the ENTSO-E. In reference to the techno-economic potential analysis of **Chapter 4**, each ENTSO-E country possess a strongly individual composition of available RES-based heat production, which is dependent on geographic, topographic, and geologic features. **Fig. 52** illustrates the quantities and distributions of total heat production per country and technology.

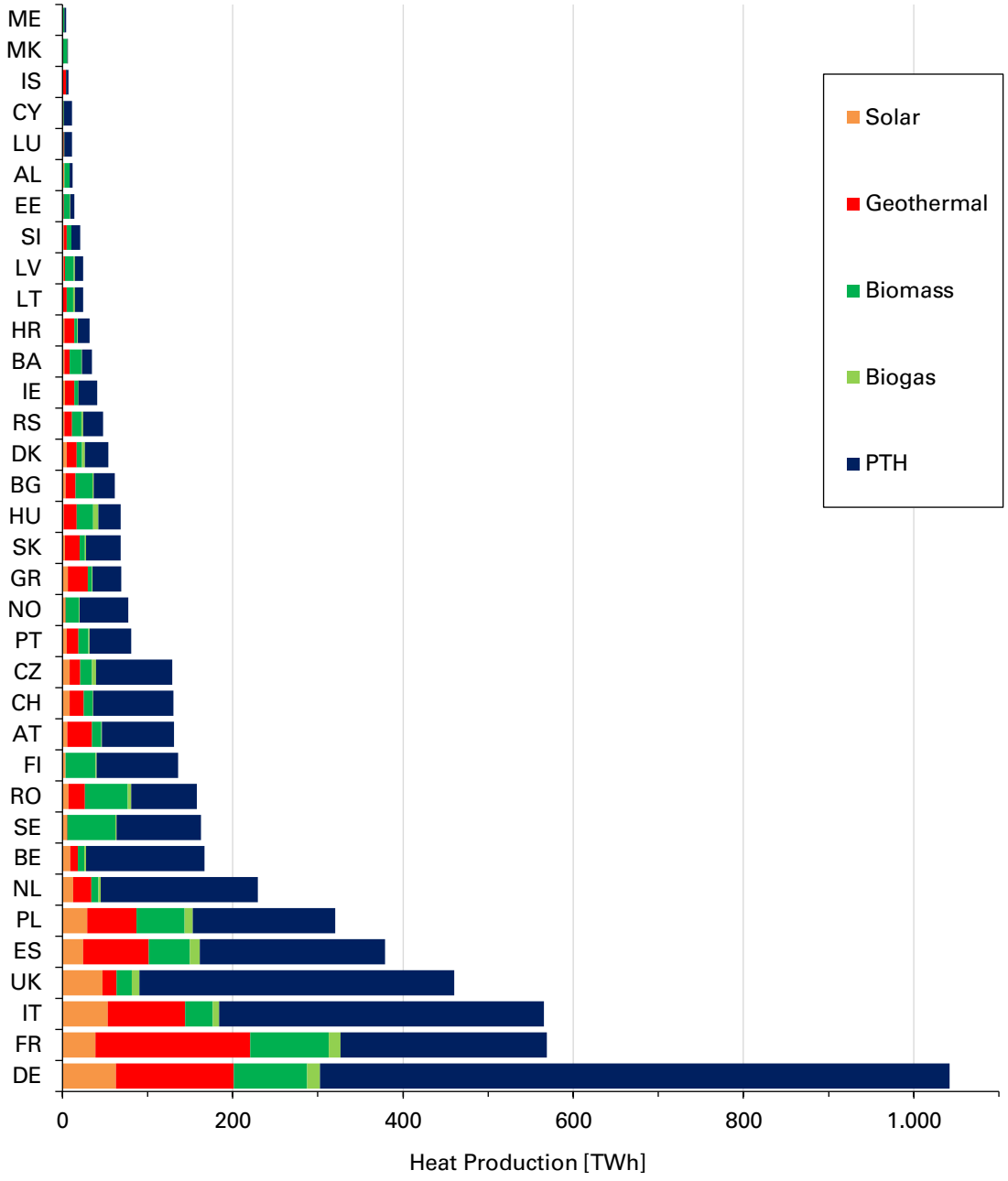

Fig. 52 Total heat production per technology and country 2050

As depicted in **Fig. 52**, countries such as France (182 TWh), Germany (138 TWh), Italy (90 TWh), Spain (77 TWh), and Poland (58 TWh) exhibit an extraordinarily large geothermal heat production potential, due to favorable geologic features. In almost all countries, PTH occupies a major share of the heat production, such as in Germany (661 TWh), Italy (395 TWh), UK (358 TWh), and Spain (220 TWh).

Depending on the domestic bioenergy production potentials, also biomass and biogas thermal power stations in countries such as France (106 TWh), Germany (101 TWh), Poland (66 TWh), Spain (60 TWh), Sweden (58 TWh), and Romania (54 TWh) contribute considerable shares. Solar thermal heat production strongly depends on the availability of rooftop space. Hence, large solar thermal shares are identified in the large-scale countries Germany (63 TWh), Italy (53 TWh), UK (47 TWh), and France (39 TWh).

Countries with low primary heat production potentials based on geothermal and bio energy, exhibit extraordinarily large shares of PTH. Among them, Germany (740 TWh), Italy (381 TWh), UK (370 TWh), the Netherlands (185 TWh), and Belgium (138 TWh).

5.7.5 Final Energy Consumption

Final energy consumption comprises gaseous and liquid energy commodities, such as biofuels, mineral oil, natural gas, and others. Moreover, it entails various PTX products, such as hydrogen, synthetic liquid fuels, and electricity. Electricity is supplied via the PTP and PTM interfaces. The PTX product synthetic natural gas (PTG-SNG) is not regarded by final energy consumption, as it is stored and exclusively supplied to the CCGT power plants in the energy transformation section, in order to account for some degree of security of supply. Moreover, primary heat from RES-based heat producers and secondary heat from PTH and thermal power stations are supplied directly. Final energy represents primary energy subtracted by energy exports, bunkering, and conversion and transmission losses. The ENTSO-E total final energy consumption accounts for 12,701 TWh. The relative composition of final energy consumption per energy technology and commodity is depicted in **Fig. 53**.

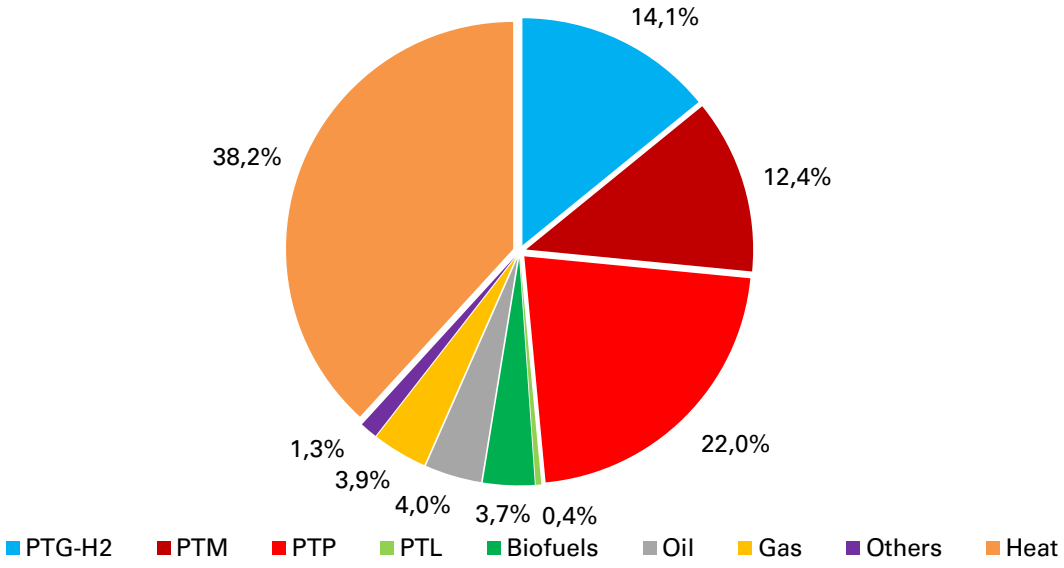

Fig. 53 Final energy consumption ENTSO-E 2050

As depicted in **Fig. 53**, heat contributes 38.2 % and, thus, the largest share of final energy consumption. Final electricity consumption accounts for 22.0 % through the PTP interface and 12.4 % through the PTM interface. Therefore, electricity represents the second largest share with 34.4 %. The PTG_{H2} product hydrogen has a share of 14.1 %. Mineral oil (4.0 %), natural gas (3.9 %), biofuels (3.7 %), other sources (1.3 %), and synthetic fuels (0.4 %) show only minor contribution with a total of 13.3 %. Final energy composition is a result of the primary energy production potentials per technology, total demand distribution, and the efficiency based linear optimization of the IES model. **Fig. 54** illustrates the quantities and distributions of the 12,701 TWh final energy consumption per country and technology.

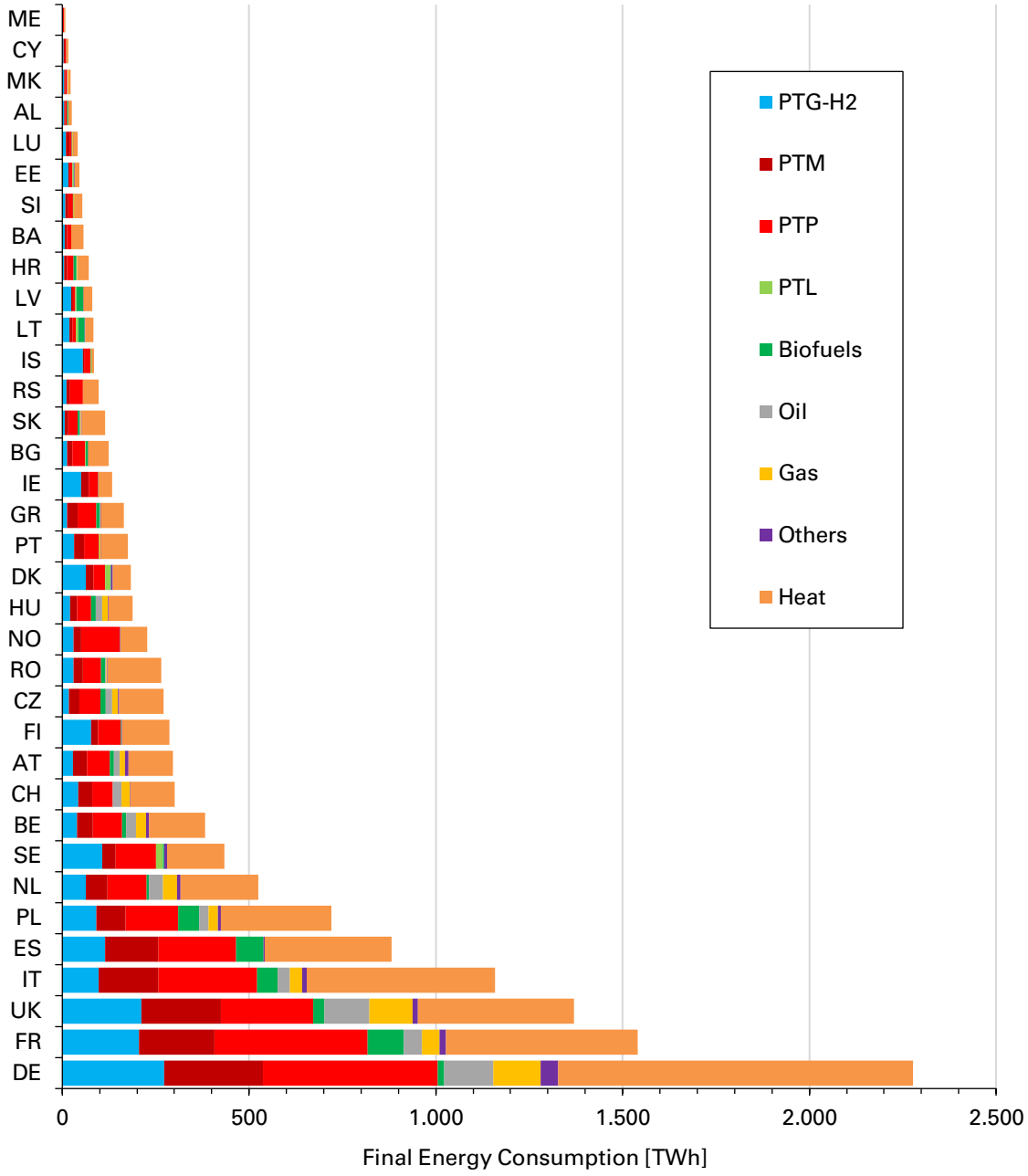

Fig. 54 Final energy consumption per technology and country 2050

In reference to **Annex XXX**, the composition of final energy consumption exhibits a heterogeneous distribution across the ENTSO-E. As indicated in **Fig. 54**, final energy consumption is dominated by the large-scale countries Germany (2,291 TWh), France (1,549 TWh), UK (1,399 TWh), and Italy (1,227 TWh), with each more than 1,000 TWh final energy consumption. Spain (874 TWh), Poland (706 TWh), and the Netherlands (523 TWh) exhibit more than 500 TWh final energy consumption. Hence, Germany (18.0 %), France (12.2 %), UK (11.0 %), Italy (9.7 %), Spain (6.9 %), Poland (5.6 %), and the Netherlands (4.1 %) possess the largest share. Remarkably, the four largest countries Germany, France, UK, and Italy contribute more than half (50.9 %) of final energy consumption. The composition of final energy consumption is strongly dependent on the individual availability of primary energy commodities.

Among those countries, especially Germany (272 TWh), UK (211 TWh), France (205 TWh), Spain (115 TWh), and Sweden (107 TWh), with each more than 100 TWh, exhibit an exceptional large PTG_{H2} hydrogen consumption. Hence, those countries embrace comparatively many time steps with excess electricity, which can be utilized for hydrogen production in the PTG process stream. In case of UK, France, Spain, and Sweden, this is mostly due to superior RES-based production. On the contrary, Germany has only moderate RES potentials compared to its superior energy demands but possess high transmission capacities to adjacent countries (compare **Annex XI**). Hence, Germany exhibits large electricity imports from adjacent countries that possess high RES-based electricity production.

The 50 TWh total PTL contribution, as a derivate of PTG_{H2} production, stems from the high RES potential countries Sweden (19 TWh), Denmark (15 TWh), Lithuania (5 TWh), Latvia (4 TWh), Estonia (3 TWh), and Iceland (3 TWh), with each more than 2 TWh. Those countries exhibit strong PTG_{H2} production, not in absolute terms but relatively to their total electricity production potential (compare **Annex XXVIII**) and belong to those countries with the largest electricity trade surplus (compare **Annex XXXI**). Hence, the aforementioned countries exhibit the largest PTG potentials. Analogous, PTM electricity consumption is led by Germany (265 TWh), UK (214 TWh), France (202 TWh), Italy (159 TWh), and Spain (142 TWh), with each more than 100 TWh. Those countries possess considerably large transport energy demands due to high population densities and GDP (compare **Annex I** and **Annex II**).

Final mineral oil demand (514 TWh) is dominated by Germany (130 TWh), UK (120 TWh), France (48 TWh), the Netherlands (39 TWh), and Italy (33 TWh), with each more than 30 TWh. Likewise, final natural gas demand (498 TWh) is led by Germany (127 TWh), UK (116 TWh), France (47 TWh), the Netherlands (37 TWh), and Italy (32 TWh), with each more than 30 TWh. Other sources account for fuel demands of industrial processes that are not mineral oil, nor natural gas. Those fuels are exclusively imported (159 TWh). Due to high economic activity, other sources imports are dominated by Germany (47 TWh), France (17 TWh), UK (14 TWh), and Italy (12 TWh), with each more than 10 TWh.

Final consumption of biofuels that are not utilized for power plant combustion processes accounts for 466 TWh and is strongly dependent on the domestic biomass and biogas production potentials. Thus, France (97 TWh), Spain (73 TWh), Poland (55 TWh), and Italy (54 TWh), with each more than 50 TWh exhibit the largest contribution. Final direct heat consumption (4,854 TWh) is dominated by Germany (964 TWh), Italy (573 TWh), France (522 TWh), UK (447 TWh), Spain (333 TWh), Poland (281 TWh), and the Netherlands (207 TWh), with each more than 200 TWh. PTP refers to final electricity demand (4,854 TWh) and exhibits the strongest contribution in Germany (467 TWh), France (410 TWh), Italy (265 TWh), UK (246 TWh), and Spain (208 TWh), with each more than 200 TWh.

5.7.6 Greenhouse Gas Emissions

A primary research question of this analysis entails the investigation of the GHG emission reduction potentials under exploitation of the techno-economic potentials of RES and integrated energy in the ENTSO-E. The analysis aims at the investigation, whether the GHG reduction goals as introduced in **Chapter 2.2** can be technically achieved. In reference to **Chapter 2.3**, GHG emissions are distinguished among direct and indirect emissions. Hence, the consecutive investigation differentiates between energy use and non-energy use direct emissions as well as indirect emissions.

Energy use and non-energy use related processes are directly supplied with fuels and various energy commodities. Therefore, they are regarded by the IES model logic as introduced in **Chapter 5.4.5**. Agriculture and waste management related emissions, which comprise waste and wastewater emissions, are caused by indirect processes. Those indirect processes are not supplied with conventional fuels and energy commodities. Hence, they are not regarded by the IES model logic. Those indirect emissions are rather caused by various GHG emitting processes, such as fermentation and fertilization as well as distribution infrastructure leakages. Indirect emissions represent a major source for climate impacting GHG gases, such as methane (CH_4) and nitrous oxide (N_2O) emissions. [Baum2018]

As depicted in **Annex XXXIII**, total GHG emissions per country and European region 2050 accumulate to 1,345 Mt CO_{2eq}. In reference to **Fig. 2** of **Chapter 2.3**, final emission sources comprise direct sources, such as fuel combustion and industrial processes, as well as indirect sources, such as agriculture and waste management emissions. In reference to the European Environment Agency (2021), indirect emissions excluding LULUCF are regarded as EU average with 13.6 % of total GHG emissions as an approximation for each ENTSO-E country (compare **Chapter 2.3**) [EEA2021].

As introduced in **Chapter 5.1–5.6**, direct emissions are prevailingly caused by fossil fuel imports that are necessary to cover energy demand during those time steps in which domestic energy production and electricity imports cannot offset the energy balance. Moreover, the non-energy demand for industrial processes is regarded as equal to the energy balances reference year 2016. In this regard, the 852 Mt CO_{2eq} (63.3 %) direct emissions are composed of 467 Mt CO_{2eq} energy use (54.9 %) and 384 Mt CO_{2eq} non-energy use (45.1 %) emissions. Indirect emissions account for 493 Mt CO_{2eq} (36.7 %).

In comparison to the 4,591 Mt CO_{2eq} total emissions of 1990, the computed emission reduction accounts for a decrease of 3,246 Mt CO_{2eq} (70.7 %). In reference to **Chapter 2.2**, this emission reduction does not match the European reduction targets, which envisage a GHG emission decrease of 80–95 % compared to the base year 1990. Moreover, countries exhibit large deviations in the GHG reduction that range from moderate to strong reduction potentials. **Fig. 55** illustrates total direct and indirect GHG emissions in Mt CO_{2eq} as well as the relative GHG emission reduction potential compared to the base year 1990 per country.

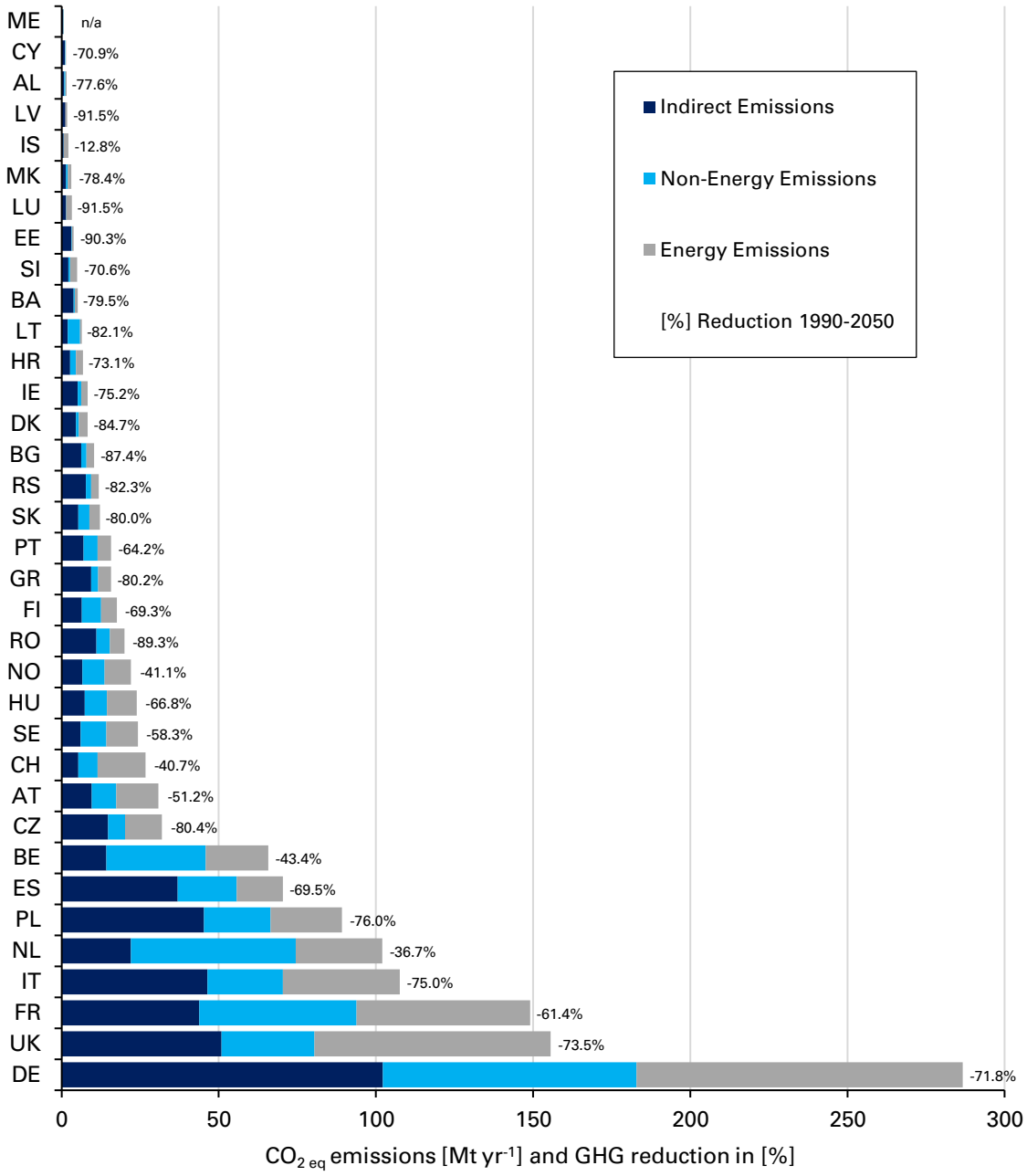

Fig. 55 Direct and indirect CO_{2eq} emissions per country 2050

As depicted in **Fig. 55**, the 35 ENTSO-E countries are quantitatively ranked regarding the accumulated direct (energy and non-energy) and indirect GHG emissions. With 287 Mt CO_{2eq} (21.3%) Germany possesses the largest total contribution, followed by 156 Mt CO_{2eq} of UK (11.6%), 149 Mt CO_{2eq} of France (11.1%), 108 Mt CO_{2eq} of Italy (8.0%), 102 Mt CO_{2eq} of the Netherlands (7.6%), 89 Mt CO_{2eq} of Poland (6.6%), 70 Mt CO_{2eq} of Spain (5.2%), and 66 Mt CO_{2eq} of Belgium (4.9%). These eight countries emit more than three-quarters (76.3%) of total GHG emissions. Among the small-scale countries, Montenegro exhibits the lowest emissions (0.64 Mt CO_{2eq}), followed by Cyprus (1.32 Mt CO_{2eq}), Albania (1.49 Mt CO_{2eq}), Latvia (1.70 Mt CO_{2eq}), Iceland (2.05 Mt CO_{2eq}), North Macedonia (3.02 Mt CO_{2eq}), Luxembourg (3.18 Mt CO_{2eq}), Estonia (3.73 Mt CO_{2eq}), and Slovenia (4.89 Mt CO_{2eq}), with each less than 5.00 Mt CO_{2eq}.

In reference to direct emissions, the large-scale countries Germany (185 Mt CO_{2eq}), France (105 Mt CO_{2eq}), UK (105 Mt CO_{2eq}), and the Netherlands (80 Mt CO_{2eq}) contribute the largest amount, followed by Italy (61 Mt CO_{2eq}), Belgium (51 Mt CO_{2eq}), Poland (44 Mt CO_{2eq}), and Spain (33 Mt CO_{2eq}). Those countries are strongly dependent on fossil fuel imports and exhibit the corresponding direct emissions, which cannot be offset by domestic RES-based energy production and electricity imports. Other large-scale country representatives, such as Austria (21 Mt CO_{2eq}), Czechia (17 Mt CO_{2eq}), and Romania (9 Mt CO_{2eq}), exhibit comparatively low direct emissions. Those countries exhibit large energy demands, but also high RES-based energy production potentials.

Under consideration of indirect emissions, 13 countries, such as Spain, Greece, Romania, Bulgaria, Poland, and Denmark, exhibit larger indirect than direct emissions. Hence, those countries are able to reduce the energy use related emissions disproportionately, due to above-average RES-based energy conversion and electricity import potentials. On the other hand, 22 countries, such as Switzerland, UK, Austria, Hungary, France, Norway, and the Netherlands, possess larger shares of direct emissions. Thus, especially the 13 countries with larger indirect emissions can reduce energy related emissions significantly. To provide a comprehensive picture of total emission quantities and distributions across the ENTSO-E 2050, GHG emissions are aggregated into five emission classes that are assigned to each country analogous to the methodology of the ENTSO-E 2019 heat map in **Fig. 5** of **Chapter 2.3**. The resulting ENTSO-E 2050 GHG emissions heat map is depicted in **Fig. 56**.

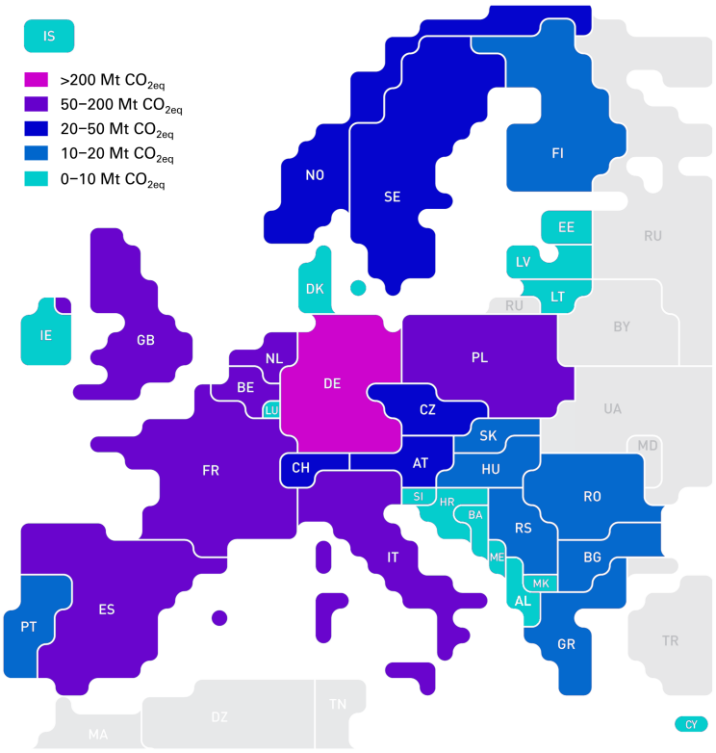

Fig. 56 GHG emissions heat map ENTSO-E 2050

As depicted in **Fig. 56**, Germany remains the leading GHG emitting country and the only country with more than 200 Mt CO_{2eq}. The previous high emitting countries UK, Italy, Poland, France, and Spain remain among the more-than-average (50–200 Mt CO_{2eq})

emitting countries. Average emitting countries (20-50 Mt CO_{2eq}) are represented by Austria, Switzerland, Belgium, and Czechia. Low emitting (10-20 Mt CO_{2eq}) and very low emitting (0-10 Mt CO_{2eq}) countries are identified in the Scandinavian, Baltic, and Balkan countries. Hence, especially the Balkan countries show excelling GHG reduction potentials, due to moderate energy demands and above-average RES potentials. In reference to the base year 1990, total GHG reductions until 2020 and future reduction potentials per region are depicted in **Fig. 57**.

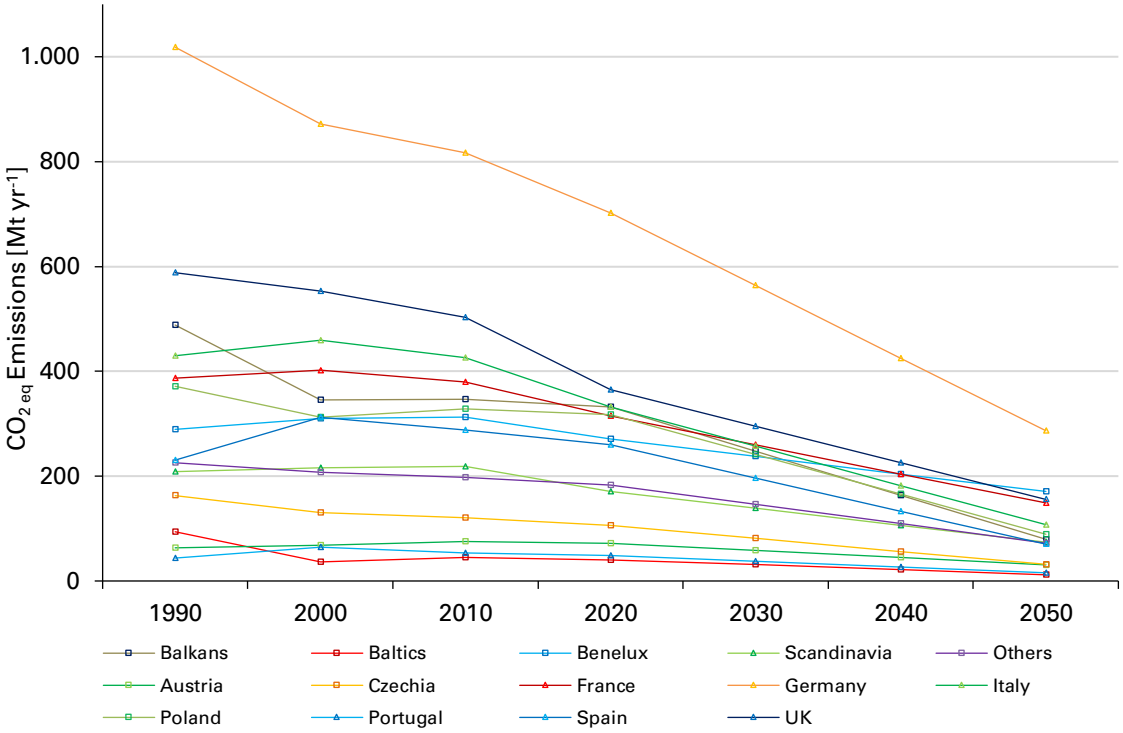

Fig. 57 GHG emission reduction potentials per region 1990–2050

As indicated in **Fig. 57** and **Annex XXXIII**, the CO_{2eq} emission reduction per region is extrapolated linearly between 2020 and 2050 in order to account for average future emission reduction potentials. However, the GHG reduction curves are likely to exhibit non-linear progression, due to unknown time-variant impacts of regulatory frameworks and legal enforcements of GHG reduction measures. Under consideration of the quantitative reduction potentials, the large-scale countries Germany (732 Mt CO_{2eq}), UK (432 Mt CO_{2eq}), Italy (323 Mt CO_{2eq}), Poland (282 Mt CO_{2eq}), France (237 Mt CO_{2eq}), Romania (167 Mt CO_{2eq}), Spain (160 Mt CO_{2eq}), and Czechia (131 Mt CO_{2eq}) exhibit the largest GHG emission reductions.

In reference to the European regions as defined in **Tab. 1** of **Chapter 2.3** and to the base year 1990, the Baltics (87.5%) and the Balkans (84.1%) exhibit the highest relative emission reduction potential, followed by Scandinavia (64.5%) and the Benelux (40.9%). The remaining small-scale countries (others) account for a reduction of 66.4%. The prevailing large-scale countries (nations) show an average GHG reduction potential of 71.6%, which is little superior to the ENTSO-E average GHG reduction potential of 70.7%. In comparison to the relative reduction potentials, those countries, except Romania (89.3%) and Czechia (80.4%), exhibit only average reduction potentials of

61–76 %. Among the large-scale countries, Germany, UK, Italy, and Poland contribute the largest quantitative reduction potentials, due to above-average emissions in the base year 1990 and robust RES potentials.

The small-scale area countries the Netherlands (36.7 %) and Belgium (43.4 %) exhibit low reduction potentials, as those countries are coined with restricted RES potentials and disproportionate energy demands, due to comparatively large population densities, small country sizes, and considerable economic activities. In reference to the base year 1990, the predominantly post USSR Baltic (87.5 %) and Balkan (84.1 %) countries show significant GHG reduction potentials due to inefficient large industrial emissions of the USSR era and considerably strong domestic RES potentials. Except Denmark (84.7 %), the Scandinavian countries Iceland (12.2 %), Norway (41.1 %), Sweden (58.3 %), and Finland (69.3 %) possess low or average GHG reduction potential due to their historically high RES share and, thus, comparatively low total emissions in 1990 (compare **Fig. 57**).

Moreover, small-scale but densely populated countries with high energy demands due to strong economic activities, such as Switzerland (40.7 %) and Austria (51.2 %), exhibit minor reduction potentials. Here, several effects come together. Both countries possess large RES contribution in 1990, due to considerable hydropower utilization. In the face of already large hydropower utilization, RES potentials remain inferior due to slope and elevation restrictions in the Alpine regions, especially regarding onshore wind power. Countries such as Sweden (58.3 %), France (61.4 %), Hungary (66.8 %), and Finland (69.3 %) exhibit above-average RES potentials but the GHG reduction potentials remain average, due to large-scale nuclear power utilization in 1990 [EUROS2021b], which must be offset by RES-based electricity production (compare **Fig. 57** and **Annex XXXIII**).

5.7.7 Energy Flow Balances

The resulting energy flow balances are depicted analogous to the Sankey methodology of **Chapter 2.4**. The left-hand side of each Sankey diagram represents the energy supply side (primary energy consumption) and the right-hand side the demand side (final energy consumption). The center of each diagram represents energy conversion and transformation. For the 2050 Sankey diagrams, the energy supply side is prevailingly dependent on the RES-based energy production potential, based on the techno-economic analysis as introduced in **Chapter 4**. The demand side is defined by the assumptions and inputs of **Chapter 5.6**. Energy conversion and transformation is determined by the PTX and storage interfaces, as presented in **Chapter 5.5**. Energy imports, exports, and conversion and transformation represent the outcome of the IES model computation. The resulting Sankey diagrams are illustrated in **Fig. 37–72** of the **Compendium**. The ENTSO-E 2050 Sankey diagram is depicted in **Fig. 58**.

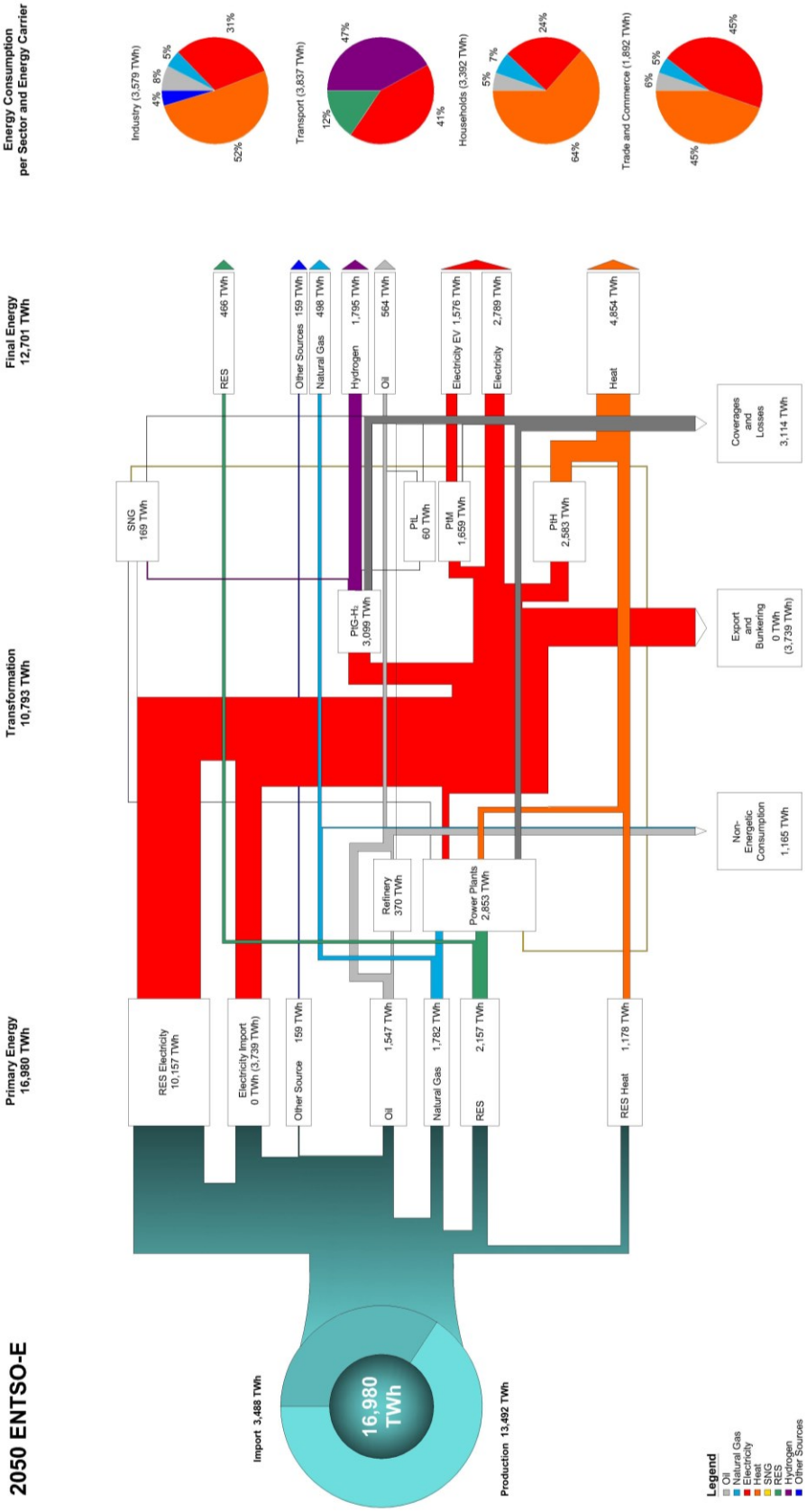

Fig. 58 Sankey energy flow diagram ENTSO-E 2050

As depicted in **Fig. 58**, the ENTSO-E 2050 energy flow chart exhibits 16,980 TWh primary energy consumption, 10,793 TWh energy conversion and transformation, and 12,701 TWh final energy consumption. Out of the primary energy consumption, 1,165 TWh oil and gas products are input into the non-energy consumption sector and 3,114 TWh are assigned to energy conversion and distribution losses. In reference to the ENTSO-E entity, electricity imports and exports are equal (3,739 TWh) as no electricity is exchanged with third-party countries. The aforementioned energy consumption and conversion sections are introduced in **Chapter 5.7.1–5.7.5**. As depicted in **Fig. 37–72** of the **Compendium**, the country-specific Sankey diagrams exhibit strong heterogeneity. Hence, the diversity of each ENTSO-E energy system is remarkable and expressed by the individual configuration of each energy consumption and conversion section.

In comparison to the 2016 Sankey diagrams as depicted in **Chapter 2.4** and **Fig. 1–36** of the **Compendium**, the 2050 Sankey diagrams significantly distinguish in the composition of primary energy supply sources and conversion technologies. The 2016 energy system strongly depends on fossil fuels, such as oil, gas, coal, and uranium. Therefore, energy conversion is dominated by conventional power plants and refineries. PTX technologies are not or only little available. On the other hand, the 2050 energy system strongly depends on RES-based energy production on the supply side. The conversion and transformation section is permeated by PTX technologies, such as PTH, PTM, and PTG. Moreover, electricity and gaseous energy storages are largely available, in order to balance the volatile supply and demand sides. Conventional power plants, such as coal and nuclear power plants, are phased out. The only remaining conventional power source is represented by natural gas fueled CCGT power plants that are able to balance the power system due to rapid ramping gradients.

In comparison to the conventional fuels dominated energy system 2016, total primary energy consumption is reduced by 12,725 TWh (42.8 %). The 10,608 TWh RES-based electricity production contributes 62.5 % of the primary energy mix. In reference to total primary energy production, the 8,877 TWh (52.8 %) wind- and solar-based electricity production represents the major primary energy input. Hence, RES-based primary energy production is increased by 9,180 TWh (940 %), whereas conventional mineral oil (1,547 TWh) and natural gas (1,782 TWh) total primary consumption is decreased by 16,859 TWh (83.5 %). Primary biofuel production accounts for 2,157 TWh and primary RES-based heat production for 1,178 TWh. Other sources for industrial applications amount to 159 TWh and remain equal compared to 2016. Energy conversion and transformation is reduced by 5,844 TWh (35.1 %).

Out of the conventional fuels, 35.0 % of mineral oil and natural gas are input into the non-energy consumption sector for industrial raw material production processes. Thus, the share of RES-based primary energy regarding the energy use consumption is rather increased. In comparison to 2016, the energy conversion and transformation sector is less dominated by power plants, thermal power stations, and refineries. Those conventional converters are largely substituted by electricity based PTX technologies and direct heat supply of primary heat sources. Thus, energy conversion and

transformation losses are strongly decreased. However, this does not regard the primary energy conversion losses of the RES-based primary converters, which are not accounted for by this analysis. Due to the anticipated end of oil and gas extraction and exploration in Europe, also the exports of conventional sources are regarded as zero.

In comparison to the 2016 conventional energy transformation processes in refineries (8,206 TWh) and power plants (7,114 TWh) as well as heat and other plants (1,317 TWh), the 2050 energy system is permeated with 7,570 TWh (69.9 %) of PTX conversion. Among the 10,793 TWh total energy conversion and transformation, PTX processes account for 3,099 TWh PTG_{H2} (28.6 %), 2,583 TWh PTH (23.9 %), 1,659 TWh PTM (15.3 %), 169 TWh PTG_{SNG} (1.6 %), and 60 TWh PTL (0.6 %) conversion. Final energy consumption accumulates to 12,701 TWh and is reduced by 861 TWh (6.4 %). Final energy consumption is distributed across the energy consumption sectors, with 3,579 TWh industry (28.2 %), 3,837 TWh transport (30.2 %), 3,392 TWh households (26.7 %), and 1,892 TWh trade and commerce (14.9 %) final consumption. As indicated on the right-hand side of the ENTSO-E Sankey diagram 2050, the quantitative and relative final energy consumptions of the sectors industry, transport, households, and trade and commerce are depicted in **Fig. 59**.

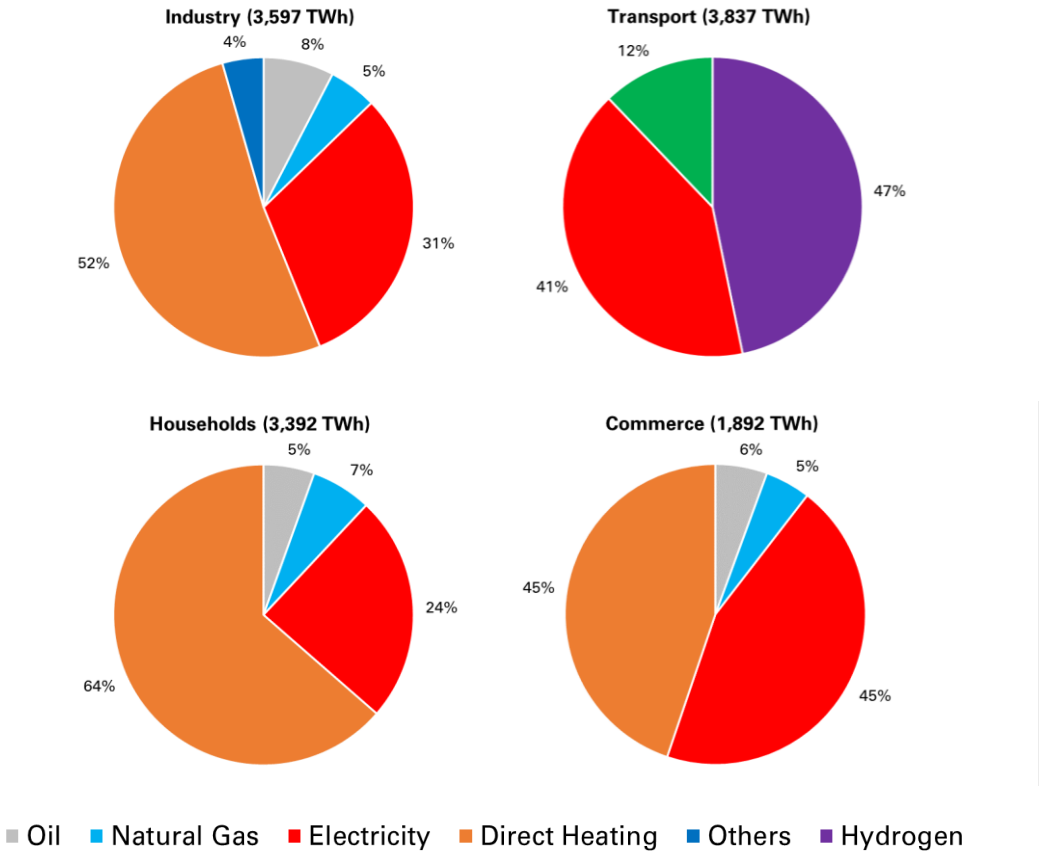

Fig. 59 Final energy consumption per sector ENTSO-E 2050

In reference to **Fig. 59**, the final energy consumption of the economic sectors industry (3,579 TWh), transport (3,837 TWh), households (3,392 TWh), and trade and commerce (1,892 TWh) exhibits a rather homogeneous composition. Industry, households and trade and commerce possess similar distributions of electricity, heat, oil, and gas

consumption. As an exception, the heat demand ratio of the household sector (64 %) is superior and electricity (24 %) inferior compared to the other sectors. In reference to the IES model assumptions of **Chapter 5**, the industry sector contains additional demands for other sources (4 %). The transport sector entails final energy consumption for hydrogen (47 %), biofuels (12 %), and electricity (41 %), as a contribution for the light- and heavy-duty transport.

Due to the assumptions of the IES model logic, hydrogen is exclusively supplied to the transport sector, whereas industry demand is covered by the conventional fossil fuels natural gas and mineral oil. However, also the industry sector exhibits large demands for hydrogen, which is predominantly produced based on steam reforming and comparable processes of natural gas. Hence, the gas and oil imports of the industry sector are likely to be substituted by hydrogen imports from third-party countries or by domestic hydrogen production. Vice versa, the imports can be utilized to cover heavy-duty demand in the transport sector. In comparison to the economic sector 2016 final energy consumption as depicted in **Fig. 8** in **Chapter 2.4**, the final energy consumption of the economic sectors 2050 shows large proportions of direct heat supply. Hence, heat production of biofuel power plants, geothermal power plants, solar thermal rooftops, and PTH substituted large shares of former heat production based on fossil fuels. The most tremendous fuel switch is identified in the transport sector. Here, the predominant oil-based consumption is largely substituted by hydrogen, electricity, and biofuels.

It is found that energy flow charts based on the Sankey methodology also provide a profound and holistic overview about primary, secondary, and final energy consumption as well as energy conversion and transformation in energy systems with large shares of RES and PTX. Moreover, energy imports, exports, and losses are accounted for. The envisaged energy transformation has tremendous implications for the configuration of the energy system itself and the corresponding Sankey diagrams. Hence, the conventional fuel-based ENTSO-E 2016 energy system, as depicted in **Fig. 7** of **Chapter 2.4**, significantly turns into a RES-based system as depicted in **Fig. 58**, which is dominated by the primary and secondary energy commodities electricity (59.8 %), biofuels (12.7 %), and heat (6.9 %). Therefore, natural gas (10.5 %), mineral oils (9.1 %), and other sources (0.9 %) contribute only minor shares. In comparison to the ENTSO-E 2016 energy system as introduced in in **Chapter 2.4**, electricity that represented a former secondary energy commodity turns to a primary energy commodity and is produced primarily by RES-based electricity converters.

6. Conclusion and Outlook

The availability of abundant energy and unrestricted access to energy commodities is the cradle of each developed and independent society. Since the extensive utilization of electricity in the late 19th century, mankind developed at an unprecedented velocity. Electricity, as the primary energy commodity of the most important RES-based energy conversion technologies, is likely to substitute common thermal energy processes in future energy systems at large scale. Those RES-based electricity converters are spearheaded by the mainstream technologies onshore wind power, offshore wind power, and utility-scale PV. At present, the ENTSO-E is strongly dependent on fossil fuel imports from third-party countries. Hence, the energy transition, security of supply, and energy dependency are likely to dominate the political discussions of the 21st century.

ENTSO-E 2016 Energy System

The ENTSO-E 2016 countries possess a heterogeneous distribution of primary energy consumption (29,705 TWh), energy transformation (16,637 TWh), and final energy consumption (13,562 TWh). This heterogeneity is historically grown and strongly dependent on the availability of domestic energy resources. Hence, some countries, such as Denmark, Iceland, and Norway, already possess large shares of RES in their primary energy mix. Whereas other countries, such as France, Italy, and Poland, are strongly dependent on depletable fossil fuels. Not only particular countries, but also the dominant energy commodities and technologies exhibit heterogeneous distributions. Denmark possesses large shares of wind power, Iceland geothermal power, and Norway hydropower. Whereas France is dominated by nuclear power, Italy by natural gas, and Poland by lignite utilization. Overall, the ENTSO-E energy system 2016 composition is strongly diverse and exhibits high degrees of energy dependencies (49.9 %). Those dependencies correspond to 9,970 TWh net imports of mineral oil, natural gas, hard coal, and uranium. The energy balances per country have been analyzed and depicted in the Sankey methodology (compare **Chapter 2.4** and the **Compendium**).

European Energy Transition Goals

Within the framework of the Energy Strategy and the Energy Union, the EU aims at the secure, sustainable, competitive, and affordable energy supply (compare **Chapter 2.2**). Promoting RES on a large scale is the most promising opportunity to significantly decrease GHG emissions by at least 80–95 % compared to the base year 1990 and to reduce energy dependencies in the ENTSO-E. The conversion of RES-based energy into various gaseous, liquid, and thermal energy commodities by the means of PTX, represents a key component to decarbonize the energy system. Hence, the exploitation of the techno-economic RES potentials and the comprehensive utilization of PTX technologies within the framework of a holistically integrated energy system are the prerequisites for a successful energy transition across all energy consumption sectors.

Integrated Energy System

The conversion of the RES-based electricity production by the means of PTX represents the most promising way to make the electricity-based RES potentials available across all economic sectors and for all specific energy commodity demands. PTX enables the interconnection of the primary energy and final energy consumption sectors. Therefore, PTH (η_{PTH}=*0.97…3.10*) and PTM (η_{PTM}=*0.95*) are coined by superior conversion efficiencies. Whereas the PTG technologies come along with significant energy losses (η_{PTG}=*0.50…0.75*) but excel in the contribution of RES-based gaseous and liquid energy commodities, such as hydrogen and SNG. Those energy commodities find application in various industrial processes and heavy-duty transportation. Moreover, they contribute to security of supply and pose resilience on the system, as they are independent from power grids and can be stored over a long time (compare **Chapter 3**).

Techno-Economic RES Potentials and IES Model

To evaluate the potential availability of domestic RES-based primary energy consumption and how this energy is efficiently transformed into the final energy consumption sectors, two model-based approaches have been developed. First, the availability of RES-based primary energy consumption is investigated in reference to the Primary and Secondary Sources analysis. The Primary Sources analysis is based on the GIS analysis of the techno-economic potentials of onshore wind power, offshore wind power, utility-scale PV, and CSP. Those technologies have been assessed based on the georeferenced analysis of environmental, economic, and regulatory restrictions per CORINE land cover. Whereas solar rooftops have been assessed based on a per capita approach. Primary Sources accumulate to 5,522 GW rated power. The remaining Secondary Sources bioenergy, hydropower, geothermal energy, and hydrokinetic energy have been evaluated based on a qualified literature review. Secondary Sources account for 4,263 TWh energy yield per year (compare **Chapter 4**). Second, the techno-economic potential analysis results are input into the IES model. Primary Sources energy conversion is computed based on historic solar and wind profiles per country. In reference to meta-analysis scenario assumptions, future energy demands are anticipated. The IES model is based on a linear optimization routine that efficiently allocates the conversion, transformation, and distribution of energy. The focus of the IES model logic lies on the minimization of CO_{2eq} GHG emissions (compare **Chapter 5**).

ENTSO-E 2050 Energy System

As a result of the techno-economic potential analysis and the IES model optimization, the ENTSO-E 2050 exhibits heterogeneous distributions of energy commodities and technologies. Likewise, primary energy consumption (16,980 TWh), energy transformation (10,793 TWh), and final energy consumption (12,701 TWh) are diversely distributed among the countries. Unlike the 2016 energy system, the ENTSO-E 2050 possess high shares of domestic RES and PTX, due to outstanding RES potentials and necessary PTX conversion. Hence, total energy dependency could be significantly decreased to 20.5 %. However, the country-specific RES-based primary energy

conversion potentials depend strongly on the individual topographic and geologic features. The RES technologies onshore wind power, utility-scale PV, solar rooftops, and bioenergy are utilized across all countries. Offshore wind power is exclusively restricted to countries with ocean access but exhibits a superior potential in most of those countries. Likewise, large-scale hydropower plants are restricted to mountainous areas and possesses significant potentials in the corresponding countries. Geothermal power and CSP plants are only available in those selected countries, which exhibit the necessary geologic and topographic features. Analogous to the ENTSO-E 2016 energy balances, the ENTSO-E 2050 energy flows have been transposed into Sankey diagrams per country (compare **Chapter 5** and the **Compendium**). The ENTSO-E 2050 energy system is a result of deterministic models. Hence, it does not represent a clearly specified future, but rather a potentially possible energy system within the framework of techno-economical constraints and the specific features of the ENTSO-E countries.

ENTSO-E 2050 Country Focus

Countries such as France, Poland, Romania, and Spain have been strongly dependent on fossil fuels and correlated energy imports. Remarkably, they are able to reduce fossil fuel demands and corresponding import dependencies significantly, due to superior RES potentials. Germany, as the largest European economy and population representative, exhibits only moderate RES potentials (1,247 TWh). The country does have access to all mainstream and unconventional RES except CSP, but total primary energy potentials are inferior due to large population density and comparably small EEZ area. As those moderate RES potentials face particular high net primary energy demands (2,880 TWh), Germany remains the largest net energy importer (1,633 TWh) with the highest energy dependency rates (56.7 %). Likewise, countries such as Belgium, Italy, Luxembourg, the Netherlands, and Switzerland are affected. Countries with already large RES shares in 2016, such as Denmark, Iceland, Norway, and Sweden, show a diverse picture. Sweden, Denmark, and Iceland become the leading net export countries due to superior domestic RES potentials and comparatively low final energy demands. Norway, as the leading energy exporter 2016, does not belong to the net export countries due to abandoned fossil fuel production and moderate RES potentials (compare **Chapter 5.7.1–5.7.5**).

ENTSO-E GHG Reduction Potentials

Total GHG emissions accumulate to 1,345 Mt CO_{2eq} that equals a reduction of 70.7 %. Despite the extensive exploitation of RES potentials, the GHG reduction goal of 80–95 % (3,673 Mt CO_{2eq}–4,362 Mt CO_{2eq}) compared to the base year 1990 (4,591 Mt CO_{2eq}) cannot be achieved. The prevailing restrictions on RES-deployment due to habitats and species protection, and persistent energy demands of performance societies, constrain GHG emission reduction potentials. Direct emissions are correlated with the country-specific RES potentials and final energy demands. Whereas indirect emissions are caused by biological and chemical processes that are not as trivial as energy combustion processes. Therefore, countries with high RES potentials and moderate demands excel in the reduction of direct emissions. On the other hand, all countries possess

comparatively large shares of indirect emissions, caused by domestic agriculture, landfilling, and wastewater management. Thus, additional measures such as imports of RES-based synthetic fuels and alternated energy consumption patterns become necessary. Apart from the increase of RES in the electricity sector, especially the emission reduction in the final heat energy demands is of high significance. Promoting direct RES-based thermal energy conversion is a straight-forward solution to reduce GHG emissions and energy dependencies in the heat sector. Moreover, the enforcement of LULUCF as carbon sink based on recultivation and reforestation is a promising means.

ENTSO-E 2050 Energy Imports

As the GHG reduction goals are not met by domestic RES production, under consideration of moderate efficiency gains across all demand sectors except air conditioning and cooling, the ENTSO-E will remain a net importer of energy commodities from third-party countries (3,488 TWh). Those energy imports must be substituted by RES-based energy commodities on a large scale, such as renewable synthetic gases and fuels. Those commodities are products of the PTG technology and rely on vast availability of solar radiation or wind energy as well as highly purified H_2O for the corresponding electrolysis processes (compare **Chapter 3.3**). Therefore, the ENTSO-E will remain dependent on energy imports from third-party countries and exhibits corresponding energy dependencies. Additional research is necessary to investigate where and to what extent those RES-based fuel imports can be sourced from, especially with the focus on security of supply and efficient provision.

Energy Efficiency and Behavioral Science

In reference to the analysis assumptions of future energy demands, it is necessary to compare energy efficiency measures with behavioral changes of energy consumption patterns as viable options to decrease GHG emissions. It is anticipated, that both options are coined with hard restrictions. The observation of the last decades of economic growth shows, that GHG emissions could be relatively reduced, but remain on a high level due to effects described as the growth paradigm, carbon lock-in, rebound effects, and the tragedy of the common goods. However, the reduction of final energy consumption represents the most straight-forward way to decrease GHG emissions and energy dependencies. Therefore, additional research should focus on the identification of robust energy efficiency gains in reference to the myriad of energy conversion processes and in the face of highly industrialized and productive countries. Likewise, the feasibility and acceptance of behavioral changes, such as alternative nutrition and mobility patterns, should be investigated in the light of behavioral sciences.

GIS Model: Environmental, Social, and Technical Assumptions

The georeferenced analysis of the techno-economic potentials for Primary Sources across the heterogeneous allocation of various environmental, social, and technical constraints across the 35 ENTSO-E countries comes along with some degree of insecurity due to the multiplicity of assumptions and the immense size of the model

region. Nonetheless, those assumptions regarding availability and suitability factors as well as technical and economical parameters represent best-practice estimates based on peer-reviewed literature research. Moreover, the assumptions have been tested and calibrated within a sensitivity analysis at the reference case of Brandenburg and Germany (compare **Chapter 4**). Hence, the GIS model analysis is considered as a robust and profound approximation of the real-world RES potentials, which are based on onsite assessments. However, country-specific regulatory frameworks and social acceptance may alter the potentials among the diverse and heterogeneous European countries.

IES Model: Grid and Storage

The massive increase of RES-based electricity producers in the power sector, foremost onshore wind power, offshore wind power, and utility-scale PV, comes along with stochastic and volatile electricity feed-in. These insecurities of supply must be compensated by strengthening the transmission and distribution grids on country and pan-European level. Additional thermal, gaseous, and electric storages, such as heat accumulators, gas storages, and batteries, become necessary to guarantee security of supply. Moreover, those storages with uni- and bidirectional power control capability must be deployed on a large scale, in order to provide ancillary services for a predominantly electricity-based energy system. The analysis of storage capacities from a techno-economical point of view as well as the quantification of ancillary services in the power system is out of the scope of this work. Therefore, additional research based on the results of this analysis is recommended.

IES Model: Curtailment and Economics

The model-based analysis and simulation comes along with some constraints. Those comprise the aforementioned technical limitations of the power grids as well as the excessive utilization of each watt-hour that becomes available in the energy supply side. Theoretically, this degree of utilization is possible, but it is not likely to be practically implemented as it comes along with tremendous technical efforts. Practically, system security measures, such as curtailment of excess energy conversion that cannot be stored or transported, are more likely to be implemented and, thus, decrease the RES-based primary energy conversion potential. Moreover, the analysis of economic costs is not regarded by this analysis. However, the GIS-based techno-economic potential analysis of Primary Sources refers to the calculation of LCOE (compare **Chapter 4**), but does not indicate total economic costs. In the face of strict economic system cost analysis, the potentials might be further reduced.

IES Model: Technological Advance and Heat Slack

On the other hand, technological advance is likely to increase RES-based energy conversion efficiencies and compensate those constraints identified in the model logic, as the anticipated efficiencies represent best-practice estimates that might be improved due to unforeseen technological advance. Especially during the summer period, a significant amount of thermal energy production is slacked by the IES model logic, due to large thermal potentials which cannot be utilized nor stored. To account for that thermal overproduction, a sensitivity analysis is recommended to fully address for the competition of thermal and electrical energy utilization in the sense of a Pareto optimal solution. Overall, the techno-economic potentials might be further reduced due to technical and economic issues, but technological advance and optimization might compensate those energy losses. Therefore, the identified energy potentials are regarded as robust and representative. However, data availability and precision of non-EU countries revealed gaps, foremost in the Balkan countries, Switzerland, and, since 2021, also in UK. Hence, a uniform and holistic data acquisition should be enforced.

Final Conclusion and Outlook

Secure, sustainable, competitive, and affordable energy supply are the cornerstones for developed and prospering societies. In the face of climate change and depleting fossil energy sources, the energy transition to a renewable and decarbonized system is inevitable. However, fossil fuels such as natural gas and most likely uranium, remain important transitional energy commodities. RES-based domestic production can decrease energy dependencies in the ENTSO-E significantly, but not exhaustively. Hence, significant amounts of RES-based synthetic fuels must be imported from third-party countries to sufficiently decrease GHG emissions. In reference to security of supply and the promotion of democratic values, those countries must be selected carefully. To further decrease those energy dependencies, highly efficient energy generation, distribution, transformation, and consumption is of importance.

Such a fundamental and radical transformation of the energy systems represents an intergenerational task, but in the face of limited time. Hence, cautious but vigorous transformation of the energy system is needed. In reference to the strong heterogeneity of RES-based primary conversion potentials, the exploitation of energy conversion and transformation potentials should be addressed country-specific to thoroughly account for individual energy conversion potentials. The ENTSO-E represents one of the largest and most important economic regions in the world and, therefore, it has strong influence on total GHG emissions as well as economic power to transform global supply chains. The implementation of a successful GHG abatement strategy remains a global task and requires the integration of all developed and developing countries, which makes the undertaking an exceptional challenge for mankind.

7. List of References

[ACEA2018] European Automobile Manufacturers' Association (ACEA) “ACEA Report Vehicles in use Europe 2018” 2018. [Online] https://www.acea.auto/files/ACEA_Report_Vehicles_in_use-Europe_2018.pdf [Accessed August 2019]

[Ademe2019] French Environment and Energy Management Agency (ADEME) “Sectoral Profile - Transport” 2019. [Online] https://www.odyssee-mure.eu/publications/efficiency-by-sector/transport/transport-eu.pdf [Accessed August 2019]

[Agora2014] Agora Energiewende “Power-to-Heat zur Integration von ansonsten abgeregeltem Strom aus Erneuerbaren Energien. Handlungsvorschläge basierend auf einer Analyse von Potenzialen und energiewirtschaftlichen Effekten” Berlin, 2014.

[Aman2018] S. Amanpour, D. Huck, M. Kuprat, H. Schwarz “Integrated energy in Germany - A critical look at the development and state of integrated energies in Germany” In: Front. Energy 12, pp. 493–500, 2018.

[Ander2015] T. Anderski, Y. Surmann, S. Stemmer, N. Grisey, E. Momot, A.C. Leger, B. Betraoui, P. van Roy “e-HIGHWAY 2050 - Modular Development Plan of the Pan-European Transmission System 2050 - D 2.2 European cluster model of the Pan-European transmission grid” European Commission, Brussels, 2015.

[Angel2013] L. Angelino, T. Boxem, P. Dumas, J. vas Wees “A prospective study on the geothermal potential in the EU” GEOELEC, Montrevault-sur-Èvre, 2013.

[Ayd2013] N. Aydin, S. Duzgun, E. Kentel “GIS-based site selection methodology for hybrid renewable energy systems - A case study from western Turkey” In: Energy Conversion Management, Vol. 70, pp. 90-106, 2013.

[Bak2015] B. Bakken, T. Anderski, E. Peirano, R. Pestana, B. de Clercq, G. Migliavacca, M. Czernie, P. Panciatici, M. Paun, N. Grisey “Europe’s future secure and sustainable electricity infrastructure - e-Highway2050 project results” RTE, La Defense, Paris, 2015.

[Baum2018] C. Baumgarten, M. Bilharz, U. Döring, A. Eisold, B. Friedrich, T. Frische, C. Gather, D. Günther, W. Große-Wichtrup, K. Hofmeier, M. Hofmeier, A. Jering, A. Klatt, L. Köder, D. Lamfried, M. Langner, W. Leujak, M. Marx, A. Matthey, V. Mohaupt, D. Osiek, G. Penn-Bressel, N.O. Plambeck, M. Pohl, J. Rechenberg, T. Scheuschner, J. Seven, A. Ullrich, I. Vogel, A.B. Walter, R. Wolter, A. Zimmermann “Daten zur Umwelt 2018: Umwelt und Landwirtschaft” Umweltbundesamt, Dessau-Roßlau, 2018.

[Bei2017] P. Beiter, W. Musial, L. Kilcher, M. Maness, A. Smith “An Assessment of the Economic Potential of Offshore Wind in the United States from 2015 to 2030” NREL, Golden, Colorado, 2017.

[Bell1999] D. Bell “The Coming of Post-Industrial Society - a Venture in Social Forecasting” Basic Books, New York, 1999.

[BFN2011] Bundesamte für Naturschutz (BFN) “Windkraft über Wald - Positionspapier des Bundesamtes für Naturschutz“ Bonn, 2011.

[Bhat2010] S.C. Bhattacharyya and G.R. Timilsina “A Review of Energy System Models” In: The International Journal of Energy Sector Management, 4(4), 2010, pp 494-518.

[Bloes2018] A. Bloessa, W.P. Schill, A. Zerrahn “Power-to-heat for renewable energy integration: A review of technologies, modeling approaches, and flexibility potentials” In: Applied Energy 212, pp. 1611–1626, 2018.

[BMVI2015] Bundesministerium für Verkehr und digitale Infrastruktur (BMVI) “Räumlich differenzierte Flächenpotenziale für erneuerbare Energie in Deutschland” BMVI, Berlin, 2015.

[Bozem2013] K. Bozem, A. Nagl, C. Rennhak “Energie für nachhaltige Mobilität - Trends und Konzepte“ Springer Gabler, Wiesbaden, 2013.

[BP2020] BP “BP Statistical Review of World Energy 2019 - 68th edition” 2020. [Online] https://www.bp.com/content/dam/bp/business-sites/en/global/corporate/pdfs/energy-economics/statistical-review/bp-stats-review-2019-full-report.pdf [Accessed February 2020]

[Brun2015] J. Brunet, A. Kotelnikova, J.P. Ponssard “The deployment of BEV and FCEV in 2015” Department of Economics, Ecole Polytechnique, CNRS, 2015. [Online] https://hal-polytechnique.archives-ouvertes.fr/hal-01212353/document [Accessed December 2019]

[BWE2012] Bundesverband Windenergie (BWE) “Potenzial der Windenergienutzung an Land” BWE, Kassel, 2012.

[Cap2016] P. Capros, A. De Vita, N. Tasios, P. Siskos, M. Kannavou, A. Petropoulos, S. Evangelopoulou, M. Zampara, D. Papadopoulos, L. Paroussos, K. Fragiadakis, S.Tsani, P. Fragkos, N. Kouvaritakis, L. Höglund-Isaksson, W. Winiwarter, P. Purohit, A. Gomez-Sanabria, S. Frank, N. Forsell, M. Gusti, P. Havlík, M. Obersteiner, H.P. Witzke, M. Kesting “EU Reference Scenario 2016 Energy, Transport and GHG Emissions Trends to 2050” Publications Office of the European Union, Luxembourg, 2016.

[CEU2009a] Council of the European Union “Presidency Conclusions 15265/1/09 REV 1 29/30” Brussels, October 2009.

[CEU2009b] Council of the European Union “Council Conclusions on EU position for the Copenhagen Climate Conference (7-18 December 2009) - 2968th Environment Council meeting” Luxembourg, 21 October 2009.

[CINEA2018] European Climate, Infrastructure and Environment Executive Agency (CINEA) “Transnational Maritime Spatial Planning in the North Sea: The Shipping Context - Report on Work-package 4 of the NorthSEE Project” 2018. [Online] https://northsearegion.eu/media/4836/northsee_finalshippingreport.pdf [Accessed September 2019]

[Ciu2020] M. Ciucci “Internal Energy Market” Brussels, 2020. [Online] https://www.europarl.europa.eu/ftu/pdf/en/FTU_2.1.9.pdf [Accessed December 2020]

[CLMS2012] Copernicus Land Monitoring Service (CLMS) “CORINE Land Cover (CLC) 2012, Version 18.5, 100 m Resolution” 2012. [Online] https://land.copernicus.eu/pan-european/corine-land-cover [Accessed May 2019]

[CLMS2018] Copernicus Land Monitoring Service (CLMS) “Technical Library - Upcoming Product CLC” 2018. [Online] https://land.copernicus.eu/user-corner/technical-library/upcoming-product-clc [Accessed March 2020]

[Crast2017] V. Crastan “Elektrische Energieversorgung 2. Energiewirtschaft und Klimaschutz, Elektrizitätswirtschaft und Liberalisierung, Kraftwerktechnik und alternative Stromversorgung, chemische Energiespeicherung“ Springer Vieweg, Wiesbaden, 2017.

[Crip2020a] M. Crippa, D. Guizzardi, M. Muntean, E. Schaaf, E. Solazzo, F. Monforti-Ferrario, J.G.J. Olivier, E. Vignati “Fossil CO2 emissions of all world countries - 2020 Report: EDGARv5.0_FT2019 dataset” EUR 30358 EN, Publications Office of the European Union, Luxembourg, 2020.

[Crip2020b] M. Crippa, D. Guizzardi, M. Muntean, E. Schaaf, E. Solazzo, F. Monforti-Ferrario, J.G.J. Olivier, E. Vignati “Fossil CO2 emissions of all world countries - 2020 Report” EUR 30358 EN, Publications Office of the European Union, Luxembourg, 2020.

[Dahl2014] T.G. Dahlgren, M.L. Schläppy, A. Šaškov, M.H. Andersson, Y. Rzhanov, I. Fer “Assessing the Impact of Windfarms in Subtidal, Exposed Marine Areas” In: M.A. Shields, A.I.L. Payne (eds.) “Marine Renewable Energy Technology and Environmental Interactions - Humanity and the Sea” Springer Science+Business Media, Dordrecht, 2014.

[Daly1974] H.E. Daly “The Economics of the Steady State” 1974. In: The American Economic Review, Vol. 64, No. 2, Papers and Proceedings of the Eighty-sixth Annual Meeting of the American Economic Association (1974), pp. 15-21.

[Delb2019] J. Delbeke, P. Vis, C. Holzleitner, D. Maedows, P. Owen, A. Paquot, A. Runge-Metzger, Y. Slingenberg, T. van Ierland, S. Vergote, P. Wehrheim, J. Werksman, P. Zapfel “Towards a climate-neutral Europe - curbing the trend” Abingdon, New York, Routledge, Brussels, 2019.

[Den2009] P. Denholm, M. Hand, M. Jackson and S. Ong “Land-use Requirements of Modern Wind Power Plants in the United States” Technical Report NREL/TP-6A2-45834," NREL, Golden, Colorado, 2009.

[DENA2018] Deutsche Energie-Agentur (dena) “Integrated Energy Transition. Impulses to shape the energy system up to 2050 - Report of the results and recommended course of action” dena, Berlin, October 2018.

[Deng2015] Y. Deng, M. Haigh, W. Pouwels, L. Ramaekers, R. Brandsma, S. Schimschar, J. Grozinger, D. de Jager “Quantifying a realistic, worldwide wind and solar electricity supply” In: Global Environmental Change, vol. 31, pp. 239–252, 2015.

[EC2013] European Commission (EC) “Commission Decision of 26 March 2013 on determining Member States’ annual emission allocations for the period from 2013 to 2020 pursuant to Decision No 406/2009/EC of the European Parliament and of the Council - Notified under document C(2013) 1708 (2013/162/EU)” Brussels, 26 March 2013.

[EC2015a] European Commission (EC) “Feasibility Study on Synchronous Interconnection of Ukrainian and Moldovan Power Systems to ENTSO-E Continental Europe Power System” Joint Operational Programme Romania-Ukraine-Republic of Moldova 2007-2013. Common borders. Common solutions. 2015. [Online] https://eepublicdownloads.entsoe.eu/clean-documents/SOC%20documents/Regional_Groups_Continental_Europe/Joint_operational_programme_Romania_Ukraine_Moldova_2007-2013.pdf [Accessed March 2022]

[EC2015b] European Commission (EC) “Energy Union Package Communication from the Commission to the European Parliament, the Council, the European Economic and Social Committee and the Committee of the Regions and the European Investment Bank - A Framework Strategy for a Resilient Energy Union with a Forward-Looking Climate Change Policy” EC COM(2015) 80 final, Brussels, 2015.

[EC2017] European Commission (EC) “Photovoltaic Geographical Information System - CM SAF Solar Radiation Data” 2017. [Online] http://re.jrc.ec.europa.eu/pvg_download/solar_radiation_cmsaf_download.html [Accessed November 2019]

[EC2017] European Commission (EC) “PVGIS Version 4, CM SAF Solar Radiation Data 2007-2016” 2017. [Online] http://re.jrc.ec.europa.eu/pvg_download/solar_radiation_cmsaf_download.html [Accessed November 2017]

[EC2018a] European Commission (EC) “Country datasheets - February 2018 update” 2018. [Online] https://ec.europa.eu/energy/en/data-analysis/country [Accessed May 2020]

[EC2018b] European Commission (EC) “A Clean Planet for all. A European strategic long-term vision for a prosperous, modern, competitive and climate neutral economy” Communication from the Commission to the European Parliament, the Council, the European Economic and Social Committee and the Committee of the Regions and the European Investment Bank” COM(2018) 773 final, Brussels, 28 November 2018.

[EC2018c] European Commission (EC) “Photovoltaic Geographical Information System (PVGIS)” 2018 [Online] https://ec.europa.eu/jrc/en/pvgis [Accessed March 2018].

[EC2019a] European Commission (EC) “Clean energy for all Europeans” Luxembourg, March 2019.

[EC2019b] European Commission (EC) “The European Green Deal Communication from the Commission to the European Parliament, the Council, the European Economic and Social Committee and the Committee of the Regions” COM(2019) 640 final Brussels, 11 December 2019.

[EC2020a] European Commission (EC) “Communication from the Commission to the European Parliament, the Council, the European Economic and Social Committee and the Committee of the Regions - Stepping up Europe’s 2030 climate ambition Investing in a climate-neutral future for the benefit of our people” COM(2020) 562 final, Brussels, 2020.

[EC2020b] European Commission (EC) “Report from the Commission to the European Parliament, the Council, the European Economic and Social Committee The state of nature in the European Union Report on the status and trends in 2013 - 2018 of species and habitat types protected by the Birds and Habitats Directives” COM(2020) 635 final, Brussels, 2020.

[EC2021] European Commission (EC) “Annex to Commission Delegated Regulation (EU) amending Regulation (EU) No 347/2013 of the European Parliament and of the Council as regards the Union list of projects of common interest” COM(2021) 8409 final, Brussels, 2021.

[EEA2009] European Environment Agency (EEA) “Europe's onshore and offshore wind energy potential: Technical Report No 6/2009” EEA, Copenhagen, 2009.

[EEA2013a] European Environment Agency (EEA) “Reference Portal for Natura 2000” 2013. [Online] https://bd.eionet.europa.eu/activities/Natura_2000/reference_portal [Accessed March 2020]

[EEA2013b] European Environment Agency (EEA) “EU bioenergy potential from a resource efficiency perspective” EEA Report No. 6/2013Publications Office of the European Union, Luxembourg, 2013.

[EEA2016] European Environment Agency (EEA) “Overview of electricity production and use in Europe” Publications Office of the European Union, Luxembourg, 2016. [Online] https://www.eea.europa.eu/data-and-maps/indicators/overview-of-the-electricity-production-1/assessment [Accessed January 2019]

[EEA2018a] European Environment Agency (EEA) “Fragmentation pressure and population density in EEA member countries” Publications Office of the European Union, Luxembourg, November 2018.

[EEA2018b] European Environment Agency (EEA) “Renewable energy in Europe – 2018 - Recent growth and knock-on effects” 2018. [Online] https://www.eea.europa.eu/data-and-maps/figures/fragmentation-pressure-and-population-density/90513_fig-6-map_fragmentation-pressure-by.eps/at_download/file [Accessed February 2019]

[EEA2020] European Environment Agency (EEA) “European CDDA version 18 (2020) - Report on the 2020 data collection and selected results” EEA, Copenhagen, 2020.

[EEA2021] European Environment Agency (EEA) “Annual European Union greenhouse gas inventory 1990–2019 and inventory report 2021 - Submission to the UNFCCC Secretariat” EEA, Copenhagen, 2021.

[Egg2006] H.S. Eggleston, L. Buendia, K. Miwa, T. Ngara, and K. Tanabe “2006 IPCC Guidelines for National Greenhouse Gas Inventories” 2006. [Online] https://www.ipcc-nggip.iges.or.jp/public/2006gl/vol3.html [Accessed February 2021]

[EMO2018] European Marine Observation and Data Network (EMODnet) “Data Portal: Human Activities” 2018. [Online] http://www.emodnet-humanactivities.eu/view-data.php [Accessed November 2018]

[ENTSO2014] European Network of Transmission System Operators for Electricity (ENTSO-E) “ENTSO-E at a Glance - Reliable, Sustainable, Connected” Brussels, 2014.

[ENTSO2015] European Network of Transmission System Operators for Electricity (ENTSO-E) “Report on Blackout in Turkey on 31st March 2015 - Final Version 1.0” Project Group Turkey, Brussels, 2015.

[ENTSO2018a] European Network of Transmission System Operators for Electricity (ENTSO-E) “Regional Groups” 2018. [Online] https://docstore.entsoe.eu/about-entso-e/system-operations/regional-groups/Pages/default.aspx [Accessed February 2020]

[ENTSO2018b] European Network of Transmission System Operators for Electricity (ENTSO-E) “Electricity in Europe 2017 - Synthetic overview of electric system consumption, generation and exchanges in 34 European countries” Brussels, 2018.

[ENTSO2019a] European Network of Transmission System Operators for Electricity (ENTSO-E) “Statistical Factsheet 2019 - Provisional values as of 5 June 2019” Brussels, 2019.

[ENTSO2019b] European Network of Transmission System Operators for Electricity (ENTSO-E) “Hourly load values 2006-2015” Brussels, 2019. [Online] https://docstore.entsoe.eu/Documents/Publications/Statistics/Monthly-hourly-load-values_2006-2015.xlsx [Accessed January 2019]

[ENTSO2019c] European Network of Transmission System Operators for Electricity (ENTSO-E) “Power Facts Europe 2019” Brussels, 2019. [Online] https://eepublicdownloads.entsoe.eu/clean-documents/Publications/ENTSO-E%20general%20publications/ENTSO-E_PowerFacts_2019.pdf [Accessed March 2019]

[ENTSO2020] European Network of Transmission System Operators for Electricity (ENTSO-E) “International Cooperation” Brussels, 2020. [Online] https://www.entsoe.eu/cooperation/ [Accessed February 2020]

[ENTSO2022] European Network of Transmission System Operators for Electricity (ENTSO-E) “Continental Europe successful synchronisation with Ukraine and Moldova power systems” 2022. [Online] https://www.entsoe.eu/news/2022/03/16/continental-europe-successful-synchronisation-with-ukraine-and-moldova-power-systems/ [Accessed March 2022][EP2018] European Parliament (EP) “2018 UN Climate Change Conference in Katowice, Poland (COP 24)” European Parliament resolution of 25 October 2018 on the 2018 UN Climate Change Conference in Katowice, Poland (COP 24) (2018/2598(RSP)). Strasbourg, 2018.

[EP2018b] European Parliament (EP) “Briefing: Economic, social and territorial situation of France - La Réunion” Policy Department for Structural and Cohesion Policies, PE 617.483, Strasbourg, 2018.

[EPEC2018] European Parliament (EP) and European Council (EUCO) “Regulation (EU) 2018/842 of the European Parliament and of the Council of 30 May 2018 on binding annual greenhouse gas emission reductions by Member States from 2021 to 2030 contributing to climate action to meet commitments under the Paris Agreement and amending Regulation (EU) No 525/2013” Strasbourg, 30 May 2018.

[EPRS2021] European Parliamentary Research Service (EPRS) “EU-UK Trade and Cooperation Agreement - An Analytical Overview” European Parliament, Brussels, 2021.

[ETH2016a] Swiss Federal Institute of Technology in Zürich (ETH Zurich) “The Renewables.ninja European wind data set – Version 1.1” 2016. [Online] https://www.renewables.ninja/static/downloads/ninja_europe_wind_v1.1.zip [Accessed August 2019]

[ETH2016b] Swiss Federal Institute of Technology in Zürich (ETH Zurich) “The Renewables.ninja European PV data set – Version 1.1” 2016. [Online] https://www.renewables.ninja/static/downloads/ninja_europe_pv_v1.1.zip [Accessed August 2019]

[ETH2019] Swiss Federal Institute of Technology in Zürich (ETH Zurich) “MERRA-2 Air Temperature (°C)” 2019. [Online] https://www.renewables.ninja/ [Accessed January 2019]

[EUCO2014] European Commission (EC) “2030 Climate and Energy Policy Framework” EUCO 169/14, Brussels, 24 October 2014.

[EUNEW2022] Euronews “The end of fossil fuels: Which countries have banned exploration and extraction?” 2022. [Online] https://www.euronews.com/green/2021/08/12/the-end-of-fossil-fuels-which-countries-have-banned-exploration-and-extraction [Accessed February 2022]

[EUROS2017] European Statistical Office (Eurostat) “Short Assessment of Renewable Energy Sources (SHARES) 2017 Summary Results” Luxembourg, Publications Office of the European Union, 2017. [Online] https://ec.europa.eu/eurostat/documents/38154/4956088/SHARES+summary+results+2017/173de00c-fe7c-43ee-98b5-a3c79aa4947c [Accessed March 2019]

[EUROS2018a] European Statistical Office (Eurostat) “Energy Balances in the MS Excel file format (2018 edition)” 2018. [Online] https://ec.europa.eu/eurostat/documents/38154/4956218/ENERGY-BALANCES-May-2018-edition.zip/310265d9-6adf-45aa-ba41-2dce8e5f78eb [Accessed September 2019]

[EUROS2018b] European Statistical Office (Eurostat) “Energy balance sheets 2016 DATA - 2018 edition” Publications Office of the European Union, Luxembourg, 2018.

[EUROS2018c] European Statistical Office (Eurostat) “Population Density by NUTS 3 region, code demo_r_d3dens” 2018. [Online] https://ec.europa.eu/eurostat/web/products-datasets/product?code=demo_r_d3dens. [Accessed March 2020]

[EUROS2018d] European Statistical Office (Eurostat) “Eurostat regional yearbook 2018” Publications Office of the European Union, Luxembourg, 2018.

[EUROS2018e] European Statistical Office (Eurostat) “Living conditions in Europe - 2018 edition” Publications Office of the European Union, Luxembourg, 2018.

[EUROS2018f] European Statistical Office (Eurostat) “EU transport in figures - statistical pocketbook 2018” Publications Office of the European Union, Luxembourg, 2018.

[EUROS2019a] European Statistical Office (Eurostat) “Energy balance sheets 2017 DATA. 2019 Edition.” Publications Office of the European Union, Luxembourg, August 2019.

[EUROS2019b] European Statistical Office (Eurostat) “Energy balance guide - Methodology guide for the construction of energy balances & Operational guide for the energy balance builder tool” Publications Office of the European Union, Luxembourg, January 2019.

[EUROS2019c] European Statistical Office (Eurostat) “Share of fuels in the final energy consumption in the residential sector for space heating, 2016 (%)” Publications Office of the European Union, Luxembourg, January 2019. [Online] https://ec.europa.eu/eurostat/statistics-explained/index.php?title=File:Share_of_fuels_in_the_final_energy_consumption_in_the_residential_sector_for_space_heating,_2016_(%25).png#file [Accessed January 2019]

[EUROS2019d] European Statistical Office (Eurostat) “EU Age 0-19” 2019. [Online] https://appsso.eurostat.ec.europa.eu/nui/submitViewTableAction.do [Accessed August 2019]

[EUROS2019e] European Statistical Office (Eurostat) “Population change - Demographic balance and crude rates at national level” 2019. [Online] https://appsso.eurostat.ec.europa.eu/nui/show.do?dataset=demo_gind&lang=en [Accessed August 2019]

[EUROS2019f] European Statistical Office (Eurostat) “Energy balance sheets 2017 DATA - 2019 edition” Publications Office of the European Union, Luxembourg, 2019.

[EUROS2020] European Statistical Office (Eurostat) “Glossary: Energy dependency rate” 2020. [Online] https://ec.europa.eu/eurostat/statistics-explained/index.php?title=Glossary:Energy_dependency_rate [Accessed February 2020]

[EUROS2021a] European Statistical Office (Eurostat) “CO_2 emissions from energy use clearly decreased in the EU in 2020” 2021. [Online] https://ec.europa.eu/eurostat/de/web/products-eurostat-news/-/ddn-20210507-1 [Accessed July 2021]

[EUROS2021b] European Statistical Office (Eurostat) “Nuclear energy SE Data2019 V19-02-2021” 2021. [Online] https://ec.europa.eu/eurostat/statistics-explained/images/c/cf/Nuclear_energy_SE_Data2019_V19-02-2021.xlsx [Accessed October 2021]

[EUROS2022a] European Statistical Office (Eurostat) “Energy production and imports 2020 v4” 2022. [Online] https://ec.europa.eu/eurostat/statistics-explained/images/a/a0/Energy_production_and_imports_2020_v4.xlsx [Accessed January 2022]

[EUROS2022b] European Statistical Office (Eurostat) “Glossary: Gross inland energy consumption” 2022. [Online] https://ec.europa.eu/eurostat/statistics-explained/index.php?title=Glossary:Gross_inland_energy_consumption [Accessed March 2022]

[EWEA2013] European Wind Energy Association (EWEA) “Deep Water: the next step for offshore wind energy” EWEA, Brussels, 2013.

[Felb2014] G. Felber and G. Stoeglehner “Onshore wind energy use in spatial planning - a proposal for resolving conflicts with a dynamic safety distance approach” Energy, Sustainability and Society, Vol. 4:22, SpringerOpen Journal, 2014.

[FFE2014] Forschungsstelle für Energiewirtschaft (FFE) “Nutzung von Wärmetechnologien. Ratgeber Wärme in Hessen“ 2014. [Online] https://www.ffegmbh.de/download/informationen/528_ihk_hessen_waerme/waermestudie-ihk-hessen-ffe_10-02-2015.pdf [Accessed March 2019]

[FFE2017] Forschungsstelle für Energiewirtschaft (FFE) “Kurzstudie Power-to-X - Ermittlung des Potenzials von PtX-Anwendungen für die Netzplanung der deutschen ÜNB” München, 2017.

[Flei2017a] T. Fleiter, R. Elsland, M. Rehfeldt, J. Steinbach, U. Reiter, G. Catenazzi, M. Jakob, R. Harmsen, C. Rutten, F. Dittmann, P. Rivière, P. Stabat "Heat Roadmap Europe 2050. Profile of heating and cooling demand in 2015 data annex. Final Data Set 15.03.2017" 2017. [Online] https://hre.aau.dk/wp-content/uploads/2018/09/HRE4-Exchange-Template-WP3_v22b_website.xlsx [Accessed November 2018]

[Flei2017b] T. Fleiter, R. Elsland, M. Rehfeldt, J. Steinbach, U. Reiter, G. Catenazzi, M. Jakob, R. Harmsen, C. Rutten, F. Dittmann, P. Rivière, P. Stabat "Heat Roadmap Europe 2050. Profile of heating and cooling demand in 2015" 2017. [Online] https://hre.aau.dk/wp-content/uploads/2018/09/3.1-Profile-of-the-heating-and-cooling-demand-in-the-base-year-in-the-14-MSs-in-the-EU28-1.pdf [Accessed November 2018]

[Frash2015] A. Frasheri "Geothermal Energy Resources in Albania-Country Update Paper" In: Proceedings World Geothermal Congress 2015, pp. 1–11, Melbourne, 2015.

[Free2016] K. Freeman, A. Roberts, B. Vaply "Future renewable energy costs: offshore wind" KIC InnoEnergy, BVG Associates, Eindhoven, Swindon, 2016.

[Götz2016] M. Götz, J. Lefebvre, F. Mörs, A. McDaniel Koch, F. Graf, S. Bajohr, R. Reimert, T. Kolb "Renewable Power-to-Gas: A technological and economic review" In: Renewable Energy Vol. 85 (2016) pp. 1371–1390, Elsevier, 2016.

[Gruen2017] W. Gründinger "Drivers of Energy Transition How Interest Groups Influenced Energy Politics in Germany" Springer VS, Wiesbaden, 2017.

[Gued2007] R. Guedes, C. Ribeiro, J. Silva, F. Ulrich "Roughness length classification of CORINE Land Cover classes" In: Proceedings of European Wind Energy Conference & Exhibition, 2007.

[Ham2011] J. Hammons "Energy Potential of the Oceans in Europe and North America: Tidal, Wave, Currents, OTEC and Offshore Wind" In: Electricity Infrastructures in the Global Marketplace, InTech, pp. 153–193, 2011.

[Hell2003] M. Hellwig "Entwicklung und Anwendung parametrisierter Standard-Lastprofile" 2003. [Online] https://mediatum.ub.tum.de/doc/601557/601557.pdf [Accessed November 2018]

[Hess2018] D. Hess, M. Wetzel, K.K. Cao "Representing node-internal transmission and distribution grids in energy system models" In: Renewable Energy, Vol. 119, April 2018, Pages 874-890.

[Hirs2018] C. von Hirschhausen, C. Gerbaulet, C. Kemfert, C. Lorenz, P.Y. Oei (eds) "Energiewende Made in Germany" Springer International, Cham, 2018.

[IASS2015] Institute for Advanced Sustainability Studies (IASS) "Long-term climate goals - Decarbonisation, carbon neutrality, and climate neutrality" DOI: 10.2312/iass.2015.029, Potsdam, 2015.

[ICCT2019] International Council on Clean Transportation (ICCT) "From Laboratory to Road - A 2018 update of official and real-world fuel consumption and CO2 values for passenger cars in Europe" 2019. [Online] https://theicct.org/sites/default/files/publications/Lab_to_Road_2018_corrected-jul2021.pdf [Accessed August 2019]

[IEA2014] International Energy Agency (IEA) "Linking Heat and Electricity Systems - Co-generation and District Heating and Cooling Solutions for a Clean Energy Future" OECD Publishing, Paris, 2014.

[IEA2016] International Energy Agency (IEA) “Energy Technology Perspectives 2016 - Annex H: Rooftop Solar PV Potential in Cities” OECD Publishing, Paris, 2016.

[IEA2018] International Energy Agency (IEA) “Renewables Information 2018” OECD Publishing, Paris, 2018.

[IEA2019] International Energy Agency (IEA) “World Energy Balances: Overview (2019 edition)” OECD Publishing, Paris, 2019.

[IHA2017] International Hydropower Association (IHA) “Hydropower Status Report 2017” 2017. [Online] https://www.hydropower.org/sites/default/files/publications-docs/2017%20Hydropower%20Status%20Report.pdf [Accessed September 2019]

[IHS2021] HIS Markit “Spain becomes fourth EU country slapping ban on new fossil fuel production” 2021. [Online] https://cleanenergynews.ihsmarkit.com/research-analysis/spain-becomes-fourth-eu-country-slamming-ban-on-fossil-fuel-ep-.html [Accessed February 2022]

[Ioan2018] A. Ioannou, A. Angus, F. Brennan “Parametric CAPEX, OPEX, and LCOE expressions for offshore wind farms based on global deployment parameters” In: Energy Source Part B: Economics, Planning, and Policy, vol. 13, pp. 281–290, 2018.

[IPCC2014] Intergovernmental Panel on Climate Change (IPCC) “Emission Factors for Greenhouse Gas Inventories” 2014. [Online] https://www.epa.gov/sites/production/files/2015-07/emission-factors_2014.xlsx [Accessed November 2019]

[IPCC2019] Intergovernmental Panel on Climate Change (IPCC) “Global Warming of 1.5°C - An IPCC Special Report on the impacts of global warming of 1.5°C above pre-industrial levels and related global greenhouse gas emission pathways, in the context of strengthening the global response to the threat of climate change, sustainable development, and efforts to eradicate poverty” IPCC, Geneva, Switzerland, 2019.

[IRENA2012] International Renewable Energy Agency (IRENA) “Renewable Energy Technologies: Cost Analysis Series: Concentrating Solar Power - Vol. 1 Power Sector” IRENA, Abu-Dhabi, 2012.

[IRENA2014] International Renewable Energy Agency (IRENA) “REmap 2030: A Renewable Energy Roadmap” IRENA, Abu-Dhabi, 2014.

[IRENA2018a] International Renewable Energy Agency (IRENA) “Global Energy Transformation: A roadmap to 2050” International Renewable Energy Agency, Abu Dhabi, 2018.

[IRENA2018b] International Renewable Energy Agency (IRENA) “Renewable Power Generation Costs in 2017” IRENA, Abu Dhabi, 2018.

[ISO2017] International Organization for Standardization (ISO) “ISO 3166 Country Codes - The International Standard for country codes and codes for their subdivisions” 2017. [Online] https://www.iso.org/obp/ui/#search/code/ [Accessed February 2017]

[IUCN2008] International Union for Conservation of Nature (IUCN) “Guidelines for Applying Protected Area Management Categories” IUCN, Gland, 2008.

[IWU1996] Institut Wohnen und Umwelt (IWU) “Jahresdauerlinien für Niedrigenergiesiedlungen Gemessene Tagesganglinien als Grundlage für die Auslegung von Blockheizkraftwerken” 1996. [Online] https://www.iwu.de/fileadmin/user_upload/dateien/energie/neh_ph/BHKW_Jahresdauerlinien.pdf [Accessed November 2018]

[Jia2017] J. Jia, P. Punys, J. Ma “Hydropower” In: W.Y. Chen, T. Suzuki, M. Lackner (eds.) “Handbook of Climate Change Mitigation and Adaptation” 2nd Edition, pp. 2085-2116, Springer International Publishing, Cham, 2017.

[JRC2018] Joint Research Centre (JRC) “NREAPs and Progress Reports Data Portal” 2018. [Online] https://iet.jrc.ec.europa.eu/remea/nreaps-and-progress-reports-data-portal [Accessed April 2019].

[Kand2014] A. Kandt and R. Romero “Implementing Solar Technologies at Airports - NREL/TP-7A40-62349” National Renewable Energy Laboratory, Golden, CO, 2014.

[Kash2013] M. Kashubsky and A. Morrison “Security of offshore oil and gas facilities: exclusion zones and ships' routeing” In: Australian Journal of Maritime and Ocean Affairs, vol. 5, pp. 1–10, 2013.

[Katso2016] G. Katsouris and A. Marina “Cost Modelling of Floating Wind Farms. ECN-E-15-078” Energy Research Center of the Netherlands (ECN), Petten, 2016.

[Kech2015] K. Kechagia and D. Latinopouls “A GIS-based multi-criteria evaluation for wind farm site selection - A regional scale application in Greece” In: Renewable Energy, Vol. 78, pp. 550–560, 2015.

[Kers2009] C. Kerschner “Economic de-growth vs. steady-state economy” 2009. In: Journal of Cleaner Production, Vol. 18 (2010), pp. 544–551.

[Kirch2011] T. Kirchner “Stand und Potenziale der geothermischen Stromerzeugung in Europa” Dissertation, Institut für Elektrizitätswirtschaft und Energieinnovation der TU Graz, Graz, 2011.

[Klaus2010] T. Klaus, C. Vollmer, K. Werner, H. Lehmann, K. Muschen “Energieziel 2050 - 100% Strom aus erneuerbaren Quellen” Umweltbundesamt, Dessau-Roßlau, 2010.

[Knop2013] B. Knopf, B. Bakken, S. Carrara, A. Kanudia, I. Keppo, T. Koljonen, S. Mima, E. Schmid, D.P. van Vuuren “Transforming the European Energy System: Member States' Prospects within the EU Framework” In: Climate Change Economics, Vol. 4, Suppl. 1, 2013.

[Komar2018] P. Komarnicki, J. Haubrock, Z.A. Styczynski “Elektromobilität und Sektorenkopplung Infrastruktur- und Systemkomponenten“ Springer Vieweg, Berlin, 2018.

[Kost2013] C. Kost, J. Mayer, J. Thomsen, N. Hartmann, C. Senkpiel, S. Philipps, S. Nold, S. Lude, T. Schlegel “Stromgestehungskosten Erneuerbare Energien” Fraunhofer-ISE, Freiburg, 2013.

[Kraut2016] J. Krautwald and J. Baier “Biologische Methanisierung - Methanogenese als mikrobiologische Alternative zur katalytischen Methanisierung“ In: AQUA & GAS No. 7/8, 2016.

[Kup2017a] M.S. Kuprat, M. Bendig, K. Pfeiffer “Possible role of power-to-heat and power to-gas as flexible loads in German medium voltage networks” In: Front. Energy 2017, 11(2), pp. 135–145, Higher Education Press and Springer-Verlag, Berlin, Heidelberg, 2017.

[Kup2017b] M.S. Kuprat “SoVieL: Sektorenkopplung - Vier Infrastrukturen, eine optimale Lösung?” MITNETZ STROM, ONTRAS, ENSO NETZ, Brandenburgische Technische Universität Cottbus-Senftenberg, Kabelsketal, Leipzig, Dresden, Cottbus, 2017.

[Kup2018] M.S. Kuprat and L. Alexandroae “Eurostat e-mail correspondence from 12th September 2018: B_100112 DIRECT USE and GROSS INLAND CONSUMPTION” Eurostat reference number ESTA44101. In: Annex CD.

[Kup2019] M.S. Kuprat and J. Gan “A novel modelling approach towards the system integration of renewable energy sources via integrated energies in ENTSO-E” In: The Seventh International Academic Conference for Graduates, NUAA 21-22, Nanjing, November 2019.

[Kup2020a] M.S. Kuprat and D.E. Huck “Geo-Spatial Analysis of Renewable Energy Potential in the European Union Under Consideration of Social, Environmental, and Technical Limitations” In: 17th International Conference on the European Energy Market (EEM), pp. 1–8, Stockholm, 2020.

[Kup2020b] M.S. Kuprat, J. Gan, H. Schwarz “A Linear Modelling Approach to Efficiently Utilize Renewable Energy Sources by the Means of Integrated Energy in the ENTSO-E” In: IEEE Conference Proceedings International Youth Conference on Radio Electronics, Electrical and Power Engineering (REEPE2020), Moscow, March 2020.

[Kurz2015] P. Kurzweil and O.K. Dietlmeier “Elektrochemische Speicher - Superkondensatoren, Batterien, Elektrolyse-Wasserstoff, Rechtliche Grundlagen“ Springer Vieweg, Wiesbaden, 2015.

[Lack2017] M. Lackner “3rd-Generation Biofuels: Bacteria and Algae as Sustainable Producers and Converters” In: W.Y. Chen, T. Suzuki, M. Lackner (eds.) “Handbook of Climate Change Mitigation and Adaptation” 2nd Edition, pp. 3173-3206, Springer International Publishing, Cham, 2017.

[Laem2017] M. Lämmle, A. Oliva, M. Hermann, K. Kramer, W. Kramer “PVT Collector technologies in solar thermal systems: A systematic assessment of electrical and thermal yields with the novel characteristic temperature approach” In: Solar Energy, vol. 155, pp. 867–879, 2017.

[Lars2018] S. Larsen, A. Hansen, H. Nielson “The role of EIA and weak assessments of social impacts in conflicts over implementation of renewable energy policies” In: Energy Policy, vol. 115, pp. 43–53, 2018.

[Lehn2014] M. Lehner, R. Tichler, H. Steinmüller, M. Koppe “Power-to-Gas: Technology and Business Models” Springer International Publishing, Basel, 2014.

[Li2013] Y. Li-Beisson and G. Peltier “Third-generation biofuels: current and future research on microalgal lipid biotechnology” OCL Vol. 20 (6) D606, EDP Sciences, 2013.

[Lig2018] Y. Ligen, H. Vrubel, H.H. Girault “Mobility from Renewable Electricity: Infrastructure Comparison for Battery and Hydrogen Fuel Cell Vehicles” Ecole Polytechnique Federale de Lausanne (EPFL), Laboratoire d’Electrochimie Physique et Analytique (LEPA), 2018. In: World Electric Vehicle Journal 2018, 9, 3.

[Liu2020] Z. Liu, P. Ciais, Z. Deng, R. Lei, S.J. Davis, S. Feng, B. Zheng, D. Cui, X. Dou, B. Zhu, R. Guo, P. Ke, T. Sun, C. Lu, P. He, Y. Wang, X. Yue, Y. Wang, Y. Lei, H. Zhou, Z. Cai, Y. Wu, R. Guo, T. Han, J. Xue, O. Boucher, E. Boucher, F. Chevallier, K. Tanaka, Y. Wei, H. Zhong, C. Kang, N. Zhang, B. Chen, F. Xi, M. Liu, F.M. Bréon, Y. Lu, Q. Zhang, D. Guan, P. Gong, D.M. Kammen, K. He, H.J. Schellnhuber “Near-real-time monitoring of global CO2 emissions reveals the effects of the COVID-19 pandemic” In: Nature Communications 11, 5172 (2020). Springer Nature, Berlin, Heidelberg, 2020.

[Luetk2012] I. Lütkehus, H. Salecker, K. Adlunger “Potenzial der Windenergie an Land” Umweltbundesamt, Dessau-Roßlau, 2012.

[META2018] METAVER Metadaten Verbund “Windkraftanlagen im Land Brandenburg” 2018. [Online] http://metaver.de/portal/ [Accessed May 2020]

[Mil2020] D. Milborrow “Wind Energy Development” In: A. Sayigh, D. Milborrow (eds.) “The Age of Wind Energy - Progress and Future Directions from a Global Perspective” Springer Nature Switzerland, Cham, 2020.

[Mura2017] H. Muraoka “Geothermal Energy” In: W.Y. Chen, T. Suzuki, M. Lackner (eds.) “Handbook of Climate Change Mitigation and Adaptation” 2nd Edition, pp. 2057-2083, Springer International Publishing, Cham, 2017.

[Nado2014] A. Nádor “Danube Region Geothermal Report” Geological and Geophysical Institute of Hungary, Budapest, 2014.

[Nee2005] M.L. Neelis, M. Patel, D.J. Gielen, K. Blok “Modelling CO_2 emissions from non-energy use with the non-energy use emission accounting tables (NEAT) model” In: Resources, Conservation and Recycling, Vol. 45, pp. 226–250, 2005.

[Nich2020] M. Nicholas and S. Wappelhorst “Regional Charging Infrastructure Requirements in Germany through 2030” 2020. [Online] https://theicct.org/sites/default/files/publications/germany-charging-infrastructure-20201021.pdf [Accessed March2021]

[NOAA2020] National Oceanic and Atmospheric Administration (NOAA) “Mauna Loa CO2 annual mean data - NOAA ESRL DATA” 2020. [Online] ftp://aftp.cmdl.noaa.gov/products/trends/co2/co2_annmean_mlo.txt [Accessed February 2020]

[NREL2014] National Renewable Energy Laboratory (NREL) “Reference Manual for the System Advisor Model’s Wind Power Performance Model” NREL, Golden, Colorado, 2014.

[NREL2016] National Renewable Energy Laboratory (NREL) “System Advisor Model Version 2017.1.17 (SAM 2017.1.17)” 2016. [Online] https://sam.nrel.gov/download/version-2017-1-17/14-sam-2017-1-17-for-windows/file.html [Accessed November 2018]

[OECD2018] Organisation for Economic Co-operation and Development (OECD) “Uranium 2014: Resources, Production and Demand” NEA No. 7413, OECD, 2018.

[Oes2018] Oesterreichs Energie “Abschlussbericht des EP Elektromobilität - EP Elektromobilität des AK Verteilernetze“ 2018. [Online] https://oesterreichsenergie.at/files/Downloads%20Netze/Abschlussbericht_EP-Elektromobilit%C3%A4t.pdf [Accessed April 2019]

[Oliv2016] J.G.J. Olivier, G. Janssens-Maenhout, M. Muntean, J.A.H.W. Peters “Trends in global CO2 emissions: 2016 Report” PBL Netherlands Environmental Assessment Agency, European Commission, Joint Research Centre, The Hague, Ispra, 2016.

[OPSD2019] Open Power System Data (OPSD) “National generation capacity - Package Version 2019-02-22” 2019. [Online] https://data.open-power-system-data.org/national_generation_capacity/2019-02-22/national_generation_capacity.xlsx [Accessed November 2019]

[Palen2019] P. Palensky, M. Cvetković, T. Keviczky (eds) “Intelligent Integrated Energy Systems” Springer International, Cham, 2019.

[Papa2018] M. Papaelias, F. Pedro G. Márquez, I. Segovia Ramirez “Concentrated Solar Power: Present and Future” In: F. P. García Márquez, A. Karyotakis, M. Papaelias (eds.) “Renewable Energies - Business Outlook 2050” Springer Nature Switzerland, Cham, 2018.

[Pat2017] J. Patronen, E. Kaura, C. Torvestad “Nordic heating and cooling Nordic approach to EU's Heating and Cooling Strategy” 2017. [Online] https://norden.diva-portal.org/smash/get/diva2:1098961/FULLTEXT01.pdf [Accessed November 2018]

[Pers2015] U. Persson and S. Werner “Stratego. Quantifying the Heating and Cooling Demand in Europe. Work Package 2, Background Report 4” 2015. [Online] http://stratego-

project.eu/wp-content/uploads/2014/09/Stratego_Final_Report_download.pdf [Accessed November 2018]

[Pfen2014] S. Pfenninger, A. Hawkes, J. Keirstead "Energy systems modeling for twenty-first century energy challenges" In: Renewable and Sustainable Energy Reviews Vol. 33, pp. 74–86, 2014.

[Pfen2016] S. Pfenninger and I. Staffell "Long-term patterns of European PV output using 30 years of validated hourly reanalysis and satellite data" In: Energy, Vol. 114, pp. 1251–1265, November 2016.

[Ponc2015] K. Poncelet, H.P. Höschle, E. Delarue, W. D'haeseleer "Selecting representative days for investment planning models" In: TME Working Paper - Energy and Environment Draft Version, June 1th 2015. In: WP EN2015-10. 2015.

[Popo2004] K. Popovski and S.P. Vasilevska "Geothermal Energy Use In Macedonia - State-of/the Art and Experience of Agricultural Uses" In: Proceedings of International Geothermal Days POLAND 2004, pp. 284–294, September 2004.

[Priet2013] P.A. Prieto and C. A.S. Hall "Spain's Photovoltaic Revolution - The Energy Return on Investment" Springer, New York, 2013.

[Prog2014] Prognos, EWI, GWS "Entwicklung der Energiemärkte – Energiereferenzprognose. Projekt Nr. 57/12" Studie im Auftrag des Bundesministeriums für Wirtschaft und Technologie. Basel, Köln, Osnabrück, 2014. [Online] https://www.bmwi.de/Redaktion/DE/Publikationen/Studien/entwicklung-der-energiemaerkte-energiereferenzprognose-endbericht.pdf?__blob=publicationFile&v=7 [Accessed December 2018]

[Purr2016] K. Purr, D. Osiek, M. Lange, K. Adlunger, A. Burger, B. Hain, K. Kuhnhenn, T. Klaus, H. Lehmann, L. Mönch, K. Müschen, C. Proske, M. Schmied, C. Vollmer "Integration of Power to Gas/Power to Liquids into the ongoing transformation process" German Environment Agency, Dessau-Roßlau, 2016.

[Rast2019] A.A. Rastegari, Ajar Nath Yadav, Arti Gupta (eds.) "Prospects of Renewable Bioprocessing in Future Energy Systems" Springer Nature, Cham, 2019.

[REC2015a] Regional Environmental Center "The typology of the residential building stock in Albania and the modelling of its low-carbon transformation - Support for Low-Emission Development in South Eastern Europe (SLED)" 2015. [Online] http://sled.rec.org/documents/SLED_Albania_BUILDING_ENG.pdf [Accessed August 2019]

[REC2015b] Regional Environmental Center "The typology of the residential building stock in Serbia and modelling its low-carbon transformation - Support for Low-Emission Development in South Eastern Europe (SLED)" 2015. [Online] http://documents.rec.org/publications/SLED_Serbia_BUILDING_ENG.pdf [Accessed August 2019]

[Rin2018] S. Rinne "Radioinactive: Are nuclear power plant outages in France contagious to the German electricity price?" 2018. CIW Discussion Paper, No. 3/2018, Westfälische Wilhelms-Universität Münster, Centrum für Interdisziplinäre Wirtschaftsforschung (CIW), Münster.

[Ruiz2015] P. Ruiz, A. Sgobbi, W. Nijs, C. Thiel, F. Longa, T. Kober, B. Elberson, G. Hengeveld "The JRC-EU-TIMES model: Bioenergy potentials for EU and neighbouring countries - JRC Policy Report ISBN 978-92-79-53879-7" Joint Research Centre, Ispra, 2015.

[Schmi2016] M. Schmidt, T. Raksha, J. Jöhrens, U. Lambrecht, N. Gerhardt, M. Jentsch "MKS-Studie - Analyse von Herausforderungen und Synergiepotenzialen beim Zusammenspiel von Verkehrs- und Stromsektor im Rahmen der Wissenschaftlichen Begleitung, Unterstützung und Beratung des BMVI in den Bereichen Verkehr und Mobilität mit besonderem Fokus auf

Kraftstoffen und Antriebstechnologien sowie Energie und Klima. München, Heidelberg, Kassel, 2016.

[Schmi2017] M. Schmidt, S. Schwarz, B. Stürmer, L. Wagener, U. Zuberbühler "Technologiebericht 4.2a Power-to-gas (Methanisierung chemisch-katalytisch)" In: Wuppertal Institut, ISI, IZES (Hrsg.): Technologien für die Energiewende. Teilbericht 2 an das Bundesministerium für Wirtschaft und Energie (BMWi). Wuppertal, Karlsruhe, Saarbrücken, 2017.

[Shur2019] N. Shurpali, A.K. Agarwal, V.K. Srivastava "Greenhouse Gas Emissions - Challenges, Technologies and Solutions" Springer Nature, Singapore, 2019.

[Sliz2013] B. Sliz-Szkliniarz "Energy Planning in Selected European Regions" Karlsruhe Institute of Technology Scientific Publishing, Karlsruhe, 2013.

[SM2019] Simple Maps "World Cities Database" 2019. [Online] https://simplemaps.com/static/data/world-cities/basic/simplemaps_worldcities_basicv1.73.zip [Accessed March 2019]

[SN2016] swissnuclear (SN) "Nukleare Stromproduktion 2016 - Schweizer Kernkraftwerke mit leicht reduzierter Produktion im Jahr 2016" 2016. [Online] https://www.swissnuclear.ch/upload/cms/news/20170222_Communiqu_swissnuclear_Betrieb_KKW_2016_de1.pdf [Accessed September 2018]

[Staf2016] I. Staffell and S. Pfenninger "Using bias-corrected reanalysis to simulate current and future wind power output" In: Energy, Vol. 114, pp. 1224–1239, November 2016.

[Stef2018] U. Steffen "Neue Chancen für Kommunen und Stadtwerke durch aktuelle Akzeptanzmaßnahmen bei den Erneuerbaren Energien - Maßnahmenpaket der Landesregierung Brandenburg Erneuerbare Energien und Bürgerinteressen im fairen Miteinander (6 - Punkte Plan)" Ministerium für Wirtschaft und Energie des Landes Brandenburg, Potsdam, 2018.

[Stry2015] G. Stryi-Hipp, J.B. Eggers, A. Steingrube "Berechnung zeitlich hochaufgelöster Energieszenarien im Rahmen des Projektes Masterplan 100%" 2015. [Online] https://www.masterplan100.de/fileadmin/user_upload/content/pdf/2015-02-04_EnSzenarien_KomMod4FFM_ISE_final_2.pdf [Accessed November 2018]

[Tan2014] Z. Tan "Air Pollution and Greenhouse Gases - From Basic Concepts to Engineering Applications for Air Emission Control" Springer Science+Business Media, Singapore, 2014.

[Töp2017] J. Töpler and J. Lehmann "Wasserstoff und Brennstoffzelle Technologien und Marktperspektiven - 2., aktualisierte und erweiterte Auflage" Springer Vieweg, Wiesbaden, 2017.

[Trieb2009] F. Trieb, C. Schillings, M. O'Sullivan, T. Pregger, C. Hoyer-Klick "Global Potential of Concentrating Solar Power" In: Proceedings SolarPaces Conference, Berlin, 2009.

[UBA2016] Umweltbundesamt (UBA) "Climate Change - CO2 Emission Factors for Fossil Fuels" Emissions Situation (Section I 2.6) German Environment Agency (UBA), Dessau-Roßlau, 2016.

[UBA2019] Umweltbundesamt (UBA) "Integration erneuerbarer Energien durch Sektorkopplung: Analyse zu technischen Sektorkopplungsoptionen Climate Change 03/2019 - Umweltforschungsplan des Bundesministeriums für Umwelt, Naturschutz und nukleare Sicherheit - Forschungskennzahl FZK 3714 41 107 2 UBA-FB 002739/1" Dessau-Roßlau, 2019.

[UBA2020] Umweltbundesamt (UBA) “Berichterstattung unter der Klimarahmenkonvention der Vereinten Nationen und dem Kyoto-Protokoll 2020 Nationaler Inventarbericht zum Deutschen Treibhausgasinventar 1990 – 2018” Umweltbundesamt - UNFCCC-Submission, Dessau-Roßlau, 2020.

[UN1994] United Nations (UN) “United Nations Convention on the Law of the Sea (UNCLOS)“ 1994. [Online] https://www.un.org/depts/los/convention_agreements/texts/unclos/unclos_e.pdf [Accessed October 2018]

[UN1998] United Nations (UN) “Kyoto Protocol to the United Nations Framework Convention on Climate Change“ 1998. [Online] https://unfccc.int/resource/docs/convkp/kpeng.pdf [Accessed February 2020]

[UN2015] United Nations (UN) “Paris Agreement“ 2015. [Online] https://unfccc.int/files/essential_background/convention/application/pdf/english_paris_agreement.pdf [Accessed February 2020]

[UN2018] United Nations (UN) “International Recommendations for Energy Statistics (IRES) - Statistical Papers Series M No. 93“ Department of Economic and Social Affairs, New York, 2018.

[UNC2020] United Nations Conference on Trade and Development (UNCTAD) “Global population and population projections, 1850–2100” 2020. [Online] https://stats.unctad.org/Dgff2016/annexes/data/Fig1.xls/ [Accessed February 2020]

[UNSD2020] United Nations Statistics Division (UNSD) “Methodology - Standard country or area codes for statistical use (M49)” 2020. [Online] https://unstats.un.org/unsd/methodology/m49/ [Accessed October 2020]

[UO2007] University of Oregon (UO) “Solar Radiation Monitoring Laboratory - Sun Path Chart Program” 2007. [Online] http://solardat.uoregon.edu/SunChartProgram.html [Accessed November 2019]

[Vart2015] E. Vartiainen, G. Masson, C. Breyer “PV LCOE in Europe 2015-2050” In: 31st European Photovoltaic Solar Energy Conference and Exhibition, Munich, 2015.

[Ven2021] D.J. van de Ven, I. C. Peréz, I. Arto, I. Cazcarro, C. de Castro, P. Pate, M. Gonzalez-Eguino “The potential land requirements and related land use change emissions of solar energy” In: Scientific Reports, Nature, Vol. 11, No. 2907, 2021.

[WBG2019a] The World Bank Group (WBG) “Land area” 2019. [Online] http://api.worldbank.org/v2/en/indicator/AG.LND.TOTL.K2?downloadformat=excel [Accessed February 2020]

[WBG2019b] The World Bank Group (WBG) “Population” 2019. [Online] http://api.worldbank.org/v2/en/indicator/SP.POP.TOTL?downloadformat=excel [Accessed February 2020]

[WBG2019c] The World Bank Group (WBG) “Gross domestic product 2018” 2019. [Online] http://api.worldbank.org/v2/en/indicator/NY.GDP.MKTP.CD?downloadformat=excel [Accessed February 2020]

[WE2017] WindEurope “Unleashing Europe's offshore wind potential: a new resource assessment” WindEurope, Brussels, 2017.

[Wees2013] J.D. van Wees, T. Boxem, L. Angelino, P. Dumas “GEOELEC - A prospective study on the geothermal potential in the EU - Deliverable No. 2.5” 2013. [Online] http://www.geoelec.eu/wp-content/uploads/2011/09/D-2.5-GEOELEC-prospective-study.pdf [Accessed October 2019]

[Wess2017] V. Wesselak, T. Schabbach, T. Link, J. Fischer “Handbuch Regenerative Energietechnik“ 3. Auflage, Springer Vieweg, Berlin, Wiesbaden, 2017.

[Wu2019] Q.H. Wu, J. Zheng, Z. Jing, X. Zhou “Large-Scale Integrated Energy Systems - Energy Systems in Electrical Engineering” Springer, Singapore, 2019.

[Yah2012] S. Al-Yahyai, Y. Charabi, A. Gastil, A. Al-Badi “Wind farm land suitability indexing using multi-criteria analysis” In: Renewable Energy, Vol. 44, pp. 80–87, 2012.

[Yilm2017] H.Ü. Yilmaz, R. Hartel, D. Keles, R. McKenna, W. Fichtner “Analysis of the potential for Power-to-Heat/Cool applications to increase flexibility in the European electricity system until 2030” 2017 [Online] https://bib.irb.hr/datoteka/889378.PtH_C_final_version_final.pdf [Accessed November 2019]

[Zapf2017] M. Zapf “Stromspeicher und Power-to-Gas im deutschen Energiesystem - Rahmenbedingungen, Bedarf und Einsatzmöglichkeiten” Springer Vieweg, Wiesbaden, 2017.

[Zaun2018] B. Zaunbrecher, B. Daniels, M. Roß-Nickoll, M. Ziefle “The social and ecological footprint of renewable power generation plants - Balancing social requirements and ecological impacts in an integrated approach” In: Energy Research & Social Science, Vol. 45, pp. 91–106, 2018.

Appendix

List of Annexes

Annex I ISO country codes, area, population, and GDP ENTSO-E 2016

Source: In reference to [ISO2017] [WBG2019a] [WBG2019b] [WBG2019c]

Country Name	ISO Code	Land Area	Population	GDP
		[km²]	[No.]	[Bil. USD]
Albania	AL	27,400	2,854,191	15
Austria	AT	82,520	8,879,920	445
Belgium	BE	30,280	11,488,980	535
Bosnia	BA	51,200	3,300,998	20
Bulgaria	BG	108,560	6,975,761	69
Croatia	HR	56,590	4,065,253	62
Cyprus	CY	9,240	1,198,574	26
Czechia	CZ	77,200	10,671,870	252
Denmark	DK	40,000	5,814,422	348
Estonia	EE	43,470	1,326,898	31
Finland	FI	303,920	5,521,606	269
France	FR	547,559	67,287,893	2,736
Germany	DE	349,380	83,092,962	3,888
Greece	GR	128,900	10,721,582	205
Hungary	HU	91,260	9,771,141	164
Iceland	IS	100,830	360,563	25
Ireland	IE	68,890	4,934,340	399
Italy	IT	297,790	59,762,945	2,011
Latvia	LV	62,090	1,913,822	34
Lithuania	LT	62,630	2,794,137	55
Luxembourg	LU	2,430	620,001	70
Macedonia	MK	25,220	2,076,694	13
Montenegro	ME	13,450	622,028	6
Netherlands	NL	33,670	17,344,874	910
Norway	NO	365,108	5,347,896	405
Poland	PL	306,170	37,965,475	597
Portugal	PT	91,606	10,286,263	240
Romania	RO	230,080	19,371,648	250
Serbia	RS	87,460	6,945,235	52
Slovakia	SK	48,080	5,454,147	105
Slovenia	SL	20,136	2,088,385	54
Spain	ES	499,603	47,133,521	1,393
Sweden	SE	407,310	10,278,887	534
Switzerland	CH	39,676	8,613,300	738
United Kingdom	UK	241,940	66,870,033	2,879
ENTSO-E		4,951,648	543,756,245	19,835

Annex II Area, population, and GDP ENTSO-E 2016

Source: In reference to [WBG2019a] [WBG2019b] [WBG2019c]

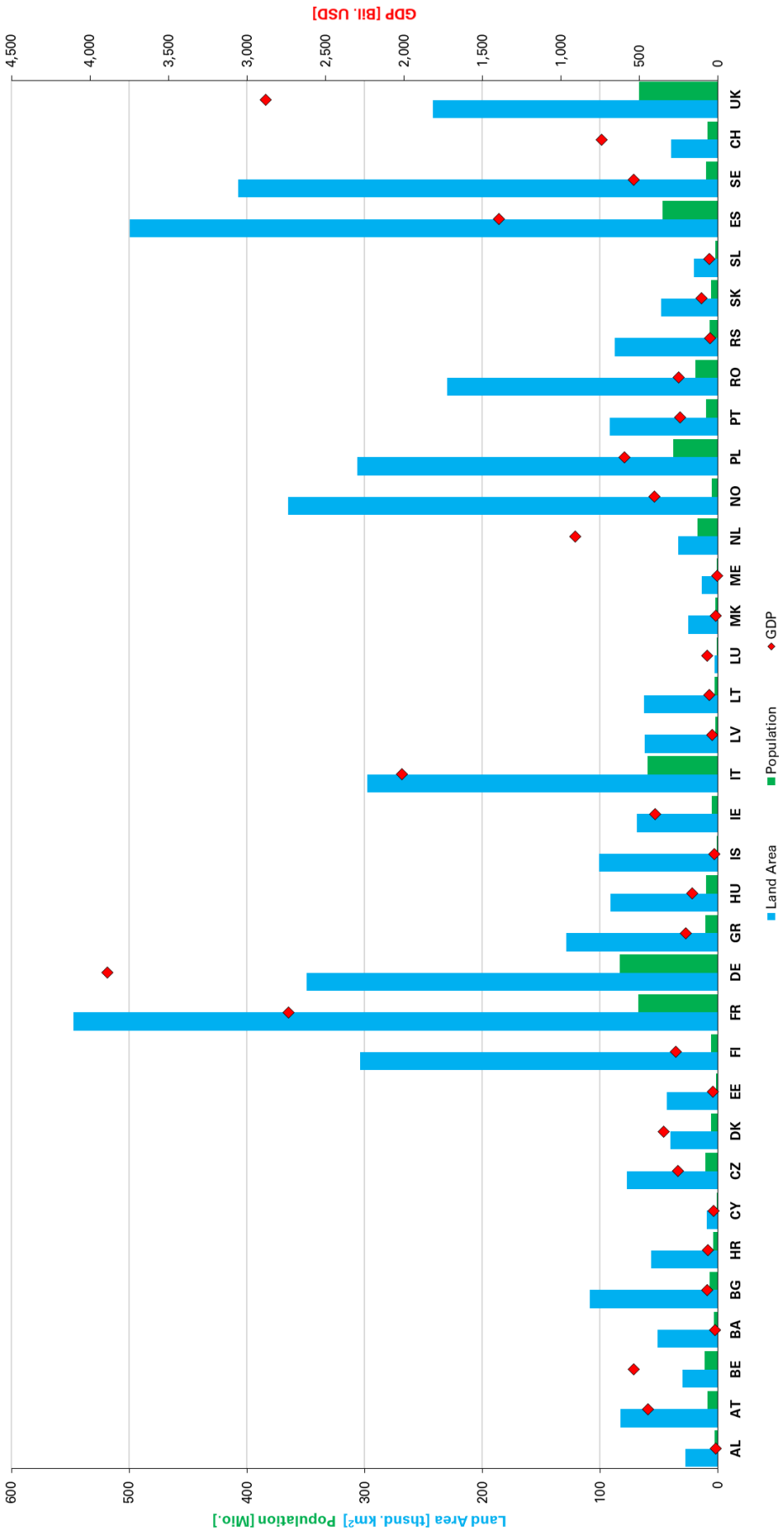

Annex III Net energy commodity imports and dependency rates per country 2016

Country	Solid Fuels [16]		Mineral Oil		Natural Gas		Electricity	
	[TWh]	[%]	[TWh]	[%]	[TWh]	[%]	[TWh]	[%]
AL	0.6	96.0	4.2	28.9	0.0	0.0	0.0	-0.6
AT	32.8	95.5	131.1	92.1	71.6	85.8	7.2	9.9
BA	7.1	14.9	20.8	100.0	2.1	100.0	-3.8	-26.8
BE	32.6	94.9	350.7	100.0	167.2	100.0	6.2	6.8
BG	6.5	9.8	48.1	97.8	30.1	96.5	-6.4	-16.6
CH	1.4	94.6	99.6	97.9	34.3	98.4	0.0	0.0
CY	0.0	0.0	29.9	100.0	0.0	0.0	0.0	0.0
CZ	-1.8	-0.9	93.4	97.2	78.1	95.7	-11.0	-15.4
DE	445.5	49.6	1,250.6	98.8	724.4	88.6	-50.5	-8.5
DK	18.6	84.6	2.4	3.0	-14.9	-44.4	5.1	14.2
EE	0.0	0.0	8.0	60.4	5.0	100.0	-2.0	-20.1
ES	90.1	76.0	703.5	100.0	287.5	98.7	7.7	2.7
FI	31.6	60.1	108.1	97.5	23.9	99.7	19.0	21.6
FR	93.2	93.5	868.8	99.4	440.8	98.9	-41.5	-8.1
GR	2.2	4.4	168.6	100.0	40.3	99.2	8.8	14.6
HR	7.7	100.0	29.3	77.0	8.5	33.5	5.5	30.5
HU	9.1	34.5	72.8	89.3	73.6	78.9	12.7	28.5
IE	13.3	54.7	86.5	100.0	19.8	40.1	-0.7	-2.4
IS	1.2	100.0	11.1	100.0	0.0	0.0	0.2	1.1
IT	124.6	97.5	608.4	94.6	619.8	91.8	37.0	11.4
LT	2.0	89.3	33.4	100.0	21.5	100.0	8.3	69.2
LU	0.6	100.0	30.7	100.0	8.2	99.3	6.3	88.9
LV	0.4	84.5	22.9	100.0	10.7	83.4	1.0	13.9
ME	-0.1	-2.7	4.0	100.0	0.0	0.0	0.3	8.8
MK	1.2	12.1	12.8	100.0	2.0	100.0	2.0	26.5
NL	108.1	91.0	494.0	100.0	-114.5	-32.7	4.9	4.1
NO	7.8	77.4	-845.5	-855.2	-257.9	-1122.0	-15.9	-15.0
PL	-68.3	-12.0	288.5	93.5	133.4	78.4	2.0	1.2
PT	33.9	100.0	128.0	100.0	49.6	99.1	-5.1	-9.4
RO	12.5	20.2	61.7	56.9	13.7	13.0	-5.0	-8.4
RS	0.0	0.0	46.2	79.6	24.0	79.6	-2.0	-5.2
SE	25.9	100.0	156.2	100.0	9.5	99.2	-11.7	-8.1
SI	2.3	17.2	29.4	100.0	8.2	99.4	-1.2	-7.8
SK	31.2	83.3	37.6	91.8	42.1	92.8	2.7	9.0
UK	69.5	50.8	291.8	35.1	376.1	46.5	17.5	5.0
ENTSO-E	1,143.4	38.2	5,487.5	79.4	2,938.8	64.6	0.0	0.0

[16] In the context of energy imports, solid fuels predominantly account for hard coal (bituminous coal) and coking coal, whereas lignite is almost exclusively produced domestically [EUROS2018b].

Annex IV Net energy imports and dependency rates per country 2016 and 2050

Country	2016		2050		2016–2050	
	Net Import	Dependency Rate	Net Import	Dependency Rate	Reduction	
	[TWh]	[%]	[TWh]	[%]	[p.p.]	[%]
AL	7.0	25.0	-8.7	-30.9	-55.9	-223.7
AT	242.0	62.1	180.1	49.9	-12.2	-25.6
BA	26.0	32.9	-5.8	-10.5	-43.5	-122.3
BE	484.0	71.4	415.1	81.4	10.0	-14.2
BG	78.0	37.0	-6.7	-5.1	-42.1	-108.6
CH	155.0	51.7	239.8	67.2	15.5	54.7
CY	28.0	96.6	1.3	5.9	-90.6	-95.3
CZ	150.0	31.4	170.2	52.0	20.7	13.5
DE	2,323.0	62.4	1,632.9	56.7	-5.7	-29.7
DK	14.0	7.2	-169.3	-66.9	-74.1	-1,308.9
EE	28.0	42.4	-50.2	-82.3	-124.7	-279.3
ES	969.0	69.5	-85.4	-7.9	-77.4	-108.8
FI	166.0	42.8	-136.2	-36.6	-79.4	-182.0
FR	1,332.0	46.2	108.0	5.5	-40.7	-91.9
GR	201.0	71.5	19.0	9.0	-62.5	-90.5
HR	48.0	48.0	6.8	8.1	-39.9	-85.8
HU	166.0	55.5	64.3	25.7	-29.8	-61.3
IE	114.0	67.5	-95.8	-53.8	-121.3	-184.1
IS	11.0	16.7	-144.7	-117.6	-134.3	-1,415.4
IT	1,373.0	77.0	633.6	44.0	-33.0	-53.9
LT	63.0	76.8	-76.8	-66.8	-143.6	-221.9
LU	47.0	95.9	41.1	83.9	-12.0	-12.5
LV	22.0	44.0	-104.7	-104.7	-148.7	-575.8
ME	4.0	33.3	-0.1	-1.0	-34.3	-102.5
MK	19.0	61.3	0.4	1.5	-59.8	-97.8
NL	310.0	33.2	445.7	60.1	26.8	43.8
NO	-1,095.0	-405.6	14.0	4.5	410.0	-101.3
PL	321.0	28.3	7.9	0.9	-27.4	-97.5
PT	195.0	72.5	-0.5	-0.2	-72.7	-100.2
RO	83.0	22.1	-14.5	-4.8	-26.9	-117.4
RS	69.0	30.3	6.0	5.0	-25.2	-91.4
SE	164.0	28.7	-229.8	-41.3	-70.0	-240.1
SI	37.0	46.8	29.1	46.9	0.1	-21.4
SK	111.0	58.4	50.2	36.9	-21.5	-54.8
UK	705.0	32.8	551.2	31.6	-1.2	-21.8
ENTSO-E	9,970.0	49.9	3,487.8	20.5	-29.4	-65.0

Annex V Onshore wind exclusion areas and buffer zones

Source: In reference to [Ayd2013] [Deng2015] [Free2016] [Luetk2012] [Sliz2013]

CLC No.	CLC Land Category	Exclusion	Buffer Zone
			[m]
111	Continuous urban fabric	YES	1,000
112	Discontinuous urban fabric	YES	1,000
121	Industrial and commercial units	YES	500
122	Road, rail networks, associated land	YES	200
123	Port areas	NO	-
124	Airports	YES	3,000
131	Mineral extraction sites	YES	150
132	Dump sites	YES	150
133	Construction sites	YES	150
141	Green urban areas	YES	1,000
142	Sport and leisure facilities	YES	500
211	Non-irrigated arable land	NO	-
212	Permanently irrigated land	YES	50
213	Rice fields	YES	50
221	Vineyards	YES	100
222	Fruit trees and berry plantations	YES	100
223	Olive groves	YES	100
231	Pastures	NO	-
241	Annual permanent crops	NO	-
242	Complex cultivation patterns	NO	-
243	Agriculture land with significant areas of natural vegetation	NO	-
244	Agro-forestry areas	NO	-
311	Broad-leaved forest	NO	-
312	Coniferous forest	NO	-
313	Mixed forest	NO	-
321	Natural grasslands	NO	-
322	Moors and heathland	NO	-
323	Sclerophyllous vegetation	NO	-
324	Transitional woodland-shrub	NO	-
331	Beaches, dunes, sands	YES	1,000
332	Bare rocks	YES	50
333	Sparsely vegetated areas	NO	-
334	Burnt areas	NO	-
335	Glaciers and perpetual snow	YES	50
411	Inland marshes	YES	50
412	Peat bogs	YES	50
421	Salt marshes	YES	50
422	Salines	YES	50
423	Intertidal flats [17]	YES	100
511	Water courses [17]	YES	100
512	Water bodies [17]	YES	100
521	Coastal lagoons [17]	YES	100
522	Estuaries [17]	YES	100
523	Sea and ocean [17]	YES	100

[17] In reference to Lütkehus et al. (2012), a 65 m buffer is necessary to meet safety and regulatory standards [Luetk2012]. For this analysis, 100 m is anticipated to account for safety, soil quality, construction, and operation requirements.

Annex VI Utility-scale PV exclusion areas and buffer zones

Source: In reference to [Ayd2013] [Sliz2013]

CLC No.	CLC Land Category	Exclusion	Buffer Zone
			[m]
111	Continuous urban fabric	YES	500
112	Discontinuous urban fabric	YES	500
121	Industrial and commercial units	NO	-
122	Road, rail networks, associated land	YES	150
123	Port areas	YES	500
124	Airports	NO	-
131	Mineral extraction sites	NO	-
132	Dump sites	NO	-
133	Construction sites	YES	500
141	Green urban areas	YES	500
142	Sport and leisure facilities	YES	500
211	Non-irrigated arable land	NO	-
212	Permanently irrigated land	NO	-
213	Rice fields	NO	-
221	Vineyards	NO	-
222	Fruit trees and berry plantations	NO	-
223	Olive groves	NO	-
231	Pastures	NO	-
241	Annual permanent crops	NO	-
242	Complex cultivation patterns	NO	-
243	Agriculture land with significant areas of natural vegetation	NO	-
244	Agro-forestry areas	NO	-
311	Broad-leaved forest	YES	0
312	Coniferous forest	YES	0
313	Mixed forest	YES	0
321	Natural grasslands	YES	0
322	Moors and heathland	NO	-
323	Sclerophyllous vegetation	NO	-
324	Transitional woodland-shrub	NO	-
331	Beaches, dunes, sands	YES	500
332	Bare rocks	NO	50
333	Sparsely vegetated areas	YES	-
334	Burnt areas	NO	-
335	Glaciers and perpetual snow	NO	-
411	Inland marshes	YES	50
412	Peat bogs	YES	50
421	Salt marshes	YES	50
422	Salines	YES	50
423	Intertidal flats	YES	50
511	Water courses	YES	65
512	Water bodies	YES	65
521	Coastal lagoons	YES	50
522	Estuaries	YES	50
523	Sea and ocean	YES	50

Annex VII CSP exclusion areas and buffer zones

Source: In reference to [Ayd2013] [Sliz2013]

CLC No.	CLC Land Category	Exclusion	Buffer Zone [m]
111	Continuous urban fabric	YES	1,000
112	Discontinuous urban fabric	YES	1,000
121	Industrial and commercial units	YES	500
122	Road, rail networks, associated land	YES	200
123	Port areas	YES	100
124	Airports	YES	3,000
131	Mineral extraction sites	YES	150
132	Dump sites	YES	150
133	Construction sites	YES	150
141	Green urban areas	YES	1,000
142	Sport and leisure facilities	YES	500
211	Non-irrigated arable land	NO	-
212	Permanently irrigated land	YES	50
213	Rice fields	YES	50
221	Vineyards	YES	100
222	Fruit trees and berry plantations	YES	100
223	Olive groves	YES	100
231	Pastures	NO	-
241	Annual permanent crops	YES	50
242	Complex cultivation patterns	YES	50
243	Agriculture land with significant areas of natural vegetation	YES	50
244	Agro-forestry areas	YES	0
311	Broad-leaved forest	YES	0
312	Coniferous forest	YES	0
313	Mixed forest	YES	0
321	Natural grasslands	NO	-
322	Moors and heathland	NO	-
323	Sclerophyllous vegetation	NO	-
324	Transitional woodland-shrub	NO	-
331	Beaches, dunes, sands	YES	1,000
332	Bare rocks	YES	50
333	Sparsely vegetated areas	NO	-
334	Burnt areas	YES	50
335	Glaciers and perpetual snow	YES	50
411	Inland marshes	YES	50
412	Peat bogs	YES	50
421	Salt marshes	YES	50
422	Salines	YES	50
423	Intertidal flats	YES	100
511	Water courses	YES	100
512	Water bodies	YES	100
521	Coastal lagoons	YES	100
522	Estuaries	YES	100
523	Sea and ocean	YES	100

Annex VIII Suitability factors onshore wind, utility-scale PV, CSP

Source: In reference to [Deng2015] [Free2016] [Luetk2012] [Sliz2013] [Yah2012]

CLC No.	CLC Land Category	Onshore Wind	Utility-Scale PV	CSP
121	Industrial and commercial units	-	0.250	-
123	Port areas	0.010	-	-
124	Airports	-	0.300	-
131	Mineral extraction sites	-	0.010	-
132	Dump sites	-	0.010	-
211	Non-irrigated arable land	0.120	0.016	0.010
212	Permanently irrigated land	-	0.016	-
213	Rice fields	-	0.012	-
221 222 223	Plantation: Vineyards, fruit, olives	-	0.012	-
231	Pastures	0.050	0.024	0.010
241 242 243	Cropland, cultivation, agriculture	0.020	0.016	-
244	Agro-forestry areas	0.020	0.024	-
321	Natural grasslands	0.100	0.024	0.010
311 312 313	Forest	0.020	-	-
322	Moors and heathland	0.100	-	0.020
323	Sclerophyllous vegetation	0.020	0.024	0.020
324	Transitional woodland-shrub	0.100	0.018	0.020
332	Bare rocks	-	0.030	-
333	Sparsely vegetated areas	0.020	0.030	0.020
334	Burnt areas	0.100	0.030	-

Annex IX Primary Sources potential analysis results per country

Country	Onshore Wind	Offshore Wind	Floating Wind	Utility-Scale PV	CSP	Rooftop PV	Rooftop Thermal
	[GW]	[GW]	[GW]	[GW]	[GW]	[GW]	[GW]
AL	0.1	0.0	0.0	6.5	0.0	8.6	3.0
AT	1.3	0.0	0.0	4.9	0.0	33.9	9.2
BA	0.5	0.0	0.0	12.6	0.0	12.0	3.7
BE	4.8	0.3	0.0	3.4	0.0	28.8	12.0
BG	12.9	0.4	0.0	18.2	0.0	35.5	7.4
CH	0.0	0.0	0.0	0.2	0.0	16.8	8.9
CY	3.3	0.0	0.0	2.9	0.3	4.0	0.9
CZ	4.8	0.0	0.0	10.6	0.0	41.1	11.1
DE	166.8	27.3	0.0	45.8	0.0	242.1	87.1
DK	66.2	56.3	0.5	4.2	0.0	21.3	4.1
EE	31.7	6.0	0.0	3.2	0.0	8.4	2.1
ES	193.4	3.9	0.4	88.7	4.2	186.8	48.8
FI	120.8	14.9	0.0	3.9	0.0	40.8	5.8
FR	343.3	17.7	9.6	78.1	0.1	247.6	68.3
GR	6.2	1.9	0.3	23.7	0.0	45.3	11.3
HR	2.5	0.0	0.0	7.8	0.0	19.3	4.3
HU	3.0	0.0	0.0	20.4	0.0	40.4	10.3
IE	49.9	8.4	24.7	5.3	0.0	22.4	5.0
IS	102.4	33.2	109.7	7.4	0.0	2.9	0.4
IT	32.1	1.9	0.0	50.8	0.1	196.2	63.7
LT	55.9	1.3	0.0	7.2	0.0	17.0	2.9
LU	0.5	0.0	0.0	0.3	0.0	2.0	0.6
LV	59.0	7.2	0.0	5.0	0.0	11.4	2.0
ME	0.4	0.0	0.0	0.0	0.0	2.8	0.6
MK	0.0	0.0	0.0	7.9	0.0	7.5	2.2
NL	28.7	40.5	0.0	7.8	0.0	40.7	18.0
NO	66.3	3.1	0.2	14.1	0.0	28.5	5.5
PL	194.6	5.3	0.1	28.6	0.0	148.1	39.9
PT	36.1	0.5	0.0	13.9	3.1	36.7	10.8
RO	12.9	1.1	0.0	39.5	0.0	90.7	20.6
RS	0.0	0.0	0.0	7.6	0.0	19.4	9.2
SE	187.9	17.1	1.6	8.4	0.0	63.9	9.6
SI	0.0	0.0	0.0	1.5	0.0	9.1	2.2
SK	0.5	0.0	0.0	6.2	0.0	23.6	5.7
UK	155.4	66.3	43.4	38.5	0.0	162.8	64.3
ENTSO-E	1,943.8	314.4	190.6	584.8	7.8	1,918.4	561.7

Annex X Secondary Sources potential analysis results per country

Country	Bioenergy	Hydro-power	Geoth. El.	Geoth. Heat	Hydro-kinetic	SUM
	[TWh]	[TWh]	[TWh]	[TWh]	[TWh]	[TWh]
AL	15.3	5.6	0.0	0.0	0.0	20.9
AT	56.1	45.8	10.7	21.4	0.0	134.0
BA	28.7	5.5	0.0	0.0	0.0	34.3
BE	32.7	0.6	3.5	7.0	0.0	43.9
BG	31.2	4.2	11.5	23.0	0.0	69.9
CH	21.6	31.2	6.9	13.7	0.0	73.4
CY	1.5	0.0	0.0	0.0	0.0	1.5
CZ	55.2	3.9	5.0	9.9	0.0	74.0
DE	235.3	30.7	55.4	110.8	0.0	432.2
DK	22.1	24.8	4.6	9.3	0.3	61.1
EE	18.4	0.1	0.3	0.6	0.0	19.4
ES	202.6	34.8	55.8	111.6	0.4	405.2
FI	75.2	16.4	0.0	0.0	0.0	91.6
FR	322.0	77.8	104.0	208.0	2.3	714.1
GR	23.2	5.6	13.0	26.0	0.0	67.8
HR	16.6	6.8	8.0	16.0	0.0	47.4
HU	68.3	1.1	27.8	55.6	0.0	152.8
IE	10.3	1.5	4.3	8.6	0.5	25.2
IS	0.3	12.2	51.4	102.7	0.0	166.5
IT	141.4	53.9	36.2	72.4	0.3	304.1
LT	38.8	1.1	3.0	6.1	0.0	49.0
LU	1.0	0.2	0.5	1.0	0.0	2.6
LV	42.5	3.3	0.5	1.0	0.0	47.3
ME	3.3	1.8	0.0	0.0	0.0	5.1
MK	9.2	2.5	0.0	0.0	0.0	11.7
NL	30.0	0.1	8.3	16.6	1.0	56.1
NO	33.3	144.0	0.0	0.0	0.0	177.3
PL	196.8	4.4	23.0	46.0	0.0	270.2
PT	28.1	19.1	10.1	20.2	0.9	78.5
RO	123.4	17.0	16.8	33.6	0.0	190.8
RS	27.1	10.1	0.0	0.0	0.0	37.3
SE	121.5	75.7	0.2	0.3	0.3	197.9
SI	11.9	5.8	1.3	2.6	0.0	21.5
SK	20.7	5.8	8.8	17.6	0.0	52.9
UK	91.3	5.6	6.7	13.4	7.9	124.9
ENTSO-E	2,157.1	658.9	477.6	955.1	13.8	4,262.5

Annex XI Power transmission capacities per country

Source: In reference to [Ander2015] [Bak2015]

Country	Link	Capacity [MW]
AL	AL-GR	1,400
	AL-IT	1,732
	AL-ME	1,660
	AL-RS	1,605
	AL-MK	1,218
AT	AT-IT	11,868
	AT-SI	2,945
	AT-HU	2,951
	AT-DE	32,310
	AT-CZ	8,621
	AT-CH	4,107
BA	BA-ME	2,779
	BA-RS	5,908
	BA-HR	8,086
BE	BE-LU	2,280
	BE-NL	16,127
	BE-DE	6,000
	BE-UK	12,000
	BE-FR	8,030
BG	BG-MK	1,404
	BG-GR	3,308
	BG-RO	4,702
	BG-RS	1,460
CH	CH-AT	4,107
	CH-IT	11,261
	CH-FR	14,026
	CH-DE	12,739
CY	CY-GR	2,000
CZ	CZ-PL	8,572
	CZ-SK	3,706
	CZ-AT	8,621
	CZ-DE	5,727
DE	DE-DK	25,569
	DE-NO	19,494
	DE-SE	16,200
	DE-PL	20,753
	DE-FR	11,484
	DE-LU	4,413
	DE-CH	12,739
	DE-AT	32,310
	DE-CZ	5,727
	DE-BE	6,000
	DE-NL	14,282
DK	DK-NO	3,889
	DK-SE	7,221
	DK-NL	3,987
	DK-DE	25,569
EE	EE-LV	7,000
	EE-FI	6,000
ES	ES-PT	16,210
	ES-FR	21,120
FI	FI-EE	6,000
	FI-NO	100
	FI-SE	7,000
FR	FR-IT	8,292
	FR-CH	14,026
	FR-IE	7,000
	FR-UK	16,000
	FR-BE	8,030
	FR-DE	11,484
	FR-ES	21,120
GR	GR-AL	1,400
	GR-IT	7,000
	GR-BG	3,308
	GR-MK	1,720
	GR-CY	2,000
HR	HR-RS	1,405
	HR-BA	8,086
	HR-IT	1,732
	HR-SI	5,713
	HR-HU	4,157
HU	HU-RO	4,494
	HU-RS	1,109
	HU-HR	4,157
	HU-AT	2,951
	HU-SK	11,422
	HU-SI	1,386
IE	IE-FR	7,000
	IE-UK	3,000
IS	-	-
IT	IT-SI	6,710
	IT-ME	3,732
	IT-HR	1,732
	IT-GR	7,000
	IT-AL	1,732
	IT-FR	8,292
	IT-CH	11,261
	IT-AT	11,868
LT	LT-PL	13,554
	LT-LV	7,000
	LT-SE	3,000
LU	LU-DE	4,413
	LU-BE	2,280
LV	LV-LT	7,000
	LV-EE	7,000
ME	ME-RS	4,658
	ME-AL	1,660
	ME-IT	3,732
	ME-BA	2,779
MK	MK-GR	1,720
	MK-AL	1,218
	MK-RS	3,654
	MK-BG	1,404
NL	NL-NO	16,633
	NL-DE	14,282
	NL-DK	3,987
	NL-UK	5,000
	NL-BE	16,127
NO	NO-NL	16,633
	NO-DE	19,494
	NO-DK	3,889
	NO-FI	100
	NO-UK	7,000
	NO-SE	8,500
PL	PL-SK	4,621
	PL-SE	1,000
	PL-LT	13,554
	PL-DE	20,753
	PL-CZ	8,572
PT	PT-ES	16,210
RO	RO-RS	3,712
	RO-BG	4,702
	RO-HU	4,494
RS	RS-BG	1,460
	RS-MK	3,654
	RS-AL	1,605
	RS-HU	1,109
	RS-RO	3,712
	RS-HR	1,405
	RS-BA	5,908
	RS-ME	4,658
SE	SE-DE	16,200
	SE-DK	7,221
	SE-PL	1,000
	SE-NO	8,500
	SE-FI	7,000
	SE-LT	1,000
SI	SI-HU	1,386
	SI-HR	5,713
	SI-AT	2,945
	SI-IT	6,710
SK	SK-HU	11,422
	SK-CZ	3,706
	SK-PL	4,621
UK	UK-FR	16,000
	UK-BE	12,000
	UK-NL	5,000
	UK-IE	3,000
	UK-NO	7,000

Annex XII Wind power generation profile ENTSO-E

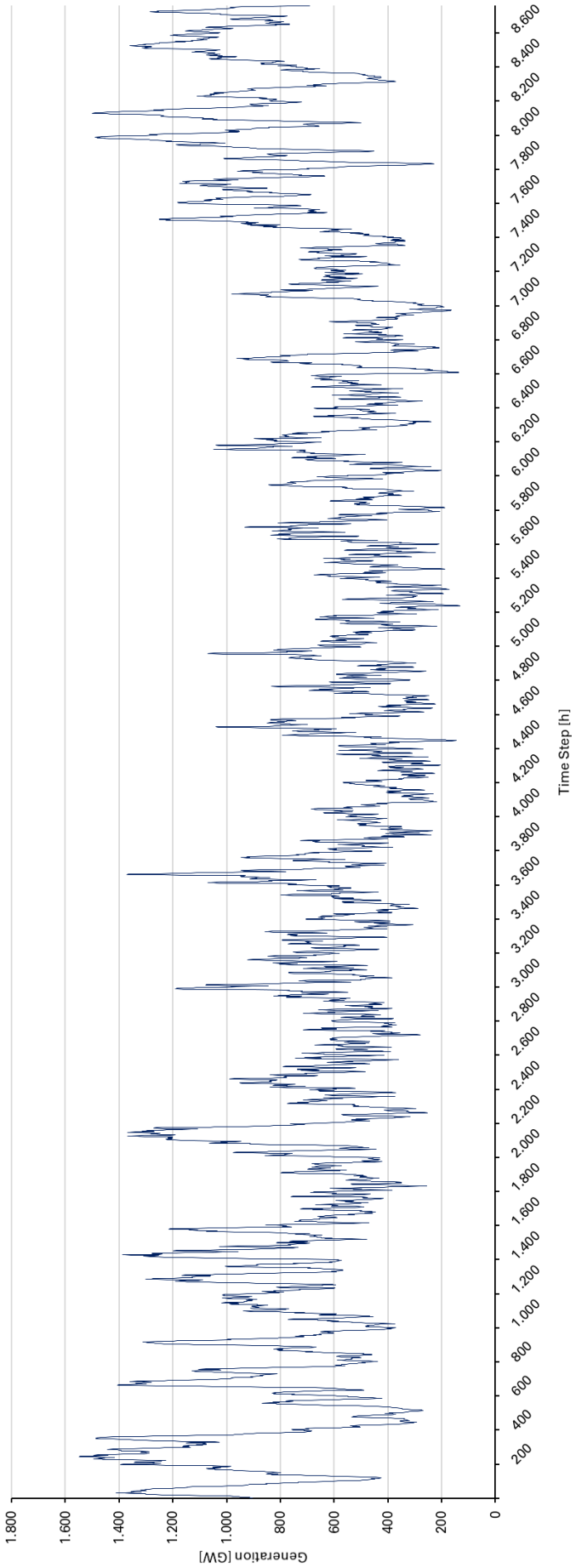

Annex XIII PV generation profile ENTSO-E

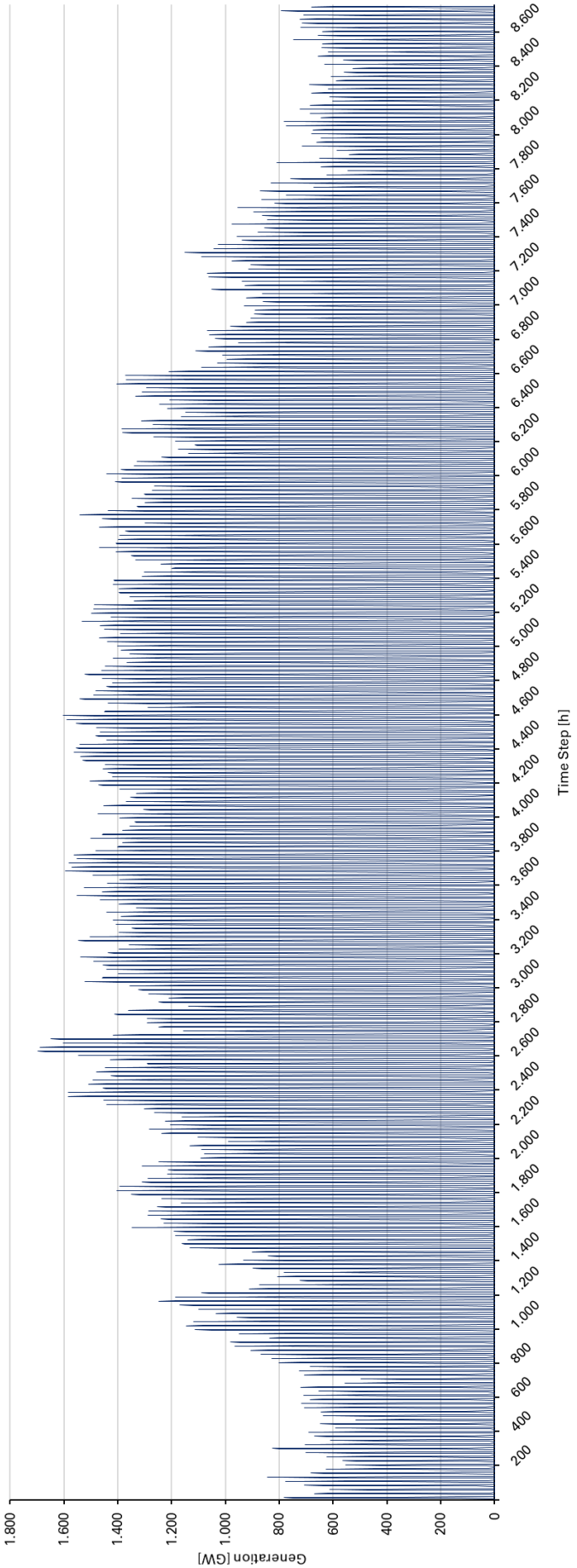

Annex XIV Solar thermal production profile ENTSO-E

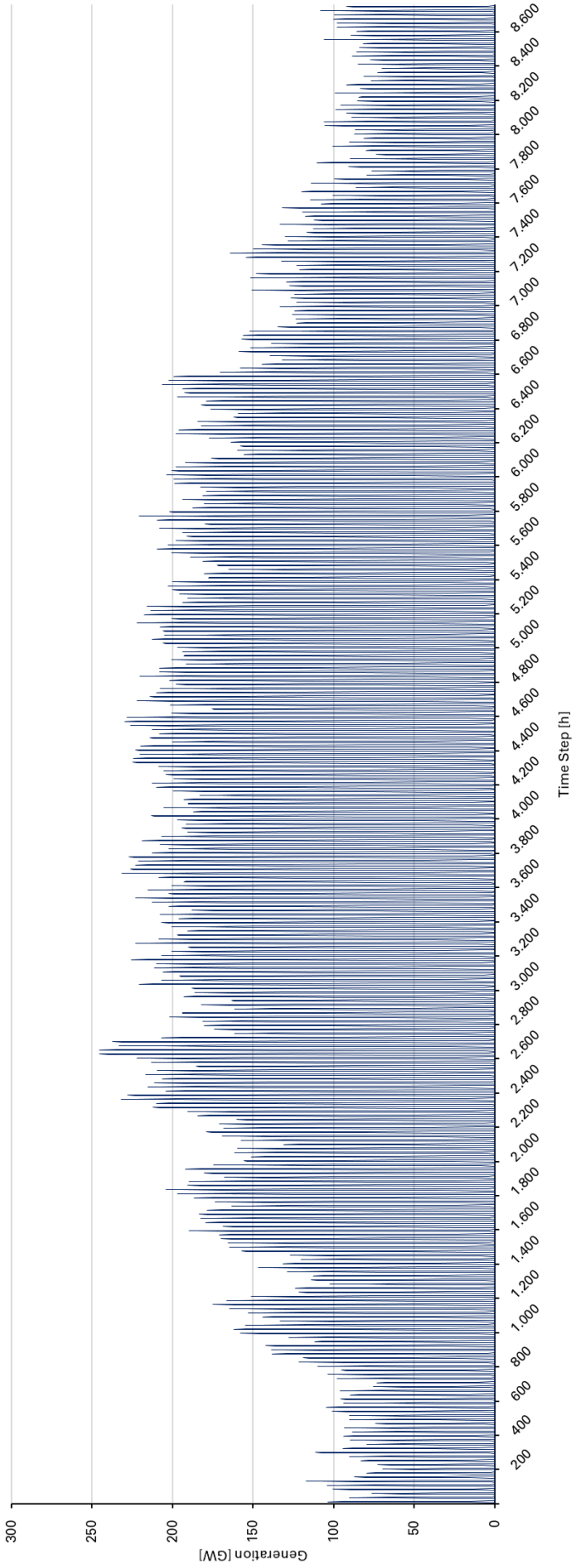

Annex XV Hydropower, bioenergy, geothermal production profiles ENTSO-E

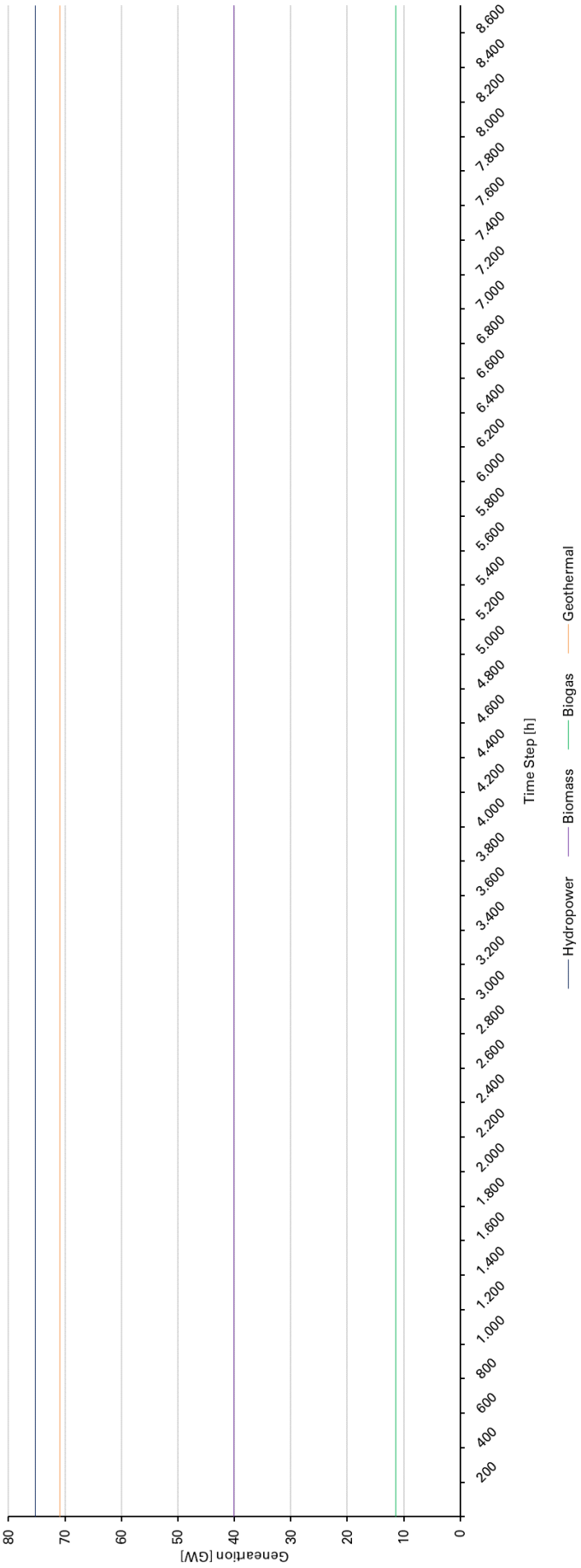

Annex XVI Bioenergy and geothermal heat production profiles ENTSO-E

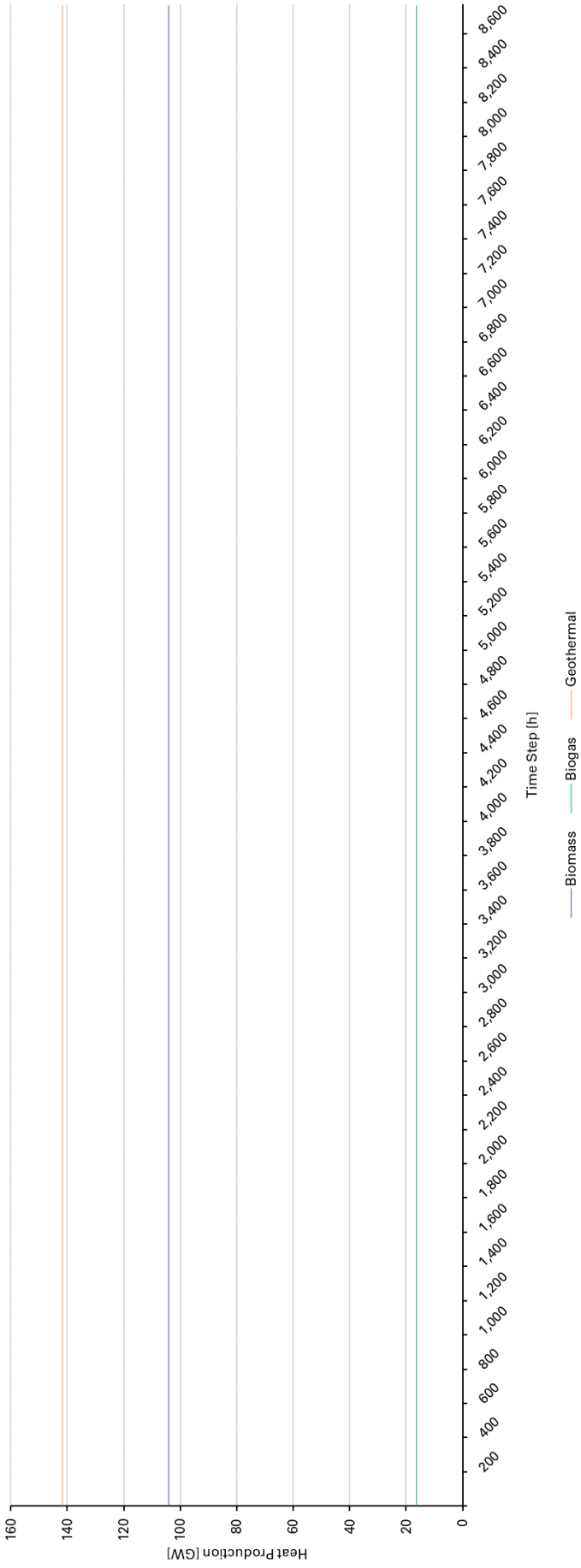

Annex XVII Heat load profiles methodology

In reference to Hellwig (2003), the development of heat load profiles to derive the typical consumer behavior is a common approach in energy economics. In principle, different methods such as regression analysis, neural networks and cluster analysis are suitable. Basically, all of the methods comprise the following two techniques. [Hell2003]

- Replication of nominally scaled factors, such as demand type or weekday.
- Replication of interval scaled factors, such as temperature.

Regarding this analysis, a novel approach is developed. To deduct the seasonal and daily demand for each country, the nominally scaled factor "user behavior of the weekday" and the interval scaled factors "outdoor temperature" and "time of the day" are combined in order to calculate individual heat demand profiles for each country and time step. Therefore, the heat and cooling load profiles are developed in regards to local average outdoor temperature ϑ in an hourly resolution and for the year 2015. The integrated energy model distinguishes among demand for industrial process heat and cold and demand for space heating and cooling input.

To address for individual variations in the local demand for space heating, a representative heat load matrix is developed. The matrix accounts for the hourly average outdoor temperature and the typical user behavior at each time of the day. Thus, the model is able to account for various seasons in relation to temperature and behavior. To calculate the interval scaled space heating demand, the individual heat load value of each time step is derived from the particular outdoor temperature. According to Hellwig (2003), it is anticipated that with temperatures above ϑ=*20°C* all heating serves the purpose of hot water production. Thus, the heating profile for each temperature above ϑ_{+20}=*20°C* equals the one for ϑ=*20°C*. Analogous, the heat profile for temperatures below ϑ_{-15}=*-15°C* equals the profile for ϑ=*-15°C* due to the assumption that the average rated power of common heating devices is calibrated to this extreme temperature. The heat load values of the heat load matrix in **Annex XVIII** are calculated according to the modified transcendental growth function **Eq. (XII.1)**. [Hell2003]

$$h_t = \frac{A}{1 + \left(\frac{B}{\vartheta - \vartheta_0}\right)^C} + D \qquad [\vartheta_0 = 31°C] \qquad \text{(XII.1)}$$

$A = 2.794$ $B = -37.2$ $C = 5.40$ $D = 0.171391$

The parameters to calculate the heat load h_t are chosen according to the values for modernized single family houses, as they represent the average curve spread within the various building types. The parameters have been determined empirically. The resulting coefficients *A* and *D* describe the limits of the function, whereas the negative coefficient *B* stretches the function to the left. The increase of coefficient *C* flattens the curve progression and positions the turning point outside the symmetry. ϑ represents the particular temperature of each time step in °C. The point of discontinuity ϑ_0 is set to

$\vartheta_0=31°C$ in order to avoid discontinuities within the expected temperature range [Hell2003]. In order to achieve the representative heat load Q_T for each reference temperature, the maximum value of h_t is scaled according to $h_T=Q_{-15}=1$ and all other values are derived from the maximum value $Q_{-15}=1$. This approach leads to the S-shaped sigmoid function with two distinctive kink points at $\vartheta=-15°C$ and $\vartheta=20°C$, as indicated in **Fig. 61**.

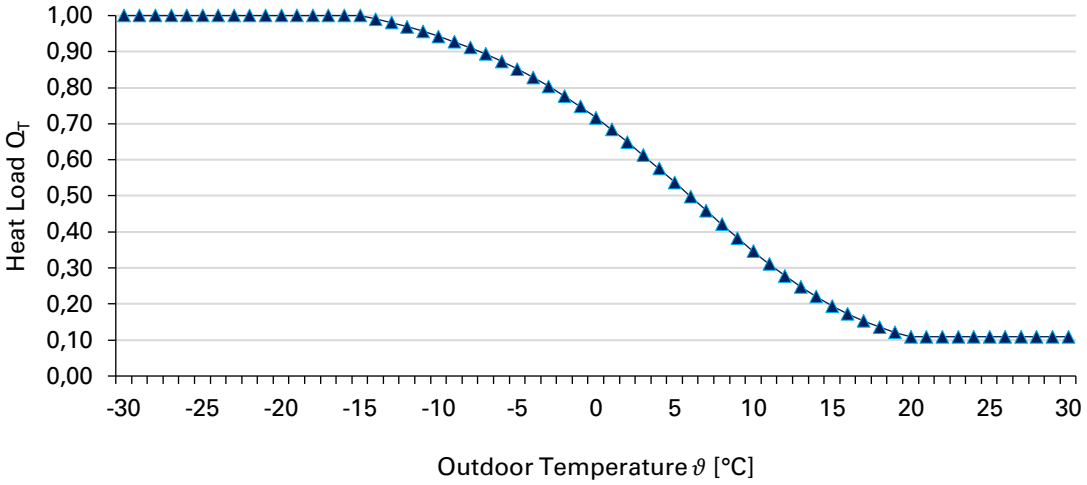

Fig. 60 Heat load Sigmoid diagram per outdoor temperature

The sigmoid function accounts for the particular heat load regarding specific outdoor temperatures, but does not incorporate the typical user behavior patterns. To account for the user behavior patterns, typical user behavior profiles are derived from the VDI-Directive 2067, which describes typical day specific profiles for the space heating and hot water demand in summers, winters, and the transition period [IWU1996]. The selected reference heat load Q_T profile of a clear winter day is depicted as heat load per time of day $Q_{T(t)}$ in **Fig. 62**.

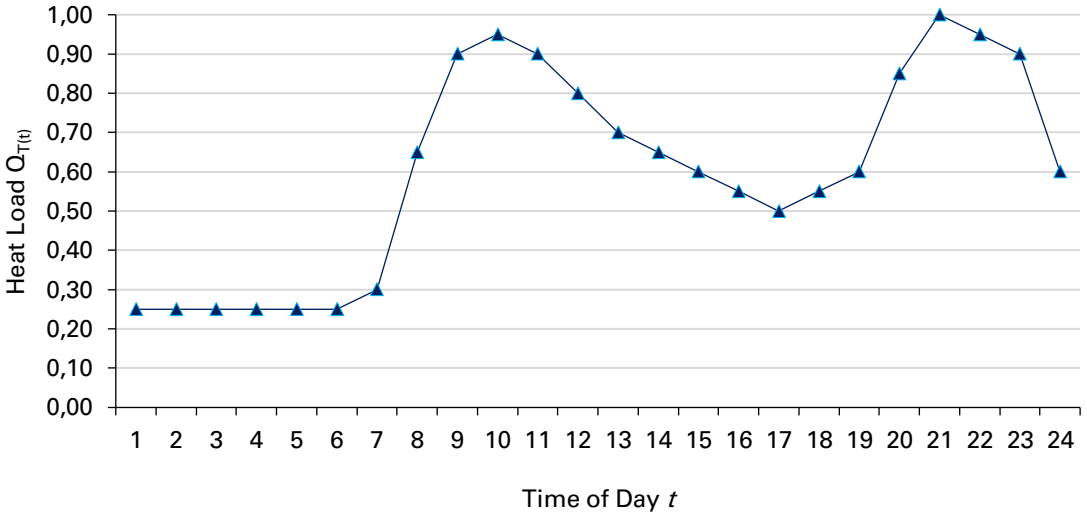

Fig. 61 Typical winter day heat load profile
Source: In reference to [IWU1996]

The heat load profile in **Fig. 62** shows an increasing heat load from 07:00 am to the first peak at 10:00 am. The maximum peak is reached at 21:00 pm, whereby the heat load is decreasing until midnight and continuous with approximately 25 % of the maximum load during the night-time heating reduction until 6:00 am of the next day. The load profile is scaled from $Q_{T(t)}=0.25$ (minimum heat load) to $Q_{T(t)}=1$ (maximum heat load). Thereby, it is anticipated that the maximum heat load of $Q_{T(t)}=1$ is reached at $\vartheta=-15°C$.

To calculate the total space heating and hot water demand for each time step, the interval and nominal scaled heat load values of each time step, temperature and user behavior load values, are multiplied with each other and result into the final heat load matrix, as depicted in **Annex XVIII**. Thereby, the column of $\vartheta=-15°C$ equals the profile of **Fig. 62** as it is scaled to the maximum heating load at the minimum calibration temperature. Thus, the correlation of the outdoor temperature and the behavior is realized through a scaling approach and reaches the positive kink point at $\vartheta=20°C$. Consequently, each value of the matrix is a product of the typical heat load of the time of day and the heat load according to the outdoor temperature.

As a simplification, the demand for industrial process heat is considered as independent from the outdoor temperature and accounts only for two types of industries. According to Stryi et al. (2015), industries, such as the chemical industry, operate their processes continuously and general manufacturers are subject to the working hours from 8:00 am to 18:00 pm. The latter is considered to be closed on holidays and Sundays [Stry2015]. For Europe, the following holidays are regarded on a national level, whereas Easter Saturday is an irregular holiday:

- Christmas (24th, 25th and 26th December)
- New Year (31st December and 1st January)
- Easter (Good Friday, Easter Saturday, Easter Sunday, Easter Monday
- Labor Day (1st May)
- Pentecost (Mondays)

Other holidays are not taken into account as they are deviating from country to country and region to region. Scaling up the results of the empirical investigation leads to the standardized profiles for working days and holidays, as indicated in **Fig. 63**.

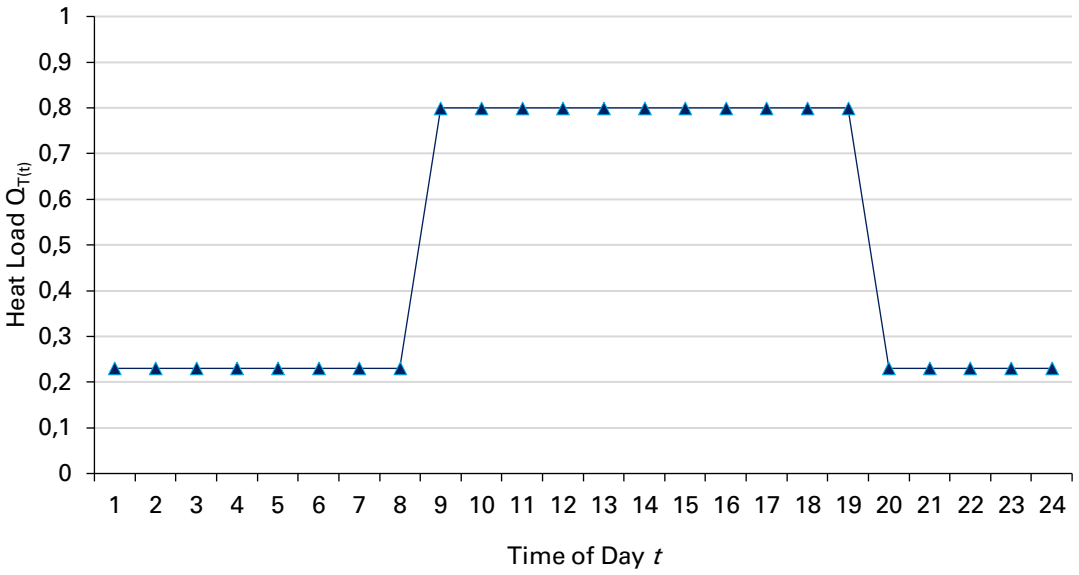

Fig. 62 Typical industry heat load profile
Source: In reference to [IWU1996]

The yearly total demand for process heat and space heating of each country is derived from the Heat Roadmap Europe 2050 and accounts for the year 2015 [Flei2017a]. In order to determine the absolute space heating demand for each time step, the yearly space heating demand of a country is multiplied with the corresponding load value of the space heating demand matrix and divided by the sum of all ratio values applying to the 8,760 time steps of a year. Correspondingly, the total process heat demand of a country is divided by 8,760 time steps and multiplied with the suitable load factor of the process heat profile of **Fig. 63** to account for the yearly heat demand in the balance. The space and process heat demands are summed up to the total demand of each time step.

The Heat Roadmap Europe 2050 does not provide heat demand data for those ENTSO-E countries that are non-EU. According to Fleiter et al. (2017b), Patronen et al. (2017), and Persson and Werner (2015), the heat demand data for those countries, especially the distinction in process heat and space heating, is not available in any other sources [Flei2017b] [Pat2017] [Pers2015]. Consequently, a scaled per capita approach is applied and the demand for process and space heating as well as cooling is derived from an appropriate adjacent country with similar properties regarding the geographic position and GDP. The countries under consideration are composed of the following.

- Albania
- Bosnia
- Iceland
- Macedonia
- Montenegro
- Norway
- Serbia
- Switzerland

In reference to the methodology of the heat matrix, the demand for space and process cooling is derived. The space cooling matrix is based on a linear increase in relation to the outdoor temperature. According to the German Technical Rules for Workplaces 2018, space cooling is required at outdoor temperatures greater than $\vartheta=26°C$ [ASTA2018]. Therefore, it is anticipated that space cooling begins with a rated power of $P_{\vartheta 25}=0.5$ at $\vartheta=25°C$ and linearly increases to the rated power of $P_{\vartheta 40}=1.0$ at $\vartheta=40°C$. Analogous to the heating user behavior, the cooling demand is correlated to the time of day, as depicted in **Fig. 62**. Again, the total space cooling demand is scaled to the total demand of each country. The process cooling demand is calculated analogous to the approach for process heating.

To anticipate the energy demand for heating and cooling in 2050, the scenario technique is applied. Therefore, the development of the demands is anticipated based on the demands for each country in 2015. According to Prognos et al. (2014), the space heating demand can be reduced by approximately 50 % due to increasing efficiency measures and improved insulations of the buildings. The demand for process heating and cooling can be reduced by 10 % due to efficiency gains in the industrial processes.

However, the demand will not reduce further as the European countries will stay industrialized and the production of innovative products is energy intensive. The demand for hot water remains equal. Unlike the demand for space heating, the demand for space cooling will increase by nearly 100 % as more air conditioning will be required in well insulated buildings [Prognos2014]. Due to global warming and increasing comfort effects, this study anticipates an increase of 200 % of the space cooling demand.

The average outdoor temperature per time step and country of 2015 is derived from the MERRA-2 database [ETH2019]. The final heating and cooling demand profiles are used as the heating and cooling demand input for the energy system simulation for each ENTSO-E country and for the year 2050. The resulting total heat demand profile for the ENTSO-E is depicted in **Annex XX**. The resulting total cooling demand profile is depicted in **Annex XXI**.

Annex XVIII Heat load per outdoor temperature matrix

Time	Temp. [°C]	-15	-14	-13	-12	-11	-10	-9	-8	-7	-6	-5	-4	-3	-2	-1	0	1	2	3	4	5	6	7	8	9	10	11	12	13	14	15	16	17	18	19	20
	Heat Load	**1,00**	**0,99**	**0,98**	**0,97**	**0,96**	**0,94**	**0,93**	**0,91**	**0,89**	**0,87**	**0,85**	**0,83**	**0,80**	**0,78**	**0,75**	**0,72**	**0,68**	**0,65**	**0,61**	**0,58**	**0,54**	**0,50**	**0,46**	**0,42**	**0,38**	**0,35**	**0,31**	**0,28**	**0,25**	**0,22**	**0,19**	**0,17**	**0,15**	**0,14**	**0,12**	**0,11**
00:00	**0,25**	0,25	0,25	0,25	0,24	0,24	0,24	0,23	0,23	0,22	0,22	0,21	0,21	0,20	0,19	0,19	0,18	0,17	0,16	0,15	0,14	0,13	0,12	0,11	0,11	0,10	0,09	0,08	0,07	0,06	0,06	0,05	0,04	0,04	0,03	0,03	0,03
01:00	**0,25**	0,25	0,25	0,25	0,24	0,24	0,24	0,23	0,23	0,22	0,22	0,21	0,21	0,20	0,19	0,19	0,18	0,17	0,16	0,15	0,14	0,13	0,12	0,11	0,11	0,10	0,09	0,08	0,07	0,06	0,06	0,05	0,04	0,04	0,03	0,03	0,03
02:00	**0,25**	0,25	0,25	0,25	0,24	0,24	0,24	0,23	0,23	0,22	0,22	0,21	0,21	0,20	0,19	0,19	0,18	0,17	0,16	0,15	0,14	0,13	0,12	0,11	0,11	0,10	0,09	0,08	0,07	0,06	0,06	0,05	0,04	0,04	0,03	0,03	0,03
03:00	**0,25**	0,25	0,25	0,25	0,24	0,24	0,24	0,23	0,23	0,22	0,22	0,21	0,21	0,20	0,19	0,19	0,18	0,17	0,16	0,15	0,14	0,13	0,12	0,11	0,11	0,10	0,09	0,08	0,07	0,06	0,06	0,05	0,04	0,04	0,03	0,03	0,03
04:00	**0,25**	0,25	0,25	0,25	0,24	0,24	0,24	0,23	0,23	0,22	0,22	0,21	0,21	0,20	0,19	0,19	0,18	0,17	0,16	0,15	0,14	0,13	0,12	0,11	0,11	0,10	0,09	0,08	0,07	0,06	0,06	0,05	0,04	0,04	0,03	0,03	0,03
05:00	**0,25**	0,25	0,25	0,25	0,24	0,24	0,24	0,23	0,23	0,22	0,22	0,21	0,21	0,20	0,19	0,19	0,18	0,17	0,16	0,15	0,14	0,13	0,12	0,11	0,11	0,10	0,09	0,08	0,07	0,06	0,06	0,05	0,04	0,04	0,03	0,03	0,03
06:00	**0,30**	0,30	0,30	0,29	0,29	0,29	0,28	0,28	0,27	0,27	0,26	0,26	0,25	0,24	0,23	0,22	0,22	0,21	0,19	0,18	0,17	0,16	0,15	0,14	0,13	0,11	0,10	0,09	0,08	0,07	0,07	0,06	0,05	0,05	0,04	0,04	0,03
07:00	**0,65**	0,65	0,64	0,64	0,63	0,62	0,61	0,60	0,59	0,58	0,57	0,55	0,54	0,52	0,50	0,49	0,47	0,44	0,42	0,40	0,37	0,35	0,32	0,30	0,27	0,25	0,23	0,20	0,18	0,16	0,14	0,13	0,11	0,10	0,09	0,08	0,07
08:00	**0,90**	0,90	0,89	0,88	0,87	0,86	0,85	0,84	0,82	0,80	0,79	0,77	0,75	0,72	0,70	0,67	0,65	0,62	0,58	0,55	0,52	0,48	0,45	0,41	0,38	0,34	0,31	0,28	0,25	0,22	0,20	0,18	0,16	0,14	0,12	0,11	0,10
09:00	**0,95**	0,95	0,94	0,93	0,92	0,91	0,90	0,88	0,87	0,85	0,83	0,81	0,79	0,76	0,74	0,71	0,68	0,65	0,62	0,58	0,55	0,51	0,47	0,44	0,40	0,36	0,33	0,30	0,26	0,24	0,21	0,19	0,16	0,15	0,13	0,12	0,10
10:00	**0,90**	0,90	0,89	0,88	0,87	0,86	0,85	0,84	0,82	0,80	0,79	0,77	0,75	0,72	0,70	0,67	0,65	0,62	0,58	0,55	0,52	0,48	0,45	0,41	0,38	0,34	0,31	0,28	0,25	0,22	0,20	0,18	0,16	0,14	0,12	0,11	0,10
11:00	**0,80**	0,80	0,79	0,78	0,78	0,77	0,75	0,74	0,73	0,71	0,70	0,68	0,66	0,64	0,62	0,60	0,57	0,55	0,52	0,49	0,46	0,43	0,40	0,37	0,34	0,31	0,28	0,25	0,22	0,20	0,18	0,16	0,14	0,12	0,11	0,10	0,09
12:00	**0,70**	0,70	0,69	0,69	0,68	0,67	0,66	0,65	0,64	0,63	0,61	0,60	0,58	0,56	0,54	0,52	0,50	0,48	0,45	0,43	0,40	0,38	0,35	0,32	0,29	0,27	0,24	0,22	0,19	0,17	0,15	0,14	0,12	0,11	0,10	0,08	0,08
13:00	**0,65**	0,65	0,64	0,64	0,63	0,62	0,61	0,60	0,59	0,58	0,57	0,55	0,54	0,52	0,50	0,49	0,47	0,44	0,42	0,40	0,37	0,35	0,32	0,30	0,27	0,25	0,23	0,20	0,18	0,16	0,14	0,13	0,11	0,10	0,09	0,08	0,07
14:00	**0,60**	0,60	0,59	0,59	0,58	0,57	0,57	0,56	0,55	0,54	0,52	0,51	0,50	0,48	0,47	0,45	0,43	0,41	0,39	0,37	0,35	0,32	0,30	0,28	0,25	0,23	0,21	0,19	0,17	0,15	0,13	0,12	0,10	0,09	0,08	0,07	0,07
15:00	**0,55**	0,55	0,54	0,54	0,53	0,53	0,52	0,51	0,50	0,49	0,48	0,47	0,46	0,44	0,43	0,41	0,39	0,38	0,36	0,34	0,32	0,30	0,27	0,25	0,23	0,21	0,19	0,17	0,15	0,14	0,12	0,11	0,09	0,08	0,07	0,07	0,06
16:00	**0,50**	0,50	0,50	0,49	0,48	0,48	0,47	0,46	0,46	0,45	0,44	0,43	0,41	0,40	0,39	0,37	0,36	0,34	0,32	0,31	0,29	0,27	0,25	0,23	0,21	0,19	0,17	0,16	0,14	0,12	0,11	0,10	0,09	0,08	0,07	0,06	0,05
17:00	**0,55**	0,55	0,54	0,54	0,53	0,53	0,52	0,51	0,50	0,49	0,48	0,47	0,46	0,44	0,43	0,41	0,39	0,38	0,36	0,34	0,32	0,30	0,27	0,25	0,23	0,21	0,19	0,17	0,15	0,14	0,12	0,11	0,09	0,08	0,07	0,07	0,06
18:00	**0,60**	0,60	0,59	0,59	0,58	0,57	0,57	0,56	0,55	0,54	0,52	0,51	0,50	0,48	0,47	0,45	0,43	0,41	0,39	0,37	0,35	0,32	0,30	0,28	0,25	0,23	0,21	0,19	0,17	0,15	0,13	0,12	0,10	0,09	0,08	0,07	0,07
19:00	**0,85**	0,85	0,84	0,83	0,82	0,81	0,80	0,79	0,77	0,76	0,74	0,72	0,70	0,68	0,66	0,64	0,61	0,58	0,55	0,52	0,49	0,46	0,42	0,39	0,36	0,33	0,29	0,26	0,24	0,21	0,19	0,17	0,15	0,13	0,12	0,10	0,09
20:00	**1,00**	1,00	0,99	0,98	0,97	0,96	0,94	0,93	0,91	0,89	0,87	0,85	0,83	0,80	0,78	0,75	0,72	0,68	0,65	0,61	0,58	0,54	0,50	0,46	0,42	0,38	0,35	0,31	0,28	0,25	0,22	0,19	0,17	0,15	0,14	0,12	0,11
21:00	**0,95**	0,95	0,94	0,93	0,92	0,91	0,90	0,88	0,87	0,85	0,83	0,81	0,79	0,76	0,74	0,71	0,68	0,65	0,62	0,58	0,55	0,51	0,47	0,44	0,40	0,36	0,33	0,30	0,26	0,24	0,21	0,19	0,16	0,15	0,13	0,12	0,10
22:00	**0,90**	0,90	0,89	0,88	0,87	0,86	0,85	0,84	0,82	0,80	0,79	0,77	0,75	0,72	0,70	0,67	0,65	0,62	0,58	0,55	0,52	0,48	0,45	0,41	0,38	0,34	0,31	0,28	0,25	0,22	0,20	0,18	0,16	0,14	0,12	0,11	0,10
23:00	**0,60**	0,60	0,59	0,59	0,58	0,57	0,57	0,56	0,55	0,54	0,52	0,51	0,50	0,48	0,47	0,45	0,43	0,41	0,39	0,37	0,35	0,32	0,30	0,28	0,25	0,23	0,21	0,19	0,17	0,15	0,13	0,12	0,10	0,09	0,08	0,07	0,07

Annex XIX Cooling load per outdoor temperature matrix

Time	Temp. [°C]	25	26	27	28	29	30	31	32	33	34	35	36	37	38	39	40
	Cool. Load	0,50	0,53	0,57	0,60	0,63	0,67	0,70	0,73	0,77	0,80	0,83	0,87	0,90	0,93	0,97	1,00
00:00	0,25	0,13	0,13	0,14	0,15	0,16	0,17	0,18	0,18	0,19	0,20	0,21	0,22	0,23	0,23	0,24	0,25
01:00	0,25	0,13	0,13	0,14	0,15	0,16	0,17	0,18	0,18	0,19	0,20	0,21	0,22	0,23	0,23	0,24	0,25
02:00	0,25	0,13	0,13	0,14	0,15	0,16	0,17	0,18	0,18	0,19	0,20	0,21	0,22	0,23	0,23	0,24	0,25
03:00	0,25	0,13	0,13	0,14	0,15	0,16	0,17	0,18	0,18	0,19	0,20	0,21	0,22	0,23	0,23	0,24	0,25
04:00	0,25	0,13	0,13	0,14	0,15	0,16	0,17	0,18	0,18	0,19	0,20	0,21	0,22	0,23	0,23	0,24	0,25
05:00	0,25	0,13	0,13	0,14	0,15	0,16	0,17	0,18	0,18	0,19	0,20	0,21	0,22	0,23	0,23	0,24	0,25
06:00	0,30	0,15	0,16	0,17	0,18	0,19	0,20	0,21	0,22	0,23	0,24	0,25	0,26	0,27	0,28	0,29	0,30
07:00	0,65	0,33	0,35	0,37	0,39	0,41	0,43	0,46	0,48	0,50	0,52	0,54	0,56	0,59	0,61	0,63	0,65
08:00	0,90	0,45	0,48	0,51	0,54	0,57	0,60	0,63	0,66	0,69	0,72	0,75	0,78	0,81	0,84	0,87	0,90
09:00	0,95	0,48	0,51	0,54	0,57	0,60	0,63	0,67	0,70	0,73	0,76	0,79	0,82	0,86	0,89	0,92	0,95
10:00	0,90	0,45	0,48	0,51	0,54	0,57	0,60	0,63	0,66	0,69	0,72	0,75	0,78	0,81	0,84	0,87	0,90
11:00	0,80	0,40	0,43	0,45	0,48	0,51	0,53	0,56	0,59	0,61	0,64	0,67	0,69	0,72	0,75	0,77	0,80
12:00	0,70	0,35	0,37	0,40	0,42	0,44	0,47	0,49	0,51	0,54	0,56	0,58	0,61	0,63	0,65	0,68	0,70
13:00	0,65	0,33	0,35	0,37	0,39	0,41	0,43	0,46	0,48	0,50	0,52	0,54	0,56	0,59	0,61	0,63	0,65
14:00	0,60	0,30	0,32	0,34	0,36	0,38	0,40	0,42	0,44	0,46	0,48	0,50	0,52	0,54	0,56	0,58	0,60
15:00	0,55	0,28	0,29	0,31	0,33	0,35	0,37	0,39	0,40	0,42	0,44	0,46	0,48	0,50	0,51	0,53	0,55
16:00	0,50	0,25	0,27	0,28	0,30	0,32	0,33	0,35	0,37	0,38	0,40	0,42	0,43	0,45	0,47	0,48	0,50
17:00	0,55	0,28	0,29	0,31	0,33	0,35	0,37	0,39	0,40	0,42	0,44	0,46	0,48	0,50	0,51	0,53	0,55
18:00	0,60	0,30	0,32	0,34	0,36	0,38	0,40	0,42	0,44	0,46	0,48	0,50	0,52	0,54	0,56	0,58	0,60
19:00	0,85	0,43	0,45	0,48	0,51	0,54	0,57	0,60	0,62	0,65	0,68	0,71	0,74	0,77	0,79	0,82	0,85
20:00	1,00	0,50	0,53	0,57	0,60	0,63	0,67	0,70	0,73	0,77	0,80	0,83	0,87	0,90	0,93	0,97	1,00
21:00	0,95	0,48	0,51	0,54	0,57	0,60	0,63	0,67	0,70	0,73	0,76	0,79	0,82	0,86	0,89	0,92	0,95
22:00	0,90	0,45	0,48	0,51	0,54	0,57	0,60	0,63	0,66	0,69	0,72	0,75	0,78	0,81	0,84	0,87	0,90
23:00	0,60	0,30	0,32	0,34	0,36	0,38	0,40	0,42	0,44	0,46	0,48	0,50	0,52	0,54	0,56	0,58	0,60

Annex XX Heat demand profile ENTSO-E

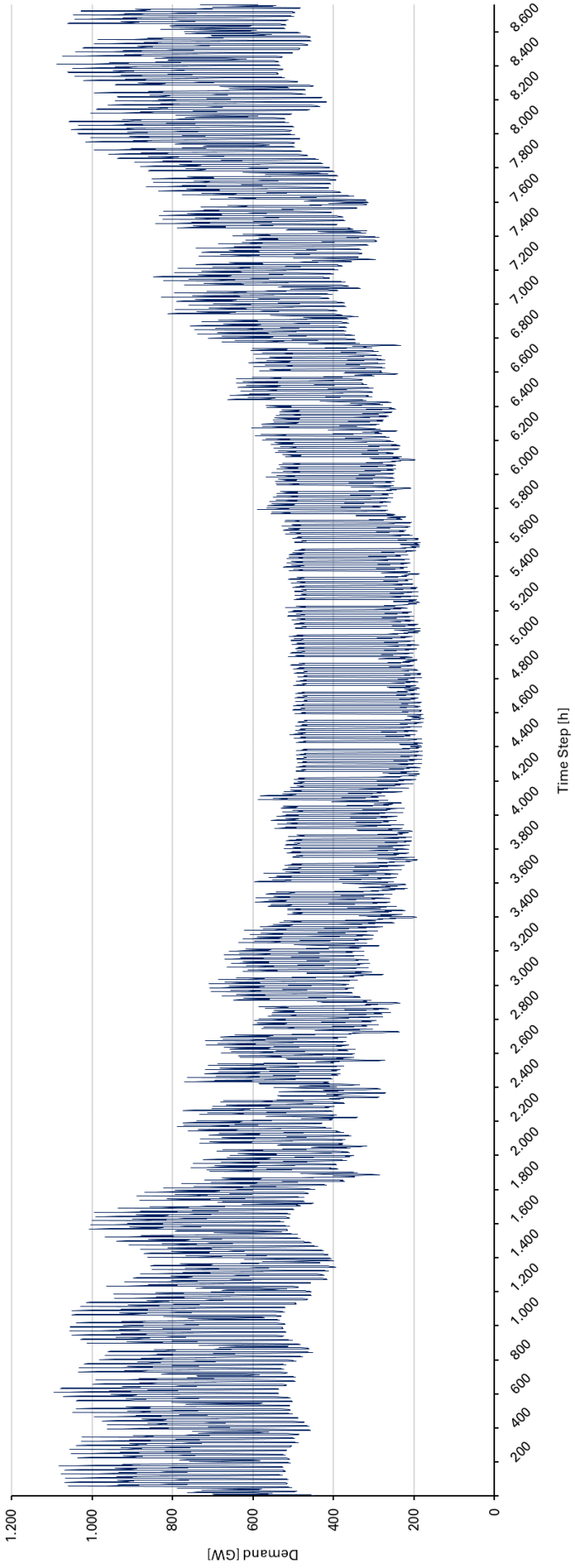

Annex XXI Cold demand profile

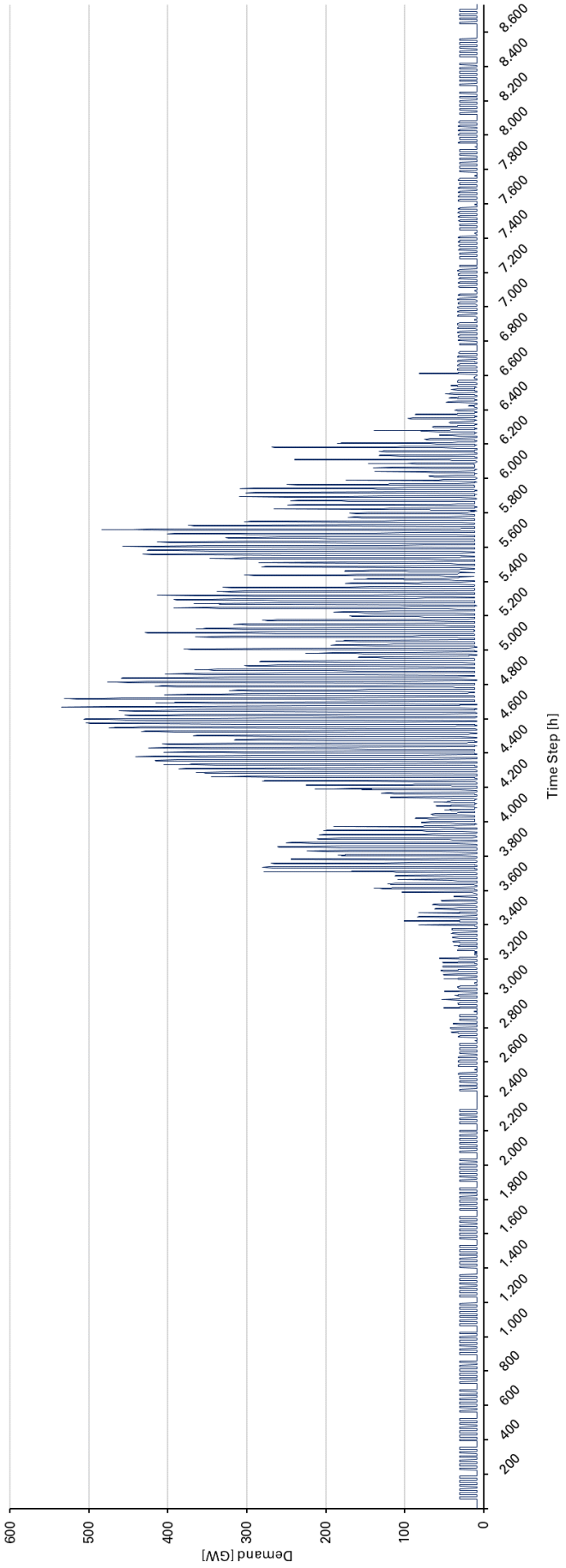

Annex XXII Electricity demand profile

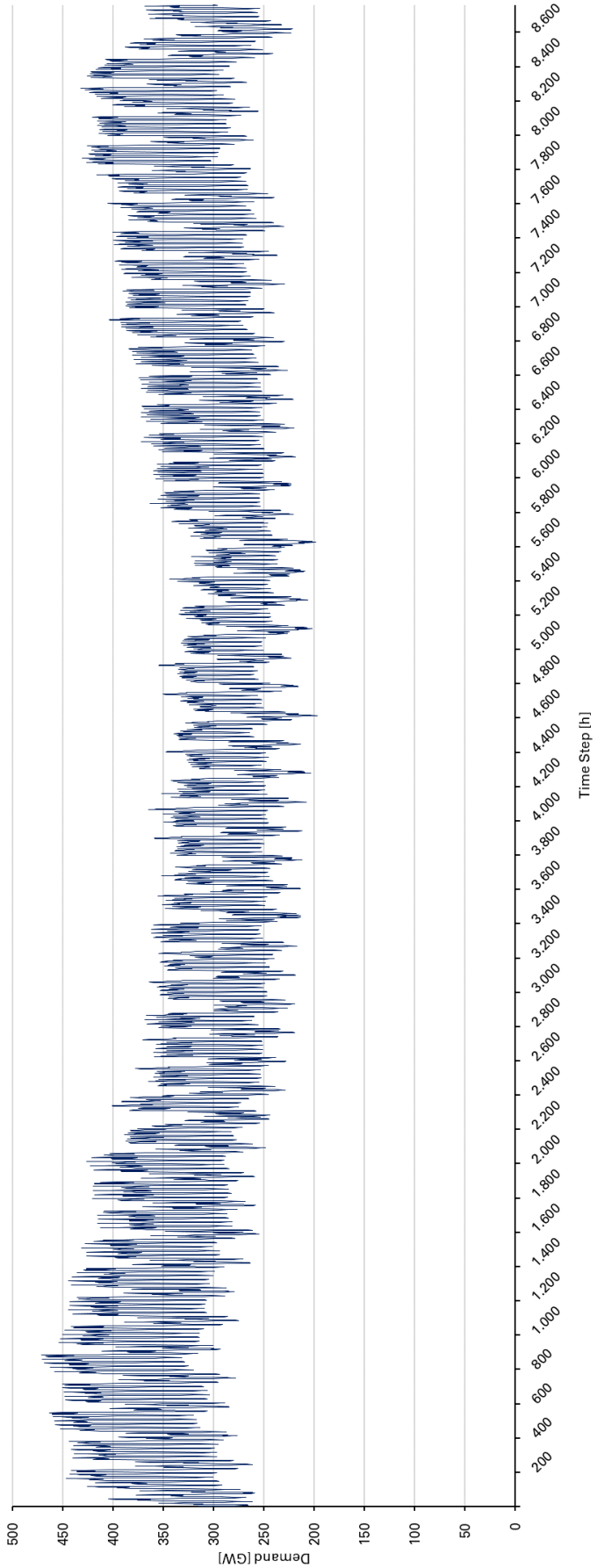

Annex XXIII BEV load profiles methodology

The charging time and location of battery electric vehicles (BEV) strongly depends on the housing and employment background of the BEV owner. As a basic assumption, owner of private parking spaces or garages are more likely to charge at home, whereas people who live in flats are more likely to charge in public spaces or at the employer's place. Generally, BEV charging in reference to passenger cars can be distinguished among charging in the subsequent spaces. [Nich2020]

- Public
- Semi-public
- Corporate
- Private

Public space refers to charge stations that are located at public roads and parking spaces. Semi-public space refers to charge stations in semi-public spaces, such as retailers and malls. Corporate spaces are those spaces which allow employees to charge at the workplace. Private spaces refer to private homes, usually located in one- and two-family houses or multi-storey buildings which are equipped with private parking spaces. As a simplification, here public spaces refer to semi-public and corporate spaces too.

Under consideration of various charging opportunities and the corresponding charging times, such as charging at home over night or at the workplace during the day, BEV charging profiles are created. Analogous to the development of heat demand profiles as depicted in **Annex XVII**, BEV charging profiles consider particular features, attributes, and assumptions. Therefore, the BEV charging profile development is based on the following inputs per country.

- Number of total passenger cars
- Number of inhabitants
- Type of housing
- Ratio of working and driving inhabitants
- Electrification rates of houses and passenger cars
- Average fuel and electricity consumption per passenger car

To facilitate the assessment of each ENTSO-E country, several inputs represent average ratios of the afore-mentioned attributes. Those inputs serve as basis for the calculation of the total electricity consumption for BEV of each country. The derived average ENTSO-E ratios are summarized in **Tab. 22**.

Tab. 22 Average ratios BEV load profile calculation
Source: [Ademe2019] [EUROS2018d] [EUROS2018e] [EUROS2019d] [ICCT2019]

Category	Number	Unit
Electrification Rate Passenger Cars	0.8	
Electrification Rate Detached Houses	0.9	
Electrification Rate Semi-Detached Houses	0.5	
Electrification Rate Flats	0.1	
Average Travelled Distance	12,000	km
Average Fuel Consumption per 100km	10	$dm^3\ 100km^{-1}$
Energy Content per 1l fuel (gas and diesel)	9.1	$kWh\ dm^{-3}$
Total Consumption per Fuel Car	10,920	$kWh\ dm^{-3}$
Average El. Consumption per 100km	20.5	$kWh\ dm^{-3}$
Total Consumption per BEV	2460	kWh
El. Consumption per Day	6.74	kWh
Fuel Equivalent	4.44	
No. EU Citizens	513,481,691	
Percentage Citizen 0–19yr	0.21	
No. EU Citizens 19–100yr	406,677,499	
No. Working People	245,799,000	
Ratio Working People	0.60	

In reference to the inputs of **Tab. 22**, the total electricity demand for BEV passenger cars of each ENTSO-E country is calculated, as depicted in **Annex XXIV**. Based on the distribution of housing background and working inhabitants, assumptions regarding the charging opportunities are taken. Therefore, charging can either be conducted at home or at public places. Charging at home usually is conducted during nighttime, whereas charging at public spaces is conducted during daytime. Thus, a typical, here simplified, distribution of charging load over the course of the day is derived. The average distribution of charging load in the ENTSO-E is depicted in **Fig. 64**.

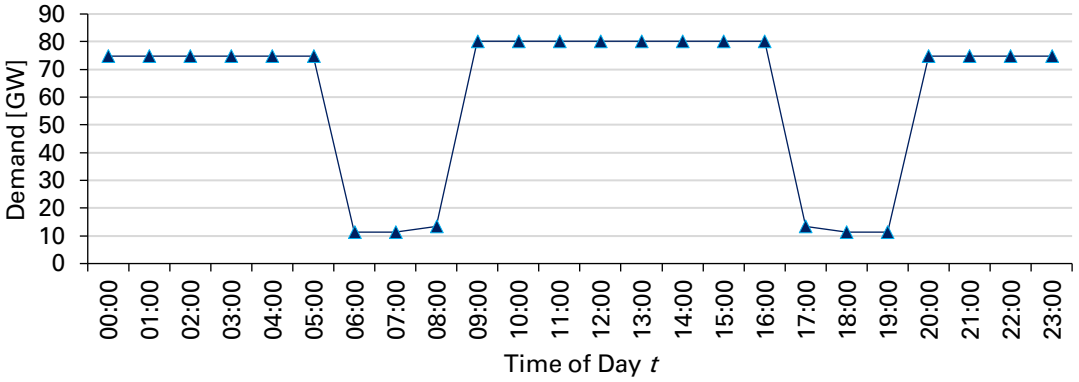

Fig. 63 Average BEV load profile

The resulting BEV load profiles in megawatt (MW) per ENTSO-E country and time of day *h* are derived, as depicted in **Annex XXV**. For the IES model computation of each country, those BEV load profiles are added to the electricity demand as of **Chapter 5.6.2** and subtracted from the transport demand as of **Chapter 5.6.3**.

Annex XXIV Calculation of total BEV electricity demand per country

Source: In reference to [ACEA2018] [EUROS2018d] [EUROS2018e] [EUROS2018f] [EUROS2019e] [REC2015a] [REC2015b]

Country	No. Passenger Cars	Ratio Detached Houses	Ratio Semi-Detached Houses	Ratio Flats	No. BEV	Total Elec. Consumption	Total Elec. Consumption per Day	Fuel Equivalent	Ratio Home Charging	Ratio Public Charging	Elec. Charged Home	Elec. Charged Public	Total Elec. per Day
						[MWh]	[MWh]	[MWh]			[MWh]	[MWh]	[MWh]
Albania	403,680	0.49	0.15	0.35	322,944	794,442	2,177	3,526,548	0.56	0.44	1,212	965	2,177
Austria	4,821,557	0.47	0.07	0.45	3,857,246	9,488,825	25,997	42,121,126	0.50	0.50	13,105	12,892	25,997
Belgium	5,669,764	0.38	0.40	0.22	4,535,811	11,158,095	30,570	49,531,056	0.56	0.44	17,180	13,390	30,570
Bosnia	828,730	0.49	0.15	0.35	662,984	1,630,941	4,468	7,239,785	0.56	0.44	2,487	1,981	4,468
Bulgaria	3,144,000	0.43	0.12	0.45	2,515,200	6,187,392	16,952	27,465,984	0.49	0.51	8,284	8,667	16,952
Croatia	1,540,260	0.71	0.08	0.21	1,232,208	3,031,232	8,305	13,455,711	0.70	0.30	5,813	2,491	8,305
Cyprus	508,000	0.48	0.25	0.26	406,400	999,744	2,739	4,437,888	0.58	0.42	1,589	1,150	2,739
Czechia	5,368,660	0.37	0.10	0.52	4,294,928	10,565,523	28,947	46,900,614	0.44	0.56	12,696	16,251	28,947
Denmark	2,477,478	0.55	0.13	0.31	1,981,982	4,875,676	13,358	21,643,243	0.59	0.41	7,903	5,455	13,358
Estonia	703,151	0.32	0.05	0.62	562,521	1,383,802	3,791	6,142,729	0.38	0.62	1,438	2,354	3,791
Finland	2,629,432	0.46	0.19	0.34	2,103,546	5,174,723	14,177	22,970,722	0.55	0.45	7,741	6,437	14,177
France	31,999,953	0.45	0.24	0.32	25,599,962	62,975,907	172,537	279,551,585	0.55	0.45	95,137	77,400	172,537
Germany	45,803,560	0.26	0.16	0.57	36,642,848	90,141,406	246,963	400,139,900	0.37	0.63	91,253	155,710	246,963
Greece	5,126,024	0.34	0.09	0.57	4,100,819	10,088,015	27,638	44,780,943	0.41	0.59	11,218	16,420	27,638
Hungary	3,308,495	0.63	0.05	0.31	2,646,796	6,511,118	17,839	28,903,012	0.62	0.38	11,124	6,714	17,839
Iceland	240,000	0.33	0.18	0.49	192,000	472,320	1,294	2,096,640	0.43	0.57	562	732	1,294
Ireland	2,026,977	0.40	0.53	0.07	1,621,582	3,989,092	10,929	17,707,675	0.63	0.37	6,874	4,055	10,929
Italy	37,876,138	0.23	0.25	0.53	30,300,910	74,540,239	204,220	330,885,937	0.38	0.62	77,399	126,821	204,220
Latvia	663,091	0.31	0.03	0.66	530,473	1,304,964	3,575	5,792,765	0.36	0.64	1,284	2,291	3,575
Lithuania	1,190,146	0.36	0.06	0.58	952,117	2,342,208	6,417	10,397,118	0.41	0.59	2,624	3,793	6,417
Luxembourg	380,860	0.38	0.28	0.30	304,688	749,532	2,054	3,327,193	0.51	0.49	1,054	999	2,054
Macedonia	383,833	0.49	0.15	0.35	307,066	755,382	2,070	3,353,161	0.56	0.44	1,152	918	2,070
Malta	283,000	0.05	0.39	0.55	226,400	556,944	1,526	2,472,288	0.30	0.70	456	1,069	1,526
Montenegro	174,073	0.49	0.15	0.35	139,258	342,575	939	1,520,697	0.56	0.44	522	416	939
Netherlands	8,439,318	0.18	0.58	0.19	6,751,454	16,608,577	45,503	73,725,878	0.47	0.53	21,432	24,071	45,503
Norway	2,662,910	0.50	0.09	0.41	2,130,328	5,240,607	14,358	23,263,182	0.54	0.46	7,686	6,672	14,358
Poland	21,675,388	0.52	0.05	0.43	17,340,310	42,657,163	116,869	189,356,185	0.54	0.46	62,712	54,157	116,869
Portugal	4,600,000	0.37	0.18	0.45	3,680,000	9,052,800	24,802	40,185,600	0.47	0.53	11,575	13,227	24,802
Romania	5,470,578	0.62	0.02	0.36	4,376,462	10,766,097	29,496	47,790,965	0.60	0.40	17,783	11,713	29,496
Serbia	1,797,427	0.66	0.02	0.32	1,437,942	3,537,337	9,691	15,702,327	0.63	0.37	6,143	3,548	9,691
Slovakia	2,124,972	0.46	0.02	0.52	1,699,978	4,181,946	11,457	18,563,760	0.48	0.52	5,466	5,991	11,457
Slovenia	1,143,218	0.66	0.05	0.29	914,574	2,249,852	6,164	9,987,148	0.64	0.36	3,971	2,193	6,164
Spain	22,876,247	0.12	0.22	0.66	18,300,998	45,020,455	123,344	199,846,898	0.28	0.72	34,734	88,610	123,344
Sweden	4,768,060	0.46	0.09	0.45	3,814,448	9,383,542	25,708	41,653,772	0.50	0.50	12,867	12,841	25,708
Switzerland	4,524,000	0.22	0.24	0.54	3,619,200	8,903,232	24,392	39,521,664	0.37	0.63	9,111	15,282	24,392
UK	34,378,386	0.25	0.60	0.14	27,502,709	67,656,664	185,361	300,329,582	0.54	0.46	99,557	85,803	185,361

Annex XXV BEV load profiles per country

Country	Albania	Austria	Belgium	Bosnia	Bulgaria	Croatia	Cyprus	Czechia	Denmark	Estonia	Finland	France	Germany	Greece	Hungary	Iceland	Ireland	Italy
Time of Day	[MW]	[MW]	[MW]	[MW]	[MW]	[MW]	[MW]	[MW]	[MW]	[MW]	[MW]	[MW]	[MW]	[MW]	[MW]	[MW]	[MW]	[MW]
00:00	91	1,216	1,262	187	817	235	108	1,532	514	222	607	7,298	14,681	1,548	633	69	382	11,957
01:00	91	1,216	1,262	187	817	235	108	1,532	514	222	607	7,298	14,681	1,548	633	69	382	11,957
02:00	91	1,216	1,262	187	817	235	108	1,532	514	222	607	7,298	14,681	1,548	633	69	382	11,957
03:00	91	1,216	1,262	187	817	235	108	1,532	514	222	607	7,298	14,681	1,548	633	69	382	11,957
04:00	91	1,216	1,262	187	817	235	108	1,532	514	222	607	7,298	14,681	1,548	633	69	382	11,957
05:00	91	1,216	1,262	187	817	235	108	1,532	514	222	607	7,298	14,681	1,548	633	69	382	11,957
06:00	14	184	191	28	124	36	16	232	78	34	92	1,106	2,224	235	96	10	58	1,812
07:00	14	184	191	28	124	36	16	232	78	34	92	1,106	2,224	235	96	10	58	1,812
08:00	24	262	344	50	166	116	32	254	158	29	155	1,903	1,825	224	222	11	137	1,548
09:00	145	1,573	2,062	298	994	698	191	1,524	948	173	929	11,416	10,950	1,346	1,335	67	825	9,288
10:00	145	1,573	2,062	298	994	698	191	1,524	948	173	929	11,416	10,950	1,346	1,335	67	825	9,288
11:00	145	1,573	2,062	298	994	698	191	1,524	948	173	929	11,416	10,950	1,346	1,335	67	825	9,288
12:00	145	1,573	2,062	298	994	698	191	1,524	948	173	929	11,416	10,950	1,346	1,335	67	825	9,288
13:00	145	1,573	2,062	298	994	698	191	1,524	948	173	929	11,416	10,950	1,346	1,335	67	825	9,288
14:00	145	1,573	2,062	298	994	698	191	1,524	948	173	929	11,416	10,950	1,346	1,335	67	825	9,288
15:00	145	1,573	2,062	298	994	698	191	1,524	948	173	929	11,416	10,950	1,346	1,335	67	825	9,288
16:00	145	1,573	2,062	298	994	698	191	1,524	948	173	929	11,416	10,950	1,346	1,335	67	825	9,288
17:00	24	262	344	50	166	116	32	254	158	29	155	1,903	1,825	224	222	11	137	1,548
18:00	14	184	191	28	124	36	16	232	78	34	92	1,106	2,224	235	96	10	58	1,812
19:00	14	184	191	28	124	36	16	232	78	34	92	1,106	2,224	235	96	10	58	1,812
20:00	91	1,216	1,262	187	817	235	108	1,532	514	222	607	7,298	14,681	1,548	633	69	382	11,957
21:00	91	1,216	1,262	187	817	235	108	1,532	514	222	607	7,298	14,681	1,548	633	69	382	11,957
22:00	91	1,216	1,262	187	817	235	108	1,532	514	222	607	7,298	14,681	1,548	633	69	382	11,957
23:00	91	1,216	1,262	187	817	235	108	1,532	514	222	607	7,298	14,681	1,548	633	69	382	11,957

Country	Latvia	Lithuania	Luxembourg	Macedonia	Malta	Montenegro	Netherlands	Norway	Poland	Portugal	Romania	Serbia	Slovakia	Slovenia	Spain	Sweden	Switzerland	UK
Time of Day	[MW]	[MW]	[MW]	[MW]	[MW]	[MW]	[MW]	[MW]	[MW]	[MW]	[MW]	[MW]	[MW]	[MW]	[MW]	[MW]	[MW]	[MW]
00:00	216	358	94	87	101	39	2,270	629	5,106	1,247	1,104	335	565	207	8,355	1,211	1,441	8,090
01:00	216	358	94	87	101	39	2,270	629	5,106	1,247	1,104	335	565	207	8,355	1,211	1,441	8,090
02:00	216	358	94	87	101	39	2,270	629	5,106	1,247	1,104	335	565	207	8,355	1,211	1,441	8,090
03:00	216	358	94	87	101	39	2,270	629	5,106	1,247	1,104	335	565	207	8,355	1,211	1,441	8,090
04:00	216	358	94	87	101	39	2,270	629	5,106	1,247	1,104	335	565	207	8,355	1,211	1,441	8,090
05:00	216	358	94	87	101	39	2,270	629	5,106	1,247	1,104	335	565	207	8,355	1,211	1,441	8,090
06:00	33	54	14	13	15	6	344	95	774	189	167	51	86	31	1,266	183	218	1,226
07:00	33	54	14	13	15	6	344	95	774	189	167	51	86	31	1,266	183	218	1,226
08:00	26	52	21	23	9	10	429	154	1,254	232	356	123	109	79	695	257	182	1,991
09:00	154	315	127	138	55	63	2,405	922	7,525	1,389	2,134	737	656	477	3,735	1,544	1,093	11,947
10:00	154	315	127	138	55	63	2,405	922	7,525	1,389	2,134	737	656	477	3,735	1,544	1,093	11,947
11:00	154	315	127	138	55	63	2,405	922	7,525	1,389	2,134	737	656	477	3,735	1,544	1,093	11,947
12:00	154	315	127	138	55	63	2,405	922	7,525	1,389	2,134	737	656	477	3,735	1,544	1,093	11,947
13:00	154	315	127	138	55	63	2,405	922	7,525	1,389	2,134	737	656	477	3,735	1,544	1,093	11,947
14:00	154	315	127	138	55	63	2,405	922	7,525	1,389	2,134	737	656	477	3,735	1,544	1,093	11,947
15:00	154	315	127	138	55	63	2,405	922	7,525	1,389	2,134	737	656	477	3,735	1,544	1,093	11,947
16:00	154	315	127	138	55	63	2,405	922	7,525	1,389	2,134	737	656	477	3,735	1,544	1,093	11,947
17:00	26	52	21	23	9	10	429	154	1,254	232	356	123	109	79	695	257	182	1,991
18:00	33	54	14	13	15	6	344	95	774	189	167	51	86	31	1,266	183	218	1,226
19:00	33	54	14	13	15	6	344	95	774	189	167	51	86	31	1,266	183	218	1,226
20:00	216	358	94	87	101	39	2,270	629	5,106	1,247	1,104	335	565	207	8,355	1,211	1,441	8,090
21:00	216	358	94	87	101	39	2,270	629	5,106	1,247	1,104	335	565	207	8,355	1,211	1,441	8,090
22:00	216	358	94	87	101	39	2,270	629	5,106	1,247	1,104	335	565	207	8,355	1,211	1,441	8,090
23:00	216	358	94	87	101	39	2,270	629	5,106	1,247	1,104	335	565	207	8,355	1,211	1,441	8,090

Annex XXVI Residual, transport, BEV demand profiles

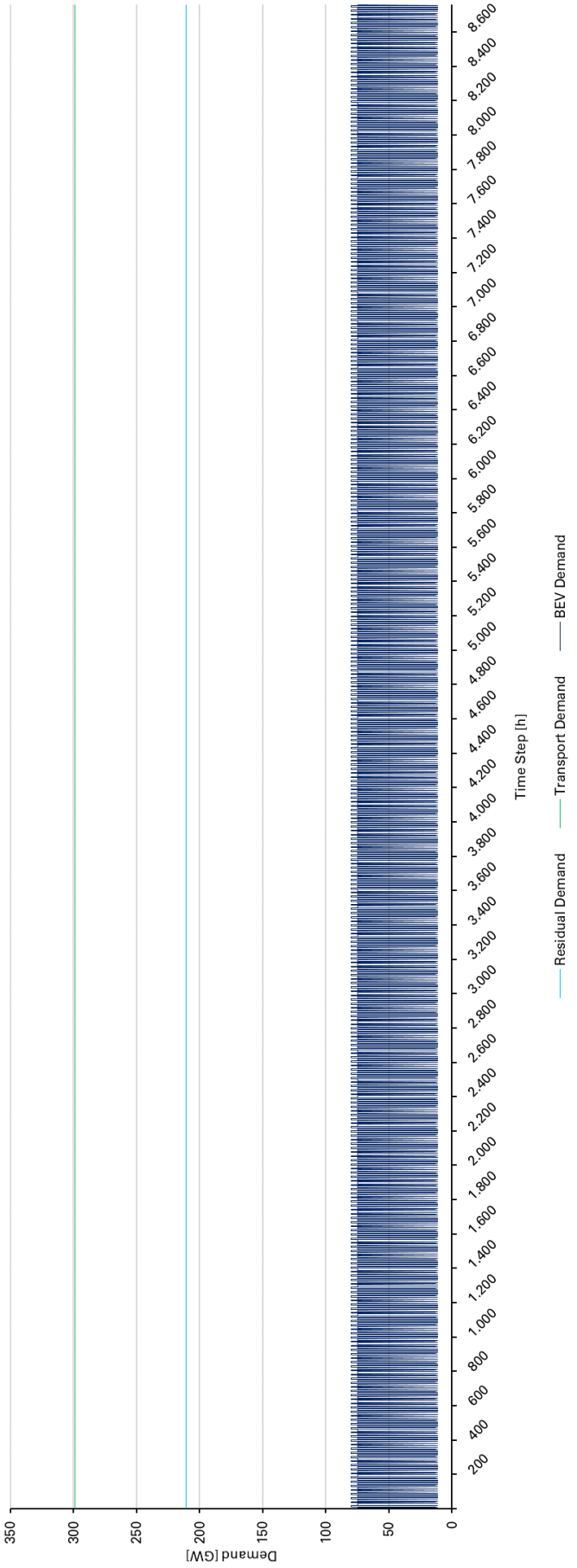

Annex XXVII Primary energy consumption per country 2050

Country	Wind	Solar El.	Geoth. El.	Hydro	El. Import	Solar Heat	Geoth. Heat	Bio-energy	Oil	Gas	Other	Sum
	[TWh]	[TWh]	[TWh]	[TWh]	[TWh]	[TWh]	[TWh]	[TWh]	[TWh]	[TWh]	[TWh]	[TWh]
AL	9.0	12.6	0.0	5.6	2.4	2.4	0.0	15.3	1.2	2.0	0.0	50.4
AT	20.7	29.2	14.4	45.8	118.9	5.7	28.7	56.1	35.7	44.8	8.6	408.5
BA	14.0	19.8	4.9	5.5	2.3	1.9	6.8	28.7	1.2	4.8	0.0	90.0
BE	24.2	24.7	4.4	0.6	282.0	9.0	8.8	32.7	114.3	70.3	7.1	578.0
BG	50.8	47.9	13.4	4.2	9.6	3.3	11.8	31.2	1.7	17.1	0.3	191.4
CH	14.8	22.2	8.6	31.2	191.9	8.1	17.2	21.6	39.1	51.2	2.0	407.7
CY	8.8	8.0	0.0	0.0	2.3	0.7	0.0	1.5	0.5	0.7	0.2	22.7
CZ	31.4	39.9	6.2	3.9	116.4	8.4	12.4	55.2	32.1	37.7	3.2	346.7
DE	433.8	277.2	69.2	30.7	1,133.7	62.6	138.4	235.3	352.1	351.5	47.2	3,131.7
DK	297.2	93.4	5.8	24.8	82.1	5.3	11.6	22.1	2.9	9.1	4.6	558.9
EE	77.5	27.6	0.4	0.1	32.4	0.8	0.8	18.4	0.5	1.9	0.7	161.2
ES	524.2	341.5	69.8	34.8	42.6	24.4	76.7	202.6	51.7	82.7	2.5	1,453.3
FI	340.6	118.4	0.0	16.4	37.6	3.7	0.0	75.2	17.8	25.4	2.8	638.0
FR	852.7	423.4	130.6	77.8	109.2	38.6	181.9	322.0	189.7	225.5	17.3	2,568.6
GR	54.4	61.4	16.2	5.6	3.8	6.1	23.6	23.2	5.9	22.6	0.6	223.5
HR	16.2	21.5	10.0	6.8	4.2	2.1	11.9	16.6	3.9	13.2	0.1	106.5
HU	34.0	46.2	34.8	1.1	29.2	1.7	15.3	68.3	33.3	31.8	1.6	297.2
IE	196.8	67.0	5.4	1.5	30.5	3.1	10.8	10.3	3.1	10.0	0.7	339.1
IS	173.2	55.0	64.4	12.2	106.2	0.0	4.0	0.3	0.2	7.8	0.0	423.3
IT	170.8	210.2	45.2	53.9	484.5	53.5	90.4	141.4	100.0	148.3	12.4	1,510.5
LT	120.1	46.9	3.8	1.1	59.7	1.1	4.0	38.8	2.4	11.5	0.6	289.9
LU	1.8	1.9	0.6	0.2	41.4	0.4	1.2	1.0	3.3	5.1	0.4	57.4
LV	134.1	45.7	0.6	3.3	76.2	1.4	1.2	42.5	1.1	1.3	0.4	307.9
ME	2.5	3.3	0.0	1.8	0.3	0.5	0.0	3.3	0.4	1.0	0.0	13.1
MK	7.9	11.2	0.1	2.5	2.9	0.9	0.1	9.2	3.3	3.4	0.0	41.5
NL	171.7	70.4	10.4	0.1	204.6	12.9	20.8	30.0	177.1	105.9	9.3	813.3
NO	95.9	50.5	0.0	144.0	8.7	3.6	0.0	33.3	21.4	45.2	0.6	403.3
PL	437.4	217.0	28.8	4.4	60.2	29.2	57.6	196.8	67.3	102.1	7.8	1,208.4
PT	99.7	64.8	12.6	19.1	8.4	5.0	13.6	28.1	15.8	17.2	2.2	286.5
RO	87.7	100.7	21.0	17.0	13.2	7.2	19.4	123.4	13.3	23.2	0.8	426.9
RS	25.7	37.5	18.3	10.2	4.5	1.9	9.4	27.1	5.0	13.3	0.0	153.0
SE	504.8	177.8	0.2	75.7	135.8	5.4	0.4	121.5	24.1	46.4	8.2	1,100.3
SI	5.3	8.1	1.6	5.8	22.1	1.6	3.2	11.9	4.1	8.1	0.5	72.2
SK	14.5	21.9	11.0	5.8	27.9	3.2	16.8	20.7	9.5	16.3	2.1	149.6
UK	726.0	292.1	8.4	5.6	251.4	46.8	16.8	91.3	211.7	223.9	14.1	1,887.9
ENTSO-E	5,780.0	3,096.6	621.1	659.0	0.0	362.3	815.6	2,157.1	1,546.7	1782.3	158.8	16,979.6

Annex XXVIII Total electricity production per country 2050

Country	Wind PP	PV PP	Biomass PP	Biogas PP	Geoth. PP	Hydro PP	Gas PP	Sum
	[TWh]	[TWh]	[TWh]	[TWh]	[TWh]	[TWh]	[TWh]	[TWh]
AL	9.0	12.6	3.0	0.2	0.0	5.6	1.2	31.6
AT	20.7	29.2	5.6	1.3	14.4	45.8	15.4	132.3
BA	14.0	19.8	7.0	0.2	4.9	5.5	2.8	54.3
BE	24.2	24.7	4.2	2.0	4.4	0.6	19.4	79.4
BG	50.8	47.9	10.4	1.4	13.4	4.2	8.4	136.5
CH	14.8	22.2	5.1	0.4	8.6	31.2	14.3	96.5
CY	8.8	8.0	0.2	0.3	0.0	0.0	0.4	17.8
CZ	31.4	39.9	7.1	4.5	6.2	3.9	11.9	104.9
DE	433.8	277.2	44.3	13.8	69.2	30.7	115.0	984.0
DK	297.2	93.4	2.9	3.2	5.8	24.8	5.6	432.9
EE	77.5	27.6	3.3	0.8	0.4	0.1	1.2	110.9
ES	524.2	341.5	24.9	10.4	69.8	34.8	47.7	1,053.3
FI	340.6	118.4	17.9	1.2	0.0	16.4	15.5	510.0
FR	852.7	423.4	47.2	12.8	130.6	77.8	100.6	1,645.0
GR	54.4	61.4	2.3	1.2	16.2	5.6	12.4	153.6
HR	16.2	21.5	1.8	0.5	10.0	6.8	3.9	60.7
HU	34.0	46.2	9.6	6.1	34.8	1.1	5.4	137.1
IE	196.8	67.0	2.3	0.3	5.4	1.5	6.2	279.5
IS	173.2	55.0	0.1	0.0	64.4	12.2	4.8	309.7
IT	170.8	210.2	16.7	7.1	45.2	53.9	65.8	569.6
LT	120.1	46.9	3.7	2.1	3.8	1.1	0.7	178.4
LU	1.8	1.9	0.2	0.0	0.6	0.2	1.4	6.1
LV	134.1	45.7	5.5	0.8	0.6	3.3	0.8	190.9
ME	2.5	3.3	0.8	0.0	0.0	1.8	0.6	9.1
MK	7.9	11.2	2.2	0.1	0.1	2.5	1.1	25.1
NL	171.7	70.4	4.4	2.3	10.4	0.1	26.4	285.7
NO	95.9	50.5	8.1	0.3	0.0	144.0	27.9	326.7
PL	437.4	217.0	28.9	9.1	28.8	4.4	30.7	756.2
PT	99.7	64.8	5.9	1.4	12.6	19.1	9.2	212.7
RO	87.7	100.7	25.7	3.6	21.0	17.0	10.4	266.1
RS	25.7	37.5	5.4	1.9	18.3	10.2	8.2	107.3
SE	504.8	177.8	28.9	1.4	0.2	75.7	27.9	816.7
SI	5.3	8.1	2.9	0.1	1.6	5.8	3.3	27.0
SK	14.5	21.9	3.3	1.3	11.0	5.8	5.9	63.5
UK	726.0	292.1	9.2	8.4	8.4	5.6	59.7	1,109.3
ENTSO-E	5,780.0	3,096.6	350.9	100.5	621.1	659.0	672.1	11,280.4

Annex XXIX Heat production per country 2050

Country	Solar Thermal	Geoth. PP	Biomass PP	Biogas PP	PTH	Sum
	[TWh]	[TWh]	[TWh]	[TWh]	[TWh]	[TWh]
AL	2.4	0.0	5.9	0.2	3.3	11.8
AT	5.7	28.7	10.9	1.4	84.3	130.9
BA	1.9	6.8	13.8	0.2	11.9	34.6
BE	9.0	8.8	8.1	2.1	138.5	166.5
BG	3.3	11.8	20.3	1.5	24.2	61.2
CH	8.1	17.2	10.1	0.4	94.7	130.4
CY	0.7	0.0	0.3	0.3	10.0	11.3
CZ	8.4	12.4	13.8	4.8	89.5	128.9
DE	62.6	138.4	86.6	14.9	739.6	1,042.1
DK	5.3	11.6	5.7	3.5	27.5	53.5
EE	0.8	0.8	6.5	0.9	5.0	14.0
ES	24.4	76.7	48.7	11.2	218.2	379.2
FI	3.7	0.0	34.9	1.3	96.1	136.0
FR	38.6	181.9	92.2	13.7	242.4	568.9
GR	6.1	23.6	4.6	1.3	33.3	68.9
HR	2.1	11.9	3.6	0.5	13.7	31.8
HU	1.7	15.3	18.8	6.6	26.2	68.5
IE	3.1	10.8	4.6	0.3	22.2	40.9
IS	0.0	4.0	0.1	0.0	2.6	6.7
IT	53.5	90.4	32.6	7.6	381.3	565.4
LT	1.1	4.0	7.2	2.2	9.9	24.5
LU	0.4	1.2	0.5	0.0	9.3	11.4
LV	1.4	1.2	10.8	0.9	9.7	24.0
ME	0.5	0.0	1.6	0.0	2.1	4.2
MK	0.9	0.1	4.4	0.1	1.0	6.5
NL	12.9	20.8	8.6	2.5	184.6	229.4
NO	3.6	0.0	15.9	0.3	57.7	77.5
PL	29.2	57.6	56.4	9.8	167.5	320.5
PT	5.0	13.6	11.6	1.5	48.8	80.5
RO	7.2	19.4	50.2	3.9	76.8	157.6
RS	1.9	9.4	10.6	2.1	24.0	47.9
SE	5.4	0.4	56.4	1.5	99.1	162.8
SI	1.6	3.2	5.7	0.1	9.9	20.5
SK	3.2	16.8	6.4	1.4	40.8	68.6
UK	46.8	16.8	17.9	9.0	369.7	460.2
ENTSO-E	362.3	815.6	686.2	108.0	3,375.6	5,347.6

Annex XXX Final energy consumption per country 2050

Country	PTG-H2	PTM	PTP	PTL	Biofuels	Oil	Gas	Others	Heat	Sum	PTG-SNG [18]
	[TWh]	[TWh]	[TWh]	[TWh]	[TWh]	[TWh]	[TWh]	[TWh]	[TWh]	[TWh]	[TWh]
AL	4.3	3.4	5.0	0.0	2.8	0.0	0.0	0.0	5.4	20.9	0.2
AT	29.0	37.4	61.1	0.0	10.6	15.5	15.0	8.6	119.8	296.9	1.8
BA	7.3	4.9	10.9	0.0	0.0	0.3	0.3	0.0	18.5	42.2	0.3
BE	39.5	42.8	77.5	0.0	10.4	27.3	26.5	7.1	154.0	385.2	2.5
BG	12.8	14.2	34.9	1.2	5.2	0.0	0.0	0.3	37.6	106.3	1.6
CH	43.3	37.4	53.8	0.0	0.0	23.2	22.5	2.0	114.8	297.0	0.5
CY	3.2	3.8	2.5	0.0	0.0	0.0	0.0	0.2	11.4	21.2	0.4
CZ	17.5	27.4	57.7	0.0	14.0	16.6	16.1	3.2	118.7	271.2	5.7
DE	272.3	265.3	466.9	0.0	18.5	130.5	126.5	47.2	963.8	2,291.0	17.6
DK	62.5	20.8	30.6	15.0	1.4	0.0	0.0	4.6	51.5	186.2	4.1
EE	16.5	3.3	7.0	2.8	2.7	0.0	0.0	0.7	11.2	44.2	1.1
ES	115.1	142.3	208.4	0.0	73.1	0.0	0.0	2.5	332.6	874.0	13.3
FI	76.3	20.2	60.9	0.0	0.3	0.0	0.0	2.8	123.4	283.8	1.6
FR	205.4	202.0	410.4	0.0	96.9	48.2	46.5	17.3	522.4	1,549.1	16.2
GR	13.6	27.6	49.5	0.0	10.5	0.7	0.6	0.6	78.4	181.5	1.5
HR	4.8	8.8	15.9	0.0	8.0	2.2	2.1	0.1	27.9	69.8	0.6
HU	20.2	18.5	38.6	0.0	12.4	16.7	16.2	1.6	65.8	190.0	7.8
IE	51.1	20.1	23.9	0.0	0.0	0.0	0.0	0.7	38.0	134.0	0.4
IS	55.6	2.6	17.8	2.8	0.0	0.0	0.0	0.0	4.4	83.3	0.0
IT	98.1	159.2	264.5	0.0	54.5	33.2	32.0	12.4	573.1	1,227.0	9.0
LT	19.6	8.0	9.2	5.5	18.1	0.0	0.0	0.6	18.6	79.4	2.7
LU	9.7	9.9	5.2	0.0	0.1	2.8	2.7	0.4	10.8	41.5	0.0
LV	24.5	4.7	5.7	3.8	18.1	0.0	0.0	0.4	18.3	75.4	1.1
ME	1.1	1.0	2.3	0.0	0.0	0.0	0.0	0.0	3.3	7.6	0.0
MK	5.2	2.8	4.2	0.0	0.0	1.6	1.6	0.0	4.1	19.6	0.1
NL	62.8	58.2	104.4	0.0	5.8	38.6	37.4	9.3	206.7	523.1	2.9
NO	29.3	21.8	103.3	0.0	0.0	0.0	0.0	0.6	69.1	224.1	0.0
PL	91.0	78.3	141.2	0.0	55.4	26.1	25.2	7.8	280.8	705.7	11.6
PT	30.9	27.6	38.3	0.0	0.3	2.3	2.2	2.2	64.3	168.1	1.8
RO	29.8	24.5	49.4	0.0	10.2	3.1	2.9	0.8	115.6	236.4	4.6
RS	10.5	8.7	36.4	0.0	0.0	0.0	0.0	0.0	37.2	92.8	2.4
SE	106.6	36.8	107.5	19.3	2.2	0.0	0.0	8.2	130.4	411.1	1.7
SI	7.9	7.8	12.4	0.0	0.0	2.6	2.5	0.5	17.4	51.2	0.1
SK	5.9	10.1	25.6	0.0	4.0	2.6	2.5	2.1	58.3	110.9	1.6
UK	210.9	214.1	246.0	0.0	30.8	119.6	116.2	14.1	447.1	1,398.8	10.6
ENTSO-E	1,794.6	1,576.3	2,789.0	50.3	466.1	513.5	497.7	158.8	4,854.4	12,700.6	127.4

[18] PTG_{SNG} production is exclusively supplied to CCGT power plants in the energy conversion section. Therefore, it is not assigned to final energy consumption (compare **Chapter 5**).

Annex XXXI Energy and electricity trade balance 2050

Country	Electricity Export	Electricity Import	Gas	Oil	Others	Electricity Balance	Energy Balance
	[TWh]	[TWh]	[TWh]	[TWh]	[TWh]	[TWh]	[TWh]
AL	14.2	2.4	2.0	0.0	0.0	11.8	9.8
AT	27.9	118.9	40.9	16.3	8.6	-91.0	-156.8
BA	14.1	2.3	4.8	0.3	0.0	11.8	6.7
BE	58.6	282.0	59.8	28.9	7.1	-223.4	-319.2
BG	35.4	9.6	13.7	0.0	0.3	25.9	11.8
CH	44.4	191.9	47.0	24.5	2.0	-147.5	-221.0
CY	2.3	2.3	0.7	0.0	0.2	0.0	-0.8
CZ	19.2	116.4	36.3	17.5	3.2	-97.2	-154.2
DE	251.7	1,133.7	321.0	137.8	47.2	-882.0	-1,388.1
DK	267.9	82.1	9.1	0.0	4.6	185.8	172.2
EE	85.8	32.4	1.9	0.0	0.7	53.4	50.7
ES	264.9	42.6	77.5	0.0	2.5	222.3	142.3
FI	219.8	37.6	25.0	0.0	2.8	182.2	154.4
FR	433.6	109.2	212.6	50.9	17.3	324.4	43.6
GR	13.9	3.8	20.9	0.7	0.6	10.1	-12.1
HR	14.6	4.2	8.8	2.3	0.1	10.4	-0.8
HU	31.6	29.2	26.1	17.6	1.6	2.4	-42.9
IE	140.1	30.5	10.0	0.0	0.7	109.7	99.0
IS	258.9	106.2	7.8	0.0	0.0	152.7	144.9
IT	111.6	484.5	140.7	35.0	12.4	-372.9	-561.1
LT	150.9	59.7	1.7	0.0	0.6	91.2	89.0
LU	9.1	41.4	5.1	2.9	0.4	-32.3	-40.7
LV	183.7	76.2	1.3	1.1	0.4	107.5	104.7
ME	1.7	0.3	1.0	0.0	0.0	1.4	0.5
MK	9.2	2.9	3.4	1.7	0.0	6.3	1.2
NL	51.3	204.6	83.2	40.7	9.3	-153.3	-286.6
NO	61.9	8.7	45.2	0.0	0.6	53.2	7.4
PL	229.3	60.2	77.6	27.6	7.8	169.2	56.2
PT	44.1	8.4	17.2	2.5	2.2	35.7	13.8
RO	65.0	13.2	20.0	3.2	0.8	51.8	27.8
RS	16.9	4.5	13.3	0.0	0.0	12.3	-1.0
SE	444.2	135.8	45.3	0.0	8.2	308.5	254.9
SI	5.6	22.1	8.0	2.8	0.5	-16.5	-27.7
SK	5.6	27.9	12.3	2.7	2.1	-22.3	-39.4
UK	149.8	251.4	219.3	126.3	14.1	-101.6	-461.3
ENTSO-E	3,738.8	3,738.8	1,620.8	543.5	158.8	0.0	-2,323.1

Annex XXXII Energy transformation input per country 2050

Country	PP Gas	PP Bioenergy	PP SNG	Oil Refineries	PTG-H_2	SNG-H_2-El.	PTL	PTM	PTH	Sum	SNG-CO_2[19]
	[TWh]	[TWh]	[TWh]	[TWh]	[TWh]	[TWh]	[TWh]	[TWh]	[TWh]	[TWh]	[mio. t]
DE	176.9	216.7	17.6	94.1	452.8	23.3	0.0	279.2	568.9	1,829.6	0.1
FR	154.8	225.1	16.2	34.8	347.2	21.5	0.0	212.6	186.5	1,198.7	0.7
UK	91.9	60.5	10.6	86.2	344.9	14.1	0.0	225.4	284.4	1,118.0	0.1
IT	101.3	86.9	9.0	23.9	168.2	11.9	0.0	167.6	284.9	853.6	1.0
ES	73.6	129.5	13.3	0.0	202.6	17.6	0.0	149.8	167.8	754.2	0.6
PL	47.2	141.4	11.6	18.8	162.2	15.3	0.0	82.4	128.8	608.0	0.2
SE	43.1	119.3	1.7	0.0	202.9	2.3	23.1	38.8	76.3	507.5	0.2
NL	40.6	24.3	2.9	27.8	102.3	3.9	0.0	61.3	142.0	405.0	2.3
FI	23.8	75.0	1.6	0.0	120.4	2.1	0.0	21.2	73.9	317.9	7.0
BE	29.8	22.2	2.5	19.7	65.6	3.3	0.0	45.1	106.5	294.8	1.6
RO	15.9	113.1	4.6	2.2	54.8	6.1	0.0	25.8	59.1	281.8	0.4
CH	21.9	21.6	0.5	16.7	67.6	0.6	0.0	39.4	72.8	241.1	5.3
AT	23.6	45.6	1.8	11.2	48.1	2.4	0.0	39.4	64.8	236.9	0.6
DK	8.7	20.8	4.1	0.0	131.7	5.4	18.0	21.9	21.2	231.7	6.5
CZ	18.3	41.2	5.7	12.0	38.0	7.6	0.0	28.9	68.8	220.5	0.6
NO	43.1	33.3	0.0	0.0	45.1	0.0	0.0	23.0	44.4	188.8	0.2
HU	8.3	55.9	7.8	12.0	46.1	10.3	0.0	19.4	20.1	179.9	3.1
PT	14.1	27.9	1.8	1.7	51.1	2.4	0.0	29.0	37.6	165.6	0.2
IE	9.6	10.3	0.4	0.0	79.5	0.5	0.0	21.2	17.1	138.5	0.0
GR	19.1	12.7	1.5	0.5	23.8	2.0	0.0	29.1	25.6	114.3	3.6
IS	7.4	0.2	0.0	0.0	90.7	0.0	3.3	2.7	2.0	106.4	1.1
BG	12.9	26.0	1.6	0.0	25.1	2.1	1.5	15.0	18.7	102.9	0.0
LT	1.2	20.7	2.7	0.0	45.3	3.5	6.6	8.4	7.6	96.0	0.4
RS	12.7	27.1	2.4	0.0	20.9	3.2	0.0	9.2	18.4	94.0	0.0
LV	1.3	24.4	1.1	0.0	46.7	1.4	4.5	5.0	7.4	91.8	0.0
SK	9.0	16.8	1.6	1.8	12.3	2.2	0.0	10.6	31.4	85.7	1.2
EE	1.9	15.7	1.1	0.0	32.6	1.4	3.3	3.5	3.8	63.2	0.2
BA	4.3	28.7	0.3	0.2	11.8	0.4	0.0	5.2	9.2	60.0	4.6
SI	5.1	11.9	0.1	1.9	12.4	0.2	0.0	8.2	7.6	47.3	0.7
HR	6.0	8.6	0.6	1.6	8.5	0.8	0.0	9.3	10.6	45.8	1.9
LU	2.2	1.0	0.0	2.0	15.0	0.0	0.0	10.4	7.2	37.7	1.0
AL	1.9	12.5	0.2	0.0	7.1	0.3	0.0	3.6	1.0	26.5	0.7
MK	1.6	9.2	0.1	1.2	8.3	0.2	0.0	3.0	0.8	24.3	0.1
CY	0.7	1.5	0.4	0.0	5.7	0.5	0.0	4.0	3.8	16.6	0.7
ME	0.9	3.3	0.0	0.0	1.7	0.0	0.0	1.0	1.6	8.6	4.2
ENTSO-E	1,034.7	1,691.0	127.4	370.3	3,098.7	168.8	60.3	1,659.3	2,582.8	10,793.2	51.1

[19] SNG-CO_2 input refers to substance input into the PTG_{SNG} processes. It does not refer to energy related conversion and is not accounted for in the energy conversion section (compare **Chapter 5**).

Annex XXXIII GHG emissions and reduction potentials per country and region

Region	Country	GHG 1990		GHG 2019		GHG 2050		Reduction 2019-2050		Reduction 1990-2050	
		[Mt CO_{2eq}]		[Mt CO_{2eq}]		[Mt CO_{2eq}]		[%]		[%]	
Balkans	AL	502.2	6.6	342.3	5.7	79.6	1.5	76.7	73.7	84.1	77.6
	BA		24.6		33.5		5.0		84.9		79.5
	BG		82.3		43.3		10.4		76.1		87.4
	HR		25.2		19.1		6.8		64.6		73.1
	GR		79.2		65.6		15.7		76.1		80.2
	MK		14.0		10.5		3.0		71.3		78.4
	ME[20]		-		2.5		0.6		74.6		-
	RO		187.3		78.6		20.0		74.6		89.3
	RS		66.4		70.7		11.8		83.3		82.3
	SI		16.6		15.4		4.9		68.2		70.6
Baltics	EE	93.9	38.5	40.7	18.5	11.8	3.7	71.1	79.8	87.5	90.3
	LV		20.1		8.4		1.7		79.7		91.5
	LT		35.3		13.8		6.3		54.0		82.1
Benelux	BE	288.9	116.0	270.6	104.4	170.9	65.6	36.8	37.1	40.9	43.4
	LU		11.8		9.7		3.2		67.3		72.9
	NL		161.2		156.4		102.0		34.8		36.7
Nations	AT	3293.9	62.9	2517.3	72.4	936.5	30.7	62.8	57.5	71.6	51.2
	CZ		162.8		105.7		31.9		69.8		80.4
	FR		386.4		314.7		149.0		52.7		61.4
	DE		1018.2		702.6		286.7		59.2		71.8
	IT		430.1		331.6		107.5		67.6		75.0
	PL		371.4		317.7		89.2		71.9		76.0
	PT		43.7		48.5		15.6		67.8		64.2
	ES		230.4		259.3		70.3		72.9		69.5
	UK		588.1		364.9		155.6		57.4		73.5
Others	CY	215.0	4.5	172.5	7.4	72.2	1.3	58.1	82.2	66.4	70.9
	HU		72.1		53.2		23.9		55.0		66.8
	IE		32.9		36.5		8.2		77.7		75.2
	SK		60.5		36.0		12.1		66.3		80.0
	CH		45.0		39.4		26.6		32.3		40.7
Scand.	DK	208.6	53.6	171.2	31.1	74.0	8.2	56.8	73.7	64.5	84.7
	FI		57.3		43.4		17.6		59.5		69.3
	IS		2.3		3.9		2.0		47.9		12.8
	NO		37.3		48.0		22.0		54.2		41.1
	SE		58.1		44.7		24.2		45.9		58.3
ENTSO-E		4591.0		3517.1		1345.0		61.8		70.7	

[20] In 1990, the emission repository was accounted for together with Serbia. Hence, Montenegro cannot be compared individually and the GHG emissions are assigned to Serbia. [Crip2020a]

Annex CD Digital annex

The **Annex CD** is not included in this publication.